2019-07-17

Adaptations of Adipose Tissue Expandability in Gestation are Associated with Maternal Glucose Metabolism

Raziel Rojas-Rodriguez
University of Massachusetts Medical School

Let us know how access to this document benefits you.

Repository Citation

University of Massachusetts Medical School Publications

2019

Adaptations of Adipose Tissue Expandability in Gestation are Associated with Maternal Glucose Metabolism

Raziel Rojas-Rodriguez

ال*منارة* للاستشارات

www.manaraa.com

ADAPTATIONS OF ADIPOSE TISSUE EXPANDABILITY IN GESTATION ARE ASSOCIATED WITH MATERNAL GLUCOSE METABOLISM

A Dissertation Presented

by

RAZIEL ROJAS-RODRIGUEZ

Submitted to the Faculty of the
University of Massachusetts Graduate School of Biomedical Sciences, Worcester
in partial fulfillment of the requirements for the degree of

DOCTOR OF PHILOSOPHY

July 17th, 2019

Translational Sciences

ADAPTATIONS OF ADIPOSE TISSUE EXPANDABILITY IN GESTATION ARE ASSOCIATED WITH MATERNAL GLUCOSE METABOLISM

A Dissertation Presented

by

RAZIEL ROJAS-RODRIGUEZ

The signatures of the Dissertation Defense Committee signify completion and approval as to style and content of the Dissertation

_____

Silvia Corvera, MD, Thesis Advisor

_____

Michael Thompson, MD, Member of Committee

_____

Yong-Xu Wang, PhD, Member of Committee

_____

Laura Alonso, MD, Member of Committee

_____

Susan K. Fried, PhD, Member of Committee

The signature of the Chair of the Committee signifies that the written dissertation meets the requirements of the Dissertation Committee

_____

Pranoti Mandrekar, PhD, Chair of Committee

The signature of the Dean of the Graduate School of Biomedical Sciences signifies that the student has met all graduation requirements of the school

_____

Mary Ellen Lane, PhD
Dean of the Graduate School of Biomedical Sciences
Translational Science Program

July 17th, 2019

Acknowledgements

First, I want to give my most sincere gratitude to my thesis mentor, Dr. Silvia Corvera for providing me with both scientific guidance and personal support during my training as a graduate student. The microscopy approach presented in this thesis has been possible thanks to the imaging acquisition and analysis training provided by Dr. Karl Bellvé and Dr. Lawrence Lifshitz, they have been great colleagues and I hope we can keep collaborating in the future. I want to give a special thank you to Dr. Tiffany Moore-Simas for guiding me in the path of translational research and making possible the recruitment of human subjects for my studies. In addition, I want to recognize the group of Information Technology-Data Sciences and the collaborators of the Obstetrics/Gynecology department, specially Kathy Leung, for their help in clinical data collection and analysis.

Thank you to Dr. Olga Gaelikman for technical training as an adipose biologist. Dr. So Yun Min, my sister in science, thank you for being there for me at all times. To the Corvera lab group: cheers for the great team we make. Last, I want to express my appreciation to my family and loved ones for their emotional support in all these years.

Abstract

Pregnancy induces maternal metabolic adaptations including mild glucose intolerance and weight gain in order to support fetal development and lactation. Adipose tissue (AT) function in gestation is featured by reduced insulin sensitivity and fat mass accrual which partly accounts for the weight gain in pregnant women and adaptation of glucose metabolism. A common metabolic pregnancy complication is gestational diabetes mellitus (GDM), a disease characterized by impaired glucose tolerance with onset in gestation. However, the relationship between AT expandability and glucose metabolism in gestation is not well understood. The goal of this thesis was to investigate the adaptations of human AT expansion induced by pregnancy, how these changes are reflected in pregnancies complicated with GDM and characterize a mouse model to study the mechanisms underlying this disease. This dissertation illustrates that pregnancy promotes AT expandability by a signaling mechanism between placental pregnancy-associated plasma protein-A (PAPP-A) and AT- insulin-like growth factor binding protein-5 (IGFBP5). In addition, gravidas with GDM showed impaired AT expansion. Studies investigating the relationship between PAPP-A and glycemic state demonstrated that low levels of PAPP-A in the 1st trimester are highly associated with the development of GDM. Moreover, PAPP-A knockout mice exhibit reduced insulin sensitivity and impaired AT growth exclusively in gestation. These results expand the knowledge of AT biology in

gestation and have the potential to improve maternal care by proposing PAPP-A as an early biomarker and possible therapeutic for GDM. It also introduces a new mouse model to study the etiology of gestational diabetes.

Table of Contents

List of Tables

List of Figures

Chapter IV

Appendix

List of Copyrighted Materials Produced by the Author

Chapter 2 has previously been published as:

Raziel Rojas-Rodriguez, Lawrence M. Lifshitz, Karl Bellve, So Yun Min,

Jacqueline Pires, Katherine Leung, Crina Boeras, Aylin Sert, Jacqueline T.

Draper, Silvia Corvera, and Tiffany A. Moore-Simas. (2015). Human adipose

tissue expansion in pregnancy is impaired in gestational diabetes mellitus.

Diabetologia, *58,* 2106-2114.

Author Contributions:

SC and TAMS conceived the study. CB, AS, JTD identified patients and obtained

their consent. RRR prepared samples for analysis. KDB and RRR developed the

multiwell plate imaging platform for the angiogenesis assay. LML, SYM, and

RRR developed the image analysis methods. JP and RRR performed and

analyzed mRNA expression experiments. LML, KL, and SC performed statistical

analyses. All authors contributed to writing the manuscript.

Chapter 3 has been submitted for publication as:

Raziel Rojas-Rodriguez, Sana Majid, Rachel Ziegler, Aylin S. Madore, Veronica A. Pace, Daniel Nachreiner, David Alfego, Jomol Mathew, Katherine Leung, Tiffany A. Moore-Simas, and Silvia Corvera. (2019). PAPP-A-mediated adipose tissue remodeling mitigates insulin resistance and protects against gestational diabetes in mice and humans. *Manuscript under review.*

Author Contributions:

RRR, SC, TAMS designed the study. AS identified patients. AS and RRR obtained patient consent. RRR prepared samples for analysis. RRR performed the experiments with human and mouse tissue. AS, DN, DA, JM, and KL collected and analyzed data for the retrospective study. RZ and RRR maintained the breeding colony. RRR performed the in vivo experiments on mice. SM and RRR did the imaging quantifications. VP and RRR performed and analyzed mRNA expression experiments. RRR and SC performed statistical analyses and wrote the manuscript.

The publication included in the Appendix has been published as:

Author Contributions:

OG and SC designed the study. RRR, OG, and SYM prepared samples for analysis. RRR, OG, and SYM performed the experiments with human and mouse tissue. RRR, OG, SYM, MEK, BR, and KR collected and analyzed data. KDB and RRR developed the multiwell plate imaging platform for the angiogenesis assay. LML, RRR, and OG developed the image analysis methods. SC and OG performed statistical analyses. All authors contributed to writing the manuscript.

CHAPTER I: Introduction

Maternal metabolic adaptations during gestation promote fetal development

During pregnancy, metabolic changes in women occur in order to support fetal growth and to prepare for lactation. An increase in maternal blood glucose is essential since the feto-placental unit utilizes glucose as its main energy source (Angueira et al., 2015) (Leturque et al., 1986) (Herrera, 2000). Maternal adipose tissue, skeletal muscle, and liver, which are organs directly involved in glucose metabolism, reduce their insulin sensitivity while the beta cells from the pancreas increase their insulin production and secretion (Sonagra, Biradar, Dattatreya, & Murthy, 2014) (Kuhl, 1991). The reduction of insulin sensitivity in pregnancy has been longitudinally measured utilizing the hyperinsulinemic-euglycemic clamp technique. Decreased glucose infusion rates (Catalano, Tyzbir, Roman, Amini, & Sims, 1991) (Kirwan et al., 2002) and reduced insulin suppression of endogenous glucose production in the third trimester (Catalano et al., 1992) (Sivan, Chen, Homko, Reece, & Boden, 1997) favors a state of hyperglycemia and accounts for the 65% decrease of insulin sensitivity observed in late gestation. These metabolic adaptations of maternal peripheral organs are the key

1

events favoring glucose availability for fetal uptake (Barbour et al., 2007) (Musial et al., 2016).

Besides increased blood glucose and reduced insulin sensitivity, weight gain is also observed in gestation due to an increase in blood volume, fetal mass, and maternal fat stores (Larciprete et al., 2003) (Berggren et al., 2017) (Pirani, Campbell, & MacGillivray, 1973) (Abrams & Selvin, 1995). The growth in maternal fat mass, or adipose tissue accrual, is accompanied by the expansion of adipose tissue stores (Kinoshita & Itoh, 2006) (Kopp-Hoolihan, van Loan, Wong, & King, 2017). The expansion of adipose tissue is necessary for maintaining metabolic homeostasis, since as pregnancy advances, fat utilization is the preferred fuel source by maternal peripheral organs (Rebuffe-Scrive et al., 1985) (Herrera & Ortega-Senovilla, 2010).

The remodeling of energy balance in gestation highlights the role of adipose tissue in supporting maternal metabolism. The main function of adipose tissue is to store energy from excess calorie intake in the form of triglycerides and release them as free fatty acids in response to energy demands (Trayhurn & Beattie, 2008). The lipid availability from maternal adipose tissue stores is dependent on the effects of insulin action according to the stage of pregnancy. In early gestation, rapid weight gain and enhanced insulin sensitivity in the adipose tissue

2

results in lipid accumulation and fat mass gain. In late gestation, adipose tissue reduces its sensitivity to insulin, favoring lipolysis and lipid mobilization to maternal peripheral tissues (Knopp, Saudek, Arky, & O'sullivan, 1973) (Herrera, 2000) (Lain & Catalano, 2007). The excess release of free fatty acids (Pusukuru et al., 2016) (Poveda et al., 2018) and the increase in the mean rate of glycerol production (Diderholm, Stridsberg, Ewald, Lindeberg-Nordén, & Gustafsson, 2005) is likely to contribute to the development of peripheral reduced insulin sensitivity and to decrease maternal glucose utilization. The excess glucose is then available for fetal uptake. The changes in maternal lipid metabolism feature the importance of adipose tissue adaptations to pregnancy.

3

Gestational diabetes mellitus: A common pregnancy complication affecting glucose metabolism

In a normal pregnancy, the reduction of insulin mediated glucose disposal is accompanied by an enhancement of insulin secretion to maintain euglycemia (Kuhl, 1991). However, maternal maladaptation to changes in glucose metabolism can lead to adverse pregnancy outcomes that can affect both mother and baby during gestation, immediately post-partum, and later in life (Gaillard, Steegers, Franco, Hofman, & Jaddoe, 2015) (The HAPO Study Cooperative Research Group, 2008).

In 1915, EP Joslin reported in the Boston Medical and Surgical Journal (now New England Journal of Medicine) the presence of glycosuria in pregnant women (Joslin, 1915). Interestingly, the report mentions that the glycosuria disappears after child birth but it can worsen with following pregnancies and a "severe form of diabetes" may result. Since then, scientific studies in the field of maternal metabolism have defined the pathologic glucose intolerance with first recognition during pregnancy as gestational diabetes mellitus (GDM). The pathogenesis of this condition is based on insufficient pancreatic β-cell insulin secretion needed to compensate for the reduced insulin sensitivity of peripheral tissues in mid to late gestation (Mørkrid et al., 2012), excessive insulin resistance of peripheral tissues (Catalano et al., 2002) (Friedman et al., 1999) (Barbour, McCurdy, Hernandez, &

4

Friedman, 2011) (Okuno et al., 1995), or a combination of both (Akbay et al., 2003) (Fasshauer, Blüher, & Stumvoll, 2014). In general, GDM develops due to the impaired ability of peripheral tissues to adapt to glucose metabolism changes in pregnancy.

Prevalence, risks, diagnosis, and prognosis of GDM

Worldwide, 1 in 7 of live births are affected by GDM (International Diabetes Federation, 2017). Until 2016, between 7.6%-8.2% of women have been diagnosed with GDM in United States (Casagrande, Linder, & Cowie, 2018) (Zhou et al., 2018). The prevalence of GDM is increasing due to new diagnostic criteria, the obesogenic epidemic, and sedentary lifestyles. Pre-pregnancy body mass index (BMI), maternal age, ethnicity, and a family history of type-2 diabetes are risk factors associated with GDM (Noctor & Dunne, 2015).

As part of the standard prenatal care, all pregnant women receive a glucose test between 24-28 weeks of gestation to screen for hyperglycemia. Two tests are currently accepted for GDM diagnosis. The most used in clinics consists of a two-step approach: 1-hour 50g oral glucose challenge screening test where abnormal results are followed by a 3-hour 100g oral glucose tolerance test (Harper et al., 2016). Diagnostic values follow the cut-offs described by either the National Diabetes Data Group (National Diabetes Data Group, 1979) or Carpenter-

5

Coustan criteria (Carpenter & Coustan, 1982) (Table 1.1). However, the cut-offs

values for both criteria were challenged by the results obtained from the

Hyperglycemia and Adverse Pregnancy Outcomes (HAPO) study. The HAPO

study demonstrated the continuous relationship of maternal glucose levels below

the established diagnostic cut-off for diabetes with increased birth weight and

cord-blood serum C-peptide from over 23,000 subjects from nine countries (The

HAPO Study Cooperative Research Group, 2008). The International Association

of Diabetes and Pregnancy Groups (IADPSG) utilized the HAPO study as

initiative to propose an alternative test for GDM, which consists of a one-step

approach as a 2-hour 75g oral glucose challenge test (International Association

of Diabetes and Pregnancy Study Groups (IADPSG) Consensus Panel, 2010)

(Table 1.1).

Two-step Approach			One-step Approach
Carpenter and Coustan		**National Diabetes Data Group**	**International Association of Diabetes and Pregnancy Study Groups**
Screening: 1hr 50g glucose challenge test Plasma glucose cut-off values (mg/dl)			**No screening test**
≥130		≥140	
Diagnosis: 3hr 100g glucose tolerance test Plasma glucose cut-off values (mg/dl) (two or more abnormal)			**Diagnosis:** 2hr 75g glucose tolerance test Plasma glucose cut-off values (mg/dl) (one or more abnormal)
Fasting	≥95	≥105	≥92
1hr	≥180	≥190	≥180
2hr	≥155	≥165	≥153
3hr	≥140	≥145	N/A

Table 1. 1 Threshold values for screening and diagnosis of GDM according to criteria from Carpenter-Coustan, National Diabetes Data Group, and International Association of Diabetes Study Groups.

The controversy of which test and diagnostic criteria to use when diagnosing GDM presents a challenge when it comes to determining the actual incidence and standards of care that must be followed in GDM.

The impact of hyperglycemia and GDM on both mother and child has been described in a series of clinical and population studies. Babies born from mothers with GDM have a higher incidence of neonatal hyperinsulinemia, hypoglycemia, macrosomia and larger fat mass composition than babies born from normoglycemic women (Sreelakshmi et al., 2015) (The HAPO Study Cooperative Research Group, 2008) (Uebel et al., 2014) (Zhao, Li, & Li, 2014) (International Association of Diabetes in Pregnancy Study Group (IADPSG) Working Group on Outcome Definitions et al., 2015). In addition, multicenter studies have shown a direct relationship between maternal hyperglycemia and childhood impaired glucose tolerance and insulin resistance (Scholtens et al., 2019) (Lowe et al., 2019). A systematic review reported that 50% of the women with a history of GDM develop type-2 diabetes five to ten years after the index pregnancy (C. Kim, Newton, & Knopp, 2002) and data included in a meta-analysis showed that women with previous GDM have a seven-fold increase risk of type-2 diabetes than women who were normoglycemic during their pregnancy (Bellamy, Casas, Hingorani, & Williams, 2009). Global health agencies have expressed their urge for understanding the biology of gestational diabetes in

8

order to establish prevention programs and possible therapeutics for this condition.

Pathogenesis of GDM

The molecular basis of GDM is under investigation; however, it has been established that women with GDM have reduced muscle glucose uptake (Friedman et al., 1999), decreased insulin suppression of hepatic glucose production (Catalano et al., 1993), and higher serum triglycerides (Koukkou, Watts, & Lowy, 1996) than normoglycemic gravidas. Moreover, gestational diabetes is characterized by peripheral insulin resistance to glucose disposal (Catalano, Huston, Amini, & Kalhan, 1999), low grade inflammation (Wolf et al., 2004) (Moore-Simas & Corvera, 2014), and dysregulation of adipokines (Tsiotra et al., 2018) (Altinova et al., 2007) (Fasshauer et al., 2014). Due to the increase in adipose tissue stores and the direct impact of adipose tissue function on glucose and lipid metabolism in pregnancy, studies investigating this physiology in the context of GDM are needed to elucidate what molecular and cellular mechanisms are driving the impaired ability of fat to adapt to gestation. Understanding the etiology of GDM will provide possibilities for early diagnosis, prevention and even treatment that will break the cycle of the transgenerational effects of this metabolic disease.

9

Adipose tissue expansion and its role in glucose metabolism during gestation

Fat storage location determines maternal insulin sensitivity

The depot distribution of fat mass is a key determinant of maternal insulin sensitivity (Straughen, Trudeau, & Misra, 2013) (Mazaki-Tovi et al., 2015). Subcutaneous fat mass deposition presents as fat accumulation beneath the skin in the abdominal, subscapular, gluteal and femoral areas and is associated with insulin sensitivity (Snel et al., 2012) (McLaughlin, Lamendola, Liu, & Abbasi, 2011). Visceral adiposity presents fat deposition inside the intra-abdominal cavity, in close proximity to the liver and intestines. Due to its close location to the liver, visceral fat accumulation increases the availability of adipose tissue hormones and adipokines into the portal circulation, affecting metabolic health by altering glucose and lipid metabolism (Kabir et al., 2005) (Frank, de Souza Santos, Palmer, & Clegg, 2018). Therefore, the preferential location of fat deposition in the subcutaneous depot prevents the ectopic deposition of lipids in visceral tissues with consequent development of insulin resistance (Snel et al., 2012) (M. Zhang, Hu, Zhang, & Zhou, 2015).

Clinical studies have investigated the association of fat distribution and risk of gestational diabetes. Two studies reported the relationship between maternal

10

abdominal adiposity measured via ultrasound at the first trimester of gestation and GDM risk assessed by oral glucose test at weeks 24-28 of gestation. The results demonstrated that gravidas with a higher content of visceral adipose tissue had higher risk of developing GDM than those with lower accumulation of visceral fat (Gur et al., 2014) (De Souza, Berger, Retnakaran, Maguire, et al., 2016). Others have also found a positive relationship between ectopic lipid deposition, measured via sonographic features of fatty liver at 11-14 weeks of gestation, and the risk for GDM at the time of diagnosis (De Souza, Berger, Retnakaran, Vlachou, et al., 2016) (Lee et al., 2019). The literature available agrees in the positive association between visceral adiposity and the development of GDM. Since pregnancy is a period of rapid weight gain, maternal adipose stores must coordinate their lipid deposition in subcutaneous depots to avoid developing metabolic complications later in gestation that can lead to hindered glucose metabolism.

Adipocyte hypertrophy and hyperplasia are associated with gestational insulin sensitivity

Different cell populations reside in adipose tissue including adipocytes, macrophages, fibroblasts, endothelial cells, pericytes and mesenchymal stem cells. Adipocytes are insulin-sensitive cells that store lipid in the form of triglycerides and release lipids as free fatty acids in response to energy needs

11

giving adipose tissue a flexible and rapid adaptation to metabolic demands. Adipocytes can grow via two mechanisms: hypertrophy and hyperplasia. Hypertrophy occurs when existing adipocytes store lipid by enlargement of their lipid droplet, therefore increasing in cellular volume. Hyperplasia, on the other hand, consists on the differentiation of adipocyte progenitors into mature adipocytes. Therefore, hypertrophy equals to an enlargement in the size of existing adipocytes while hyperplasia results in an increase of adipocyte number (Arner, 2018).

The relationship between adipocyte size and insulin sensitivity has been studied in diverse clinical settings. In an obese cohort, subcutaneous and omental (visceral) adipocyte size had a positive correlation with increased plasma insulin and triglyceride levels while a negative association with insulin sensitivity (Rydén, Andersson, Bergström, & Arner, 2014). Interestingly, subcutaneous adipocyte number positively correlated with insulin sensitivity but had a negative association with plasma insulin and triglyceride levels (Rydén et al., 2014). In a weight loss after bariatric surgery (roux-en-y gastric bypass) study, fat mass and subcutaneous adipocyte volume and number were measured before and two years after surgery. Results showed that weight loss resulted in reduced fat mass and that adipocyte volume was reduced but no changes were observed with respect to adipocyte number. This reduction in adipocyte volume was positively

12

associated with improved insulin sensitivity as determined by hyperinsulinemic-euglycemic clamp studies (Andersson et al., 2014). A longitudinal study of normal weight and obese pregnant women measured abdominal subcutaneous adipocyte volume and number in the first and third trimester of gestation. The results showed that normal weight gravidas had increased adipocyte size while obese gravidas had an increase in adipocyte number suggesting that obese gravidas recruited new adipocytes to store fat. (Svensson et al., 2016). Therefore, the pre-pregnancy BMI and composition of adipose tissue could indicate how adipocytes adapt to gestation. Another longitudinal study done in normal weight women measured gluteal subcutaneous adipocyte size and number at the pre-pregnancy stage followed by early (8-12 weeks) and late (36-38 weeks) gestation (Resi et al., 2012). Interestingly, this particular subcutaneous depot showed adipose tissue growth by both hypertrophy and hyperplasia indicating that each fat depot site may present distinct mechanisms for adipose tissue expansion.

The connection between insulin resistance and impaired adipocyte growth can be explained by the limited expansion capacity of hypertrophic adipocytes. Fat cells growing via hypertrophy reach an expansion limit, driving lipid accumulation in ectopic sites (visceral organs) and causing low grade chronic inflammation in the adipose tissue (Rutkowski, Stern, & Scherer, 2015) (Wajchenberg, 2000)

(Verboven et al., 2018). In the visceral fat of obese and type-2 diabetes men, hypertrophied adipocytes secrete pro-inflammatory cytokines promoting macrophage infiltration and establishing local low-grade inflammation but lean individuals do not present these features (Verboven et al., 2018). Together, the evidence suggests that the glycemic status during pregnancy is largely due to a delicate balance between adipocyte number, volume and the site of fat accumulation.

Angiogenesis is essential for adipose tissue expansion

Besides changes in adipocyte size and number, the growth of adipose tissue is dependent on remodeling of the extracellular matrix and adipose tissue angiogenesis. In fact, adipose tissue angiogenesis (extension of the vascular network) can be considered as the rate limiting step for adipose tissue expansion as vascularization is essential for oxygen supply, nutrient intake, waste removal, and establishes the crosstalk between cells and organs through hormonal and growth factor exchange (Rupnick et al., 2002) (Cao, 2007) (Nishimura et al., 2007). Developmental origins of the adipose organ in embryonic stages demonstrate that adipocytes arise from vascular networks, since extension of the vascular bed is followed by the appearance of lipid containing cells located around the capillaries (Hausman & Richardson, 2004) (Han et al., 2011). In the adult human and murine adipose tissue, resident mesenchymal stem cells give

14

rise to adipocyte progenitors and are tightly associated with the vascular endothelium (R. Gupta et al., 2012) (Tran et al., 2012) (Min et al., 2016). In periods of metabolic adaptation, these progenitors are able to differentiate into mature adipocytes and store lipid.

Our lab has developed a technique, named the adipose tissue angiogenesis assay, where we can grow the capillary network from adipose tissue fragments obtained from human and animal fat biopsies and recapitulate *in vitro* the expansion capacity and metabolic state of the adipose tissue sample (Rojas-Rodriguez et al., 2014). The assay consists on embedding small adipose tissue explants (fragments cut into 1mm) in Matrigel and culture them under pro-angiogenic conditions which promotes the sprouting of capillary networks and proliferation of associated adipocyte progenitors. Based on this technique, our lab has published high impact work that has demonstrated the therapeutic potential of adipose tissue progenitor cells in systemic metabolism and highlighted the mechanistic role of adipose tissue expandability in glucose metabolism. For example, implantation of differentiated adipose progenitor cells (primed adipose stem cells "PADS") in Matrigel into NOD-*scidIL2rγ^{null}* (NSG) mice decreases fasting glucose and enhances glucose disposal rate when compared to mice injected with vehicle only (Min et al., 2016). Furthermore, high fat diet fed NSG mice implanted with PADS exhibit improved glucose tolerance and reduced

liver steatosis compared with controls injected only with Matrigel (Min et al., 2016).

The effect on *in vivo* insulin sensitivity on adipose tissue can be recapitulated *in vitro* via the adipose tissue angiogenesis assay, as adipose tissue explants obtained from fat biopsies of *ob/ob* mice and human subjects treated with the insulin sensitizer rosiglitazone have increased capillary sprouting when compared to untreated *ob/ob* mice and subjects in placebo (Gealekman et al., 2008) (Gealekman et al., 2012). The assay was also performed in human adipose tissue explants obtained from subcutaneous and visceral fat biopsies. Interestingly, the capacity for adipose to grow via angiogenesis is depot specific and favors the angiogenic growth via adipose capillary sprouting of the subcutaneous over visceral fat tissue (Gealekman et al., 2011).

Pregnancy, as a weight gain state, requires the expansion of adipose stores. Since adipose tissue angiogenesis is one of the initial stages of adipose tissue growth, the measurement of this parameter in the gravid state can provide insight into the preferential location of fat deposition during gestation and its relationship with systemic insulin sensitivity.

Adipokines as markers of inflammation and insulin sensitivity in gestation

As an endocrine organ, adipose tissue secretes hormones and cytokines, termed adipokines, which serve as intercellular communication peptides and regulate energy homeostasis, systemic glucose homeostasis, lipid metabolism, inflammation, adipocyte proliferation and differentiation, angiogenesis, and many other physiological events (Ouchi, Parker, Lugus, & Walsh, 2011) (Sun, Kusminski, & Scherer, 2011) (Kusminski & Scherer, 2012). The role of adipokines in adipose tissue expansion has been mostly described by their inflammatory properties in obesity and type-2 diabetes. Hypertrophied adipocytes that are metabolically dysfunctional display chronic hypoxia and secrete elevated quantities of proinflammatory and reduced amounts of anti-inflammatory adipokines (Hosogai et al., 2007). Classically activated macrophages (M1, proinflammatory) organize as crown-like structures around hypoxic and hypertrophied adipocytes which can lead to adipocyte death. Conversely, adipocytes from lean individuals preferentially secrete anti-inflammatory adipokines and the majority of the residing macrophages are alternatively activated (M2, anti-inflammatory) (Ouchi et al., 2011) (Sethi & Vidal-Puig, 2007).

Pregnancy, by itself, is a state of altered inflammation. The adipose tissue and placenta are sources of adipokines with different inflammatory roles, however, the common goal is to create a state of mild inflammation and reduced insulin

17

sensitivity to support fetal development (D'Ippolito, Tersigni, Scambia, & Di Simone, 2012). The adipokines adiponectin, leptin, and TNFα encompass the majority of the research regarding glycemic status, adipose tissue function, and mild inflammation during gestation, hence are briefly introduced.

Adiponectin

Adiponectin is an anti-inflammatory adipokine which circulating levels decrease as pregnancy advances in both human and mice. Murine studies have shown that adiponectin beneficially lowers hepatic glucose production and lipid accumulation and stimulates fatty acid oxidation in skeletal muscle via signaling through the adiponectin receptor in different cell types (Combs, Berg, Obici, Scherer, & Rossetti, 2001) (Yamauchi et al., 2001). Clinical studies have investigated the association between adiponectin and GDM. A cross-sectional study reported that at the time of GDM diagnosis, plasma adiponectin was lower in subjects with GDM than normoglycemic, and there was a negative correlation between these values and the homeostatic model assessment for insulin resistance (HOMA-IR) (Altinova et al., 2007). A retrospective study investigated if first trimester serum adiponectin could predict the development of GDM in a high-risk population as determined by obese BMI, maternal age of >40 years, ethnicity, history of polycystic ovarian syndrome (PCOS), family history of type-2 diabetes, and a previous macrosomic baby. Unadjusted logistic regression

18

demonstrated that low circulating adiponectin in the first trimester is associated with a positive screen for GDM and this interaction remained constant after adjusting for BMI, ethnicity and a family history of diabetes (Corcoran et al., 2018). Regarding tissue specific contribution of adiponectin, studies have shown that adiponectin mRNA was downregulated in placenta (J. Chen et al., 2006) and subcutaneous (Ranheim et al., 2004) (Ott et al., 2018) and visceral (Ott et al., 2018) adipose tissue of GDM when compared to normoglycemic gravidas. However, one study did not find a significant difference between GDM and controls in placenta as well as subcutaneous adipose tissue and skeletal muscle (Lappas, Yee, Permezel, & Rice, 2005). Although tissue specific adiponectin studies report contradictory findings in adiponectin gene expression and glycemic state in gestation, it is important to consider that the total amount of serum adiponectin is a combination of the secreted adipokine from both the placenta and adipose tissue. Altogether, the evidence obtained from clinical studies suggests the association between low circulating adiponectin and the presence of GDM.

Leptin

The adipokine leptin is mainly produced by the adipose tissue and acts as an appetite suppressor and energy expenditure-inducing hormone via interaction with its receptor in the hypothalamus (Ahima et al., 1996) (Domingos et al.,

2011). In addition, leptin has been shown to suppress insulin secretion from pancreatic β-cells (Kieffer, Heller, Leech, Holz, & Habener, 1997). The adipose tissue-derived leptin is produced in proportion to fat mass storage (Patif et al., 1995). The concept of leptin resistance occurs when tissues become desensitized to leptin signaling resulting in hyperphagia and obesity (Myers, Cowley, & Münzberg, 2008). In women, non-human primates, and mice the plasma levels of leptin increase with gestation and rapidly fall after birth, highlighting placental contribution to leptin circulating levels (Hardie, Trayhurn, Abramovich, & Fowler, 1997) (NF Butte, Hopkinson, & Nicolson, 1997) (M. C. Henson et al., 1999) (M. Henson & Casatracane, 1998) (Pérez-Pérez et al., 2018).

The quantification of leptin in plasma and peripheral tissues has been studied in relation to glycemic status and BMI in gestation. At the time of cesarean section, circulating leptin was elevated in normoglycemic obese compared to normoglycemic non-obese gravidas and in GDM obese compared to GDM non-obese. Leptin gene expression was higher in visceral adipose tissue of both normoglycemic and GDM obese gravidas when compared to normoglycemic non-obese controls. No differences where observed regarding leptin expression in subcutaneous fat or placenta between cohorts (Tsiotra et al., 2018), highlighting the depot-specific effect of obesity on increased leptin expression.

20

Data from this report and others (Kirwan et al., 2002) suggests that leptin levels are related to the pre-pregnancy obese state rather than the effect of pregnancy on leptin levels. Another longitudinal study measured the levels of fasting plasma leptin at week 28 of gestation and 8 weeks after delivery in normal glucose tolerance, GDM, and type-1 diabetes women. Interestingly, circulating leptin was elevated only in GDM and the values for normal glucose and type-1 cohorts were not different. Besides plasma leptin, the marked differences between cohorts was postpartum BMI, waist-to-hip ratio, and plasma triglycerides which were all elevated in GDM when compared to normoglycemic and type-1 diabetes groups (Kautzky-Willer et al., 2001a). Although fat mass was not measured in this study, is possible that the hyperleptinemia observed in GDM is due to an excess of adipose tissue stores. Overall, studies available so far imply the role of maternal obesity in the elevated circulating levels of leptin in gestation, where regional differences of fat distribution may regulate leptin production and secretion.

Tumor necrosis factor α

The tumor necrosis factor alpha (TNFα) is a proinflammatory adipokine expressed by macrophages, monocytes, T-cells, fibroblasts, neutrophils, and adipocytes and has been attributed to disrupt insulin signaling in insulin-sensitive tissues as well as inhibiting insulin secretion from β-cells (Fasshauer et al., 2014). Plasma TNFα shows a trend for reduced values in early pregnancy

21

compared to pregravid but it increases in late gestation (Kirwan et al., 2002). An inverse association between insulin sensitivity (measured via hyperinsulinemic-euglycemic clamp) and plasma TNFα was observed in late pregnancy (Kirwan et al., 2002). In addition, plasma TNFα measured at 34-36 weeks of gestation showed that obese pregnant women with GDM have elevated plasma TNFα when compared to lean normoglycemic gravidas (Kirwan et al., 2002). At the time of GDM diagnosis, serum TNFα was elevated in subjects with GDM than normoglycemic, and there was a positive correlation between these values and pre-pregnancy BMI (Altinova et al., 2007).

In vitro studies of term placental and subcutaneous adipose tissue explants demonstrated that during hyperglycemic conditions, explants obtained from GDM women release more TNFα when compared to normoglycemic gravidas. Interestingly, there was no difference between groups in omental fat explants (Coughlan, Oliva, Georgiou, Permezel, & Rice, 2001). Another study done in basal conditions reported that there was no difference in secreted TNFα when measured in placental, subcutaneous fat, and skeletal muscle (pyramidalis) explants from normal glucose and GDM cohorts (Lappas, Permezel, & Rice, 2004). At the cellular level, TNFα impairs activation of insulin signaling and glucose uptake in mouse muscle cells (C2C12 myoblast cell line) (del Aguila, Claffey, & Kirwan, 1999) and in 3T3L1 adipocytes it reduces *GLUT4* expression

22

(Stephens, Lee, & Pilch, 1997) (Ruan, Hacohen, Golub, Parijs, & Lodish, 2002) and insulin-stimulated glucose uptake (Anusree, Sindhu, Preetha Rani, & Raghu, 2018). Therefore, is possible that the effect of TNFα on reduced insulin signaling is exacerbated in gestational diabetes, contributing to the peripheral tissue insulin resistance observed in gravid women with GDM.

The association of each adipokine with glycemia in pregnancy is dependent on the parameter and population measured, the gestational age during assessment, and the source of the specimen, as some circulating peptides correlate with the development of GDM, however the tissue-specific gene and protein expression results vary (Fasshauer et al., 2014). However, clinical studies and meta-analysis up to date agree that women with GDM have lower levels of circulating adiponectin and increased values of circulating leptin than normoglycemic gravidas at the time of sampling (Bao et al., 2015) (Fasshauer et al., 2014) (Francis et al., 2019) (Atègbo et al., 2006) (Retnakaran et al., 2004) (Soheilykhah, Mojibian, Rahimi-Saghand, Rashidi, & Hadinedoushan, 2011) (Kautzky-Willer et al., 2001b) (Doruk, Uğur, Oruç, Demirel, & Yildiz, 2014) indicating the role of adipose tissue in glycemic control during pregnancy.

Adaptations of insulin and insulin-like growth factor signaling mechanisms in the gravid state

Drivers of insulin resistance

Historically, placental secretion of "diabetogenic" hormones such as progesterone, cortisol, estrogen, human placental lactogen, and human placental growth factor have been attributed to the insulin resistance observed in gestation. Nevertheless, it does not explain why some women who developed GDM present impaired fasting glucose, impaired glucose tolerance, or develop type-2 diabetes 6-12 weeks after giving birth (Kitzmiller, Dang-Kilduff, & Taslimi, 2007) (Huopio et al., 2014). The insulin action in peripheral tissues must then explain the difference between normoglycemia and GDM development.

The molecular mechanisms of insulin resistance studied at the cellular-tissue level rather than by associations between molecules and glycemic state can deepen the understanding of the etiology of GDM. Unraveling the differences in insulin signaling from peripheral tissues of normoglycemic and GDM gravidas can serve as the basis for advancements in approaches to manage this condition.

24

Molecular mechanisms of insulin action

In normoglycemia, glucose uptake in adipose tissue and skeletal muscle due to insulin action initiates when insulin binds the insulin receptor (IR) at the cell membrane. A conformational change and autophosphorylation of the tyrosine kinase IR induce phosphorylation of the insulin receptor substrate (IRS-1), which leads to an interaction and subsequent activation of phosphoinositide 3-kinase (PI3K) producing phosphatidylinositol (3,4,5)-trisphosphate (PIP3). PIP3 activates and localizes protein kinases that initiate a series of phosphorylation events that result in the activation of protein kinase B (PKB or AKT). The substrate of AKT, AS160, is responsible for translocation of GLUT-4 to the plasma membrane. Glucose enters the cell through GLUT-4 and undergoes glycolysis. AKT signaling events also regulate cellular proliferation and growth as well as metabolic functions including lipid synthesis, gluconeogenesis, and glycogen synthesis (Boucher, Kleinridders, & Kahn, 2014) (Tokarz, MacDonald, & Klip, 2018).

In pregnancy, the insulin signaling events are altered to favor reduced insulin sensitivity, but these changes are more pronounced in GDM. These changes can occur by alterations in protein concentration or tyrosine/serine phosphorylation of the molecules involved in the insulin signaling pathway. Table 1.2 summarizes

25

the findings from cross sectional studies in pregnant women with respect to the

analysis of insulin signaling molecules in muscle and adipose tissue.

Signaling Molecule	Function in Signaling Pathway	Adipose Tissue (abdominal subcutaneous)[1,4]	Muscle (rectus abdominus)[2,5] (vastus lateralis)[3]
Insulin Receptor (IR)	Binding of insulin causes auto-phosphorylation of IR tyrosine residues. IR phosphorylates the tyrosine residues of IRS-1 leading to its activation.	No difference in expression between NP-OB, P-OB-NGT, and P-OB-GDM[1]	No difference in expression between NP-OB, P-OB-NGT, and P-OB-GDM[2]
Insulin Receptor Substrate-1 (IRS-1)	Recruits the p85α/p110 subunits of the phosphoinositide 3-kinase (PI3K).	Decreased in P-OB-GDM when compared to NP-OB and P-OB-NGT[1]	Expression and tyrosine phosphorylation are decreased in P-OB-NGT and even lower values in P-OB-GDM when compared to NP-OB[2] Expression decreased but serine phosphorylation increased in P-OB-GDM over P-OB-NGT[3]
p85α	Forms a heterodimer with p110 to activate PIK3. Increased amounts of p85α subunit can inhibit PI3K activation.	Increased in P-OB-GDM when compared to NP-OB and P-OB-NGT[1]	Increased in P-OB-NGT and even higher values in P-OB-GDM when compared to NP-OB[2]
Glucose-transporter 4 (GLUT4)	Upon activation, GLUT4 translocates to the cell membrane and facilitates diffusion of glucose inside the cell.	Reduced in P-NGT and even lower quantities in P-GDM when compared to NP[4]	No difference in expression between NP-LN, NP-OB, and P-OB-GDM[5]

Table 1. 2 Adipose tissue and muscle expression of proteins from insulin/IGF signaling pathway in pregnancy and GDM.

Non-pregnant (NP), pregnant (P), lean (LN), obese (OB), normoglycemic (NGT), gestational diabetes (GDM). Data from [1](Catalano et al., 2002), [2](Friedman et al., 1999), [3](Barbour et al., 2011), [4](Okuno et al., 1995), [5](Garvey, Maianu, Hancock, Golichowski, & Baron, 1992)

27

Insulin and IGFs share signaling properties

The insulin-like growth factor-1 (IGF-1) is a hormone with similar structure and signaling properties as insulin (46.2 homology score between insulin and IGF-1 preproteins). IGF-1 is regulated by nutrition and growth hormone and is produced and secreted by liver and other peripheral tissues where it has autocrine and paracrine actions (Lewitt, Dent, & Hall, 2014) (Klement & Fink, 2016). IGF-1 can mimic insulin by stimulating glucose and amino acid uptake and inhibition of gluconeogenesis (Clemmons, 2012). IGF-1 has mitogenic properties and is involved in adipose tissue growth and glucose metabolism (Hesse et al., 2018). Besides IGF-1, IGF-2 also shares sequence similarity to insulin. The *Igf-2* gene is maternally imprinted and the role of the gene product has been mostly described in fetal development (A. Smith, Choufani, Ferreira, & Weksberg, 2007) (White et al., 2017). Circulating IGF-2 increases with age and remains unchanged through adulthood, whereas IGF-1 levels decrease after puberty (Yu et al., 1999). Both IGF-1 and IGF-2 have been described to regulate cellular proliferation and differentiation as well as angiogenesis (Yang et al., 2018)(Harris, Crocker, Baker, Aplin, & Westwood, 2011) (Chao & D'Amore, 2008).

The IGF-1 receptor (IGF-1R) has high homology to the IR. The IGF-1 binds the IGF-1 receptor and with lower affinity to the IR. Both ligands can also bind a

28

hybrid of the IR/IGF-1R, however IGF-1 has higher affinity than insulin for this heteroreceptor (Taniguchi, Emanuelli, & Kahn, 2006). Additionally, IGF-2 can bind its receptor (IGF-2R) as well as the IGF-1R and the IR (Andersen, Nørgaard-Pedersen, Brandt, Pettersson, & Slaaby, 2017) (Spicer & Aad, 2007). Interaction with the IGF-2R results in IGF-2 degradation or mitogenic signaling (Harris et al., 2011). The intracellular signaling events are also shared, involving tyrosine phosphorylation and activation of the IRS. The different effects of each hormone *in vivo* is dependent on the developmental stage, the location where it is expressed, the quantity of each ligand as well as the amount of each receptor at the target cells, and the activation of the signaling events (Werner, Weinstein, & Bentov, 2008) (Siddle, 2011) (Boucher et al., 2014). Furthermore, dysregulation of insulin action and IGF events could occur before receptor binding in target tissues, decreased availability of the cellular receptor, or defects in intracellular signal transduction.

IGFs bioavailability is dependent on IGF-binding proteins

Stability of IGF is dependent on the binding of an IGF-binding protein (IGFBP) that can either inhibit or stimulate the growth promoting effects of the ligand (Murphy, 1998). Seven IGFBPs have been identified and their function is to sequester IGF to prevent cellular receptor binding (H. Kim, Rosenfeld, & Oh, 1997) (Infante & Rodríguez, 2018). IGF-IGFBP complex availability is tissue

29

specific, thus the binding preference between ligand and binding protein depends on the location of where these molecules are interacting (Oxvig, 2015) (Mohan & Baylink, 2002).

Amongst the described IGFBPs, studies in pregnant and non-pregnant cohorts showed circulating IGF-1, IGFBP1, and IGFBP3 are elevated in pregnancy compared to the non-pregnant state (Monaghan et al., 2004) (Anderlová et al., 2018). However, gravidas that develop GDM have higher values for IGF-2 and IGFBP3 and lower concentration of IGFBP4 when compared to normoglycemic gravidas. In addition, gestation increases the expression of *IGF1, IGFBP4, and IGFBP5* in subcutaneous adipose tissue (Resi et al., 2012) (Anderlová et al., 2018). Moreover, a longitudinal study across gestation reported the levels of serum IGFBP2 were downregulated whereas values of IGF-1 and IGFBP3 upregulated during early and mid-gestation in gravidas that developed in GDM (Zhu et al., 2016).

Proteolytic Cleavage of IGFBPs

IGF release from the IGF-IGFBP complex is dependent on proteolytic cleavage of the IGFBP (Figure 1.1). The IGFBPs proteases were first described in the serum of pregnant women (Bischof, 1989). One of these proteases, pregnancy-associated plasma protein-A (PAPP-A) is a placental secreted metalloprotease synthesized by syncytiotrophoblasts (Tornehave, Chemnitz, Teisner, Folkersen,

30

& Westergaard, 1984). However, reports have demonstrated its gene expression in murine adipose tissue (Hjortebjerg et al., 2018) and protein secretion and proteolytic activity is observed in subcutaneous and visceral human adipose tissue explants (Gude et al., 2016) indicating a tissue specific function for this protease (Oxvig, 2015) (Hjortebjerg et al., 2018). Furthermore, mRNA and secreted PAPP-A has been detected in human preadipocytes from omentum, mesenteric and subcutaneous fat depot (Davidge-Pitts, Escande, & Conover, 2014). The major known function of PAPP-A is to increase IGF bioavailability in the pericellular environment through cleavage of IGFBP2, IGFBP4, and IGFBP5, highlighting the role of this protease in the insulin/IGF signaling pathway (Conover, Durham, Zapf, Masiarz, & Kiefer, 1995) (Laursen et al., 2001) (Monget et al., 2003). In mice, ablation of *Papp-A* results in dwarf animals with reduced female fertility due to decreased ovulated oocytes and shorter ovulation periods but extended longevity (~30% longer than wild-type littermates) (Nyegaard et al., 2010) (Conover & Bale, 2007).

31
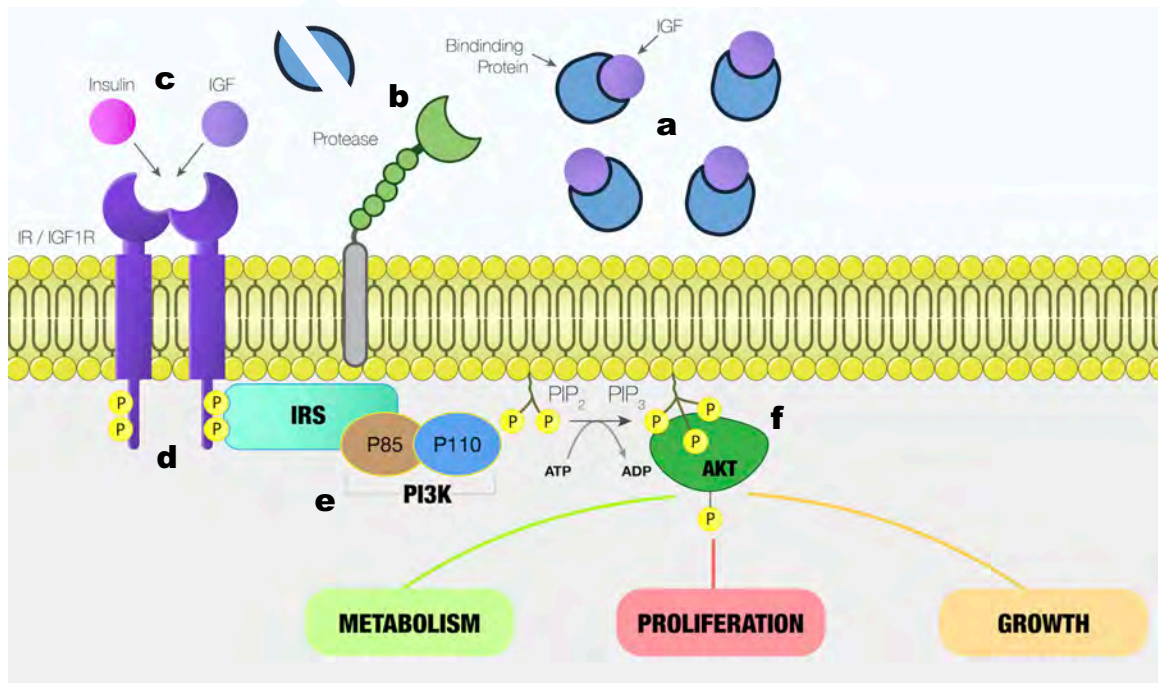
Figure 1. 1 Insulin and IGF share signaling pathways.

(a) Insulin-like growth factors (IGF) are sequestered by IGF binding proteins (IGFBP) in the pericellular environment, creating a local bioreservoir of IGFs. **(b)** IGFBP protease localizes in close proximity to the cellular insulin/IGF1 receptor (IR/IGF1R). Cleavage of IGFBPs by protease releases IGFs. **(c)** Free IGF or insulin bind the IR/IGF1R. **(d)** Upon binding, a conformational change in the IR/IGF1R causes autophosphorylation of tyrosine residues, which activates the tyrosine kinase activity that leads to increased tyrosine phosphorylation of cellular substrates. The IRS-1 and other docking proteins bind to the phosphorylated intracellular substrates, thereby transmitting the signal downstream. **(e)** Insulin stimulates the binding and activation of phosphatidylinositol-3 (PI-3)-kinase, to IRS-1. PI 3-kinase is composed of an 85 kD regulatory subunit (p85) that is associated with the phosphorylated IRS-1 and activates the catalytic 110 kD subunit. The formation of $PI(3,4,5)P_3$ is necessary for insulin action on glucose transport. The stimulation of PI 3-kinase activity is linked to AKT. **(f)** AKT phosphorylates downstream substrates that are involved in the regulation of diverse cellular functions including metabolism, proliferation, and growth. Adapted from (Taniguchi et al., 2006)

32

Clinical Relevance of PAPP-A

Currently, PAPP-A is part of the first trimester maternal screen for fetal chromosomal abnormalities, as low levels of circulating PAPP-A early in gestation are associated with trisomy 13 (Patau's syndrome), 18 (Edward's syndrome) and 21 (Down's syndrome) (Snijders, Spencer, Souter, Nicolaides, & Tul, 2003) (Wapner et al., 2003) (Driscoll & Gross, 2008) (Leguy et al., 2014). The marked presence of PAPP-A and target IGFBPs in maternal circulation and adipose tissue presents an opportunity to study this interaction in relation to adipose tissue expandability and glucose metabolism in gestation.

Animal models of gestational diabetes mellitus

Advances in the understanding of the molecular mechanisms driving the development of a disease are often dependent on the use of animal models that replicate the pathologic conditions as is observed in humans. The difficulty when developing animal models for gestational diabetes arise due to the onset of pathological hyperglycemia and insulin resistance, which needs to be present exclusively during gestation. Therefore, any established models for type-2 diabetes used in pregnant dams do not accurately describe GDM. An ideal animal study would present normoglycemic, insulin sensitive animals in the non-pregnant state and GDM pathophysiology exclusively in gestation.

Current animal models include induction of GDM in mice, rats, rabbits, dogs, sheep, and swine. Different approaches have been used to induce diabetes in pregnancy. Surgical removal of pancreatic mass is usually done before puberty and has up to 20% mortality rate (Jawerbaum & White, 2010). However, failed insulin secretion is observed in virgin females resembling to what is observed in type-1 diabetes. Chemical induction with streptozotocin or alloxan which are toxic to pancreatic β-cells, cause hyperglycemia, however the timing of treatment (before or during gestation) and the dose used results in either mild or severe hyperglycemia depending on the animal and strain (Kiss et al., 2009) (Singh et al., 2011) (Chandna et al., 2015) (Trejo-González, Chirino-Galindo, & Palomar-

34

Morales, 2015) (Y. Chen et al., 2017). High fat and high sucrose diets have also been reported to induce hyperglycemia in gestation although these models do not recapitulate the genetic variants of GDM and are more relevant for the effect of maternal obesity (Moore et al., 2010) (Coate et al., 2013) (Pereira et al., 2015) (Hosni, Abdel-Moneim, Abdel-Reheim, Mohamed, & Helmy, 2017).

Genetic models have also been employed, and the most representative in adipose tissue physiology and impaired gestational glucose metabolism are *db/+* (heterozygous for mutation in leptin receptor) and *Adipo$^{-/-}$* (knockout of adiponectin). The *db/+* females are normoglycemic and insulin sensitive when virgins and develop glucose intolerance, insulin resistance, and obesity when pregnant (Ishizuka et al., 1999). In addition, these mice give birth to macrosomic pups a feature of neonates born from GDM mothers (Ishizuka et al., 1999) and had reduced skeletal muscle insulin-stimulated tyrosine phosphorylation of IRS-1 receptor (Yamashita et al., 2001). However, experiments carried out with the *db/+* mice had conflicting results, as some reported glucose intolerance and others normoglycemia in gestation where the variables observed included the kind of chow diet and strain of controls used (Plows et al., 2017). The *Adipo$^{-/-}$* pregnant dams are glucose intolerant, have higher plasma free fatty acids and triglycerides, and had macrosomic pups compared to wild type pregnant controls. Although these animals are not insulin resistant, they have reduced β-cell islets

35

size. The caveat of this animal model is the absence of wild type and *Adipo^-/-^*

virgin controls ran in parallel with the pregnant dams (Qiao et al., 2017).

Dissecting the role of key molecules and alterations in signaling pathways during

gestation that result in failed β-cell compensation, peripheral tissue insulin

resistance, or the combination of these events is the appropriate approach to

discover the cause and possible treatments for gestational diabetes.

Scope of the thesis

Pregnancy as a weight gain state presents an ideal setting to study the physiology of adipose tissue expansion and its association with systemic glucose metabolism. Defects in adequate deposition of lipids has been reported in various animal models and patients with type-2 diabetes. Numerous prospective studies clearly indicate the increased morbidity for type-2 diabetes in pregnant women with gestational diabetes (GDM) in comparison with normoglycemic (NGT) gravidas. Therefore, there is an urgent need for understanding the biology of adipose tissue expansion in gestation and its association with glycemic control. The purpose of the work presented in this thesis is to characterize the adaptations of adipose tissue growth in late gestation and investigate how changes in adipose tissue expansion are associated with maternal glucose metabolism. The thesis aims are presented in chapters.

In Chapter 2, I characterized the late-pregnancy changes in abdominal subcutaneous and omental adipose tissue expandability of pregnant women with normoglycemia and gestational diabetes. The results demonstrated that in comparison with NGT gravid subjects, pregnant women with GDM have impaired adipose tissue growth characterized by enlarged hypertrophic adipocytes in omental fat and reduced vascularization in both adipose depots. In addition, adipose tissue whole transcriptomic analysis of NGT non-pregnant and pregnant

37

individuals revealed the upregulated expression of insulin-like growth factor binding protein 5 (*IGFBP5*) in gestation. The levels of *IGFBP5* were markedly decreased in GDM gravidas. The results from Chapter 2 in conjunction with the work published by others highlights the maladaptation of adipose tissue growth in gravidas with gestational diabetes.

In order to understand the pathology of impaired adipose tissue expansion in GDM it is necessary to acquire new knowledge regarding the biology of fat expandability in pregnancy on a normoglycemic state. The results presented in Chapter 3 consists of studies done in humans and mice exploring a potential signaling mechanism driving adipose tissue expansion in pregnancy and protecting against gestational diabetes. First, I analyzed the changes in subcutaneous adipose tissue expansion between normoglycemic non-pregnant and pregnant subjects in late gestation. The results showed that adipose tissue in pregnancy is characterized by adipocyte hypertrophy and hyperplasia and is accompanied with structural changes of the microvasculature. Re-analysis of the transcriptomic database presented in Chapter 2 by hierarchical clustering and differential expression confirmed that the gene *IGFBP5* was the most upregulated gene due to gestation in both subcutaneous and omental depots.

Next, I explored if the IGFBP5/IGF axis in the adipose tissue was associated with maternal glucose metabolism. It is known that the pregnancy associated plasma protein-A (PAPP-A) cleaves IGFBP5. PAPP-A concentration in the serum increases as pregnancy advances. In order to investigate if circulating PAPP-A in the first trimester of pregnancy is associated with maternal glycemic state we performed a retrospective study. Results showed that low levels of PAPP-A in weeks 10-14 of pregnancy are associated with high risk of developing abnormal glucose tolerance and GDM later in gestation, suggesting the potential of PAPP-A as an early biomarker of gestational diabetes. The findings from the retrospective study were possible by the collaboration with the OB/GYN department and IT-Data Sciences Technology group.

In order to elucidate the mechanistic role of PAPP-A with respect to adipose tissue growth, I leveraged a new *in vitro* technique developed by our lab that measures adipose tissue expandability. I was interested in understanding if the presence of PAPP-A would promote the expandability of adipose tissue. I found that pregnancy enhances adipose tissue growth and that the supplementation of recombinant human PAPP-A stimulated the expansion capacity of adipose tissue from pregnant women. This suggested that PAPP-A was involved in the adaptations of adipose tissue expansion during gestation.

Last, I explored if *Papp-a* knockout mice represent an animal model of impaired adipose tissue adaptations as presented in human gestational diabetes. The mice studies were done with cohorts of non-pregnant (NP) and pregnant (P) wild-type (WT) and *Papp-a* knockout (KO) dams. Analysis of adipose tissue architecture demonstrated that the changes related to adipocyte size and number distribution in normal WT gestation where absent in the KO. Expression of *Igfbp2*, which is also cleaved by PAPP-A, was upregulated by gestation but no differences where observed between genotypes. Metabolic phenotyping experiments showed the presence of insulin resistance and fatty liver only in the PKO, highlighting the similarity of the PKO with the pathology observed in gestational diabetes.

The results from cross-sectional and retrospective studies in addition to the animal experiments presented in my thesis feature molecules from the IGF signaling pathway, particularly IGFBP5 and PAPP-A as having pivotal roles in the adaptation of adipose tissue expandability in gestation and in maternal glucose metabolism. Besides my research in gestational diabetes and adipose tissue physiology, I collaborated in the design, conducted experiments, and analyzed data for other projects studying adipose tissue expandability *in vitro*. The published technique developed for this approach is presented in the Appendix section.

40

CHAPTER II: Human adipose tissue expansion in pregnancy is impaired in gestational diabetes mellitus

Abstract

During pregnancy, adipose tissue (AT) must expand to support the growing fetus and the future nutritional needs of the offspring. Limited expandability of AT is associated with insulin resistance, attributed to ectopic lipid deposition. This study aimed to investigate human AT expandability during pregnancy and its role in the pathogenesis of gestational diabetes mellitus (GDM). This cross-sectional study of omental (OM) and subcutaneous (SQ) AT collected at Caesarean delivery included fifteen pregnant women with normal glucose tolerance (NGT), six with GDM, and three with type 2 diabetes mellitus. Adipocyte size, capillary density, collagen content and capillary growth were measured. Affymetrix arrays and real-time PCR studies of gene expression were performed. Mean OM adipocyte size was greater in women with GDM than in those with NGT (p=0.004). Mean OM and SQ capillary density were lower in GDM compared with NGT (p=0.015). Capillary growth did not differ significantly between groups. The most differentially expressed AT transcript when comparing non-pregnant and pregnant women corresponded to the IGF binding protein (IGFBP)-5, the

41

expression levels of which was found by subsequent quantitative real-time PCR to be lower in women with GDM vs women with NGT (p< 0.0001). The relative OM adipocyte hypertrophy and decreased OM and SQ capillary density are consistent with impaired AT expandability in GDM. The induction of adipose tissue *IGFBP5* in pregnancy and its decrease in GDM point to the importance of the IGF-1 signaling pathway in AT expansion in pregnancy and GDM susceptibility.

Introduction

Gestational diabetes mellitus (GDM) affects 240,000 pregnancies in the USA each year, a number expected to increase to ~720,000 with changes in diagnostic criteria and increased incidence (Sacks et al., 2012) (Getahun, Nath, Ananth, Chavez, & Smulian, 2008) (Albrecht et al., 2010). GDM has been associated with intergenerational effects on risk of obesity, the metabolic syndrome and cardio-metabolic disorders (Moore Simas et al., 2010) (Metzger, 2007) (Hillier et al., 2007)(Malcolm, 2012). Of women with a history of GDM, 50% develop type 2 diabetes within 5 years (Kjos et al., 1995), and up to one-third of women with type 2 diabetes have a history of GDM (Cheung & Byth, 2003). Notwithstanding the considerable public health relevance of this disorder, its etiology remains unclear.

Appropriate expandability of adipose tissue (AT) is necessary for preventing ectopic deposition of lipids and their metabolites in tissues such as muscle, liver and pancreas, with consequent development of insulin resistance (Gray & Vidal-Puig, 2007) (Virtue & Vidal-Puig, 2010) (D. Gupta, Krueger, & Lastra, 2012) (Summers, 2006). The need for expandability is seen in mouse models in which increased AT mass results in metabolic improvement (JY Kim et al., 2007), and in epidemiological studies linking increased subcutaneous (SQ) AT with protection from type 2 diabetes risk (McLaughlin et al., 2011). Notably, while SQ

43

AT expansion is associated with diminished risk, expansion of visceral AT is associated with increased risk of metabolic disease (McLaughlin et al., 2011). This dichotomy is attributed to the propensity of visceral AT to undergo inflammation (Tchernof & Després, 2013), associated with insufficient SQ AT expandability (Alligier et al., 2013). During pregnancy, AT must rapidly expand to support the needs of the fetus and the future needs of the offspring through lactation (Herrera, 2000) (Ryan, Sullivan, & Skyler, 1985). Thus, inherent limitations in the ability of AT to expand may be unmasked during pregnancy and manifest as GDM and future susceptibility to type 2 diabetes.

It was thought that GDM arises from placental hormones that induce insulin resistance, coupled with insufficient insulin secretion. Numerous placental hormones can affect insulin sensitivity (Catalano, 2014). However, an association between these and insulin sensitivity in late pregnancy, and with GDM, has not been consistently discerned (Kirwan et al., 2002). A major factor produced by placenta is pregnancy-associated plasma protein-A (PAPP-A), a protease that can hydrolyze IGF binding proteins (IGFBPs) 4 and 5 (Laursen et al., 2001). IGFBPs bind IGF-1 and/or IGF-2 and control their bioavailability within tissues (Beattie, Allan, Lochrie, & Flint, 2006). The high affinity of IGFBPs for IGFs precludes their binding to the IGF-1 receptor (Beattie et al., 2006) (Garten, Schuster, & Kiess, 2012) . Thus, through the production of PAPP-A, the placenta

44

can exert a major effect on the growth of tissues through hydrolysis of IGFBPs and release of bound IGF-1. Obesity can affect the placenta, resulting in structural and biochemical alterations (Huang et al., 2014) (Jones & Fox, 1976) (Mele, Muralimanoharan, Maloyan, & Myatt, 2014) (O'Tierney-Ginn, Presley, Myers, & Catalano, 2015), with potential consequent maternal AT growth.

To explore the role of AT expandability in the etiology of GDM we conducted a cross-sectional analysis of AT from pregnant women undergoing elective Caesarean deliveries. Our results are consistent with the hypothesis that AT expandability is decreased in individuals with GDM. Moreover, global expression analyses reveal that *IGFBP5* is highly induced in AT during pregnancy and is decreased in GDM, suggesting a mechanism for placenta–AT communication that may be impaired in GDM.

Methods

Study settings and participants

All pregnant women with singleton gestations presenting to UMass Memorial Health Care (UMMHC) between March 2013 and June 2014 for scheduled Caesarean delivery were considered for enrolment. The Institutional Review Board of the University of Massachusetts Medical School (UMMS) approved the study, and all participants provided informed consent. Exclusion criteria were as follows: (1) pre-gestational type 1 diabetes; (2) underweight pre-pregnancy body-mass index (BMI) (<18.5 kg/m2); (3) multiple gestations; (4) reported use of substances, including alcohol and/or illicit drugs and replacement or maintenance products, in pregnancy; (5) HIV; (6) hepatitis; (7) age <18 years; (8) autoimmune disease and/or chronic steroid use; (9) prenatal care initiation after 13 completed weeks gestational age and (10) plans to move out of the area within the study period.

Diabetes status

Type 2 diabetes was diagnosed based on patient report of medical history and confirmatory review of medical records. Individuals were considered to have GDM if they did not have pre-gestational type 1 or type 2 diabetes and either met American Diabetes Association criteria (a value of ≥7.7 mmol/L (140 mg/dl) 1h

46

after a 50g dextrose load (Thermoscientific, Middletown, VA, USA) screening test followed by two or more abnormal values in the 100g 3h glucose tolerance test) at routine screening between 24 and 28 weeks of gestation, or had a value >10 mmol/l (180 mg/dl) on the 1h screening test (Landy, Gómez-Marín, & O'Sullivan, 1996) (Atilano, Lee-Parritz, Lieberman, Cohen, & Barbieri, 1999).

Covariates and other relevant data collection

Clinical and anthropometric data were collected at enrollment. Pre-pregnancy BMI was calculated as pre-pregnancy weight (kg)/height^2 (m^2). Post-pregnancy BMI was calculated from the last prenatal weight record minus the weight of the baby. Blood glucose was measured 1h after ingestion of a 50g glucose load, a test routinely performed for GDM screening in individuals without pre-gestational type 2 diabetes.

Non-pregnant individuals

Cohorts for Affymetrix arrays and gene expression by real time PCR were from non-diabetic individuals undergoing bariatric surgery, as previously described (Gealekman et al., 2011) (Table 2.2). Consent for collection of additional samples of AT was obtained from non-pregnant individuals undergoing panniculectomy surgery who had no history of type 2 diabetes.

47

Adipose tissue collection

Biological specimens were collected at the time of surgical delivery. After delivery of the baby, two segments (1cm × 1cm) of omental (OM) tissue from the midline inferior periphery were collected. After the rectus fascia was re-approximated, prior to skin closure, two samples (1cm × 1cm) of SQ AT were obtained from within the surgical incision usually placed approximately 2cm above the pubic bone (Pfannenstiel incision). In the case of repeat Caesarean deliveries, subcutaneous AT biopsies were taken from deep within the incision to decrease scar tissue sampling.

Analysis of adipocyte size and collagen staining

AT samples were fixed in 4% formaldehyde and embedded in paraffin. Tissue sections (8μm) were mounted on Superfrost Plus microscope slides (Fisher Scientific, Pittsburgh, PA, USA), and stained with hematoxylin and eosin (H&E). Investigators acquiring the images were blinded to the origin of the sample. Adipocyte size was determined using an automated procedure based on the open software platform Fiji (Schindelin et al., 2012) (Figure 2.1) . Collagen was detected using picrosirius red staining. For quantification, images were imported into Fiji, and converted into 8-bit greyscale images. After background subtraction, total intensity was recorded.

48

Analysis of capillary density

Fragments of AT were fixed in 4% formaldehyde, washed and stained with Rhodamine-Lectin UEA-1 (Vector Labs, Burlingame, CA, USA) for 1h at room temperature and then mounted between 1.5 mm coverslips sealed with Pro-Long Gold Antifade Reagent (Life Technologies, Grand Island, NY, USA). A Zeiss (Peabody, MA, USA) Axiovert 100 inverted microscope with a ×10 objective and AxioCam HRm camera was used to acquire nine Z-plane image stacks at 10µm intervals. The individual collecting the images was unaware of the group they corresponded to. Quantification of capillary density was determined after background subtraction and projection of the Z-stack maximal intensity (Figure 2.2).

AT capillary growth assay

AT biopsies were cut into small (1mm^3) pieces and embedded in individual wells of a 96-multiwell plate as described (Rojas-Rodriguez et al., 2014). After 11 days of culture in EBM-2 medium supplemented with EGM-2 MV (BulletKit CC-3202; Lonza, Allendale, NJ, USA), images were acquired using a Zeiss Axio Observer Z1 equipped with an automated stage and a Clara High Resolution CCD Camera (Andor, Concord, MA, USA). Images were taken under ×2.5 magnification as a stack composed of five Z planes at 150µm intervals and as a canvas of four quadrants per well and then combined into a single three-dimensional image.

49

Subsequent image processing and quantification of capillary growth was determined after background subtraction and projection of the Z-stack maximal intensity (Figure 2.3).

Affymetrix arrays

Total RNA was isolated using TRIzol (Life Technologies). Affymetrix (Santa Clara, CA, USA) protocols were followed for the preparation of cRNA, which was hybridized to HG-U133v2 Chips. Raw expression data collected from an Affymetrix HP GeneArrayScanner was normalised across all data sets using the RMA algorithm. Probes in which any condition resulted in raw expression values above 1,000 were included in the heat map shown in Figure 2.9a.

Quantitative real-time PCR

Total RNA was extracted from AT using the RNeasy Lipid Tissue Mini Kit (Qiagen, Valencia, CA, USA). One microgram of total RNA was reverse-transcribed using iScript cDNA synthesis kit (Bio-Rad, Hercules, CA, USA). cDNA was used as template for real-time PCR using the iQ SYBR Green Supermix kit (Bio-Rad) and the CFX96 Real-Time System (Bio-Rad). Human ribosomal protein L4 (*RPL4*) was used for normalization. To reflect the abundance of the different *IGFBPs* and *IGF-1* relative to each other and between

50

groups, all values were normalized to the content of the lowest expressed transcript, which was *IGFBP1* in the non-pregnant group.

Statistical analysis

Clinical study data were collected and managed using REDCap (Research Electronic Data Capture). Stata/MP v.13.1 or GraphPad Prism v.6.0 were used for analysis as indicated. Multiple measures for each individual were acquired for each variable investigated. For adipocyte size data, between five and ten sections per each individual were used to acquire between 38 and 117 images. For capillary density data three three-dimensional image stacks were acquired from three independent sections per each individual. For capillary growth data, between seven and 58 observations were made for each individual. For picrosirius red staining, three sections per individual were used to acquire 15 images. Each individual's data were collapsed to the mean, which was then used for group analysis. A sensitivity analysis was performed with both the mean and median value for each individual. Sensitivity analysis results were similar to the mean; therefore, we present only the mean results. To calculate the maximum adipocyte size, the single largest adipocyte in each field was recorded, and the mean value calculated for each individual. Categorical variables were described using frequency and percentage with Fisher's exact test used to compare groups. Group comparisons for adipocyte size, capillary density and

51

angiogenesis data were made using the Wilcoxon rank sum test (Mann–Whitney test in Prism 6.0). Within-subject differences between OM and SQ tissue were determined using the Wilcoxon signed-rank test. Histograms of adipocyte size distributions for each patient were generated using the same bin sizes, and groups of histograms were compared using the Wilcoxon test for histograms (Prism 6.0). Statistical analysis of difference between groups in experiments involving real-time PCR was done using two-way ANOVA with the Holms–Sidak correction for multiple comparisons.
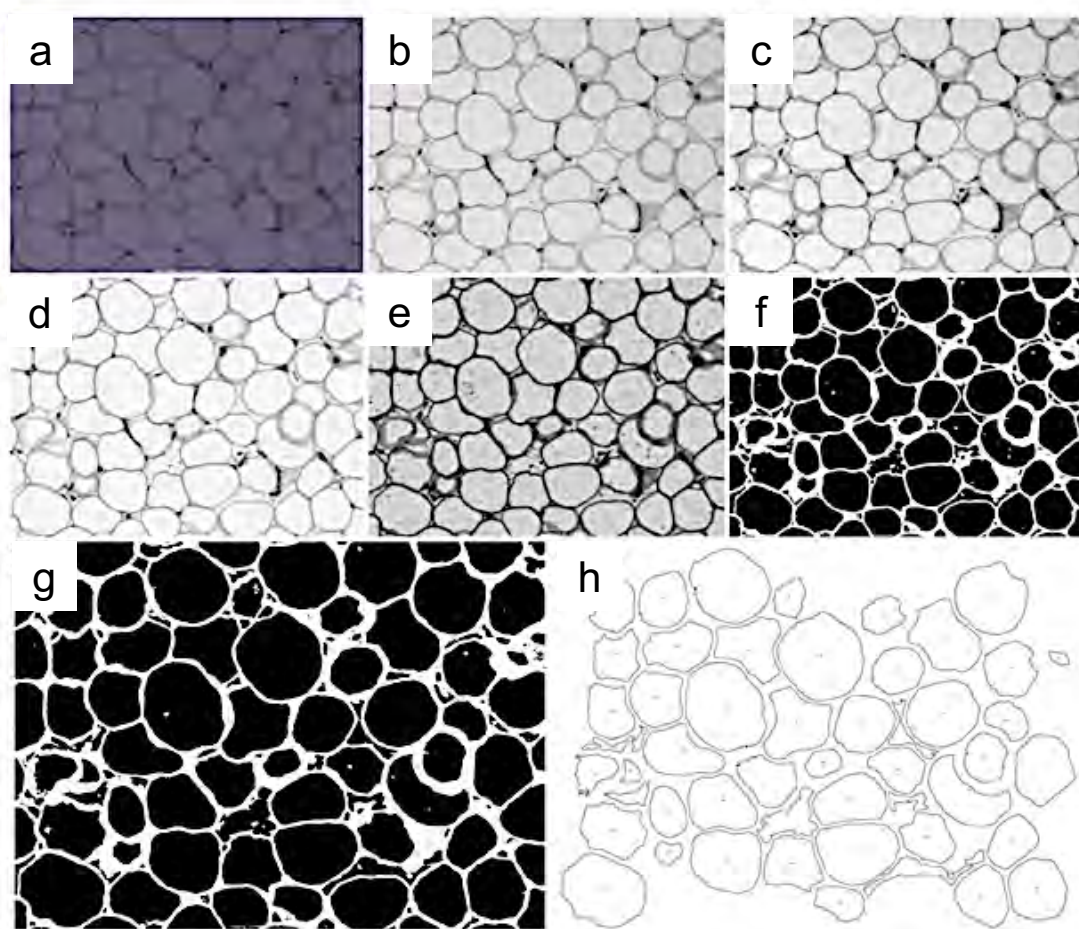
Figure 2. 1 Image processing and quantification of adipocyte size.

(a) Image of AT section stained with hematoxylin and eosin (H&E) (x10 magnification). **(b)** Image is imported to Fiji software and converted to 8-bit grayscale image. **(c)** Enhancement of image contrast (Process/Enhance Contrast/ Saturated pixels: 0.35%; normalize). **(d)** Background subtraction (Process/Subtract Background/Rolling Ball; radius=50.0pixels; Light background; Sliding paraboloid). **(e)** Enhancement of image contrast (Process/Enhance Contrast/ Saturated pixels: 10%; Normalize). **(f)** Binarized image (Image/Adjust/ Threshold/Huang; Dark background; Apply). **(g)** Processing on the binary image fills in small holes (Process/Binary/Fill Holes) **(h)** Resulting image showing the outlines of the counted objects (Analyze/Analyze Particles, Size (pixel²=1200-Infinity; Circularity=0.10-1.00; Show=Outlines; Display results; Exclude on edges). Note the reference numbers for each counted adipocyte, which is associated with the corresponding area in the results sheet.
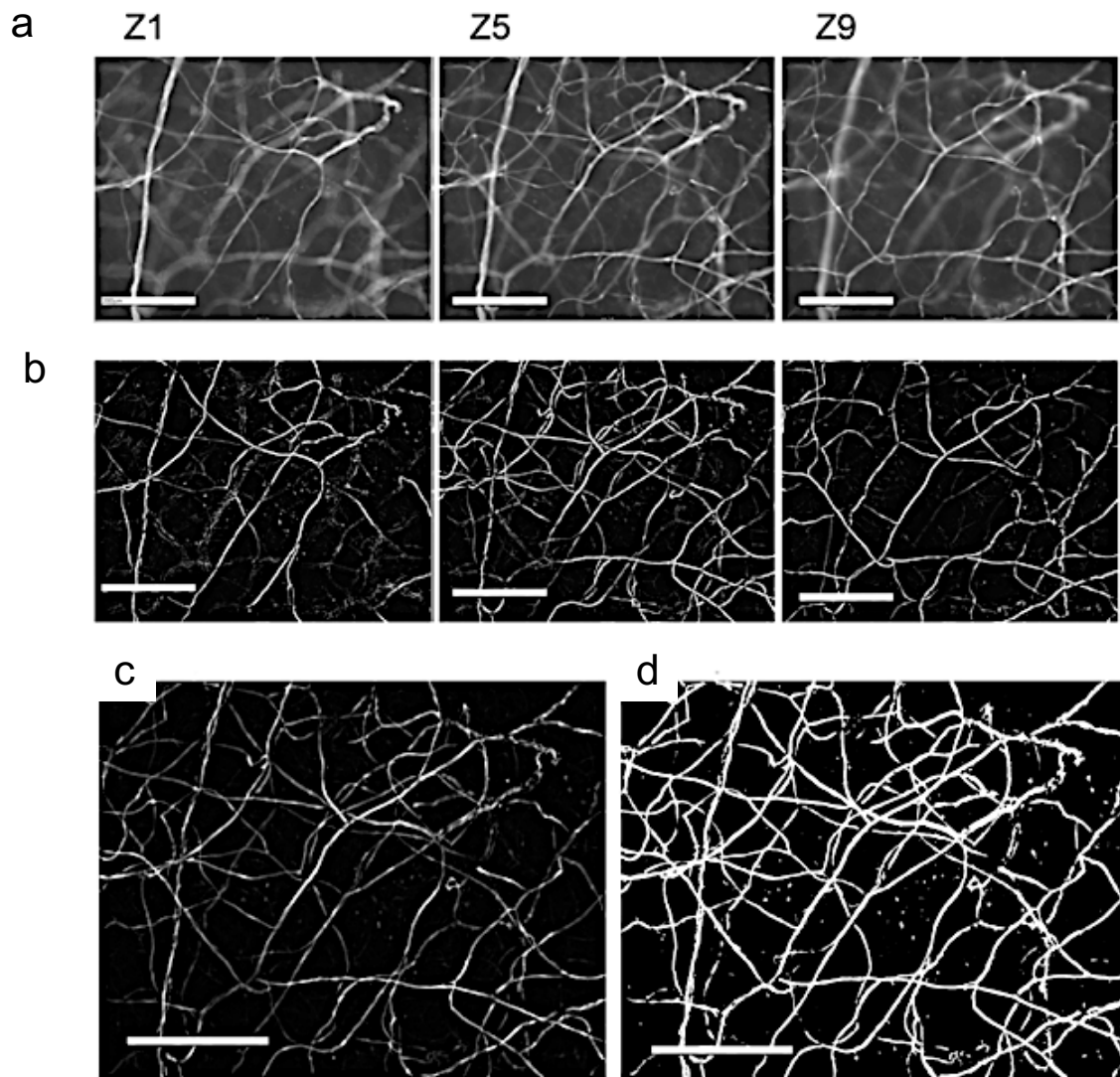
Figure 2. 2 Image processing and quantification of capillary density from whole mount adipose tissue.

(a) Selected Z-planes illustrating raw images of AT samples stained with lectin (x10 magnification). **(b)** Image stack is imported into Fiji software and the background is subtracted (Process/Subtract Background/Rolling Ball radius=5.0pixels). **(c)** A maximal intensity projection of the Z-stack is generated (Image/Stacks/Z Project/Max Intensity). **(d)** Greyscale image is converted into a binary image (Process/Binary/Make Binary/ Method:Default, Background: Dark). The number of white pixels in the image are recorded (Plugins/Feature Extraction/Feature J/Feature J Statistics).

54
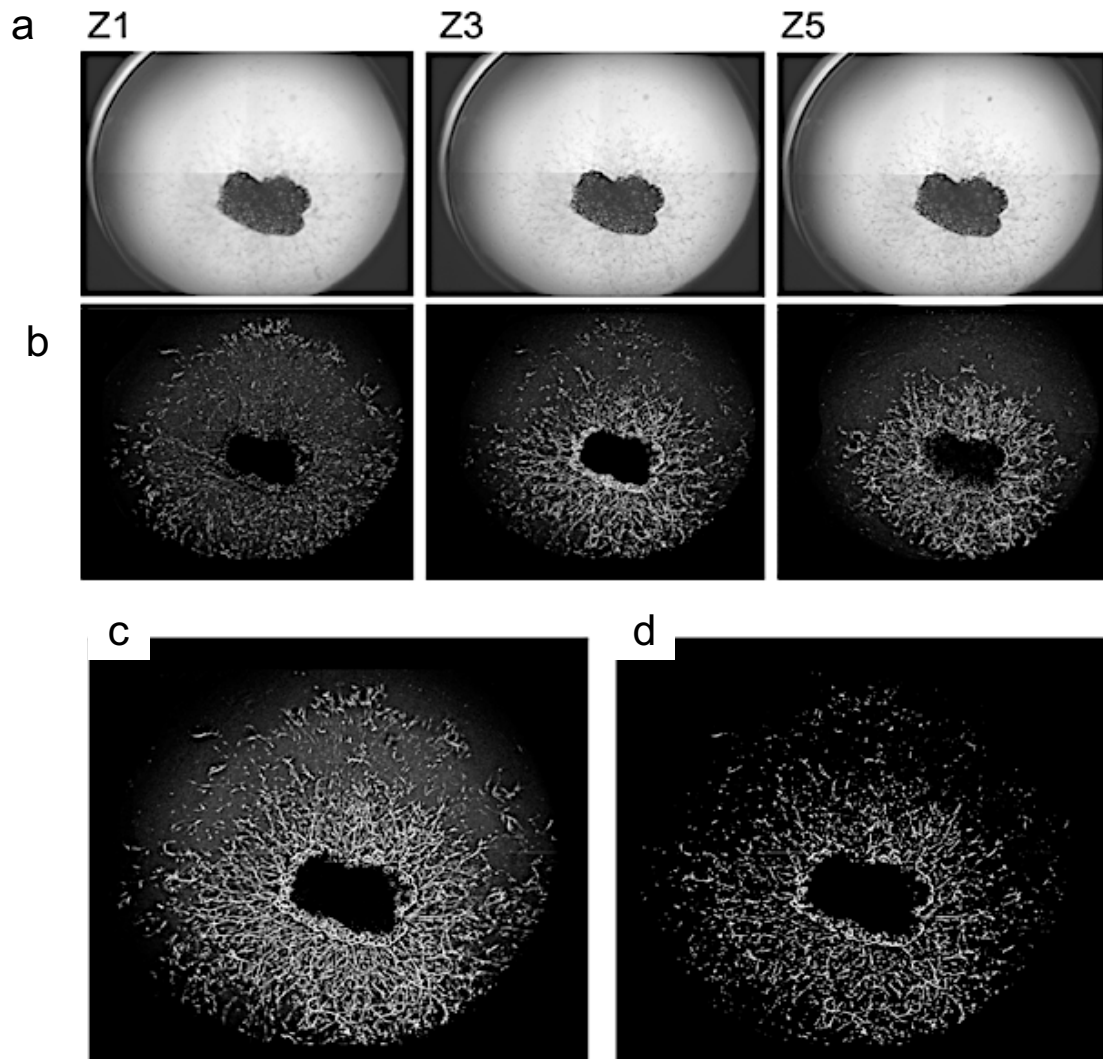
Figure 2. 3 Image processing and quantification of capillary growth from adipose tissue explants.

(a) AT explant imaged under 2.5 magnification as a stack composed of 5 z planes at 150μm intervals. **(b)** Same Z-planes after background is subtracted from the stack (Process/Subtract Background/Rolling Ball radius=5.0pixels). **(c)** Maximal intensity projection of the Z-stack (Image/Stacks/Z Project/Max Intensity). **(d)** Binarized image (Process/Binary/Make Binary/Method:Default; Background: Dark). The resulting numbers of pixels are recorded for each image (Plugins/Feature Extraction/FeatureJ/ FeatureJ Statistics).

55

Results

Patient characteristics

Relevant characteristics of the patients used for adipocyte size, capillary density, fibrosis and capillary growth assays are summarized in Table 2.1. Because the number of individuals in the type 2 diabetes category was small, comparisons were made only between the NGT and GDM groups. A trend for higher pre-pregnancy and post-delivery BMI in individuals with GDM was noted but the difference was not statistically significant. While there was a statistically significant difference in age between the groups, none of the observed variables correlated with this variable. Nevertheless, the small sample size is a limitation of this study.

www.manaraa.com

Characteristic	NGT (n=15)	GDM (n=6)	Type 2 diabetes (n=3)	p value (NGT vs GDM)
BMI pre-pregnancy (kg/m^2)	27.3 (6.2)	32.2 (6.2)	34.0 (6.6)	0.0895
BMI at term (kg/m^2)	30.6 (5.8)	33.8 (5.3)	37.4 (5.9)	0.241
Age (years)	29.7 (4.1)	35.3 (4.6)	32.3 (5.5)	0.0119
GWG (kg)	12.65 (3.9)	9.4 (6.1)	11.0 (4.4)	0.1531
GWG-baby (kg)	9.1 (3.8)	5.8 (5.9)	7.9 (4.4)	0.1292
Baby weight (kg)	3.53 (0.47)	3.68 (0.438)	3.07 (0.166)	0.7826
Serum glucose (mmol/l)[a]	7.13 (2.29)	9.36 (2.78)	N/A	0.0003

Table 2. 1 Subject characteristics of pregnant cohorts.

Data are presented as mean (SD). [a]Serum glucose measured at time of GDM screening. GWG, gestational weight gain; GWG−baby, gestational weight gain immediately after delivery of baby.

57

Parameter	Value
n	11
Age (years)	41 (32-54)
BMI at term (kg/m^2)	45.4 (39-55)
Fasting serum glucose (mg/dl)	92 (75-128)
Fasting serum insulin (mIU/ml)	9.1 (3-14)
HOMA-IR	1.4 (0.4-1.9)

Table 2. 2 Patient characteristics of non-pregnant subjects included in Affymetrix analysis.

Values are means, with range for each parameter shown in parenthesis. Data extracted from previously published parameters as described (Gealekman et al., 2011).

Adipocyte Size

Adipocyte size was quantified (Figure 2.4). The mean cell size in OM AT was 4,163 μm^2 (SD 1,380μm^2; n=13) in individuals with NGT, 7,482 μm^2 (SD 2,980μm^2; n=5) in those with GDM and 6,849 μm^2 (SD 1,060 μm^2; n=3) in those with type 2 diabetes, with a statistically significant difference between the NGT and GDM group (*p*=0.019) (Figure 2.4b). OM AT from women with GDM contained an increased number of large adipocytes (as shown by a peak in the size distribution histogram above the mean value in Figure 2.4c, arrows). The difference in the frequency distribution between NGT and GDM was statistically significant (p=0.028). A similar trend was seen in samples from three type 2 diabetes cases, also plotted but not analyzed due to the small sample size. The mean cell size in SQ AT was 7,066μm^2 (SD 2,612μm^2; n=15) in individuals with NGT, 9,045μm^2 (SD 2,340μm^2; n=5) in those with GDM and 9,102μm^2 (SD 2,503μm^2; n=3) in those with type 2 diabetes. The difference between the NGT and GDM group was not statistically significant (p=0.178) (Figure 2.4b). A trend for larger adipocyte numbers in SQ tissue from individuals with GDM was seen in the size distribution histograms (Figure 2.4d), but the difference did not reach statistical significance. In women with NGT, adipocytes from OM AT (mean size 4,178μm^2; SD 1,440μm^2; n=12) were significantly smaller (p=0.0005) than those from SQ AT (mean size 7, 581μm^2; SD 2,672μm^2; n=12); this difference was

59

eliminated in GDM (p=0.125) due to the increase in mean OM adipocyte size

(mean size 7,482μm^2; SD 2,980μm^2; n=5) (Figure 2.4b).

60
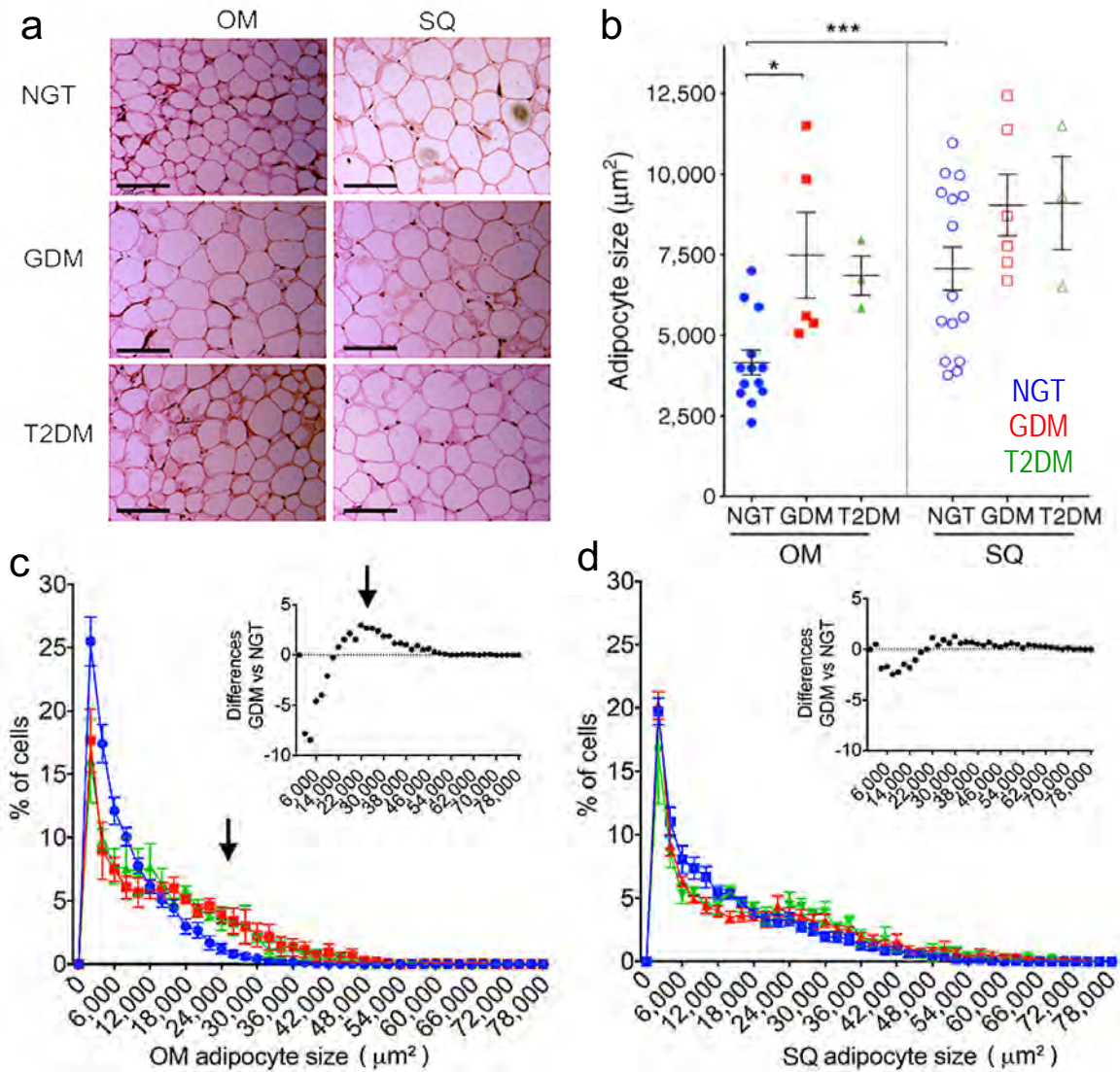
Figure 2. 4 Enlarged adipocytes are observed in OM AT of GDM gravidas.

(a) Representative images of H&E stained AT sections taken from individuals with NGT, GDM or type 2 diabetes (T2DM). Scale bar, 200μm. **(b)** Mean adipocyte size from OM (filled symbols) and SQ (white symbols) AT from women with NGT (blue circles), GDM (red squares) and type 2 diabetes (green triangles). **(c, d)**. Size distribution of adipocytes from OM **(c)** or SQ **(d)** AT. Plots show the means and SEM at each bin size of women with NGT (blue circles), GDM (red squares) and type 2 diabetes (green triangles). Symbols show the means of each individual and lines represent the means and SEM of all individuals. *$p<0.05$ and ***$p<0.001$ for indicated comparisons.

61

The increase in mean OM adipocyte size in individuals with GDM could not be explained by an increase in BMI (Figure 2.5a) or gestational weight gain (Figure 2.5b) but was highly correlated with serum glucose levels (Figure 2.5c), as was the maximal OM adipocyte size (Figure 2.5d). This finding is consistent with those of previous studies in non-pregnant individuals in which large adipocytes are associated with dyslipidemia as well as glucose and insulin abnormalities (Hoffstedt et al., 2010) (Veilleux, Caron-Jobin, Noël, Laberge, & Tchernof, 2011), revealing a similarity between a central AT feature in GDM and type 2 diabetes.
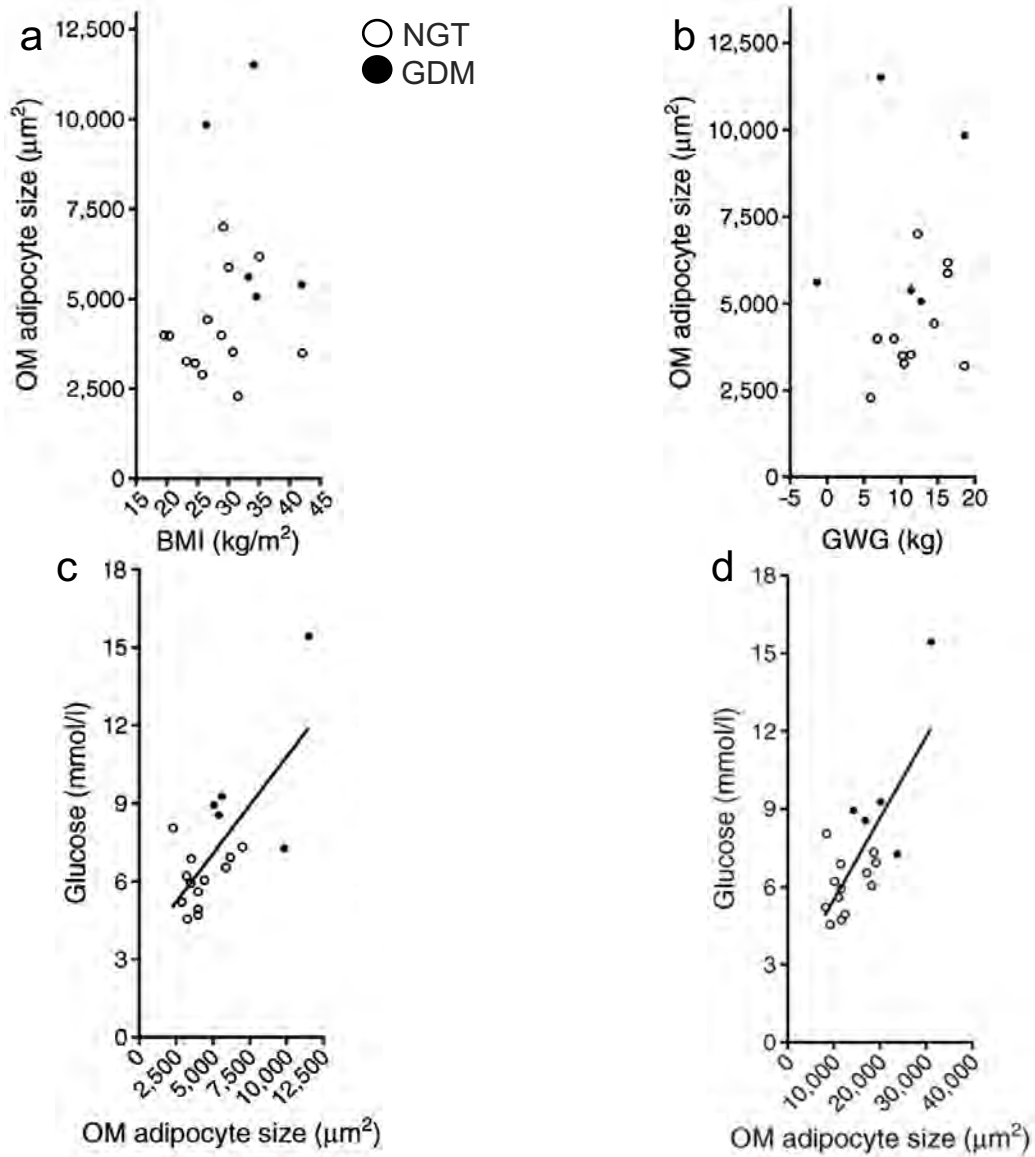
Figure 2. 5 OM adipocyte size has a positive correlation with serum glucose in pregnant women.

(a-d) Linear regression analyses: BMI vs mean OM adipocyte size (r^2=0.038; p=0.433) **(a)**; gestational weight gain (GWG) vs mean OM adipocyte size (r^2=0.149; p=0.651) **(b)**; mean OM adipocyte size vs serum glucose (r^2=0.505; p=0.0009) **(c)** and maximal OM adipocyte size vs serum glucose (r^2=0.568; p=0.0003) **(d)**. White circles, NGT; black circles, GDM.

63

Capillary density

In parallel with the growth of adipocytes, the capillary network of AT must expand to sustain adipocyte function (Bouloumié, 2002) (Hausman & Richardson, 2004). Moreover, the vasculature of AT is a developmental niche for adipocyte precursors (Tran et al., 2012) and adequate angiogenesis may be a prerequisite for adipocyte hyperplasia. Capillary density was measured in lectin-stained whole mounts (Figure 2.6). The mean area of lectin staining (as % of total area) in OM AT was 21.3% (SD 5.0%; n=11) in individuals with NGT, 13.2% (SD 4.8%; n=5) in those with GDM and 16.6% (SD 4.5%; n=3) in those with type 2 diabetes, with a statistically significance difference between the NGT and GDM group (p=0.013) (Figure 2.6b). The mean area of lectin staining in SQ AT was 20.3% (SD 5.0%; n=18) in individuals with NGTs, 13.6% (SD 3.9%; n=5) in those with GDM and 16.5% (SD 2.2%; n=3) in those with type 2 diabetes, with a statistically significant difference between the NGT and GDM group (p=0.039) (Figure 2.6b). Differences in capillary density could not be attributed to changes in adipocyte size, as the product of capillary density and adipocyte size remained significantly different (Figure 2.6c).
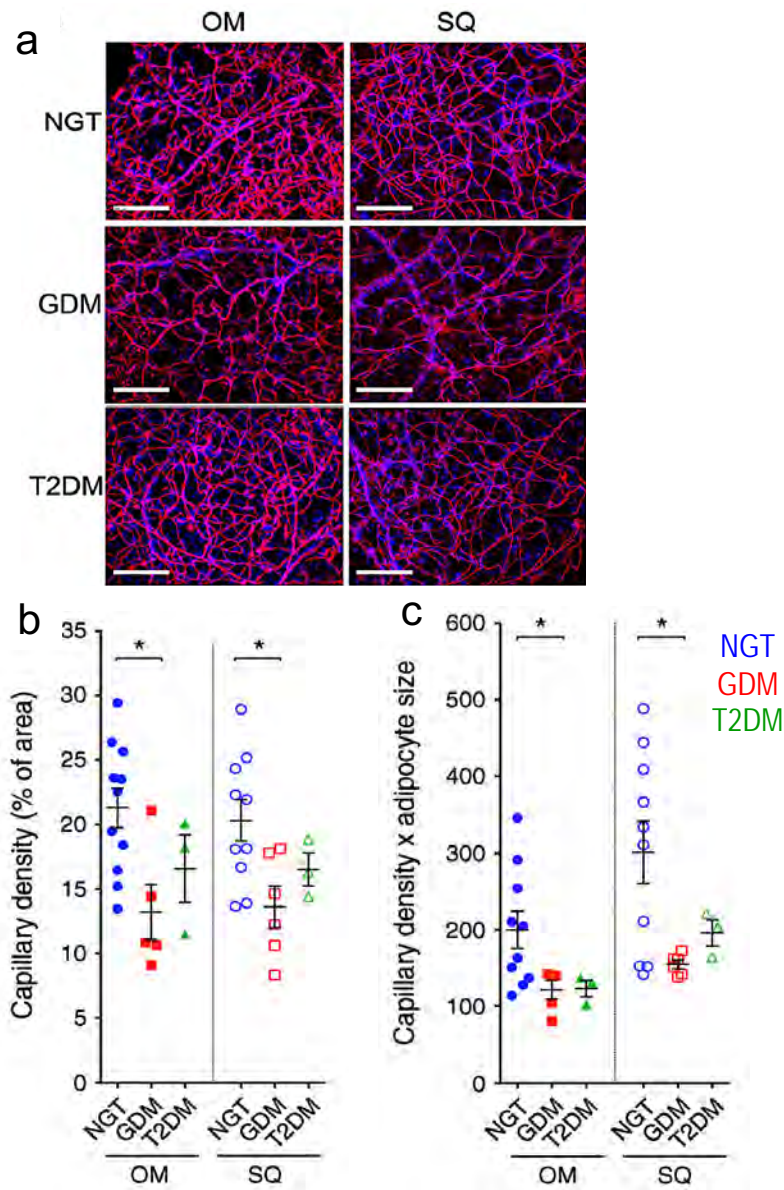
Figure 2. 6 Capillary density of OM and abdominal SQ AT is reduced in GDM gravidas.

(a) Representative images of capillary density in rhodamine-lectin UEA-1-stained AT taken from individuals with NGT, GDM or type 2 diabetes (T2DM). Scale bar, 200µm. **(b, c)** Capillary density, shown as % of area **(b)** and as % of area × mean adipocyte size **(c)**, in OM (filled symbols) and SQ (white symbols) AT taken from individuals with NGT (circles), GDM (squares), and type 2 diabetes (triangles). Symbols show the means for each individual and lines represent the mean and SEM of all individuals. *p<0.05 for indicated comparisons.

65

Collagen content

To explore other alterations in AT associated with metabolic disease, such as fibrosis (Divoux et al., 2010), we analyzed fixed sectioned tissue for collagen content using picrosirius red (Figure 2.7). No significant differences were detected between groups, possibly due to the lower BMI and early onset of metabolic disease in this population compared with previously studied bariatric surgery populations (Divoux et al., 2010) (Henegar et al., 2008).
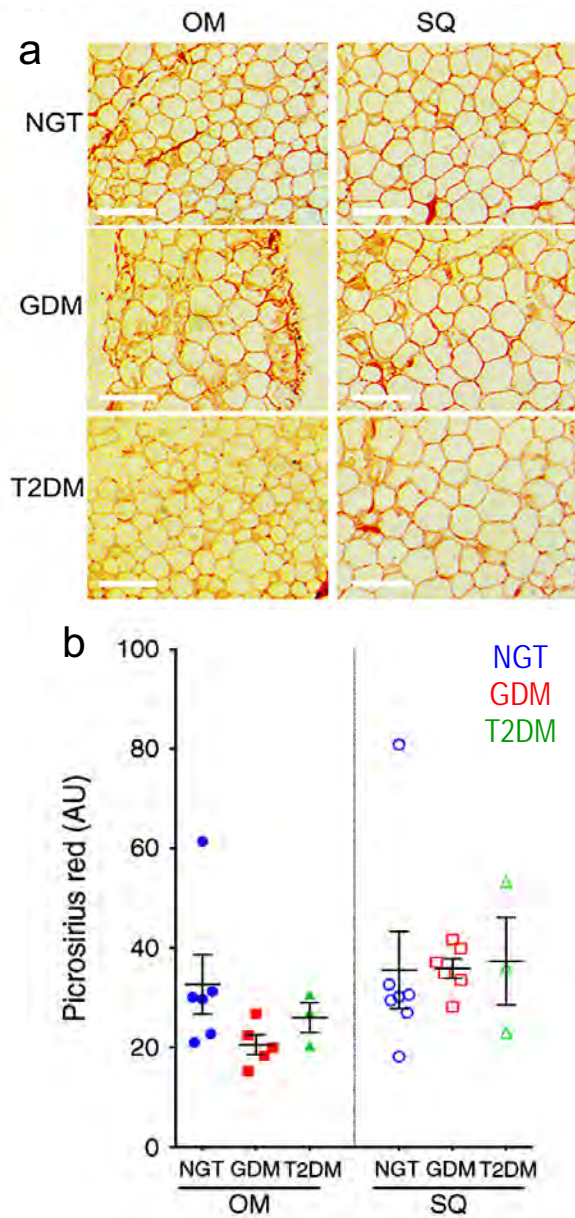
Figure 2. 7 Collagen content in OM and abdominal SQ AT is not different between NGT and GDM gravidas.

(a) Representative examples of AT sections stained with picrosirius red. Scale bar, 200μm**. (b)** Intensity of picrosirius red staining. OM (filled symbols) and SQ (white symbols) AT taken from individuals with NGT (circles), GDM (squares), and type 2 diabetes (triangles). Symbols show the means for each individual and lines represent the mean and SEM of all individuals.

67

Adipose tissue angiogenesis

To gain insight into the causes that may underlie the observed changes in capillary density seen in GDM we measured the capacity of AT to form capillaries *ex vivo* (Figure 2.8). This assay measures the competence of endothelial cells and cells associated with the vasculature to grow under ideal angiogenic conditions where growth factors are optimally supplied in the growth medium. Thus, it can help distinguish between the effects of environmental factors (e.g. decreased levels of growth factors) and those of other inherent properties of the tissue (e.g. decreased number of progenitor cells). The mean growth density (number of pixels) for SQ and OM AT from individuals with NGT was 5.32×10^7 (SD 2.43×10^7; n=12) and 3.34×10^7 (SD 2.34×10^7; n=13), respectively, with a statistically significant difference (p=0.033), consistent with our previous observations in non-pregnant obese individuals (Gealekman et al., 2011). However, no significant difference (p=0.882) was detected in OM AT when comparing individuals with NGT (3.34×10^7; SD 2.34×10^7; n=13) and those with GDM (2.94×10^7; SD 2.19×10^7; n=5) (Figure 2.8b). Also, no significant difference (p=0.349) was detected when comparing SQ AT explants from individuals with NGT (5.32×10^7; SD 2.43×10^7; n=12) with those from individuals with GDM (4.40×10^7; SD 2.09×10^7; n=6). The lower mean angiogenic potential seen in

68

tissues from two individuals with type 2 diabetes must be confirmed with a larger

sample size.
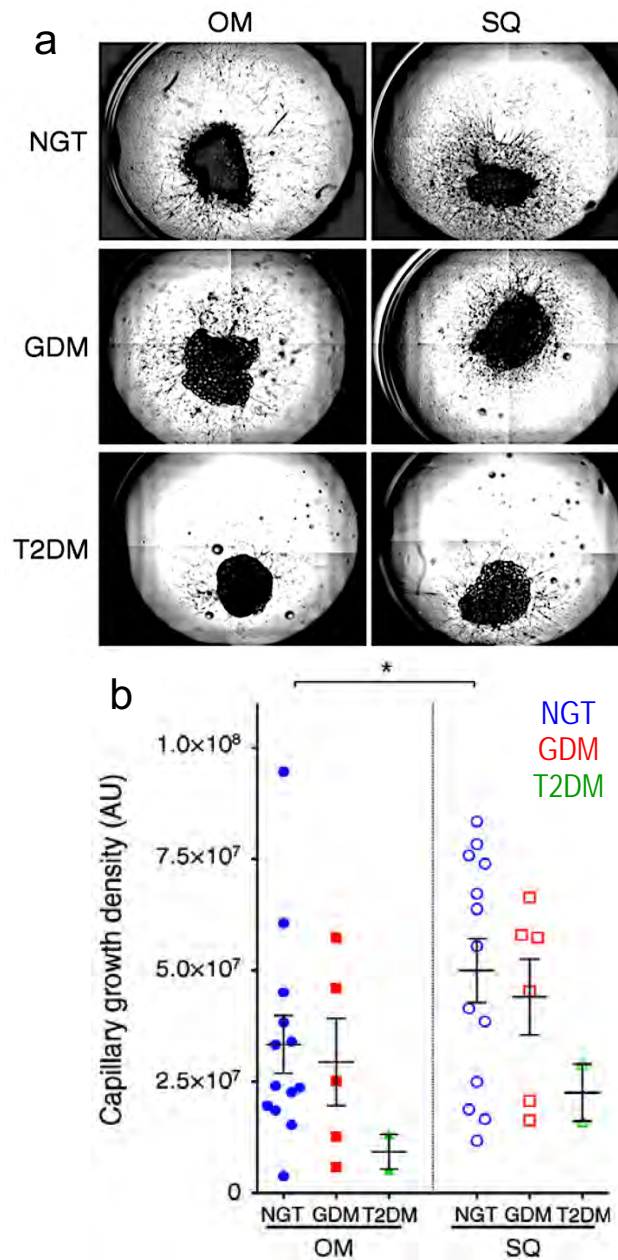
Figure 2. 8 NGT gravidas demonstrate depot-specific differences in AT angiogenic potential.

(a) Representative examples of capillary growth in AT (x2.5 magnification). **(b)** Capillary growth area density. OM (filled symbols) and SQ (white symbols) AT taken from individuals with NGT (circles), GDM (squares), and type 2 diabetes (triangles). Symbols show the means for each individual and lines represent the mean and SEM of all individuals. *p<0.05 for indicated comparisons.

70

Gene expression analysis

To explore the mechanisms involved in AT growth in pregnancy, we compared previously acquired Affymetrix gene arrays of SQ and OM AT from 11 non-pregnant, non-diabetic women undergoing bariatric surgery (Gealekman et al., 2011) (Table 2.2), with similar arrays of pregnant women with NGT (n=3 individuals; BMI 20.4, 19.6 and 19.5 kg/m^2). Numerous differences in gene expression were seen between OM and SQ AT depots, and between pregnant and non-pregnant groups (Figure 2.9a). The most differentially expressed gene when comparing AT from non-pregnant and pregnant women, for both OM and SQ AT, was *IGFBP5*. Further analysis of Affymetrix data revealed higher levels of I*GFBP5* in the OM AT than in the SQ AT of non-pregnant women, with no correlation with BMI (Figure 2.9b). No changes in expression of *IGFBP5* have been observed in SQ AT arrays from individuals with a BMI range of 16.7–50.2 kg/m^2 and normal or impaired glucose tolerance (Keller et al., 2011) (data set record GDS3961), supporting the notion that the induction seen in our study was due to pregnancy. The most significantly altered genes (p<0.0001) were used to identify pathways significantly associated with pregnancy. Kyoto Encyclopedia of Genes and Genomes (KEGG) identified the 'protein processing in the endoplasmic reticulum' and 'protein export' pathways as being enriched in differentially expressed genes (Table 2.3).

71
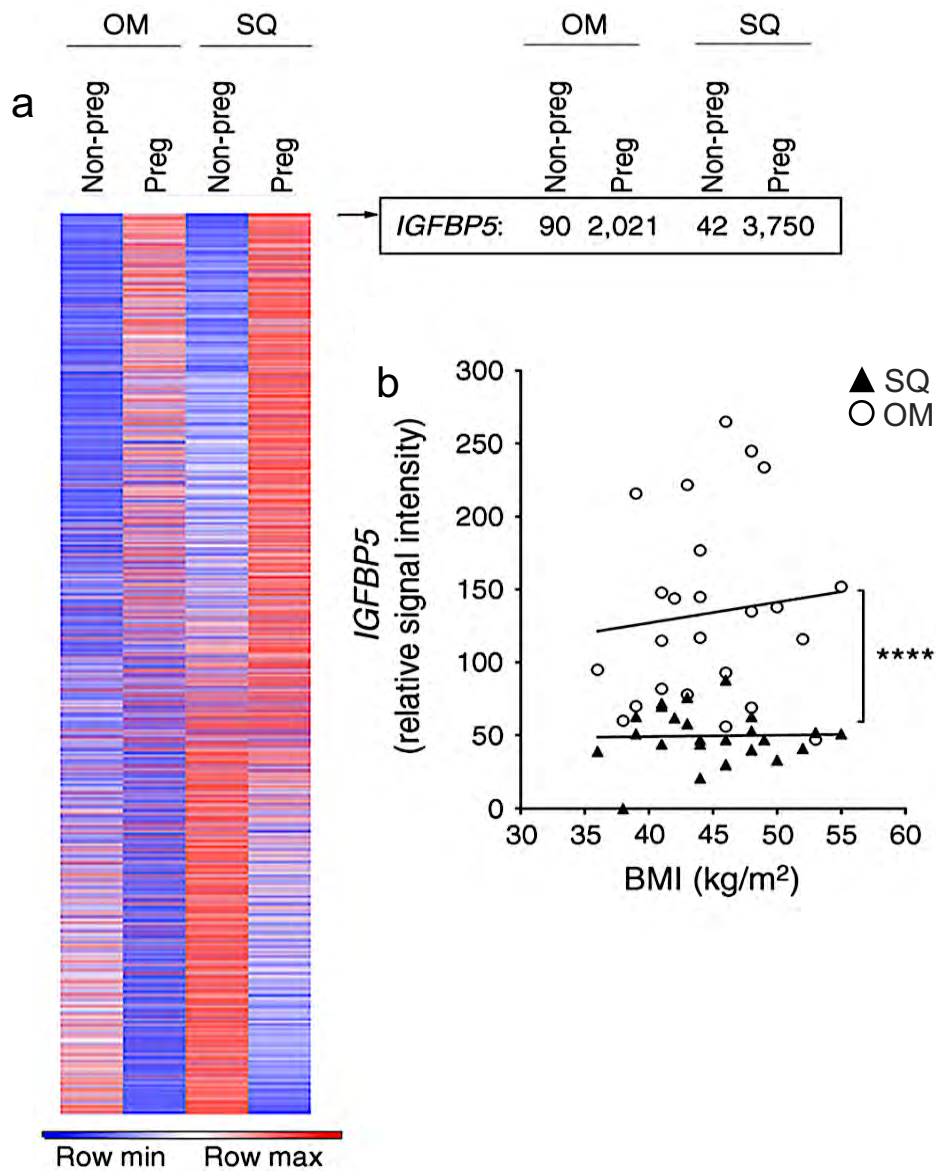
Figure 2. 9 Pregnancy induces changes in OM and abdominal SQ AT gene expression.

(a) Heat map of 22,000 genes, and specific expression values for IGFBP5 in AT from non-pregnant and pregnant women with NGT. Values for *IGFBP5* (relative signal intensity) are shown. **(b)** Relationship between BMI and *IGFBP5* levels in SQ (black triangles) and OM (white circles) AT from individuals used for the Affymetrix array. Adjusted p value ****p<0.0001 for indicated comparison.

KEGG Enrichment

Probes with KEGG annotations in above list: 188

The chip holds 5870 probes annotated to 229 pathways

Gene List	Path	Path Name	P-val
⇓ DNAJA2 OS9 CKAP4 CRYAB ERN1 SEC61G UBQLN1 STT3A MAP3K5PRKCSH SKP1 SSR1 SSR3 UBE2D1 XBP1 CAPN1 MBTPS1 PDIA4	4141	Protein processing in endoplasmic reticulum	4.77E-08
⇓ MYL9 COL6A1 COL6A2 CTNNB1 FYN PARVB ILK ITGA7 ITGB5 JUNPDGFA PPP1CB MAPK3 SHC1 THBS1 TLN1 ZYX	4510	Focal adhesion	4.35E-06
⇓ FBXO5 PPP1CB PPP2CA PPP2R1A PPP3R1 MAPK3 SKP1 YWHAECAMK2G SMC3 CDC27	4114	Oocyte meiosis	3.39E-05
⇓ CTNNB1 JUN CYCS MAPK3 TCF7L2 TGFB1 TGFB2	5210	Colorectal cancer	0.00019882
⇓ SEC61G SRP68 SRPR SEC11C	3060	Protein export	0.00027554
⇓ GNAS JUN PPP2CA PPP2R1A MAPK3 MAPK13 TGFB1 TGFB2 CFLAR	5142	Chagas disease (American trypanosomiasis)	0.00038197
⇓ CTBP1 CTNNB1 DAAM1 JUN LRP5 PPP2CA PPP2R1A PPP3R1 SKP1TCF7L2 CAMK2G	4310	Wnt signaling pathway	0.00055785
⇓ CTNNB1 FYN MAPK3 PTPN1 PVRL2 TCF7L2 IQGAP1	4520	Adherens junction	0.0006184
⇓ NEDD4L SKP1 UBA1 UBE2D1 UBE2L3 UBE2N ITCH CUL4A CUL7CDC27	4120	Ubiquitin mediated proteolysis	0.00081475
⇓ MYL9 CFL1 GSN ITGA7 ITGB5 PDGFA PPP1CB ENAH MAPK3PIP4K2B IQGAP1 ARHGEF7 ARHGEF1	4810	Regulation of actin cytoskeleton	0.00139422
⇓ PPP2CA PPP2R1A MAPK3 SKP1 TGFB1 TGFB2 THBS1	4350	TGF-beta signaling pathway	0.00157004
⇓ JUN ARHGDIB MAP3K5 NTRK2 MAPK3 MAPK13 SHC1 YWHAECAMK2G	4722	Neurotrophin signaling pathway	0.00182166

Table 2. 3 KEGG pathways enriched in AT of pregnant women.

73

To verify the arrays, we conducted real-time PCR analysis of SQ AT from additional cohorts of non-pregnant women undergoing panniculectomy surgery (mean BMI 29.6 kg/m^2; SEM 1.2 kg/m^2; n=3), pregnant women with NGT (mean BMI 19.7 kg/m^2; SEM 0.1 kg/m^2; n=3) and pregnant women with GDM (mean BMI 34 kg/m^2; SEM 4.6 kg/m^2, n=3) (Figure 2.10). These results confirmed the marked induction of *IGFBP5* by pregnancy seen in Affymetrix arrays and revealed a significant decrease in *IGFBP5* and *IGF-1* expression in tissue from individuals with GDM (Figure 2.10a). While this difference also coincided with a significant difference in BMI among the groups, the lack of correlation between *IGFBP5* expression and BMI in the individuals used for Affymetrix gene chip analysis (Figure 2.9b), and between *IGFBP5* expression and the BMI of non-pregnant individuals and those with GDM (r^2=0.28, p=0.278), suggests that the observed differences in *IGFBP5* expression between individuals with NGT and GDM is independent of BMI. In addition to differences in *IGFBP5*, differences in the expression of *IGF-1*, *IGFBP3*, *IGFBP4* and *IGFBP6* were seen (Figure 2.10a), revealing alterations in the IGF-1 signaling axis in AT in response to pregnancy and GDM. Moreover, the decrease in I*GFBP5* and *IGF-1* expression seen in GDM was not paralleled by changes in other key angiogenic factor genes, such as *VEGFA* and *FGF2*, nor by significant inflammatory alterations as inferred by unchanged gene expression of the macrophage marker *CD-68* (Figure 2.10b).

74
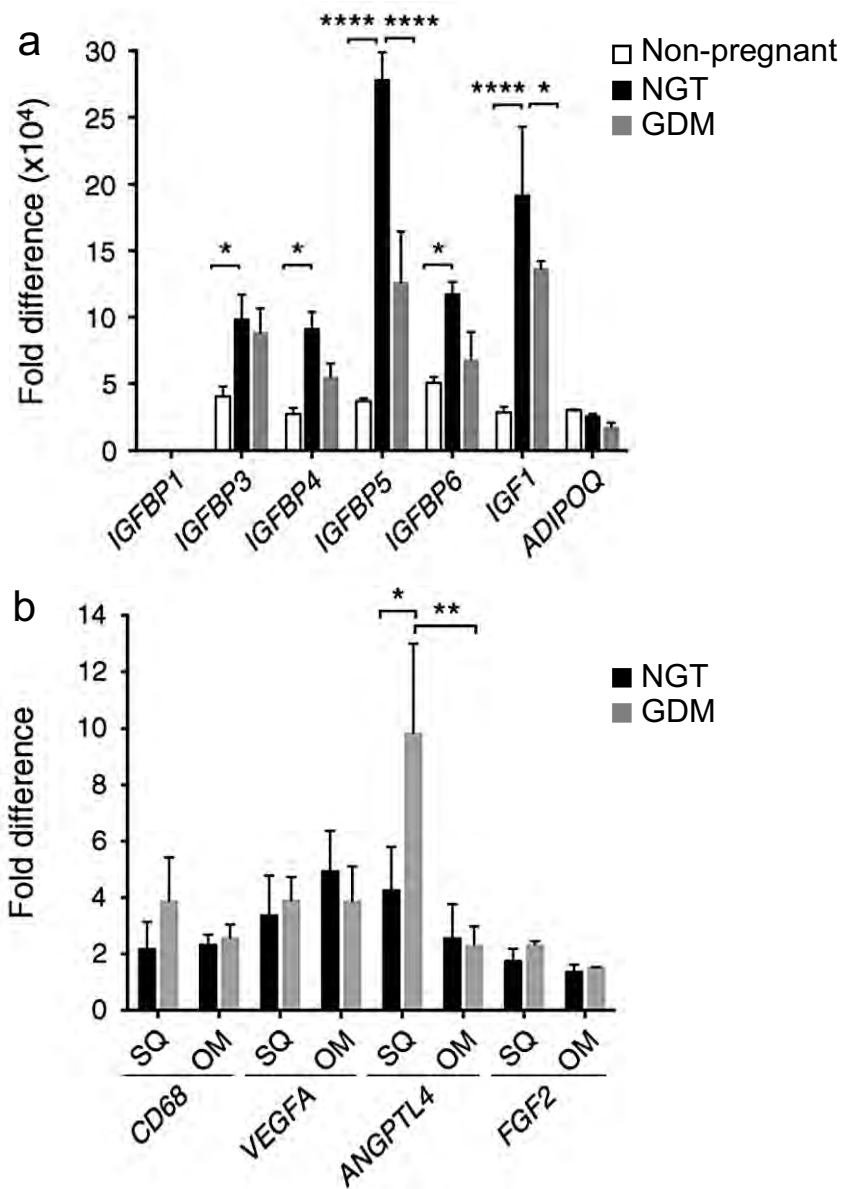
Figure 2. 10 Alterations in gene expression are observed in AT of GDM gravidas.

(a) Real-time PCR analysis of SQ AT from non-pregnant women with NGT (white bars), pregnant women with NGT (black bars) and pregnant women with GDM (grey bars). Values are normalized to the lowest expressed transcript in the NGT group, which was *IGFBP1*. **(b)** Real-time PCR analysis of SQ AT from pregnant women with NGT (black bars) and pregnant women with GDM (grey bars). Values are normalized to the lowest expressed transcript in the NGT group, which was *FGF2*. Adjusted p values: *$p<0.05$, **$p<0.01$ and ****$p<0.0001$ for indicated comparisons.

75

Discussion

Adipocyte size is an indicator of the mode of AT expansion, which can occur through two distinct processes: adipocyte hypertrophy, where each adipocyte increases in size to contain a larger lipid droplet, and hyperplasia, where more adipocytes form through differentiation of precursor cells (Hoffstedt et al., 2010) (Tchoukalova et al., 2014). AT hyperplasia (small adipocytes) is significantly associated with better glucose, insulin and lipid profiles (Hoffstedt et al., 2010) (Veilleux et al., 2011). In contrast, large adipocytes are associated with dyslipidemia, glucose and insulin abnormalities (Hoffstedt et al., 2010) (Veilleux et al., 2011), are insulin resistant (JI Kim et al., 2015) and are prone to necrosis and inflammation. Hyperplasia may be more effective at increasing total AT mass and storage capacity, thus preventing deposition of deleterious lipid species in other organs and ensuing insulin resistance. Consistent with this possibility are data from obese mouse models in which AT containing small adipocytes leads to improved glucose homeostasis (JY Kim et al., 2007) (Lu, Li, Zou, & Cao, 2014). The relative hypertrophy of adipocytes in women with GDM, together with their trend to a lower gestational weight gain (Table 2.1), suggests a decreased capacity for hyperplastic adipocyte growth and AT expansion, with consequent negative effects on glucose and insulin homeostasis. Adipocyte progenitors are tightly associated with the AT capillary network (Han et al., 2011) (Tang et al., 2008). Thus, the decreased capillary density seen in individuals with GDM could

76

underlie diminished pre-adipocyte proliferation and hyperplastic growth, with consequent hypertrophy of existing adipocytes. Insufficient vascular growth in the AT of individuals with GDM could also contribute to insulin resistance through hypoxia (Gealekman et al., 2011) (Spencer et al., 2011). Expression levels of the gene encoding angiopoietin-like 4 (*ANGPTL-4*), which is sensitive to hypoxia (Xin et al., 2013), were found to be elevated in GDM (Figure 2.10b), possibly indicating insufficient oxygenation. Other mechanisms could include failure of nutrient exchange or failure to deliver secreted hormones (adipokines) into the circulation.

Previous studies from our group identified IGFBP4 as a potential key factor in AT expansion in response to a high-fat diet in mice (Gealekman et al., 2014). The marked upregulation of *IGFBP5* seen in AT from pregnant women supports a similar role for the IGF-1 signaling pathway in adult AT expansion. IGFBP5 binds IGF-1 and IGF-2 with high affinity and has been shown in cell and animal models to inhibit signaling by sequestering these growth factors (Beattie et al., 2006). However, IGFBP5 also binds to the extracellular matrix of tissues, and can thereby serve as a local reservoir of IGF-1 (Beattie et al., 2006). The concurrent expression of *IGFBP5* in AT and secretion of PAPP-A by the placenta suggests a mechanism whereby the local concentration of IGF-1 is increased in AT through interaction with IGFBP5 and release in response to PAPP-A secretion, thereby coordinating placental function with maternal AT expansion (Figure 2.11).

77

Abnormalities in this mechanism could potentially lead to impaired AT expansion and to lipotoxicity and metabolic disruption manifesting as GDM. This hypothesis is consistent with previous studies in which type 2 diabetes has been associated with abnormalities in SQ AT levels of the IGF-1 receptor and IGFBP3 (Yamada et al., 2010). While our current study is limited by sample size and by differences in age and BMI between groups, the large magnitude of the results presented support a new model to explore the mechanism of AT expansion in pregnancy and its role in the etiology of GDM.
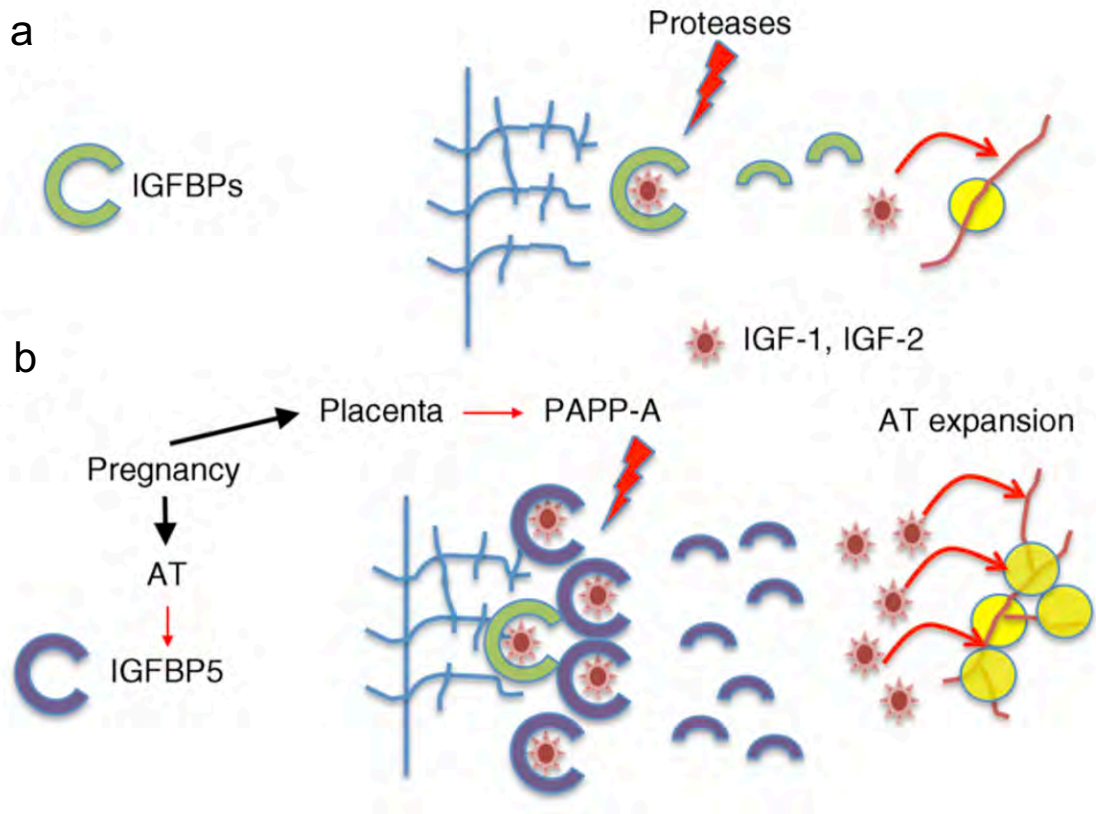
Figure 2. 11 Potential role of IGFBP5 in AT expansion during gestation.

(a) In non-pregnant women, IGFBPs sequester IGF-1 and IGF-2. Proteolysis of IGFBPs releases the growth factors, which act on AT vasculature and maintain tissue homeostasis. **(b)** In pregnancy, the induction of IGFBP5 increases the amount of sequestered IGF-1. The pregnancy-specific protease PAPP-A degrades IGFBP5 to release IGFs, promoting angiogenesis, pre-adipocyte proliferation and hyperplastic expansion.

CHAPTER III: PAPP-A mediated adipose tissue remodeling mitigates insulin resistance and protects against gestational diabetes in mice and humans

Abstract

Pregnancy is a unique physiological state in which the body must adapt to rapidly changing maternal and fetal nutritional needs. A known feature of pregnancy is the reduction of maternal insulin sensitivity allowing for appropriately enhanced glucose availability to the fetus. However, excessive insulin resistance results in maternal glucose intolerance and gestational diabetes mellitus (GDM), increasing the risk for pregnancy complications and predisposing both mothers and offspring to future metabolic disease. Here we report a previously unrecognized signaling pathway that plays a key role in mitigating insulin resistance in pregnancy. We show that in both mice and humans, pregnancy promotes adaptations in adipose tissue reflected by altered adipocyte size, vascularization and expansion capacity. We find that these adaptations are dependent on the pregnancy-associated plasma protein-A (PAPP-A), a metalloprotease secreted by human placenta that cleaves insulin-like growth factor binding proteins (IGFBP) 2, 4 and 5, and thus modulates insulin-like growth factor (IGF) bioavailability. We find levels of

circulating PAPP-A in humans are inversely correlated with glycemia and with the odds of developing GDM, and recombinant PAPP-A stimulates human adipose tissue expandability *in vitro*. Moreover, mice lacking PAPP-A display pregnancy-induced insulin resistance, hepatic steatosis and impaired adipose tissue, thereby recapitulating the pathophysiology of human GDM. These data identify PAPP-A as a critical factor in the regulation of maternal adipose tissue physiology and systemic glucose homeostasis, with potential for therapeutic use.

Introduction

Gestational diabetes mellitus (GDM) is one of the most common complications of pregnancy, affecting 240,000 U.S. pregnancies yearly, a number expected to increase to ~720,000 with potential changes in diagnostic criteria (Gariani et al., 2019). GDM is associated with increased risk of obesity, metabolic syndrome and other cardiometabolic disorders in the offspring (Patel et al., 2012) (Wicklow et al., 2018) (Farahvar, Walfisch, & Sheiner, 2019) (Kampmann et al., 2018). Furthermore, as many as 50% of women with a GDM develop type-2 diabetes mellitus (T2DM) within 5 years (Kjos et al., 1995), and GDM elevates lifetime risk of T2DM 7-fold (Bellamy et al., 2009) (Kwak et al., 2013). Understanding the etiology of GDM is crucial for developing appropriate preventive and therapeutic strategies.

The precise mechanisms underlying the development of GDM are not clear. Pregnancy is a state of rapid metabolic adaptation required to meet the nutritional needs of both mother and growing fetus, as well as anticipate those of the offspring which are met through maternal lactation. An increase in total adipose mass is characteristic of normal pregnancy (Eriksson, Löf, Olausson, & Forsum, 2010) (Kopp-Hoolihan et al., 2017) (Forsum, Sadurskis, & Wager, 1989) (Larciprete et al., 2003), with about 30% of recommended weight gain composed of fat mass. The mechanism underlying normal adipose tissue growth in

82

pregnancy, and its role in partitioning energy resources amongst mother, fetus, and offspring through lactation, has yet to be fully defined (Resi et al., 2012). Indeed, one of the major metabolic adaptations to pregnancy is a maternal decrease in insulin sensitivity, which is thought to facilitate glucose availability to the fetus. In non-pregnant subjects, adipose tissue plays a central role in regulating insulin sensitivity (Carobbio, Pellegrinelli, & Vidal-Puig, 2017), and there is increasing evidence that alterations in adipose tissue, including excessive visceral expansion (Shinar, Berger, De Souza, & Ray, 2019), changes in adipocyte size (Svensson et al., 2016) (Rojas-Rodriguez et al., 2015) and physiological inflammation (Resi et al., 2012) contribute to insulin resistance in human pregnancy and to GDM risk.

The insulin-like growth factor (IGF) -1 and -2 signaling axis plays a central role in tissue growth through their interactions with the insulin and IGF-1 receptors (Roberts & Leroith, 1988). IGFs circulate at high levels relative to other peptide growth factors and their mitogenic activities are modulated via their tight association with one of seven different IGF binding proteins, IGFBPs 1-7 (Holly, 2004) (Haruki Nishizawa et al., 2008). The IGF/IGFBP system has been implicated in regulating adipose tissue growth (Garten et al., 2012) (Hoeflich et al., 1999) (Maridas, DeMambro, Le, Mohan, & Rosen, 2017) and may play a special role in adipose tissue adaptation in pregnancy, as levels of subcutaneous

and omental *IGFBP4* and *IGFBP5* are increased in human pregnancy (Resi et al., 2012) (Rojas-Rodriguez et al., 2015). IGFBPs increase local availability of IGFs by preventing their clearance, but also impair productive binding with their receptors. Receptor binding of IGFs and induction of mitogenic signaling is dependent on the proteolytic degradation of IGFBPs.

The pregnancy-associated plasma protein A, PAPP-A, has been shown to account for the vast majority of proteolytic activity for IGFBP4 in serum from pregnant women (Byun et al., 2001) (Overgaard et al., 2000), and is a critical factor for early development in mice (Conover et al., 2004). While the vast majority of total and proteolytically active circulating PAPP-A in humans is derived from the uterus (Bischof, 1984), a significant amount is expressed in other tissues, including adipose tissue (Conover, Bale, Frye, & Schaff, 2019). In mice, *Papp-a* is expressed at high levels independent of pregnancy (Qin et al., 2002), but it has an important developmental role during gestation, as its ablation results in proportional dwarfism which is rescued by *Igf-2* expression (Bale & Conover, 2005). In addition to its role in development, Papp-a has important roles in adult animals, as evidenced by alterations in neointimal development and increased longevity in mice with *Papp-a* ablation in adulthood (Conover, Bale, & Powell, 2013) (Bale, West, & Conover, 2017). The concomitant induction of IGFBPs in adipose tissue and high levels of circulating PAPP-A in human

84

pregnancy suggested the possibility that the IGF-IGFBP-PAPP-A axis would play a role in the adaptation of adipose tissue to pregnancy, and in consequent modulation of metabolic homeostasis. In this paper, we leverage *in vitro* model systems to quantify human adipose tissue expandability, retrospective population data and mouse knockout studies to further investigate this hypothesis.

Methods

Study cohorts

For Affymetrix analysis, cohorts were as described previously (Gealekman et al., 2011) (Table 2.2). For analysis of adipose tissue features, all normoglycemic pregnant women with singleton gestations scheduled for cesarean section, and non-pregnant normoglycemic women without hypertension presenting to University of Massachusetts Memorial Health Care (UMMHC) between June 2015 and November 2016 were considered for enrollment. The Institutional Review Board (IRB) from the University of Massachusetts Medical School (UMMS) approved the study, and all participants were provided and signed informed consent. Diabetes status in the pregnant cohort was classified according to the Carpenter-Coustan criteria. The exclusion criteria included, type-1 and type-2 diabetes mellitus, underweight BMI (<18.5kg/m^2, pre-gestational BMI in Preg cohort), use of illicit substances including replacement products, HIV/AIDS, hepatitis B or C, autoimmune disease, chronic steroid use, age <18 and >45 years, and plans to move out of the area during study period. Exclusions specific to pregnant cohort included multiple gestations, initiated prenatal care after 13 completed gestational weeks, alcohol use, and previous diagnosis of T2DM.

To determine the relationship between serum PAPP-A and glycemic status, defined as normal glucose tolerance (NGT), abnormal glucose tolerance (AGT) and gestational diabetes mellitus (GDM), retrospective analyses of the electronic health records of all pregnant women with singleton gestations who delivered at UMMHC from June 2009 to March 2015 and had PAPP-A results were performed. The IRB of the UMMS approved the study. Gravidas were classified according to the Carpenter-Coustan criteria; NGT is defined as gravidas without pre-gestational diabetes and with passing value on routine 50g glucola screening (≤140mg/dl) or ≤1 abnormal value (fasting≥95, 1hr≥180, 2hr≥155, 3hr≥140mg/dl) on 100g 3hr glucose tolerance test (GTT); AGT included gravidas without pre-gestational diabetes and with failed value on routine 50g glucola screening (>140mg/dl), independent on the value of 100g 3hr GTT; GDM included gravidas without pre-gestational diabetes and with failed value on routine 50g glucola screening (>140mg/dl), and ≥2 abnormal values (fasting≥95, 1hr≥180, 2hr≥155, 3hr≥140mg/dl) on 100g 3hr GTT. Women with pre-gestational type 1 or type 2 diabetes, multiple gestation, and chronic hypertension were excluded from this study. Additionally, women who were missing critical data (e.g. prepregnancy height and weight, evidence of GDM screen) or had missing or unknown relevant demographics of interest (e.g. smoking status, maternal age, parity, race/ethnicity) were also excluded. Finally, for women with more than one

87

pregnancy during the study period, one pregnancy was selected at random for inclusion in analysis. Our final analytic sample included 6,361 women.

For analysis of the correlation between PAPP-A and serum glucose, all records containing PAPP-A and glucose values from routine 10-14-week aneuploidy and 24-28-week GDM screens (50g glucose 1h test), respectively, were extracted using Epic EHR v. 2018. In order to allow comparison of serum PAPP-A across different gestational ages, PAPP-A data was also presented as multiples of the median (MoM). PAPP-A MoM was calculated using the gestational mean for our center adjusting for maternal weight, ethnicity, and smoking status. Data from subjects complying with the inclusion/exclusion criteria defined above were used for regression analysis. This sample reflects the population of Central Massachusetts.

Human adipose tissue collection

For the pregnant cohort, specimen collection was done at the time of cesarean section after delivery of the baby. Prior to skin closure, two samples (1 cm × 1 cm) of subcutaneous (SQ) adipose tissue (AT) were obtained from within the surgical incision usually placed approximately 2 cm above the pubic bone (Pfannenstiel incision). In the case of repeat Caesarean delivery, SQ AT biopsies were taken from deep within the incision to decrease scar tissue sampling. For the non-pregnant cohort, specimen collection was done at the Clinical Trials Unit

88

of UMMS during a scheduled site visit. SQ AT needle biopsies were obtained from anterior abdominal wall just lateral and inferior to the umbilicus, both away from blood vessels and scars. For acquiring the AT specimens, a 60ml BD syringe with 14-gauge needle filled with 30ml of normal saline was used. Approximately, 1g of AT was collected.

Affymetrix arrays

For transcriptomic analysis, total RNA was extracted using the RNeasy Lipid Tissue Mini kit (Qiagen, Valencia, CA, USA). The GeneChip Human Genome U133A 2.0 Array was employed for analysis of cRNA, which was obtained following manufacturer supplied protocols (Affymetrix, Santa Clara, CA, USA). Raw expression data collected from an Affymetrix HP GeneArrayScanner was normalized across all data sets using the RMA algorithm. Differential expression was performed using Limma as implemented in DEBrowser (Kucukural, Yukselen, Ozata, Moore, & Garber, 2019). Hierarchical clustering was done using Morpheus (https://software.broadinstitute.org/morpheus/). For pathway enrichment, the list of differentially expressed genes was uploaded to ToppGene (J. Chen, Bardes, Aronow, & Jegga, 2009) via the ToppFun uploader. ToppFun default parameters were used to generate pathway lists, which were considered to be significantly enriched if the p-adjusted value was less than 0.05.

89

Analysis of adipocyte size

Samples were fixed in 4% formaldehyde and embedded in paraffin. Eight-micrometer sections were mounted on Gold Seal microscope slides (Fisher Scientific, Pittsburgh, PA, USA), and stained with hematoxylin and eosin (H&E). Investigators acquiring the images were blinded to the origin of the sample. Brightfield images were acquired using a 5X (for human studies) or 10X (for mouse studies) objective on a Zeiss Axiovert 35 microscope and a Zeiss AxioCam ICc1 digital camera. Adipocyte size was determined using an automated procedure based on the open software platform Fiji (Schindelin et al., 2012) (as described in Figure 2.1)

Analysis of microvasculature

Samples were fixed in 4% formaldehyde and rinsed in phosphate-buffered saline (PBS). Samples were cut in 1mm fragments and stained with rhodamine-labeled Ulex Europaeus Agglutinin I (UEA-1) (Vector Labs, Burlingame, CA, USA) for 1h at room temperature and then mounted on Gold Seal microscope slides, sealed with Pro-Long Gold Antifade Mountant (Life Technologies, Grand Island, NY, USA) and covered with 1.5 mm coverslips. Images were taken under 5X magnification in a Zeiss Axiovert 200M microscope equipped with Zeiss AxioCam HRm digital camera. Quantification of capillary connectivity was done using an algorithm for connected regions implemented in Image J

90

(http://homepages.inf.ed.ac.uk/s9808248/imagej/find-connected-regions/).
Images of UEA-1 stained explants were converted into 8 bit and background
corrected prior to applying the algorithm. Results quantifying the number and
mean size of regions in each image were recorded. All image acquisition and
analysis were done by operators blinded to the origin of the samples.

In vitro adipose tissue expandability assay

The *in vitro* expandability assay (adipose tissue angiogenesis) was done as
described previously (Rojas-Rodriguez et al., 2015). Briefly, AT samples were cut
into $1mm^3$ pieces and embedded in Matrigel (Corning, Bedford, MA, USA) using
single wells of a 96-well template plate. AT explants were cultured under
proangiogenic conditions for 11 days using EGM-2MV media (Lonza, Allendale,
NJ, USA). Imaging was done at day 7 and day 11 after embedding using a Zeiss
Axio Observer Z1 equipped with an automated stage and a Clara High
Resolution CCD Camera (Andor, Concord, MA, USA). Images were taken under
×2.5 magnification as a stack composed of five Z planes at 150µm intervals and
as a canvas of four quadrants per well and then combined into a single three-
dimensional image. Image processing for capillary sprouting quantification
included background subtraction, maximal intensity projection of the Z-stack and
binarization (Figure 2.3). For analysis of effects of PAPP-A *in vitro*, recombinant
human PAPP-A (R&D Systems, Minneapolis, MN, USA) was added as described

91

in each figure legend (Figure 3.9). All image acquisition and analysis were done by operators blinded to the origin of the samples.

Animal husbandry and pregnancy

All procedures were approved by UMMS Institutional Animal Care and Use Committee. The experimental animals used in this study were homozygous *Papp-a* (+/+) (wild type, WT) and *Papp-a* (-/-) (knockout, KO) littermates obtained from crosses of heterozygous *Papp-a* (+/-) mice (Conover et al., 2004). All mice were fed normal chow diet (22% protein and 5% fat, Isopro 3000) ad-libitum and housed under controlled temperature and 12-hour light/dark cycle conditions. For all experiments, 10-12 week old mice were used. For the pregnancy experiments, homozygous WT or KO animal trios consisting of 1 male and 2 females were housed together. Presence of vaginal plug was considered as day 1 of gestation. After visualization of plug, females were separated from males. All experiments with pregnant animals were carried out at day 16 of gestation.

Metabolic phenotyping of Papp-a mice

Whole body composition assessment of fat and lean mass was done in conscious mice utilizing 1H-MRS technology (Echo Medical Systems, Houston, TX, USA). For the glucose tolerance test, pregnant dams and non-pregnant controls were fasted for 6 hours (8:00am-2:00pm). Small blood samples (~5ul)

92

were obtained from tail vein at 0, 15, 30, 45, 60, 90, and 120 min after intraperitoneal (IP) injection of glucose (2g/kg dose from 20% w/v glucose solution, Sigma, St Louis, MO, USA). Blood glucose was measured using One Touch Ultra 2 glucose meter (Lifescan, Milpitas, CA, USA). For the insulin tolerance tests, pregnant dams and non-pregnant controls were fasted for 4.5 hours (8:00am- 12:30pm). Small blood samples (~5ul) were obtained from tail vein at 0, 15, 30, 45, 60, and 90min after IP injection of insulin (0.65u/kg dose, Novolin R, Novo Nordisk, Bagsværd, Denmark). Blood glucose was measured using One Touch Ultra 2 glucose meter (Lifescan). For insulin secretion measurements, pregnant dams and non-pregnant controls were fasted for 6 hours (8:00am- 2:00pm). Blood samples (~50ul) obtained from tail vein at 0 and 45 min after IP injection of glucose (2g/kg dose from 20% w/v glucose solution, Sigma) were collected in capillary tubes and transferred to EDTA coated microtubes. Plasma was obtained by centrifugation at 2000g for 10min at 4°C. Insulin concentrations were determined in each sample by a commercial ultrasensitive ELISA (Alpco, Salem, NH, USA). Hyperinsulinemic-euglycemic clamps were conducted in the National Mouse Metabolic Phenotyping Center at UMASS according to established methods (J Kim, 2009).

Mouse tissue collection

Collection of inguinal, axillar, parametrial distal and proximal to uterine horn, periovarian, retroperitoneal, mesenteric, interscapular brown adipose tissue and liver was performed using sterile microsurgery instruments. The weight of all depots and tissues was recorded using an analytical balance, and tissues were then flash frozen for further analysis.

Mouse mammary gland whole-mount staining

For visualization of the three-dimensional structure of mammary gland development in pregnant mice, mammary gland tissue along the inguinal and axillar fat pad was excised. Whole-mount staining was done with carmine alum, a nuclear stain that allows the detection of epithelial structures embedded in the adipose tissue of the mammary fat pads (Plante, Stewart, & Laird, 2011). The protocol consisted on fixing the excised tissue in Carnoy's fixative (100% EtOH, chloroform, glacial acetic acid; 6:3:1) overnight at 4°C, followed by a wash in 70% ethanol and rehydration steps. Then, whole mounts samples were stained overnight with carmine alum at room temperature. Excess staining was removed by a serial of dehydrating ethanol baths and clearing in xylene overnight. Last, mammary glands were immersed in methyl salicylate prior to examination. Images of the mammary gland were taken with a digital camera attached to a Nikon SMZ800 stereomicroscope.

Quantitative real-time PCR

Total RNA was isolated from AT utilizing the Lipid Tissue Mini Kit (Qiagen). One microgram of total RNA was reverse-transcribed using iScript cDNA synthesis kit (Bio-Rad, Hercules, CA, USA). cDNA was used as template for real-time PCR using the iQ SYBR Green Supermix kit (Bio-Rad) and the CFX96 Real-Time System (Bio-Rad). Glyceraldehyde 3-phosphate dehydrogenase (*Gapdh*) was used for normalization of each sample. Values were expressed as the fold difference of the lowest value in each data set.

Triglyceride analysis

Liver samples were homogenized in 5% Nonidet P40. Homogenates were heated at 80-100°C for 2 min and cooled to room temperature (RT) on ice. This step was repeated and then followed by centrifugation (12000g, 10min, RT). The supernatant was used to measure triglyceride content following the protocol from L-type triglyceride M assay (Fujifilm Dako Diagnostics, Richmond, VA, USA).

Statistical analysis

Statistical analysis was performed using the following tests as implemented in GraphPad Prism v.8.0, and specific tests are described in each figure legend. Difference of histograms was calculated using the Wilcoxon matched pairs test as implemented in GraphPad Prism 8, and individual p values for differences at

each size range calculated using multiplicity adjusted (Sidak) student t-tests.

Statistical significance between groups was estimated using ordinary one-way

ANOVA corrected for multiple comparisons using the Sidak test. For contingency

analyses, statistical significance between comparisons to the highest quartile

was done using Fisher's exact test. Statistical significance of the difference

between control and treated explants was calculated using paired student t-tests.

Statistical significance of the difference between doses at each timepoint was

calculated using repeated measures two-way ANOVA. Statistical significance of

the differences between fat depot, genotype and pregnant state for each gene

were calculated using three-way ANOVA corrected for multiple comparisons

using the Tukey test.

Results

Patient characteristics

Relevant characteristics of the patients used for adipocyte size, microvasculature, and *in vitro* adipose tissue expandability assays are summarized in Table 3.1. There was not a statistically significant difference in age, BMI, or smoking status between the non-pregnant and pregnant cohorts. Although there was not a significant difference in race between groups, most of the subjects in both cohorts were white.

Cohorts characteristics for the subjects included in the retrospective analysis of serum PAPP-A and diabetes status are included in Table 3.2. There was a statistically significant difference between age, BMI, and parity between groups. Notably, there was diversity in the races included in the study but the majority of the women were white. No difference between smoking status was observed between cohorts.

97

Characteristic	Total (n=25)		Non-pregnant (n=12)		Pregnant (n=13)		p value
	N	%	N	%	N	%	
Age (Mean, SD)	31.5	5.6	31.7	7.1	31.2	4.1	0.978
BMI (pre-pregnancy or at biopsy)							
Normal range	5	20.0%	1	8.3%	4	30.8%	0.267
Overweight	9	36.0%	6	50.0%	3	23.1%	
Obese	11	44.0%	5	41.7%	6	46.2%	
Race							
White	21	84.0%	11	91.7%	10	76.9%	0.48
Asian	1	4.0%	0	0.0%	1	7.7%	
Black or African American	2	8.0%	0	0.0%	2	15.4%	
Other race	1	4.0%	1	8.3%	0	0.0%	
Hispanic, Latino, or Spanish origin							
No, not of Hispanic, Latino, or Spanish origin	20	80.0%	9	75.0%	11	84.6%	0.071
Yes, Puerto Rican	2	8.0%	0	0.0%	2	15.4%	
Yes, another Hispanic, Latino or Spanish origin	3	12.0%	3	25.0%	0	0.0%	
Ever smoked							
No	16	64.0%	8	66.7%	8	61.5%	0.999
Yes	9	36.0%	4	33.3%	5	38.5%	
Current smoker							
No	23	92.0%	11	91.7%	12	92.3%	0.999
Yes	2	8.0%	1	8.3%	1	7.7%	

Table 3. 1 Patient characteristics of cohorts included in adipose tissue analysis.

Data are presented as mean and percent of the subjects included in the study.

98

Characteristic	Total (n=6361)		GDM status						p value
			NGT (n=5,703)		AGT (n=298)		GDM (n=360)		
	n or mean	%	n or mean	%	n or mean	%	n or mean	%	
Age (Mean)	29.8	5.7	29.5	5.7	31.8	4.9	32.4	4.9	<0.001
Gestational age (Mean)	12.5	0.6	12.5	0.6	12.5	0.7	12.5	0.5	0.652
BMI Categories									
< 18.5	198	3.1%	186	3.3%	6	2.0%	6	1.7%	<0.001
18.5 to < 25.0	3,042	47.8%	2,823	49.5%	117	39.3%	102	28.3%	
25.0 to < 30.0	1,757	27.6%	1,574	27.6%	83	27.9%	100	27.8%	
>= 30.0	1,364	21.4%	1,120	19.6%	92	30.9%	152	42.2%	
Race									
Asian	527	8.4%	416	7.4%	50	17.1%	61	17.2%	<0.001
Black	473	7.5%	418	7.4%	17	5.8%	38	10.7%	
Caucasian/white	4,049	64.2%	3,692	65.3%	181	61.8%	176	49.6%	
Hispanic/Latino	577	9.2%	520	9.2%	21	7.2%	36	10.1%	
Other	680	10.8%	612	10.8%	24	8.2%	44	12.4%	
Cigarette smoker									
No	5,724	93.3%	5,122	93.1%	276	94.5%	326	95.0%	0.133
Smoker	411	6.7%	378	6.9%	16	5.5%	17	5.0%	
Parity									
Nulliparous	2,763	43.4%	2,519	44.2%	107	35.9%	137	38.1%	0.002
Multiparous	3,598	56.6%	3,184	55.8%	191	64.1%	223	61.9%	

Table 3. 2 Population characteristics of subjects included in retrospective analysis of serum PAPP-A and glycemic state.

Data are presented as mean and percent of the subjects included in the study.

99

Adaptations of adipose tissue during pregnancy in humans

To characterize the changes that occur in adipose tissue during pregnancy, we compared total gene expression of subcutaneous (SQ) and omental (OM) adipose tissue obtained during cesarean section from normoglycemic pregnant subjects with those of non-diabetic, non-pregnant subjects obtained during gastric bypass surgery as described previously (Rojas-Rodriguez et al., 2015) (Gealekman et al., 2011) (Table 2.1 and Table 2.2) . We reanalyzed this data set using hierarchical clustering of the 1200 genes displaying the highest median absolute deviation among the four groups. This analysis resulted in four distinct clusters, segregated by both depot and pregnancy state (Figure 3.1a). Among the genes defining these clusters were a set that was highly enriched in pregnancy in both subcutaneous and omental depots (Figure 3.1a, bracket). To identify the specific genes and pathways modified by pregnancy in both depots, we performed differential expression analysis (Figure 3.1b,c). *IGFBP5* was the most upregulated gene, increasing by more than 60-fold and 20-fold in subcutaneous and omental adipose depots, respectively (Figure 3.1b,c). Notably, pathway enrichment analysis identified a central regulatory arm of the IGF signaling axis, the growth hormone receptor signaling pathway, among other significantly enriched pathways related to metal binding, IL-6 signaling, and heat stress response. (Figure 3.1d).

100
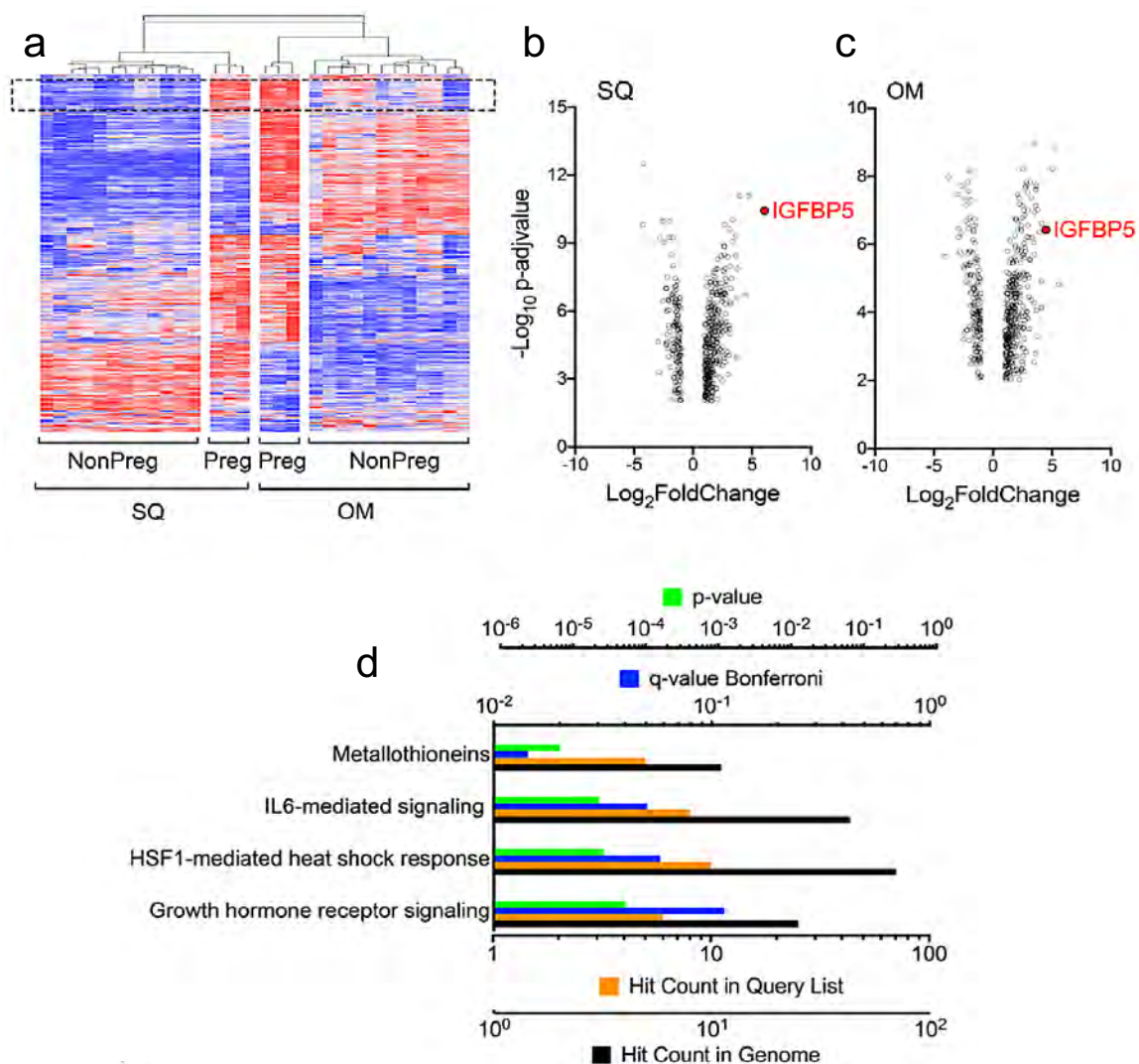
Figure 3. 1 Analysis of adipose tissue global gene expression changes highlights a particular transcriptomic signature associated with pregnancy.

(a) Hierarchical clustering of genes expressed in subcutaneous (SQ) or omental (OM) adipose tissue of non-pregnant or pregnant women. **(b,c)** Volcano plots of genes modulated by pregnancy in both depots, as expressed in each depot; IGFBP genes detected are highlighted. **(d)** KEGG enrichment analysis of genes modulated by pregnancy in both depots.

101

To distinguish adipose tissue responses specific to pregnancy relatively independent of BMI, we obtained a separate cohort of samples by needle biopsy of SQ adipose tissue from weight matched non-pregnant women (Table 3.1). The changes in adipocyte size and number are presented in Figure 3.2. The mean adipocyte size was significantly altered by pregnancy and it was the major change between cohorts (Figure 3.2b). This difference is attributable to adipocyte hypertrophy (Figure 3.2c), with a negligible decrease in the number of small adipocytes, suggesting compensatory hyperplasia during pregnancy.
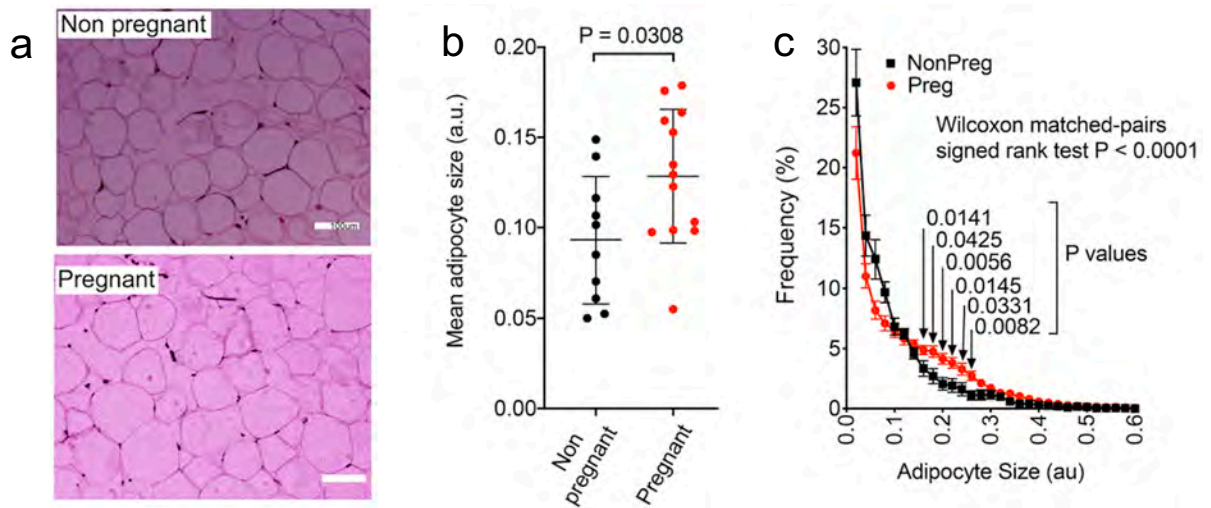
Figure 3. 2 Adipocyte size changes are observed in human pregnancy.

(a) Representative H&E stains of SQ adipose tissue sections from a non-pregnant (above) and a pregnant (below) subject with similar BMIs (26). **(b,c)** Mean adipocyte size **(b)** and frequency size distributions **(c)** from H&E stains of adipose tissue sections. Adipocytes were measured in 5-10 slides from each subject, and the mean and SEM of each subject depicted in the plots. Difference of histograms was calculated using the Wilcoxon matched pairs test as implemented in GraphPad Prism 8, and individual P values for differences at each size range calculated using multiplicity adjusted (Sidak) student t-tests.

103

As adipose tissue is densely vascularized and adipocyte progenitors are localized along the adipose tissue vasculature, we examined whether pregnancy would induce changes in the microvasculature by staining tissue fragments with lectin. This staining yielded qualitative changes in the microvasculature, with decreased homogeneity of vessel diameter and discontinuity and tortuosity of vessel structure in pregnant subject biopsies (Figure 3.3a). To quantify these observations, we applied an imaging algorithm to measure connectivity between regions. The microvasculature from pregnant women was less connected compared to that of non-pregnant women, as determined by a decrease in region size per image and an increased in total regions per image (Figure 3.3b-d). These results reveal that human adipose tissue adapts to pregnancy with a robust increase in expression of IGF signaling pathway genes, specifically *IGFBP5*, and with hypertrophy, hyperplasia and changes in microvasculature dynamics.
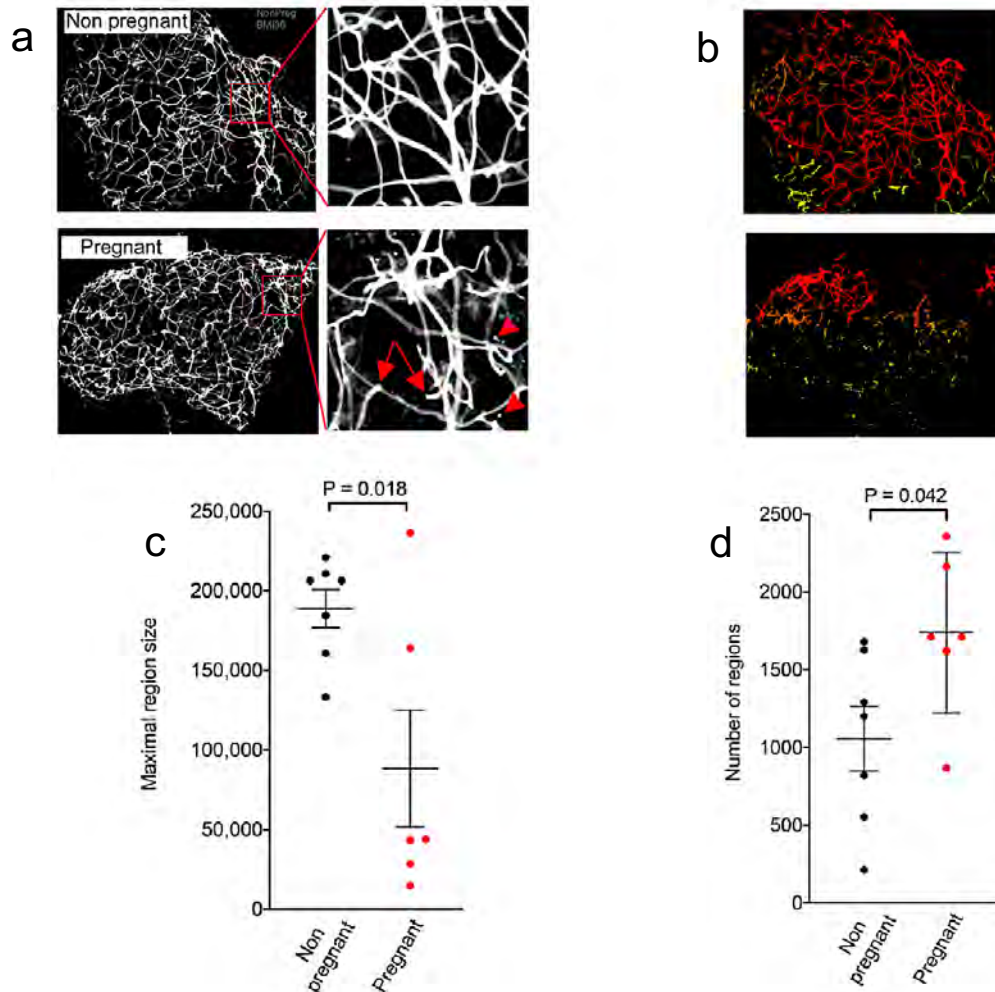
Figure 3. 3 Human gestation is accompanied by alterations in the microvasculature architecture of adipose tissue.

(a) Whole mount lectin staining of adipose tissue from a non-pregnant (above) and a pregnant (below) subject with similar BMIs (30). Arrows in magnified area indicate discontinuity, and arrowheads lectin positive cells separated from vessel structures seen in images from pregnant subjects. **(b)** Continuous regions detected in the image using Image J connected regions algorithm. **(c)** Maximal region size and **(d)** number of regions measured in 5-10 whole mount images from each subject, and the mean and SEM of each subject depicted in the plots. Statistical significance of the difference between pregnant and non-pregnant was calculated using student t-tests.

PAPP-A levels are directly associated with glycemic control in human pregnancy

If the IGFBP/IGF axis in adipose tissue is important for the regulation of glucose homeostasis during pregnancy, we reasoned that circulating levels of PAPP-A, which increases in proportion to placental growth and specifically cleaves IGFBPs 2, 4 and 5, would be associated with glycemia and/or disrupted glucose metabolism. Levels of circulating PAPP-A were significantly lower in serum samples of pregnant subjects with abnormal glucose tolerance (AGT) and GDM compared to those with normal glucose tolerance (NGT) (Table 3.2 and Figure 3.4 a). We separated all PAPP-A serum values in the population into quartiles (Figure 3.4b) and calculated the odds of AGT and GDM occurring in each PAPP-A quartile. Compared to the highest quartile of PAPP-A the odds of AGT (Figure 3.5a) and GDM (Figure 3.5b) significantly increased as the value of PAPP-A decreased.
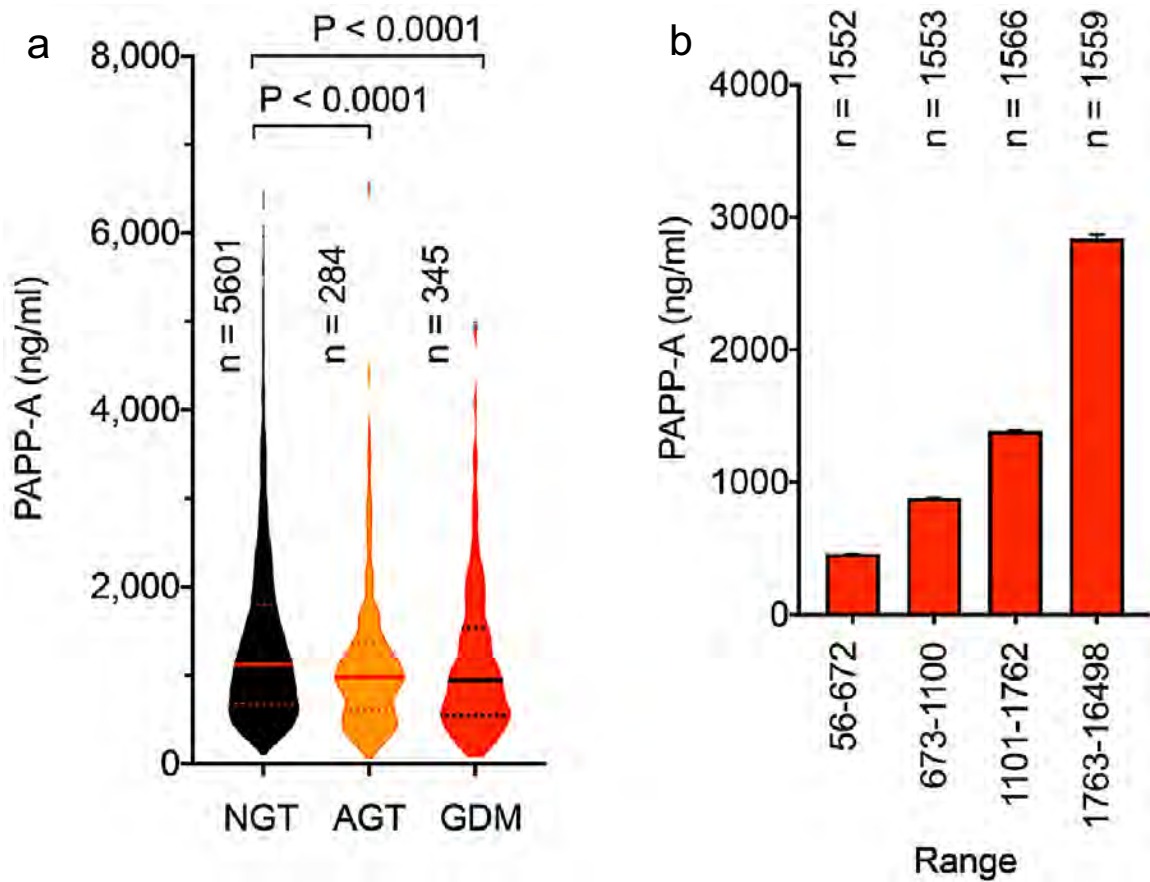
Figure 3. 4 First trimester serum PAPP-A levels are decreased in AGT and GDM gravidas.

(a) Violin plots of PAPP-A levels at 10-14 weeks of gestation in women categorized as normal glucose tolerance (NGT, n=5601), abnormal glucose tolerance (AGT, n=284), and gestational diabetes (GDM, n=345) at week 24-28 of gestation. Statistical significance was estimated using ordinary one-way ANOVA corrected for multiple comparisons using the Sidak test. Median and quartile values are indicated. **b.** Range of PAPP-A values comprising each quartile.
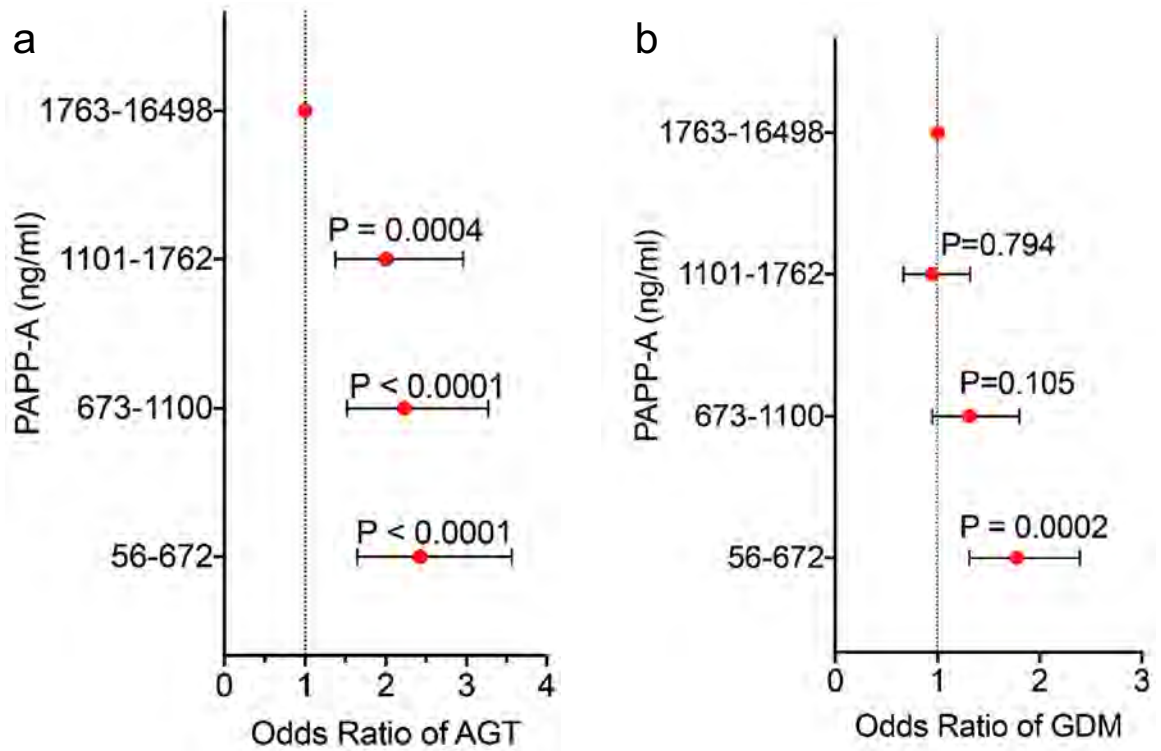
Figure 3. 5 Low first trimester serum PAPP-A is associated with the presence of abnormal glucose tolerance and gestational diabetes later in gestation.

(a,b) Odds ratio and 95% CI for AGT **(a)** or GDM **(b)**. Statistical significance between comparisons to the highest quartile was done using Fisher's exact test.

PAPP-A results are routinely expressed as multiples of the median (MOM) in order to compare values across different gestational ages, as well as factors strongly associated with increased diabetes risk in non-pregnant populations- BMI, ethnicity and smoking status. Despite these adjustments we find that the odds of GDM significantly increased as the quartile of serum PAPP-A MOM decreased (Figure 3.6) compared to the highest quartile, indicating that PAPP-A MOM is related to the odds of developing gestational diabetes independent of other factors related to diabetes in general.
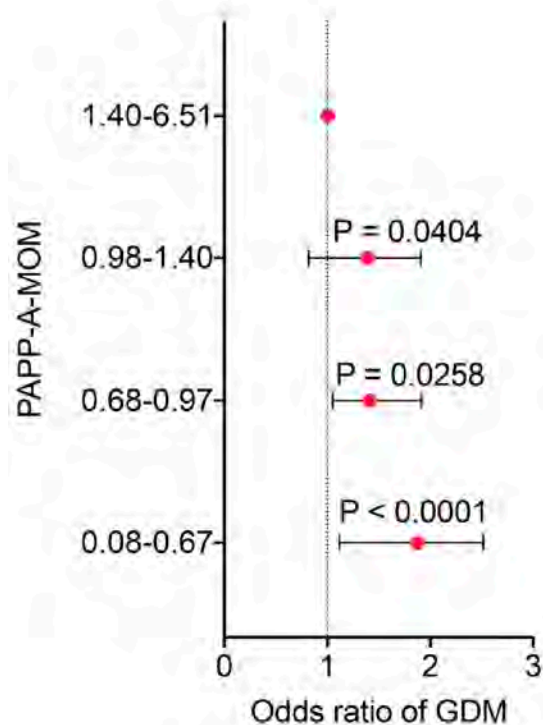
Figure 3. 6 Low first trimester PAPP-A MoM is associated with the development of gestational diabetes later in gestation.

Odds ratio and 95% CI of GDM at different quartiles of PAPP-A MOM. Statistical significance between comparisons to the highest quartile was done using Fisher's exact test.

110

To test PAPP-A association with systemic glucose metabolism independent of other factors, we compared serum PAPP-A MOM with blood glucose values after 1h of a 50g dextrose load in subjects diagnosed with normal glucose tolerance. We observed a linear, inverse relationship between PAPP-A MOM values and glucose levels (Figure 3.7).
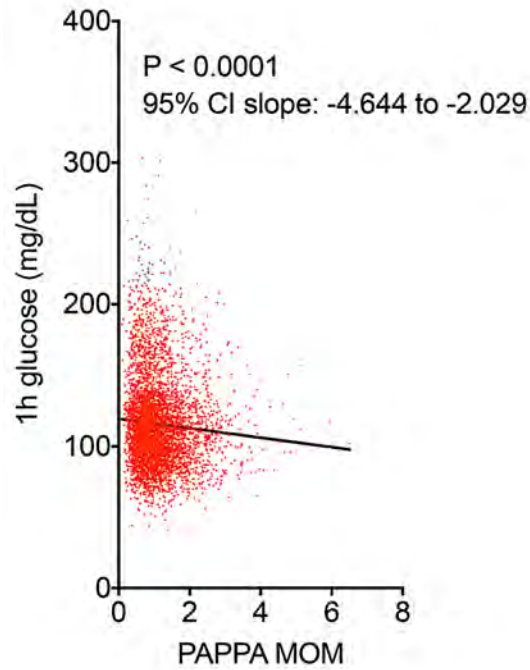
Figure 3. 7 PAPP-A MoM has a negative correlation with 1 hr glucose values of normoglycemic pregnant women.

Linear regression between PAPP-A MOM and 1-hr glucose values at week 24-28 of gestation (n=862).

112

Human adipose tissue expandability is increased in pregnancy and stimulated by PAPP-A

To directly explore whether PAPP-A cleavage of IGFBPs could mediate our observed pregnancy-induced adaptations of adipose tissue, we used an *in vitro* system that measures adipose tissue expandability. When small fragments of human adipose tissue are implanted in MatriGel and cultured in EGM2-MV medium, endothelial and mesenchymal progenitor cells emerge and proliferate, gradually covering a larger area around the explant. The area of the capillary growth covered by the sprouting cells is a surrogate measure of adipose tissue expandability, varying as a function of depot of origin and physiological state of the donor (Gealekman et al., 2011). We found that explants from subcutaneous adipose tissue from pregnant women display greater expandability compared to those from non-pregnant women (Figure 3.8), consistent with evidence of increased hyperplasia (Figure 3.2). Moreover, subcutaneous adipose tissue explants from pregnant women cultured in the presence of recombinant human PAPP-A displayed significantly greater growth area compared to vehicle control (Figure 3.9a). The effect of recombinant PAPP-A was dose dependent and increased over time in culture (Figure 3.9b). These results demonstrate that PAPP-A can directly stimulate adipose tissue expandability and are consistent with a direct effect in mediating the adaptations of adipose tissue in pregnancy.

113
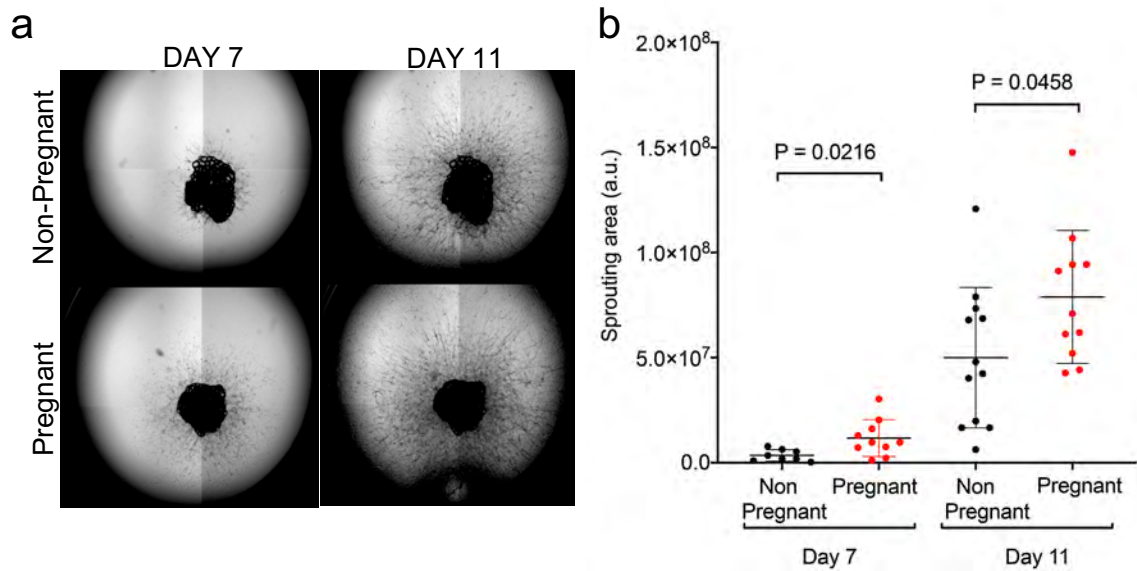
Figure 3. 8 *In vitro* adipose tissue expandability is enhanced in pregnant women.

(a) Representative images of sprouts emerging from adipose tissue explants obtained from normoglycemic non-pregnant or pregnant women. Images were taken at 7 and 11 days of culture. **(b)** Quantification of sprouting area from AT explants at the indicated timepoints. Between 10-30 explants were embedded for each subject, and each symbol represents the mean sprouting area of all explants per subject. Plotted are the means and SEM of non-pregnant and pregnant subjects. Statistical significance of differences between groups was quantified using unpaired, two-tailed student t-tests.

114
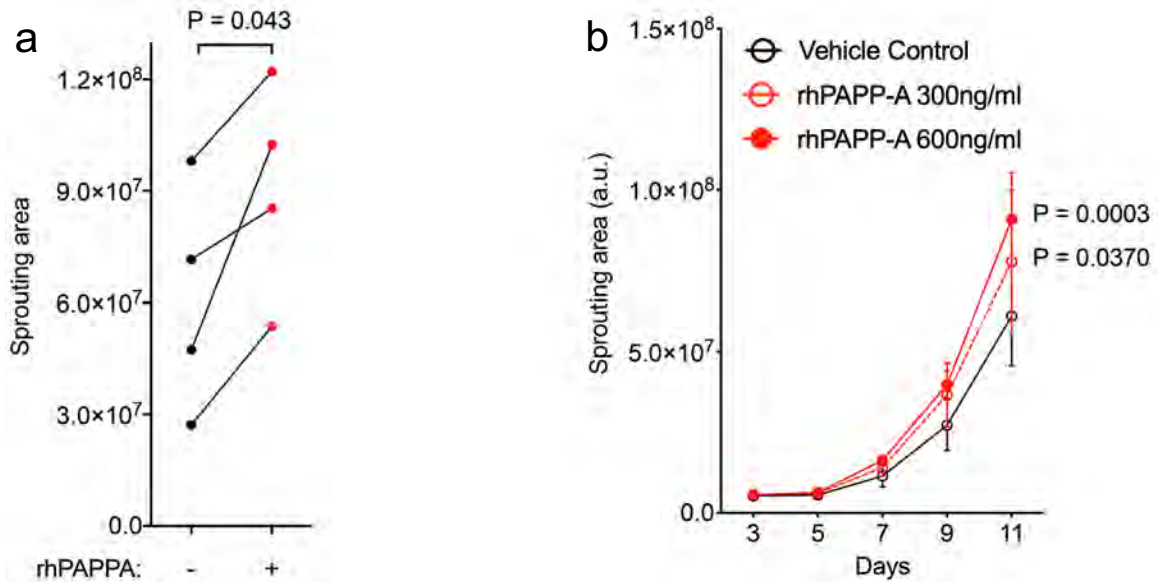
Figure 3. 9 PAPP-A stimulates *in vitro* adipose tissue expandability in pregnant women.

(a) Explants from four pregnant women (n=5-10 explants per subject) were cultured in the presence of recombinant human PAPP-A (rhPAPP-A, 600ng/ml) or vehicle control. Statistical significance of the difference between control and treated explants was calculated using paired student t-tests. **(b)** Mean and SEM of the sprouting area of 5-10 explants from 4 separate subjects treated with vehicle control or in the presence of the indicated concentration of recombinant human PAPP-A (rhPAPP-A) for the times shown. Statistical significance of the difference between doses at each timepoint was calculated using repeated measures two-way ANOVA.

115

Papp-a deletion in mice prevents pregnancy-associated adipose tissue remodeling

To directly test the role of PAPP-A in remodeling adipose tissue during pregnancy *in vivo*, we studied mice in which the *Papp-a* gene was ablated (KO). These mice have been characterized as proportional dwarfs, being viable and fertile but exhibiting only 60% of wild-type (WT) size (Conover et al., 2004). Pregnancy induced a similar proportional increase in body weight in WT littermate controls and KO mice (Figure 3.10a) which was attributable to an increase in lean body mass with no significant change in fat mass (Figure 3.10b,c) consistent with studies of pregnancy in C57BL6 mice (Qiao et al., 2019). As a percent of total (lean + fat mass), lean and fat mass are affected by pregnancy to a similar extent between WT and KO mice (Figure 3.11).
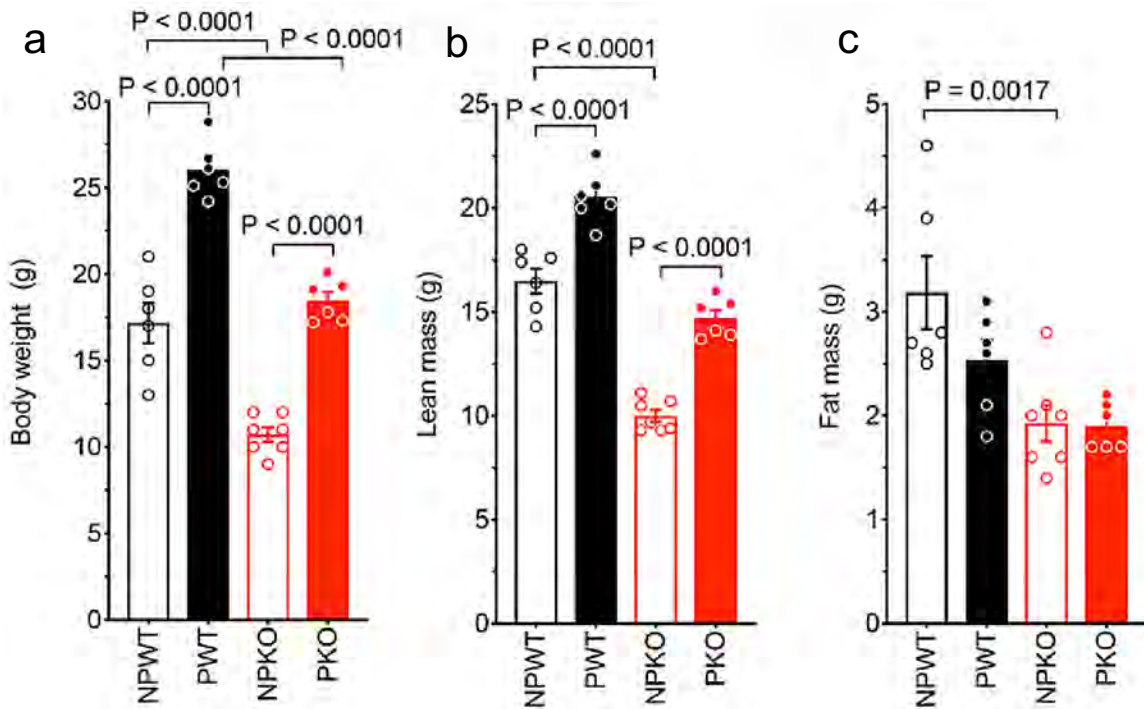
Figure 3. 10 Pregnancy increases body weight and lean mass in WT and *Papp-a* KO mice.

(a) Body weight, **(b)** total lean mass, and **(c)** total fat mass from non-pregnant or pregnant wild-type (NPWT, PWT) or non-pregnant or pregnant *Papp-a* KO mice (NPKO, PKO). Statistical significance was assessed using ordinary one-way ANOVA corrected with the Sidak test for multiple comparisons.

117
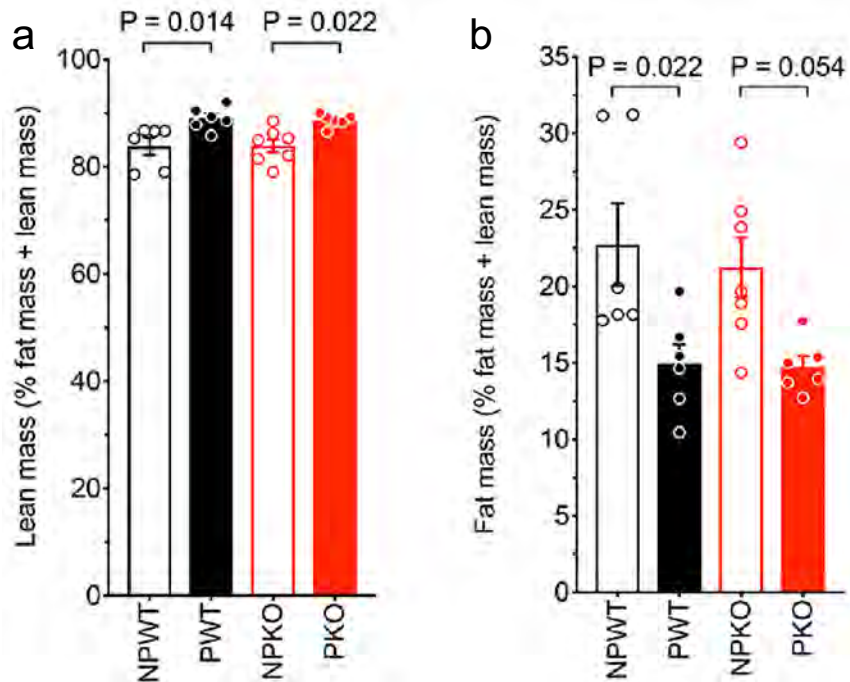
Figure 3. 11 Pregnancy decreases fat mass percent in WT and *Papp-a* KO mice.

(a) Lean mass and **(b)** fat mass percent from non-pregnant or pregnant wild-type (NPWT, PWT) or non-pregnant or pregnant *Papp-a* KO mice (NPKO, PKO). Fat and lean mass percent were calculated by normalizing to lean + fat mass. Statistical significance was assessed using ordinary one-way ANOVA corrected with the Sidak test for multiple comparisons.

118

To examine pregnancy-induced adipose tissue adaptations and the role of Papp-a, we dissected and analyzed all discernable depots in WT and KO pregnant and non-pregnant mice, following the guidelines published by S. Cinti (Cinti, 2015) (Figure 3.12).

119
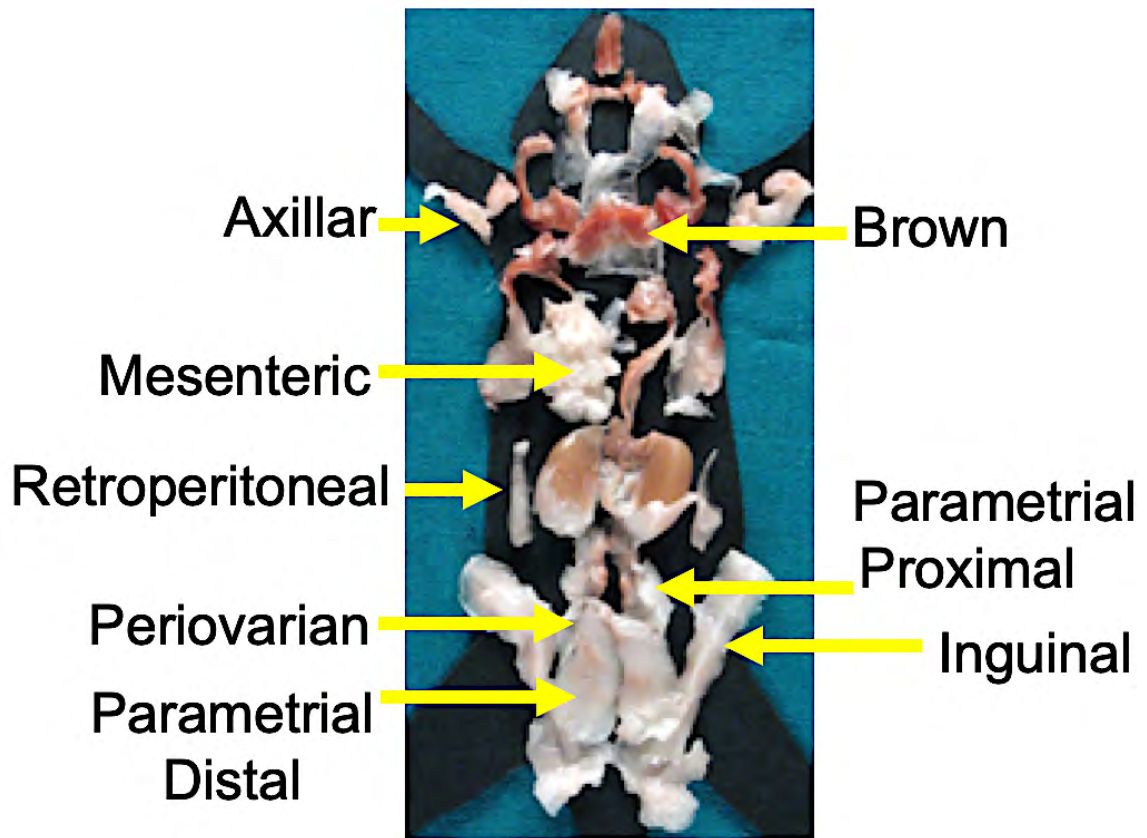
Figure 3. 12 Anatomical localization of the adipose organ.

Representative figure of the anatomical localization for the fat pads analyzed (adapted from (Cinti, 2015)).

The largest depot was the parametrial, which was comprised of a proximal and distal sections relative to the uterine horn. In WT mice, pregnancy caused a decrease in the mass of all depots with the exception of axillary and interscapular brown adipose tissue (iBAT) depots. However, with the exception of the inguinal depot, we did not see pregnancy-induced changes in depot mass in the KO mice (Figure 3.13).
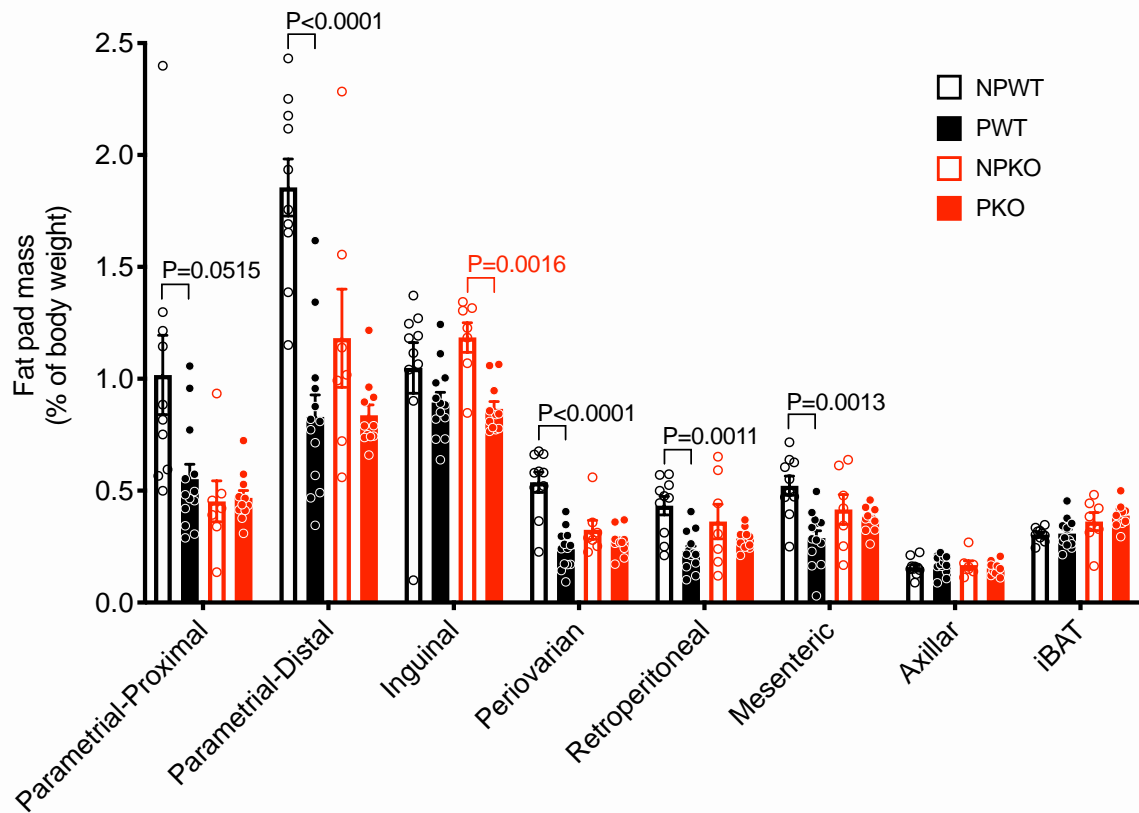
Figure 3. 13 Changes in fat pad mass due to pregnancy are absent in *Papp-a* KO.

Mass of individual fat depots expressed as % body weight. Statistical significance of differences in gene expression between non-pregnant and pregnant state within each depot was measured using multiplicity (Holm-Sidak) adjusted t-tests.

Histochemical analysis of each fat pad (Figure 3.14) revealed significant changes in the distribution of fat cell sizes induced by pregnancy in the parametrial, inguinal, periovarian, retroperitoneal and mesenteric depots. With the exception of the parametrial-distal depot, these depots exhibited a decrease in adipocyte size, and an accumulation of small-sized adipocytes, suggesting hyperplastic growth in the mentioned fat pads. These changes in adipocyte size distribution did not occur in fat depots from *Papp-a* KO mice demonstrating that pregnancy-induced remodeling of fat depots is dependent on Papp-a.

www.manaraa.com
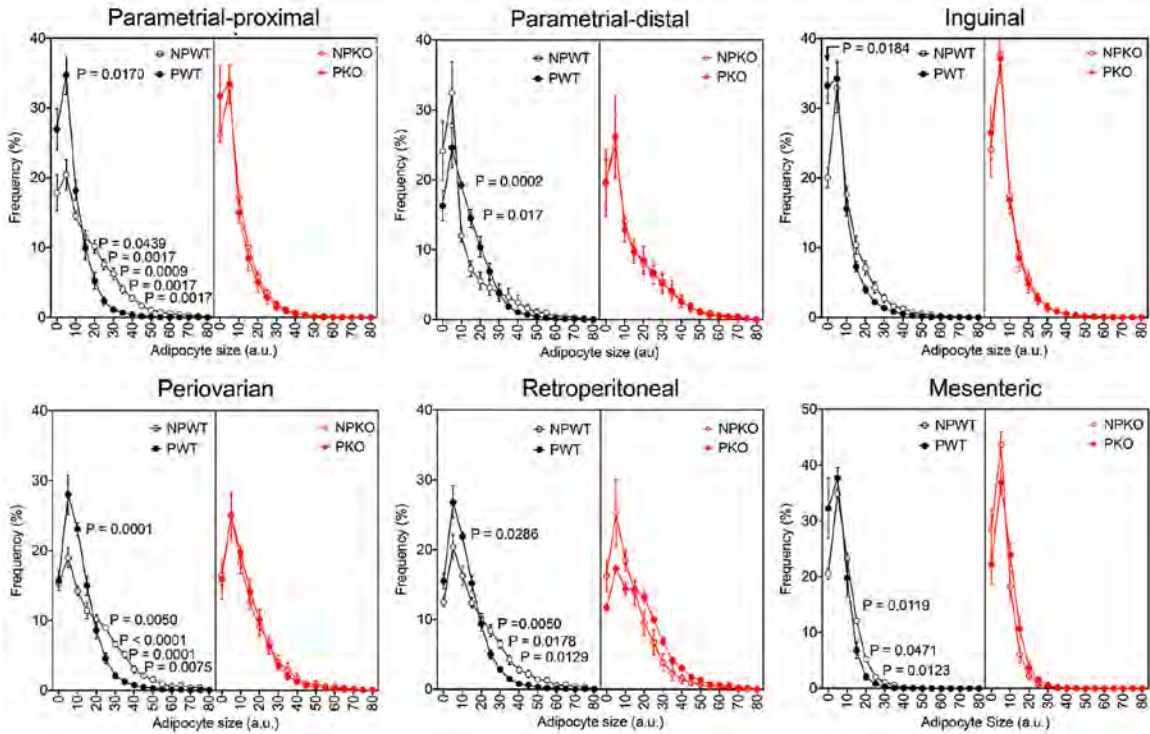
Figure 3. 14 Pregnancy-induced variations in adipocyte size and number are not observed in *Papp-a* KO.

Frequency distribution of adipocyte sizes measured in H&E stained sections (~10 images per depot) from 6 mice per group. Data shown is from the fat pads with the most difference between non-pregnant and pregnant mice. For each of the indicated fat pads, statistical significance of differences in frequency at each bin between non-pregnant and pregnant state was measured using multiplicity (Holm-Sidak) adjusted t-tests.

During the examination of H&E inguinal and axillar adipose tissue sections, we noticed an interesting feature regarding the presence of alveoli in the pregnant mice (Figure 3.15, 3.16), as the inguinal mammary glands are embedded along the inguinal fat pad and the thoracic mammary glands are located in close proximity to the axillar fat pad. The pregnant KO had reduced alveolar development in the inguinal (Figure 3.15) and their presence was almost absent in the axillar pad (Figure 3.16) as observed by both H&E staining of adipose tissue sections (Figure 3.15a, 3.16a) and whole-mount carmine-alum staining of inguinal and axillar fat pads (Figure 3.15b, 3.16b). These results, in addition to the absence of adipocyte size and number changes demonstrate that the adaptations of adipose tissue to gestation are regulated by Papp-a.
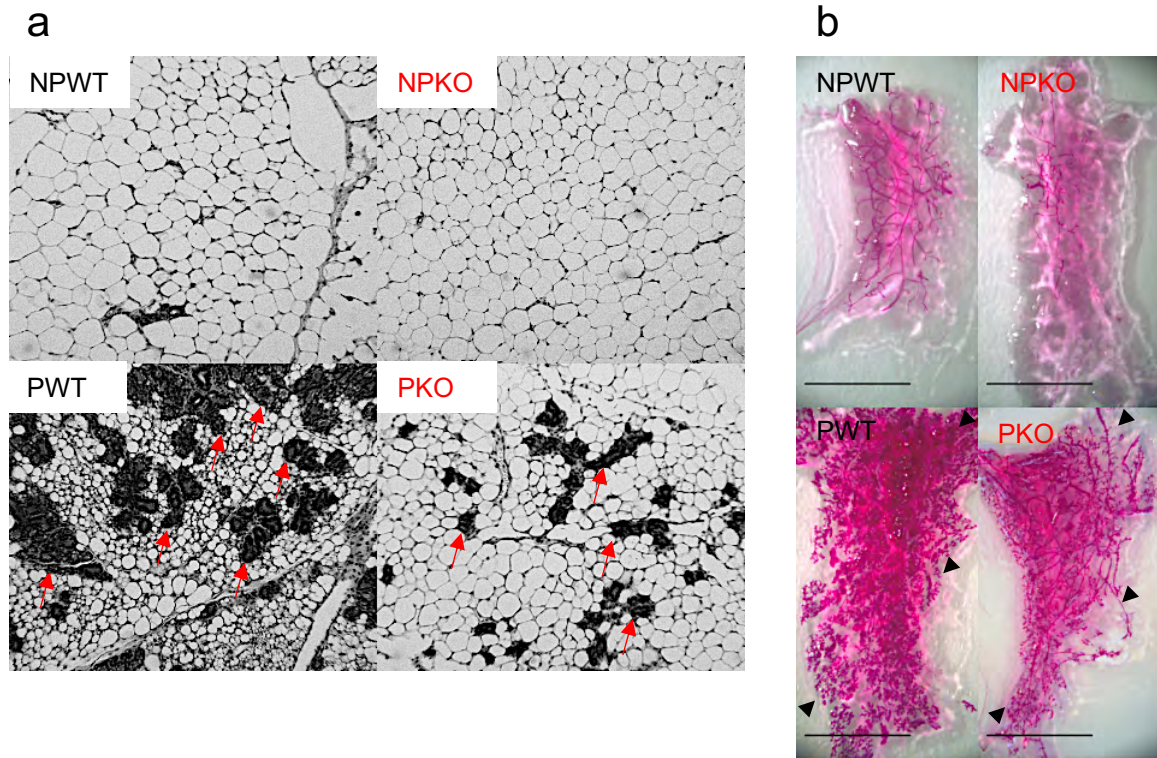
Figure 3. 15 The development of inguinal mammary glands in response to pregnancy is reduced in *Papp-a* KO.

(a) Inguinal adipose tissue sections stained with H&E from non-pregnant or pregnant wild-type (NPWT, PWT) or non-pregnant or pregnant *Papp-a* KO mice (NPKO, PKO). Images were taken under 10X magnification. Red arrows indicate the alveoli embedded within the inguinal fat pad. In addition, note the difference in adipocyte size between NPWT and PWT, which is not noticeable between NPKO and PKO. **(b)** Inguinal whole-mount carmine alum staining of non-pregnant or pregnant wild-type (NPWT, PWT) or non-pregnant or pregnant *Papp-a* KO mice (NPKO, PKO). Black arrowheads indicate areas of the epithelial ductal system. The development of mammary ducts in response to pregnancy is reduced in the PKO. Scale bar 0.5 cm.
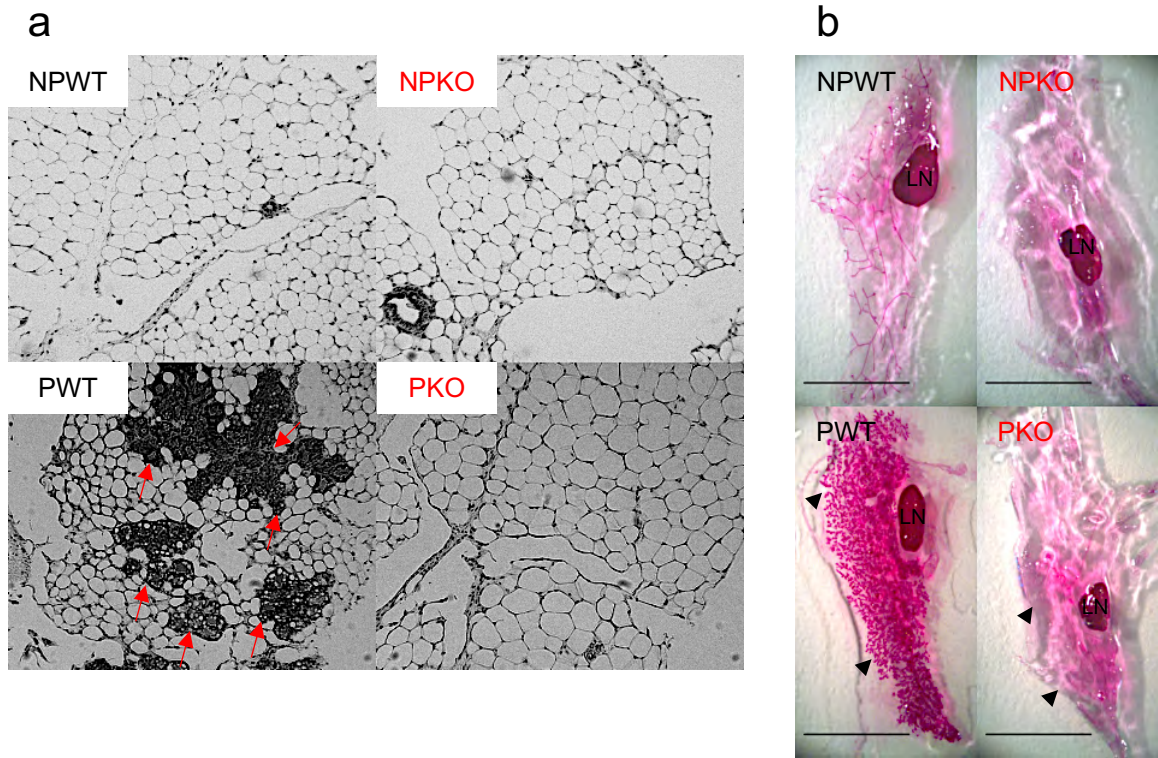
Figure 3. 16 The development of mammary glands proximal to the axillar fat pad in response to pregnancy is absent in *Papp-a* KO.

(a) Axillar adipose tissue sections stained with H&E from non-pregnant or pregnant wild-type (NPWT, PWT) or non-pregnant or pregnant *Papp-a* KO mice (NPKO, PKO). Images were taken under 10X magnification. Red arrows indicate the alveoli embedded within the inguinal fat pad. **(b)** Axillar whole-mount carmine alum staining from non-pregnant or pregnant wild-type (NPWT, PWT) or non-pregnant or pregnant *Papp-a* KO mice (NPKO, PKO). LN, lymph node. Black arrowheads indicate areas of the epithelial ductal system. The development of mammary ducts in response to pregnancy is absent in the PKO. Scale bar 0.5 cm.

www.manaraa.com

To investigate if the absence of Papp-a would impair adipose tissue expandability in gestation, we performed the *in vitro* expandability assay with explants of inguinal fat pad (Figure 3.17). Similar to the observed adipocyte hyperplasia, pregnancy induced the growth of capillary sprouts in the inguinal adipose explants of WT mice. In the KO, pregnancy did not stimulate adipose tissue expandability. These results further support the evidence that Papp-a is involved in the adaptations of adipose tissue growth in gestation.
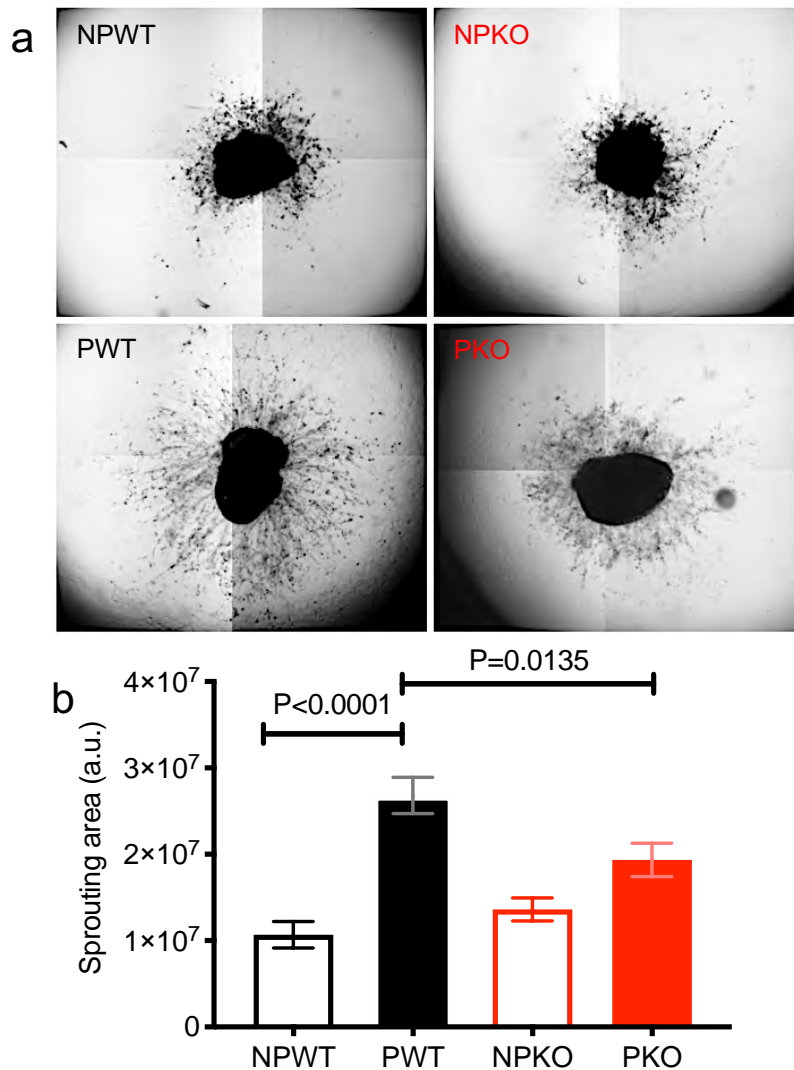
Figure 3. 17 Adipose tissue expandability is impaired in pregnant Papp-a KO.

(a) Representative images of sprouts emerging from adipose tissue explants obtained from non-pregnant or pregnant wild-type (NPWT, PWT) or non-pregnant or pregnant *Papp-a* KO mice (NPKO, PKO). Images were taken at 11 days of culture. **(b)** Quantification of sprouting area from AT explants. Between 20-30 explants were embedded for each mouse, and each symbol represents the mean sprouting area of all explants per group. Plotted are the means and SEM of non-pregnant and pregnant WT and KO mice (n=3 per group). Statistical significance was assessed using ordinary one-way ANOVA corrected with the Sidak test for multiple comparisons.

To explore the mechanisms by which Papp-a is required for adipose tissue remodeling, we measured the expression of genes in the IGF signaling pathway in fat depots from pregnant and non-pregnant WT and *Papp-a* KO mice (Figures 3.18-3.23). Depot, genotype and pregnancy-dependent changes were analyzed by three-way ANOVA. While all genes analyzed varied significantly by depot, only *Igf-2* (Figure 3.19), *Igfbp2* (Figure 3.20) and *Igfbp4* (Figure 3.21) significantly changed in pregnancy, and *Papp-a* trended towards a significant increase in the mesenteric depot in pregnancy (Figure 3.18). *Igfbp2* was the gene most strongly upregulated by pregnancy, mostly in the inguinal and axillary depots. The only gene significantly affected by the absence of Papp-a was *Igf-2,* which was upregulated in both inguinal and axillary depots to a greater extent in *Papp-a* KO than in WT mice.
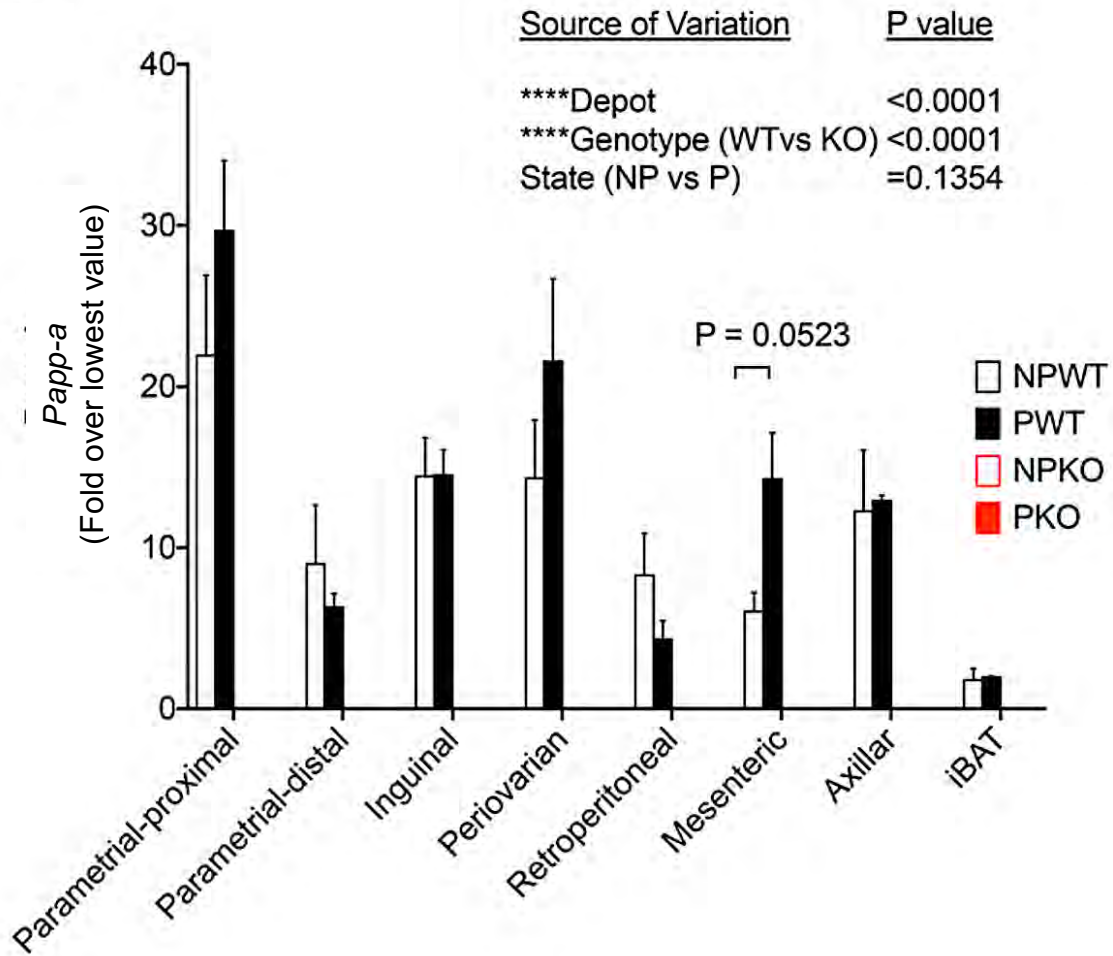
Figure 3. 18 *Papp-a* expression differs between fat pads of wild-type mice.

Real-time qPCR for *Papp-a* in fat depots from non-pregnant or pregnant wild-type (NPWT, PWT) or non-pregnant or pregnant *Papp-a* KO mice (NPKO, PKO). Fold expression values were calculated by normalization to the lowest expression value in the dataset. Graphs show mean and SEM of n=3 mice per group assayed in triplicate. Statistical significance of the differences between fat depot, genotype and pregnant state for each gene were calculated using three-way ANOVA corrected for multiple comparisons using the Tukey test. Statistical significance of differences in gene expression between states within individual depots were measured using multiplicity adjusted t-tests.

131
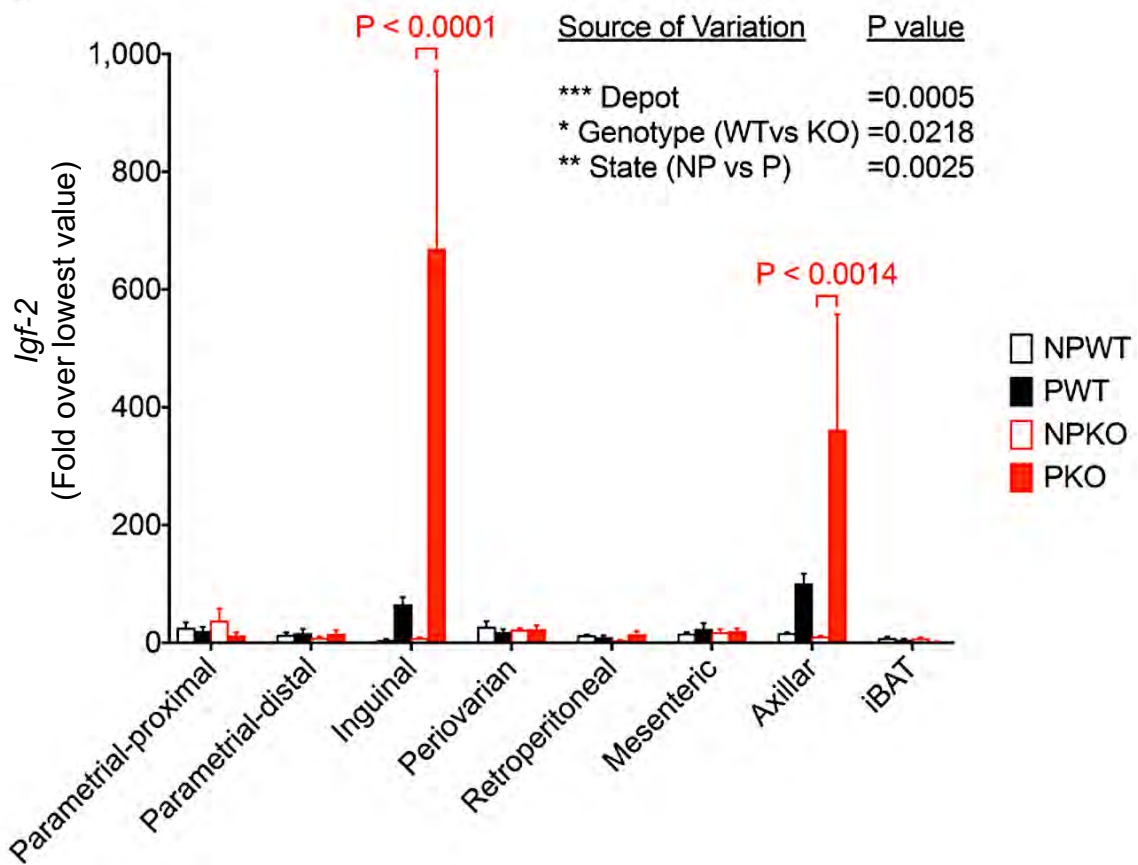
Figure 3. 19 *Igf-2* expression reveals compensation for *Papp-a* deletion in specific adipose depots of pregnant *Papp-a* KO.

Real-time qPCR for *Igf-2* in fat depots from non-pregnant or pregnant wild-type (NPWT, PWT) or non-pregnant or pregnant *Papp-a* KO mice (NPKO, PKO). Fold expression values were calculated by normalization to the lowest expression value in the dataset. Graphs show mean and SEM of n=3 mice per group assayed in triplicate. Statistical significance of the differences between fat depot, genotype and pregnant state for each gene were calculated using three-way ANOVA corrected for multiple comparisons using the Tukey test. Statistical significance of differences in gene expression between states within individual depots were measured using multiplicity adjusted t-tests.
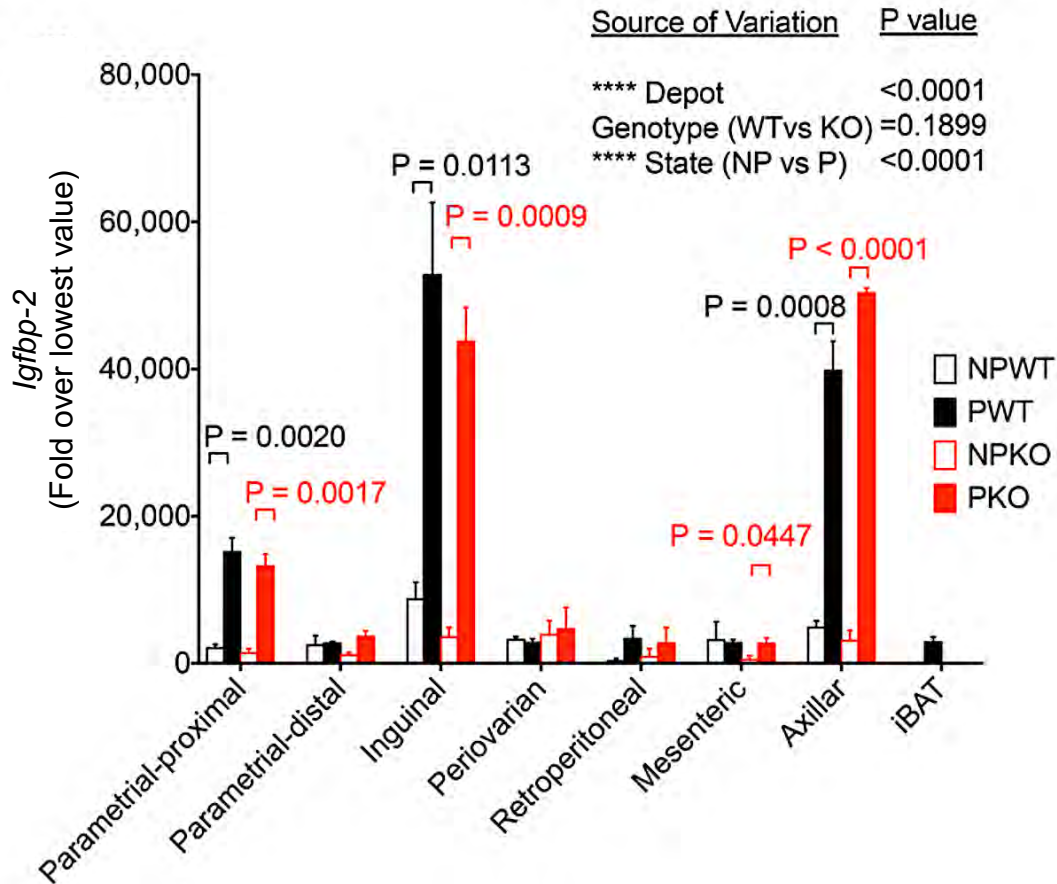
Figure 3. 20 *Igfbp2* expression is enhanced by pregnancy and differs between adipose depots in wild-type and *Papp-a* KO.

Real-time qPCR for *Igfbp2* in fat depots from non-pregnant or pregnant wild-type (NPWT, PWT) or non-pregnant or pregnant *Papp-a* KO mice (NPKO, PKO). Fold expression values were calculated by normalization to the lowest expression value in the dataset. Graphs show mean and SEM of n=3 mice per group assayed in triplicate. Statistical significance of the differences between fat depot, genotype and pregnant state for each gene were calculated using three-way ANOVA corrected for multiple comparisons using the Tukey test. Statistical significance of differences in gene expression between states within individual depots were measured using multiplicity adjusted t-tests.
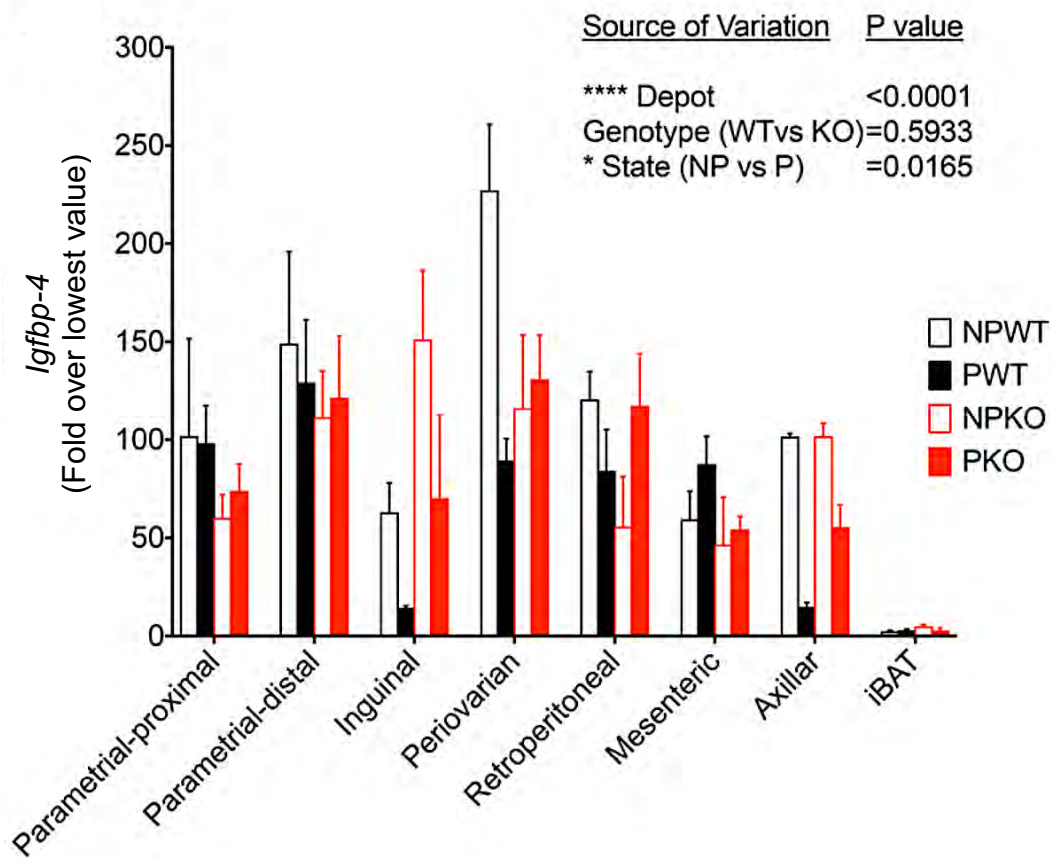
Figure 3. 21 *Igfbp4* expression varies between fat depots and pregnant state in wild-type and *Papp-a* KO.

Real-time qPCR for *Igfbp4* in fat depots from non-pregnant or pregnant wild-type (NPWT, PWT) or non-pregnant or pregnant *Papp-a* KO mice (NPKO, PKO). Fold expression values were calculated by normalization to the lowest expression value in the dataset. Graphs show mean and SEM of n=3 mice per group assayed in triplicate. Statistical significance of the differences between fat depot, genotype and pregnant state for each gene were calculated using three-way ANOVA corrected for multiple comparisons using the Tukey test.

134

Figure 3. 22 *Igfbp5* expression is different in each fat pad of wild-type and *Papp-a* KO.

Real-time qPCR for *Igfbp5* in fat depots from non-pregnant or pregnant wild-type (NPWT, PWT) or non-pregnant or pregnant *Papp-a* KO mice (NPKO, PKO). Fold expression values were calculated by normalization to the lowest expression value in the dataset. Graphs show mean and SEM of n=3 mice per group assayed in triplicate. Statistical significance of the differences between fat depot, genotype and pregnant state for each gene were calculated using three-way ANOVA corrected for multiple comparisons using the Tukey test.

135
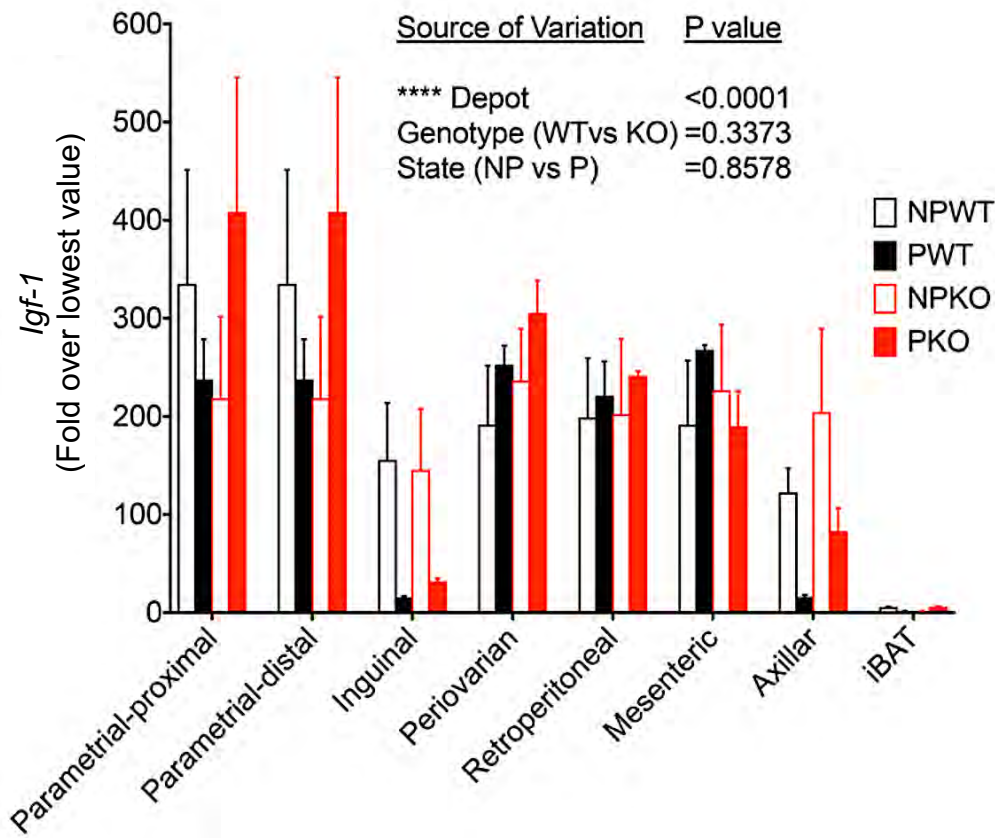
Figure 3. 23 *Igf-1* expression is different in each fat pad of wild-type and *Papp-a* KO.

Real-time qPCR for *Igf-1* in fat depots from non-pregnant or pregnant wild-type (NPWT, PWT) or non-pregnant or pregnant *Papp-a* KO mice (NPKO, PKO). Fold expression values were calculated by normalization to the lowest expression value in the dataset. Graphs show mean and SEM of n=3 mice per group assayed in triplicate. Statistical significance of the differences between fat depot, genotype and pregnant state for each gene were calculated using three-way ANOVA corrected for multiple comparisons using the Tukey test.

Papp-a deletion results in gestational insulin resistance

We then studied the metabolic consequences of the abnormalities in adipose tissue remodeling induced by Papp-a loss. Fasting blood glucose was lower in the pregnant state in both WT and KO mice, but was slightly higher in non-pregnant KO compared to WT mice (Figure 3.24). This was accompanied by trends towards higher basal insulin values in response to pregnancy, and also higher basal insulin values in KO mice compared to WT, although the data did not reach statistical significance (Figure 3.25).

137
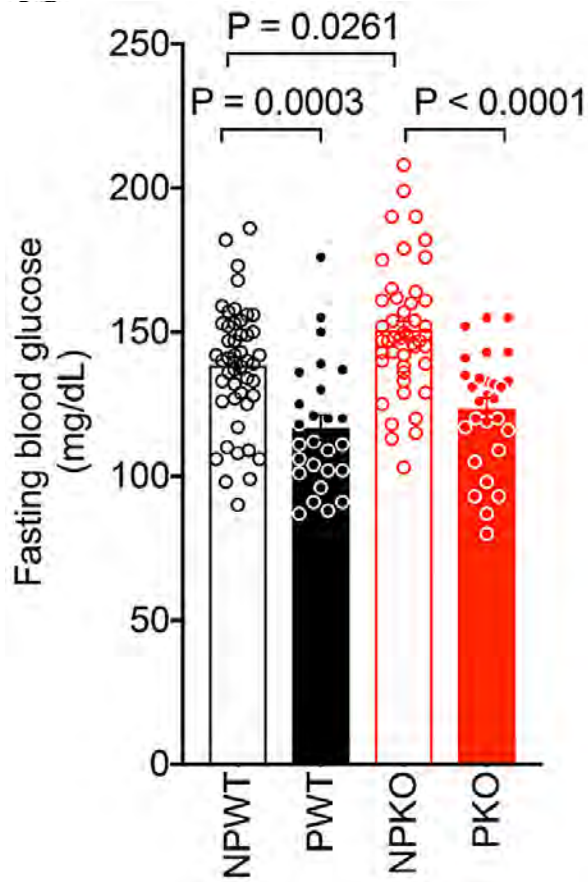
Figure 3. 24 Pregnancy reduces fasting glucose in both wild-type and *Papp-a* KO.

Blood glucose after a 6hr fast of 10-12-week old non-pregnant or pregnant wild-type (NPWT, PWT) or non-pregnant or pregnant *Papp-a* KO mice (NPKO, PKO). Statistical significance was assessed using ordinary one-way ANOVA corrected with the Sidak test for multiple comparisons.

138
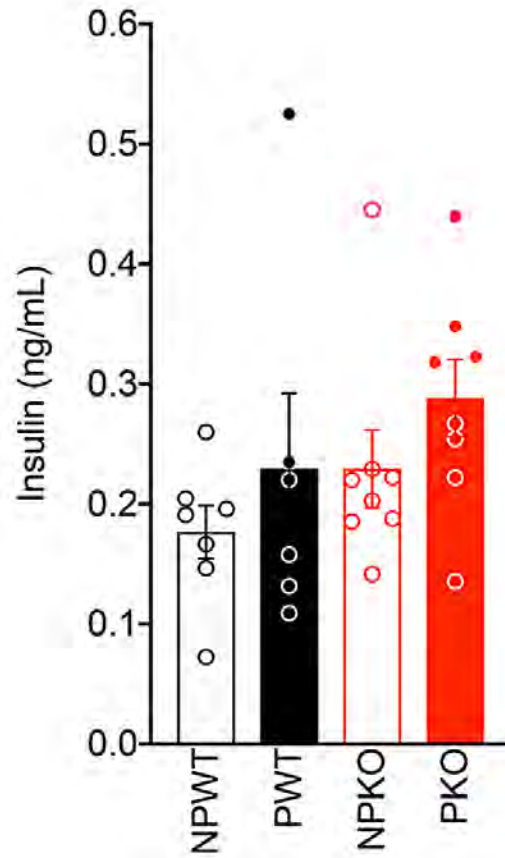
Figure 3. 25 Fasting insulin is not altered by pregnancy in wild-type and *Papp-a* KO.

Plasma insulin after a 4.5hr fast of 10-12-week old non-pregnant or pregnant wild-type (NPWT, PWT) or non-pregnant or pregnant *Papp-a* KO mice (NPKO, PKO). Statistical significance was assessed using ordinary one-way ANOVA corrected with the Sidak test for multiple comparisons.

139

To directly measure insulin sensitivity, we conducted insulin tolerance tests. These revealed a trend towards increased insulin resistance induced by pregnancy in WT mice, and this effect was much more pronounced in KO mice (Figure 3.26). Greater insulin secretion following glucose injection was seen in pregnant compared to the non-pregnant mice, however there were no differences due to *Papp-a* deletion (Figure 3.27). These results indicate that loss of Papp-a results in pregnancy-induced insulin resistance, without effects on β-cell insulin secretion.
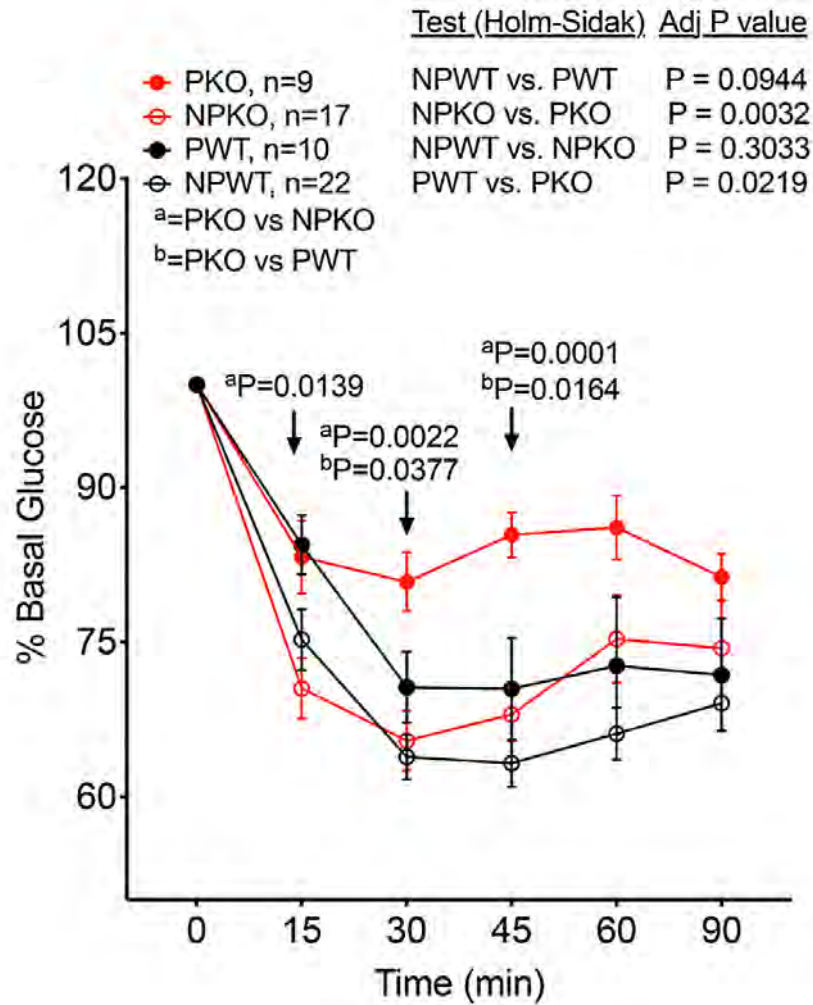
Figure 3. 26 Pregnant *Papp-a* KO exhibit reduced insulin sensitivity.

Percent of basal glucose from 10-12-week old non-pregnant or pregnant wild-type (NPWT, PWT) or non-pregnant or pregnant *Papp-a* KO mice (NPKO, PKO) during an insulin tolerance test (0.65 units of insulin/kg body weight) after 4.5 hr fast. Statistical significance between groups was assessed using repeated measures one-way ANOVA corrected for multiple comparisons using the Holm-Sidak test, and statistical significance of differences at each time point measured using multiplicity adjusted t-tests.

141
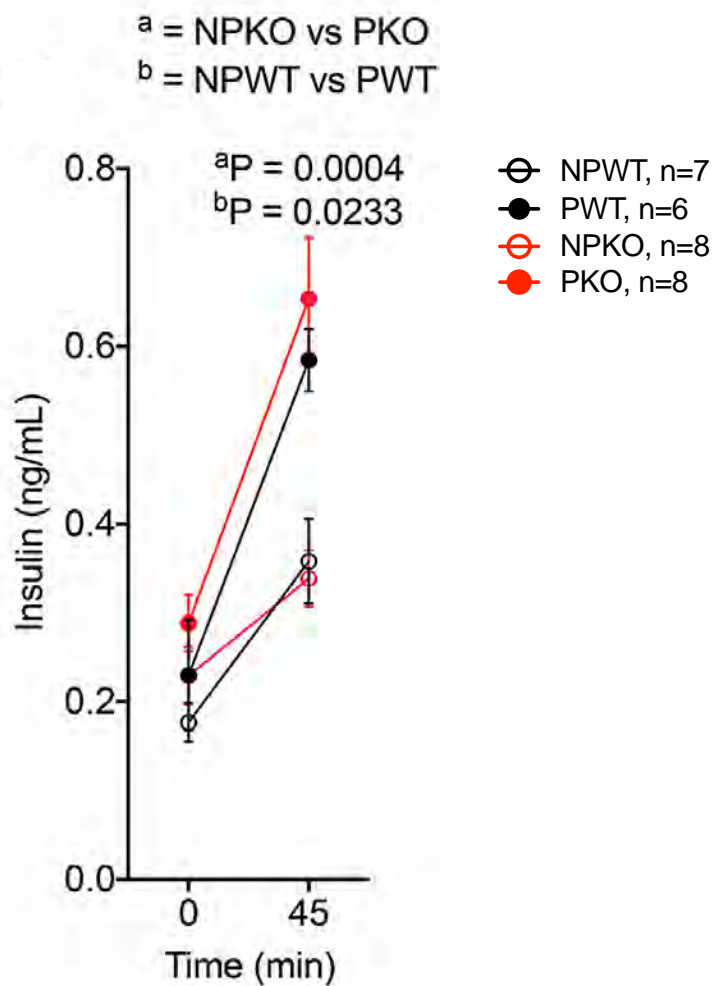
Figure 3. 27 Glucose stimulated insulin secretion is enhanced in pregnant dams.

Plasma insulin after administration of glucose (2g/kg body weight) in 10-12-week old non-pregnant or pregnant wild-type (NPWT, PWT) or non-pregnant or pregnant *Papp-a* KO mice (NPKO, PKO) following a 6hr fast. Statistical significance was assessed using ordinary one-way ANOVA corrected with the Sidak test for multiple comparisons.

To examine whether insulin resistance could be accompanied by changes in the liver, we analyzed triglyceride content and histological appearance (Figure 3.28). Liver weight increased significantly in response to pregnancy in both WT and KO mice, but livers from KO pregnant mice were larger than those from WT pregnant mice (Figure 3.28a). This increased weight could be attributed to an increase in triglyceride levels (Figure 3.28b), which was reflected by the presence of large lipid droplets (Figure 3.28c) and was only observed in pregnant KO mice. Thus, the insulin resistance induced by pregnancy in *Papp-a* KO mice was accompanied by fatty liver.

143
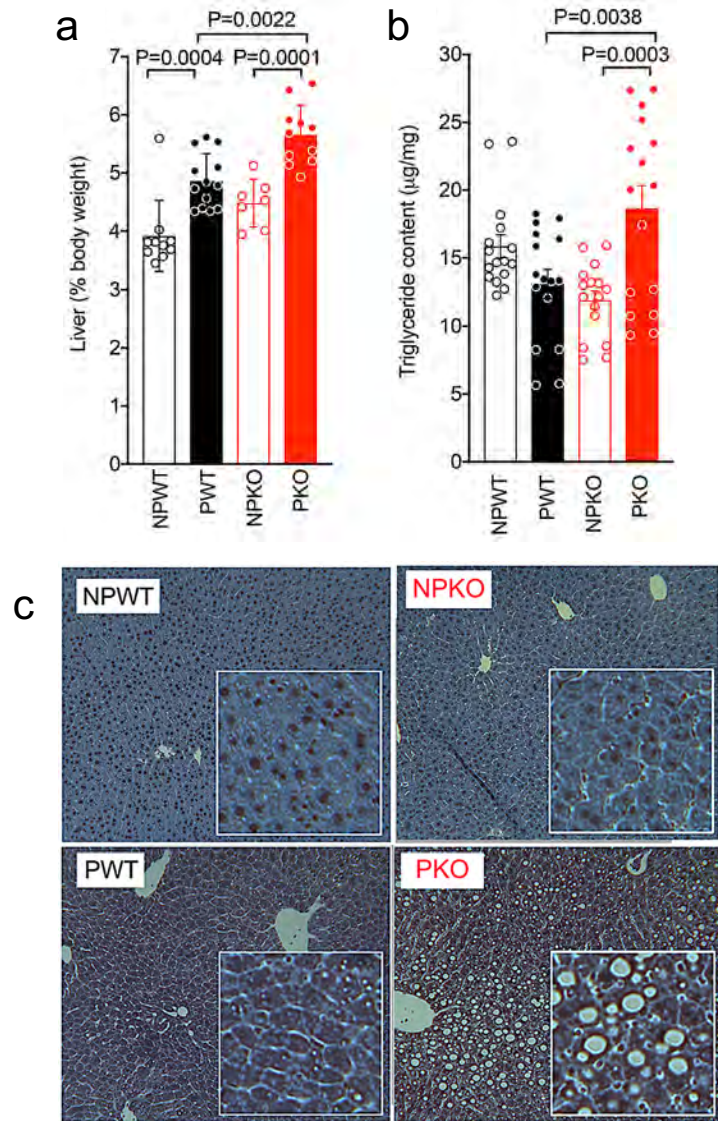
Figure 3. 28 Pregnant *Papp-a* KO have increased hepatic triglyceride content.

Liver mass (**a**) and triglyceride (**b**) content from 10-12-week old non-pregnant or pregnant wild-type (NPWT, PWT) or non-pregnant or pregnant *Papp-a* KO mice (NPKO, PKO). **(c)** Representative images of H&E liver sections taken under 10X magnification. Insets contain magnified sections of each image. Statistical significance was assessed using ordinary one-way ANOVA corrected with the Sidak test for multiple comparisons.

144

Unexpectedly, the insulin resistance and fatty liver phenotype on the pregnant KO mice was not reflected by impaired glucose tolerance. Indeed, the absence of Papp-a was accompanied by improved glucose tolerance in both non-pregnant and pregnant states (Figure 3.29). To determine potential mechanisms of enhanced glucose disposal in the KO mice, we conducted hyperinsulinemic-euglycemic clamps (Figure 3.30). KO mice required higher glucose infusion rates and displayed enhanced whole-body glucose turnover. This was accompanied by enhanced skeletal muscle glucose uptake (Figure 3.30, right panel) and increased whole body glycolysis. We also observed a trend towards higher hepatic glucose production, consistent with insulin resistance.

145
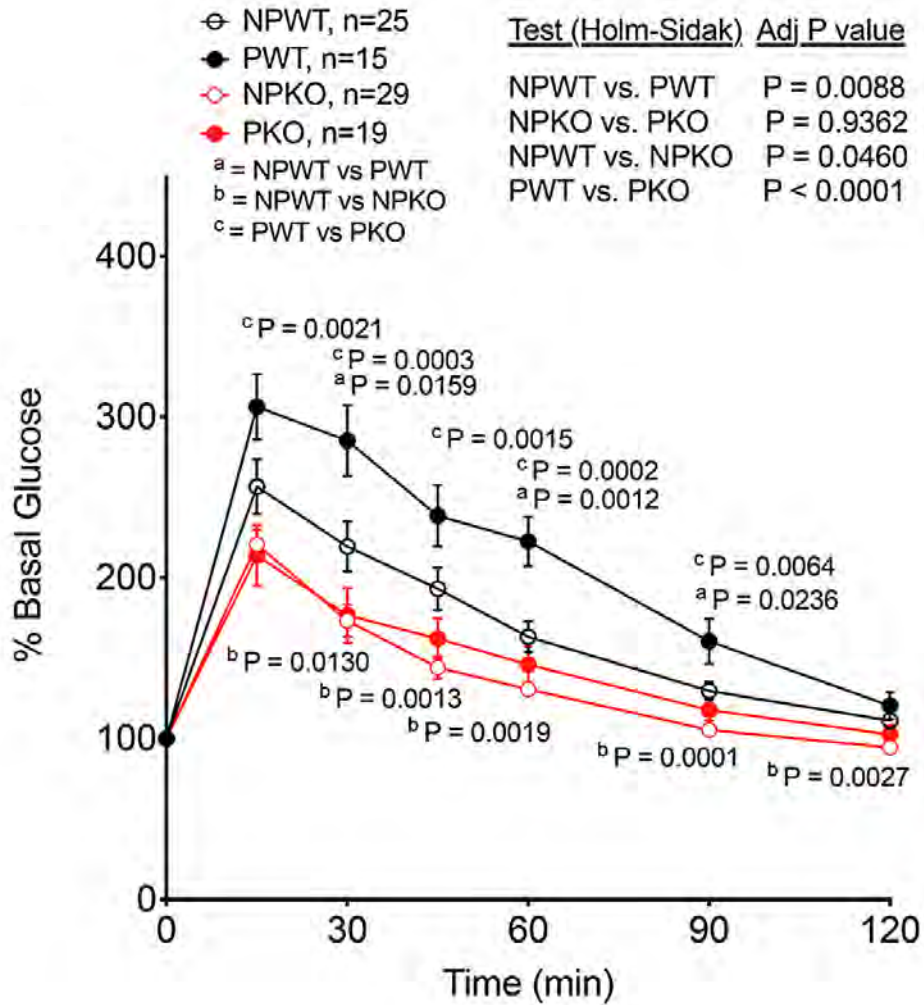
Figure 3. 29 *Papp-a* KO dams exhibit improved glucose tolerance.

Percent of basal glucose from 10-12-week old non-pregnant or pregnant wild-type (NPWT, PWT) or non-pregnant or pregnant *Papp-a* KO mice (NPKO, PKO) during a glucose tolerance test (2g glucose/kg body weight) after 6hr fast. Statistical significance between groups was assessed using repeated measures one-way ANOVA corrected for multiple comparisons using the Holm-Sidak test, and statistical significance of differences at each time point measured using multiplicity adjusted t-tests.

146
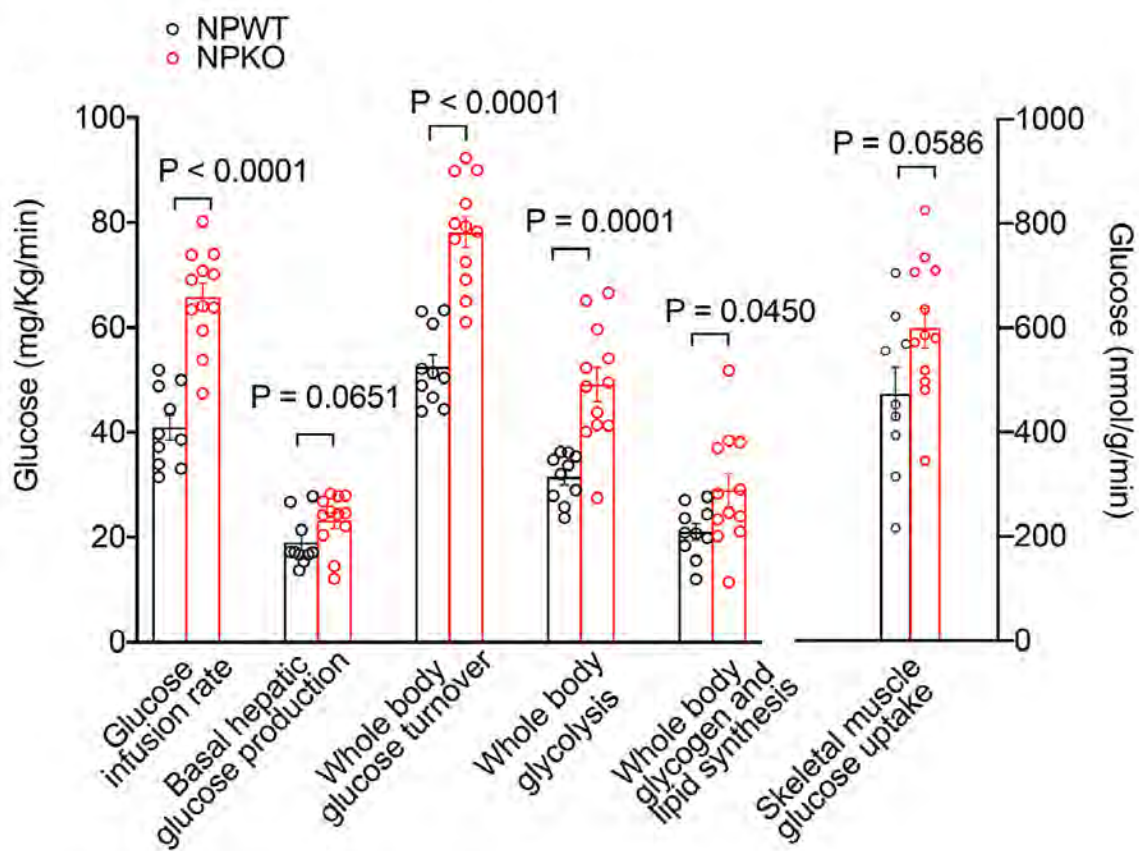
Figure 3. 30 Papp-a KO display enhanced glucose disposal under the hyperinsulinemic-euglycemic clamp.

Glucose values (left y-axis, mg/Kg/min) and muscle glucose uptake (right y-axis, nmol/g/min) during hyperinsulinemic-euglycemic clamps for each parameter measured (x axis). Bars indicate mean and SEM. Statistical significance of the differences for each parameter were calculated using unpaired Student's t-tests.

147

Discussion

The results presented in this paper demonstrate that both mouse and human pregnancy induces adipose tissue adaptations important for the regulation of insulin sensitivity. Our findings implicate PAPP-A as a key signaling molecule in this remodeling of adipose tissue. Acting on IGFBPs, this protease establishes a pregnancy-specific signaling axis in adipose tissue that can couple fetal growth to maternal fuel homoeostasis.

PAPP-A was initially described as one of three proteins produced by the human endometrium that increase dramatically after decidualization and pregnancy (R. Smith, Bischof, Hughes, & Klopper, 1979) (Bischof, 1979). Of these only PAPP-A increases progressively from very early (6-10 weeks) gestation to term (Bischof, 1989). The development of sensitive assays for PAPP-A early on revealed significant correlations with pregnancy abnormalities (Barnea, 1986) (Griffin, 1983) (Sutcliffe et al., 1982). A single low value for PAPP-A was highly significantly correlated with Down syndrome pregnancies (Brambati et al., 1993) (Wald et al., 1992), leading to its adoption for screening chromosomal abnormalities in early pregnancy, although the mechanisms behind these low values are unclear. Cloning of the *PAPP-A* gene led to its identification as a Zn+ binding metalloprotease (Kristensen, Oxvig, Sand, Hundahl Moeller, & Sottrup-Jensen, 1994), and functional studies to its subsequent identification as the

148

single protease responsible for cleavage of IGFBP4 (Conover, Oxvig, Overgaard, Christiansen, & Giudice, 1999) and capable of cleavage of IGFBP5 (Laursen et al., 2001). The key role of PAPP-A in IGFBP proteolysis and IGF signaling is evidenced by its effects on embryonic development; in humans, PAPP-A levels in early pregnancy correlate with fetal size at term (Pedersen, Sørensen, & Ruge, 1995) (Baer, Lyell, Norton, Currier, & Jelliffe-Pawlowski, 2016) (Giudice et al., 2015), and in mice ablation of *Papp-a* results in proportional dwarfism (Conover et al., 2004). In addition to its role in fetal development, total and proteolytic human PAPP-A levels progressively rise in serum throughout pregnancy (Gyrup, Christiansen, & Oxvig, 2007), suggesting a longitudinal mediation of maternal peripheral tissue adaptations to fetal growth. This view is supported by the inverse linear correlation between circulating PAPP-A and serum glucose shown in our study. Moreover, it suggests that the observed correlations between low PAPP-A levels and pregnancy abnormalities might be attributable to inadequate regulation of IGF signaling in maternal peripheral tissues, required for adaptation to the growing demands of the fetus.

In the case of diabetes, a correlation between low level first trimester PAPP-A and GDM risk has been reported in some (Beneventi et al., 2011) (Lovati et al., 2013) (Petry et al., 2017), though not in all studies (Husslein & Lausegger, 2012) (Savvidou, Syngelaki, Muhaisen, Emelyanenko, & Nicolaides, 2012). In our

149

retrospective study of over 6000 women, we found a strong positive correlation between development of GDM and second, third and fourth quartile first-trimester PAPP-A levels, compared to the highest quartile. Importantly, it has been recognized that levels of circulating PAPP-A at the three trimesters of pregnancy are affected by diverse maternal factors and medical history (Wright, Silva, Papadopoulos, Wright, & Nicolaides, 2015), including weight, age, smoking, race and diabetes status. Because these factors lower the sensitivity and accuracy of single measure PAPP-A levels for aneuploidy screening, algorithms used by clinical laboratories to report PAPP-A MOM correct for these factors.

Nevertheless, in our study we find that PAPP-A MOM levels in the lowest quartile are still associated with increased odds of development of GDM, supporting the hypothesis PAPP-A levels are an independent risk factor for the development of gestational metabolic disease. Mechanistically, our results support a model in which low levels of PAPP-A result in impaired proteolysis of adipose tissue IGFBPs, which are upregulated in adipose depots during pregnancy. In turn, IGF signaling decreases, impairing pregnancy-induced adipose tissue remodeling (Rojas-Rodriguez et al., 2015). This mechanistic view is supported by our finding of direct stimulation of human adipose tissue expandability by PAPP-A *in vitro* (Figure 3.9) reflecting *in vivo* physiology (Gealekman et al., 2014) (Pellegrinelli et al., 2018) (Gealekman et al., 2012), as well as our findings of impaired adipose

150

tissue remodeling and pregnancy-specific insulin resistance in *Papp-a* knockout mice.

Despite displaying 86% conservation between human and mouse at the amino acid level and sharing catalytic features, Papp-a is not highly produced in the placenta during pregnancy in mice (Qin et al., 2002), therefore pregnancy-specific regulation in this species may occur through its expression and function in peripheral tissues. The effects of Papp-a on murine adipose tissue can be mediated through cleavage of Igfbp2, as this binding protein was specifically upregulated by pregnancy, and is a known substrate of Papp-a (61, 62) (Gérard, Delpuech, Oxvig, Overgaard, & Monget, 2004) (Monget et al., 2003). The direct role of Papp-a in remodeling adipose depots is also supported by the finding that depots displaying lesser impairments exhibit a larger compensatory overexpression of *Igf-2*, consistent with observations that increased *Igf-2* mitigates the effects of *Papp-a* deficiency (Bale & Conover, 2005). In human adipose tissue, the largest pregnancy-induced change in a single gene is the enhanced expression of *IGFBP5*, accompanied by >10-fold elevation in circulating PAPP-A net proteolytic activity (Gyrup et al., 2007). Thus, while the specific IGF binding proteins and the source of PAPP-A may differ between mice and humans, the mechanism whereby the PAPP-A/IGF axis enables adipose tissue adaptation to pregnancy is conserved between these species.

151

The pregnancy-specific adaptations we observed in mice include a trend towards decreasing total fat pad mass, the appearance of small adipocytes, consistent with increased fat mobilization and adipose tissue growth by hyperplasia, and the enhanced expansion capacity of adipose explants. The molecular mechanisms that remodel adipose tissue during pregnancy appear to be variations on mechanisms already known to play a major role in adipose tissue development. In non-pregnant humans, the IGF signaling pathway is known to play a major role in the regulation of adipose tissue expandability (Garten et al., 2012) (Maridas et al., 2017) (Gealekman et al., 2014) (Hjortebjerg et al., 2018) (Rajkumar, Krsek, Dheen, & Murphy, 1996) (Silha, Gui, & Murphy, 2002). In mice, expression of *Igfbp4* is regulated by age and obesity, and it can directly modulate adipose tissue expandability *in vitro* (Gealekman et al., 2014).

Adipose tissue expandability is increasingly recognized to play a central role in the regulation of insulin sensitivity through secretion of cytokines and preventing lipotoxicity (Carobbio et al., 2017). Failure of adipose tissue to suppress lipolysis or insufficient adipose tissue storage capacity leads to increased lipid delivery to the liver and enhanced gluconeogenesis and hepato-steatosis (Kabir et al., 2005) (Reilly et al., 2015). Interestingly, we find that non-pregnant *Papp-a* KO mice display a trend to increased hepatic glucose production, although enhanced glucose utilization prevents glucose intolerance. This enhanced glucose

152

utilization, which is unusual in the context of insulin resistance, is reflected in hyperinsulinemic clamps by increased glucose uptake in skeletal muscle and may result from an increased muscle oxidative metabolism previously reported in aged *Papp-a* KO mice (Conover, Bale, & Nair, 2016). Moreover, a striking phenotype is seen in response to pregnancy, where *Papp-a* KO mice display much greater insulin resistance evidenced by insulin tolerance tests accompanied by fatty liver, consistent with impaired adipose tissue function.

Our model from this presented data does carry limitations. We cannot be certain that circulating PAPP-A derived from the placenta is mediating subcutaneous human adipose tissue IGFBP5 cleavage. Although the vast majority of circulating PAPP-A in human pregnancy is derived from the uterus (Bersinger & Klopper, 1984), other tissue also expresses a significant amount (Gude et al., 2016). Further studies assessing adipose tissue adaptations during the course of pregnancy and their correlation with subcutaneous adipose tissue *PAPP-A* gene expression and circulating levels of total and active PAPP-A over time may help answer this question. Another approach studying tissue-specific ablation in mice may determine whether circulating Papp-a can affect remodeling in adipose tissue-specific KO mice and the extent to which each tissue contributes to the metabolic adaptations to pregnancy. In addition, the finding of reduced alveolar development needs to be explored further as in humans it has been described

153

that women with glucose intolerance during pregnancy (either gestational, type 1, or type 2 diabetes) have greater odds of low milk supply during the lactation period (Riddle & Nommsen-Rivers, 2016). Therefore, is possible that the role of PAPP-A in adipose tissue remodeling also impacts mammary gland adaptations to pregnancy in both human and mice. Nevertheless, our current findings identify, for the first time, the important PAPP-A dependent effects of pregnancy on adipose tissue remodeling in human and mice critical for maternal metabolic homeostasis.

Gestational diabetes is a growing medical concern, with increasingly recognized long-term health consequences for mothers and their offspring (Farahvar et al., 2019) (C. Zhang et al., 2019). Our finding that PAPP-A insufficiency may drive GDM development opens the possibility of therapeutic use of this protease. Through gathering a better understanding of PAPP-A/IGF signaling, initiating a targeted investigation of *PAPP-A* expression regulation, and directly studying the action of PAPP-A as a biologic, we will determine its potential as a therapeutic option in mitigating GDM and its transgenerational pathologies.

CHAPTER IV: Discussion

Overview

Research in metabolism emphasize the endocrine role of adipose tissue in glucose homeostasis.

In periods of excess calorie intake, the adipose tissue expands in response to insulin signaling by storing glucose as triglycerides. Glucose uptake and storage by the adipose tissue and other insulin sensitive tissues prevents hyperglycemia and the stored triglycerides can be released as free fatty acids at times of energy need (Choe, Huh, Hwang, Kim, & Kim, 2016). The rapid adaptations of adipose tissue expandability led by changes on insulin sensitivity in pregnancy features the metabolic role of adipose tissue as a regulator of energy sources between maternal tissues and the feto-placental unit (N Butte, 2000) (Lain & Catalano, 2007).

Adipose tissue metabolism in gestation can be described in two phases. The first half of pregnancy is characterized by fat mass accrual accompanied by adipose tissue growth, which is facilitated by enhanced insulin sensitivity. The second half of gestation is highlighted by lipid mobilization from adipose tissue stores due to

155

reduced insulin sensitivity. This metabolic adaptation to gestation favors glucose uptake by fetal tissues while maternal tissues rely on lipid as energy source (King, 2000) (Wiznitzer et al., 2009).

The maintenance of glucose homeostasis in periods of adipose tissue growth is dependent on the site and composition of fat mass.

The main site for lipid storage is in the subcutaneous adipose tissue, however, once it reaches an expansion limit, the deposition of lipids gets shifted to ectopic sites leading to an insulin resistance state (Virtue & Vidal-Puig, 2010). Reports from various studies across populations from different ethnicities coincide that visceral adiposity is associated with the development and the presence of insulin resistance and type-2 diabetes (Gastaldelli et al., 2002) (Anjana et al., 2004) (Usui et al., 2010) (Neeland et al., 2012) (Nordström, Hadrévi, Olsson, Franks, & Nordström, 2016). Furthermore, individuals with fat accumulation in the subcutaneous depot have improved insulin profiles and lower risk of metabolic disease than those with preferential visceral fat accumulation (Porter et al., 2009) (McLaughlin et al., 2011).

In addition to fat localization, the mechanisms of adipocyte growth have been implicated in the maintenance of systemic insulin sensitivity. Hyperplastic growth via differentiation of adipocyte progenitors aids in the maintenance of insulin

sensitivity, contrary to hypertrophic adipocytes leading to inflammation and insulin resistance (Isakson, Hammarstedt, Gustafson, & Smith, 2009) (Lönn, Mehlig, Bengtsson, & Lissner, 2010) . Adipocyte growth is accompanied by extension of the vasculature, therefore adipose tissue angiogenesis is also a key determinant of insulin sensitivity (Corvera & Gealekman, 2014).

Importance of studying adipose tissue expansion in gestation

The association between visceral fat deposition and type-2 diabetes in non-pregnant individuals have prompted the studies on the effect of visceral adiposity in glucose metabolism on gravid women particularly due to the state of rapid weight gain that pregnancy imposes. Most of the work for depot-specific fat mass content assessment along gestation has been done utilizing non-invasive approaches. Others have biopsied and analyzed the composition of subcutaneous adipose tissue longitudinally across gestation. In depth study of the adaptations of adipose tissue expansion and its effect on insulin state requires the analysis of both subcutaneous and visceral fat depots in order to elucidate what molecular mechanisms are driving the growth of adipose tissue and how they are altered in gestational diabetes. Evidence obtained from these studies can then be applied for the development of animal models that can lead the discovery of potential molecules with preventive and therapeutic roles for gestational diabetes.

157

Major results of the thesis

Cross-sectional studies: Morphological and gene expression changes in adipose tissue due to gestation and glycemic state in pregnancy

In this thesis work, I performed two independent cross-sectional studies for the characterization of the morphological changes in adipose tissue expansion due to gestation and how these effects are altered in pregnancies with GDM. The adipocyte size and number distribution, vascularization level via capillary density and capacity for adipose tissue growth of subcutaneous adipose tissue where determined for normoglycemic non-pregnant and pregnant women. These parameters were also measured in a paired analysis of subcutaneous and omental adipose tissue of normoglycemic and gestational diabetes gravid women. Altogether, the results presented in this thesis demonstrate that pregnancy induces adipose tissue expansion via adipocyte hypertrophy and hyperplasia and extension of the vascular network in the subcutaneous adipose tissue. The presence of GDM resulted in a distinctive pattern of inadequate adipose tissue expansion. Namely, omental fat depots contained hypertrophied adipocytes and both the subcutaneous and omental adipose tissue had reduced vascularization.

158

Moreover, adipose tissue gene expression analysis from Affymetrix array and real-time PCR indicate the upregulation of *IGFBP5* expression due to pregnancy and the reduced expression levels of this gene in GDM.

Retrospective study: First trimester circulating PAPP-A and the association with maternal glycemic state at the time of screening for gestational diabetes

PAPP-A is a metalloprotease secreted by the placenta which circulating levels increase as pregnancy advances and has been shown to cleave IGFBP2, IGFBP4, and IGFBP5. Due to the observations of *IGFBP5* expression changes in adipose tissue with maternal glycemic state, I was interested in investigating the relationship between PAPP-A and the development of glucose intolerance in gestation. Analysis of a retrospective study in gravid women delivering at UMMHC showed that pregnant women with low levels of circulating PAPP-A at weeks 10-14 of gestation had higher odds for developing abnormal glucose tolerance or GDM later in pregnancy.

PAPP-A effects on human adipose tissue expandability in pregnancy

Based on the results from this thesis, a normoglycemic pregnancy is characterized by high levels of circulating PAPP-A, enhanced adipose tissue expansion and upregulation of adipose tissue *IGFBP5*. Since IGFBP5 is a substrate for PAPP-A, I explored if PAPP-A stimulates the expansion capacity of

159

adipose tissue *in vitro*. Indeed, the presence of recombinant human PAPP-A enhances the expansion capacity of adipose tissue explants from pregnant women.

Characterization of the impact of Papp-a deletion on glycemic state and adipose tissue expandability in murine pregnancy

The findings of inadequate adipose tissue expandability and low levels of PAPP-A in pregnant women with GDM prompted me to investigate a possible mouse model for this disease. To fulfill this end, I utilized a whole-body *Papp-a* knockout mouse line and performed metabolic phenotyping as well as analysis of adipose tissue histology and gene expression of the molecules involved in IGF signaling in wild-type and *Papp-a* knockout non-pregnant and pregnant dams. Overall, the results demonstrate that *Papp-a* knockout pregnant dams have reduced insulin sensitivity and fatty liver when compared to *Papp-a* knockout non-pregnant and wild-type pregnant controls. Also, the changes in adipocyte size and number observed due to pregnancy in wild-type animals were absent in *Papp-a* knockouts. Last, only *Igfbp2* expression was increased by pregnancy with no difference in relative abundance between wild-type and knockout pregnant dams.

In general, the work presented in this thesis characterized the morphological changes of adipose tissue expansion in gestation and how these adaptations are

160

altered in GDM. The proposed molecular mechanism between placental PAPP-A and adipose tissue IGFBP-5 feature the role of adipose tissue expandability in maintaining maternal glucose metabolism and highlights the use of PAPP-A as an early biomarker and therapeutic for gestational diabetes. In addition, a mouse model of *Papp-a* knockout is proposed for the study of gestational diabetes.

Major conclusions and implications of the work

Gravid women with GDM have impaired adipose tissue expansion

In chapter 2, I demonstrated that pregnant women with GDM have impaired adipose tissue expansion. The increased amounts of enlarged adipocytes observed in the omental fat suggest that GDM women tend to store lipid via hypertrophy in a visceral site, which is one of the features that can lead to insulin resistance and altered lipid profiles. On the contrary, normoglycemic gravid women have in their omental fat depot a higher number of small adipocytes, which is characteristic of hyperplasia and associated with insulin sensitivity.

The effect of hypertrophic adipocytes on metabolism has been described in both human and mice where enlarged fat cells have increased rates of lipolysis, secrete pro-inflammatory adipokines and have reduced insulin sensitivity with decreased GLUT-4 trafficking than smaller adipocytes (JI Kim et al., 2015) (Verboven et al., 2018). In a paired analysis of subcutaneous and omental adipose tissue from lean and obese non-pregnant women, isolated adipocytes where categorized as hypertrophic or hyperplastic according to their size and number and associated with the lipid profiles for each subject (Veilleux et al., 2011). Women with omental hypertrophic adipocytes had deleterious lipid profiles than subjects with omental adipocyte hyperplasia while no differences in lipid

162

profiles were observed among individuals with hyperplastic or hypertrophic subcutaneous adipocytes. Logistic regression analysis estimated that a 10% enlargement of omental adipocytes increased the risk for hypertriglyceridemia by more than 4-fold, and this association was not observed for subcutaneous adipocyte size. Therefore, the size of omental adipocytes can be associated with the state of lipid metabolism.

The differences in adipocyte size between fat depots has also been studied by others in different stages of pregnancy. Rebuffé-Scrive et al collected subcutaneous abdominal and femoral adipose biopsies of non-pregnant, early gestation (8-11 weeks gestational age), and lactating women (Rebuffe-Scrive et al., 1985). Femoral fat cells were larger than abdominal in all groups and, interestingly, adipocytes in both subcutaneous regions were larger in lactating women compared to the other cohorts. In addition, basal lipolysis rates were increased in lactating women with a pronounced effect in the femoral region indicating a depot-specific response to lipid metabolism in response to lactation. Similar to the approach utilized in my thesis research, Huda and colleagues analyzed isolated omental and subcutaneous adipocytes from fat biopsies of healthy pregnant women at the time of cesarean section. Their report demonstrated that omental adipocytes had smaller diameter and were less lipolytic than subcutaneous adipocytes, supporting my observations of depot-

163

specific differences in adipocyte size (Huda et al., 2014). Therefore, each stage of pregnancy will present a unique metabolic adaptation reflected, in part, by fat depot-specific changes in adipocyte size regulating lipid storage and mobilization.

In normoglycemic gravidas, the subcutaneous and omental fat where highly vascularized. The subcutaneous had increased expansion capacity (measured via angiogenic potential) than the omental depot indicating that both depots are capable of healthy expansion, however the subcutaneous had an enhanced capacity for growth. The reduced vascularization observed in both the omental and subcutaneous fat of GDM women is characteristic of dysfunctional adipose tissue growth. The biology of fat expansion consists on an initial acute hypoxic state that induces signaling events resulting in mild inflammation which promotes remodeling of the extracellular matrix and extension of the vascular network via angiogenesis (Resi et al., 2012) (Wernstedt Asterholm et al., 2014) (Attie & Scherer, 2009) (Crewe, An, & Scherer, 2017). Unhealthy adipose tissue expansion creates a state of chronic hypoxia resulting in a condition of unresolved inflammation leading to fibrosis and impaired angiogenesis (Michailidou et al., 2012) (Lin, Chun, & Kang, 2016) (Crewe et al., 2017). The importance of vascularization specific to the expanding adipose tissue relies not only in oxygenation, nutrient supply and growth factor/hormone exchange, but

164

also on the mesenchymal stem cell progenitors residing in the vascular endothelium of adipose tissue that proliferate and differentiate into mature adipocytes driving the hyperplastic fat growth (Tran et al., 2012) (Min et al., 2016). Studies done in mice with adipose tissue overexpression of the vascular-endothelial growth factor (VEGF), a potent activator of angiogenesis, demonstrated that animals fed a high-fat diet had formation of functional vessels and were protected from diet-induced glucose intolerance and insulin resistance (Elias et al., 2012). Also, when C57BL/6J and *ob/ob* mice are treated with the insulin sensitizer rosiglitazone, these animals have an adipose tissue pro-angiogenic effect that increases the capillary network when compared to untreated controls (Gealekman et al., 2008) suggesting the relationship between adipose tissue microvasculature and insulin sensitivity.

In humans, subcutaneous adipose tissue changes in basal and the early phase of weight gain induced by overfeeding results in an increase of capillary density and upregulation of genes involved in angiogenesis indicating that the initial stages of adipose tissue expansion begin with extension of the vascular network (Alligier et al., 2012). Therefore, based on the results obtained from the GDM women included in this thesis I conclude that the adipose tissue of GDM gravidas failed in adapting to the changes that maintain a healthy adipose expansion. It is possible that the impact of reduced vascularization is more prominent in the

165

omental depot due to the presence of hypertrophic adipocytes that could drive a state of chronic-low grade inflammation and lead to insulin resistance.

To my knowledge, this is the first study that examined the morphological changes of adipocyte growth along with differences in both angiogenesis and vascular network of subcutaneous and omental adipose tissue in normoglycemic and GDM gravidas at the end of gestation. However, there are some caveats regarding the experimental approach and design of the study. The technique for measuring adipose tissue vascularization relies on a whole-mount lectin staining of a small fat fragment. Ideally, the measurements of capillary density are analyzed relative to the adipocyte number and surface area. A more accurate measure for fat vascularization could be done by co-staining adipose tissue fragments with lectin and perilipin, which will also give more insight into the architectural differences of adipose tissue between normoglycemic and GDM gravidas. Regarding adipocyte size and number, I can only estimate the changes in adipocyte morphology since I don't have the measurement of the depot and therefore cannot adjust for adipose organ size. An alternative approach can be to weight the fat biopsy, isolate the adipocytes from the stromovascular fraction, measure adipocyte diameter and volume from 100-300 cells and adjust for the weight of the adipose tissue biopsy. It will still be an approximation; however more precise than the method I utilized. The measures of capillary density and

166

adipocyte size are usually adjusted by BMI. However, in pregnancy, BMI is not an accurate measurement due to the increase in total body water and the difficulty for distinguishing between maternal and fetal mass. There are methods that have been used to detect differences in regional fat in gestation including ultrasound and anthropometry. However, ultrasound does not estimate total body composition and anthropometry has its limitations in late pregnancy stages. So again, this is another technical limitation of the study.

The small sample size included in the cohorts does not provide enough evidence that the abnormal morphological changes observed in the GDM group are representative of the disease in the population. Following this line, an appropriate comparison with pregnant women that had pre-existing type-2 diabetes was not possible, since only three subjects were included in the study and the adipose biopsy obtained from them was relatively small. In addition, the cohorts were overweight or obese prior to becoming pregnant, so the predisposition to an obese state could underlie an additional metabolic stress that was observed in the adipose tissue morphology and was accounted primarily to the glycemic state of the gravid woman. Additional experiments to support the work in this chapter will include a larger cohort of normal, overweight, and obese pre-pregnancy BMI of normoglycemic, GDM, and type-2 diabetes. The data obtained will indicate if the changes in adipose tissue architecture are due to a pre-existing obese state

and differentiate the morphological characteristics between GDM and type-2 diabetes. Last, the cellular mechanisms driving insulin resistance in the adipose tissue of pregnant women need to be explored and characterized in the different glycemic states in order to determine what are the molecular drivers specific to the adipose tissue promoting the development of gestational diabetes.

Pregnancy induces the upregulation of IGFBP5 expression in the adipose tissue

Chapter 2 and 3 include different analysis techniques of Affymetrix gene arrays from abdominal subcutaneous and omental adipose tissue of normoglycemic non-pregnant and pregnant women. The most differentially upregulated gene was *IGFBP5* in both depots of pregnant women compared to non-pregnant controls. The upregulation of *IGFBP5* and other genes of the insulin/IGF signaling pathway was also observed in gluteal subcutaneous adipose tissue at late gestation compared to pregravid in a normoglycemic cohort (Resi et al., 2012). The reduced expression of *IGFBP5* and *IGF1* in our GDM cohort indicates that there is a deficiency in the adaptations of subcutaneous adipose tissue remodeling induced by pregnancy via the IGF signaling pathway. Based on these results, I can conclude that pregnancy enhances the expression of *IGFBP5* in the subcutaneous adipose tissue regions which has been shown to expand in response to pregnancy (Resi et al., 2012). The caveats for this conclusion include the small cohort of gravidas and that I only measured gene expression.

168

Validation of the upregulation of adipose tissue *IGFBP5* should be done in larger cohorts with normal, overweight and obese BMI pregnant women and confirmed with the presence of higher concentration of bioactive IGFBP5 peptides in adipose tissue of pregnant compared to non-pregnant women. However, these experiments along with the morphological measurements described in the previous section, will require larger amounts of adipose tissue samples which is not always possible to obtain.

Adipocyte hypertrophy and hyperplasia are accompanied with extension of the vascular network during adipose tissue remodeling in late gestation

In chapter 3, I explored the changes in adipose tissue morphology that occur in response to a normal pregnancy given that the adaptations of adipose tissue to gestation are altered due to glycemic state. Histological analysis using non-pregnant biopsies as controls showed that pregnancy induces an enlargement of existing adipocytes in the abdominal subcutaneous fat depot and no differences in the number of small adipocytes, suggesting compensatory hyperplasia and hypertrophy in the expansion of adipose tissue at late gestation. In addition to changes in adipocyte size and number, remodeling of the adipose tissue microvasculature and increased expansion capacity determined from the *in vitro* expandability assay is also observed in late pregnancy. As mentioned before,

169

www.manaraa.com

extension of the vascular network is critical for the proliferation of progenitors and adipocyte differentiation.

The morphological changes in adipocyte size and number obtained from my results were also observed in late gestation compared to pregravid in the longitudinal study mentioned previously (Resi et al., 2012), although just in gluteal subcutaneous samples. However, another group reported an increase in adipocyte diameter and volume in abdominal subcutaneous fat biopsies between the first and third trimester of normal weight gravid women, but no changes in adipocyte number (Svensson et al., 2016). There was a different approach used to determine fat cell size and number between these studies. In my experiments, similar to Resi and colleagues, I analyzed adipocyte distribution from adipose tissue sections. Svensson digested the adipose tissue with collagenase and determined the size from isolated adipocytes. Although measuring isolated adipocyte volume seems more relevant to the actual size, analysis of multiple adipose tissue sections gives more resolution of the size and number distribution in the sample.

In conclusion, the adaptations of adipose tissue remodeling in late gestation are a dynamic process that includes adipocyte growth via hypertrophy and hyperplasia as well as extension of the vascular network. The limitations for this

170

section in chapter 3 are specific to the approaches for measuring capillary density and fat cell size (as discussed previously in pages 166-167) and the time of sample collection. Since fat mas accrual starts in the first trimester, I propose a longitudinal study where adipose biopsies are collected from the abdominal (lateral) and gluteo-femoral depot in the pregravid state, followed by first, second and third trimester. Inclusion of both subcutaneous depots is necessary since most of the fat mass gain localizes subcutaneously in the abdominal trunk and femoral region. Adaptations of adipose tissue to pregnancy not only includes changes in adipocyte size and number but also angiogenesis. The inflammatory component of the expanding adipose tissue and remodeling of the extracellular matrix are also key elements influencing the metabolic health of the expanding adipose tissue and should be measured along gestation. Furthermore, the adipokine secretion should be investigated due to their leading roles in adipogenesis and insulin sensitivity as well as inflammatory agents driving the low-grade immune response in the initial stages of adipose tissue growth.

First trimester PAPP-A is associated with the development of gestational diabetes

The reduced expression of *IGFBP5* in GDM led me to examine if PAPP-A, as a protease for IGFBP5 (Laursen et al., 2001), is also related to glycemic state in pregnancy. PAPP-A can be detected after 28 days of implantation in maternal

171

circulation and is part of the first maternal screen for fetal chromosomal abnormalities (Wapner et al., 2003). Early detection of maternal abnormal glucose metabolism is important since lifestyle interventions can ameliorate the metabolic burden that glucose intolerance has in both mother and child. Thus, the retrospective study presented in Chapter 3 examined if low levels of PAPP-A between weeks 10-14 of gestation were associated with abnormal glucose metabolism at the time of screening for gestational diabetes. The results from the large cohort showed that gravid women with low concentrations of circulating PAPP-A early in gestation have higher odds for developing abnormal glucose tolerance and gestational diabetes. This finding was constant even after adjusting for gestational age (PAPP-A MoM), as PAPP-A concentration steadily increases from week 6-13 of pregnancy (Bischof, DuBerg, Herrmann, & Sizonenko, 1981) and other variables associated with diabetes (BMI, ethnicity, smoking status). Wright and colleagues also investigated if there was a relationship between circulating PAPP-A and glycemic state in gestation (Wright et al., 2015). They conducted a prospective study and found that low levels of PAPP-A were observed in pregnant women with pre-existing type-2 diabetes, with a greatest decrease in patients that needed insulin therapy. The results from the retrospective study included in this thesis and the evidence from other clinical reports suggest PAPP-A as a mediator in glycemic control specifically during pregnancy.

172

Other studies in the field further support my conclusion as there is evidence of a positive association between low first trimester PAPP-A MoM and glucose intolerance, although cohorts in these studies were smaller (Kulaksizoglu et al., 2013) (Petry et al., 2017). Wells and colleagues showed that PAPP-A MoM decreased with the severity of diabetes when analyzing subjects that developed GDM, were diagnosed with diabetes early in gestation, or had pre-existing type-2 diabetes (Wells et al., 2015). Maternal age, BMI and sex of the baby were not confounders of this relationship, only parity. In comparison with this report, a large prospective observational study in London (n=31,225) showed that early pregnancy (11-13 weeks) PAPP-A MoM was lower in women who developed GDM and further decreased in gravidas that further needed insulin treatment (Syngelaki, Kotecha, Pastides, Wright, & Nicolaides, 2015). Contrarily, other groups have described that there is no relationship between first trimester PAPP-A MoM and the presence of GDM. However, these results were obtained from small cohorts (Kavak, Basgul, Elter, Uygur, & Gokaslan, 2006) (Husslein & Lausegger, 2012) or only found a relationship between low PAPP-A early in gestation with pregnant women that had pre-existing type-2 diabetes (Savvidou et al., 2012). It is important to note that extremely high PAPP-A is not associated with adverse maternal outcomes (Aitken et al., 2003).

173

Based on the results from our study which include a reasonable cohort size, I can conclude that low PAPP-A in the first trimester can predict the development of gestational diabetes. The limitations of this conclusion are based on the cohort of our study which was mainly Caucasian and the majority of the GDM cases were obese. In addition, our retrospective study was done utilizing the two-step approach and the Carpenter and Coustan criteria for the diagnosis of abnormal glucose tolerance and GDM, which is the routine method at the clinics that were enrolled in this study. Since the continuous relationship of maternal glucose levels below the established diagnostic cut-off for diabetes with averse pregnancy outcomes has been characterized (The HAPO Study Cooperative Research Group, 2008) (Scholtens et al., 2019) (Lowe et al., 2019), I consider that implementing the one-step approach for diagnosis, as is suggested by the International Association of Diabetes in Pregnancy Study Groups, will result in an even stronger association between the low levels of PAPP-A in the first trimester and the development of gestational diabetes.

PAPP-A stimulates adipose tissue expandability in vitro

The results of my thesis demonstrate that a healthy, normoglycemic pregnancy is distinguished by increased levels of circulating PAPP-A, adipose tissue- *IGFBP5* upregulation, along with enhanced adipose tissue expandability. These findings prompted me to investigate how the molecules involved in the IGF signaling

174

pathway regulate adipose tissue expansion in pregnancy. IGFBP5 serves as a bioreservoir of IGF in the pericellular environment. Cleavage of IGFBP5 is needed for the release of IGF (Allard & Duan, 2018). Free IGF is then available for binding to its receptor and activation of the intracellular events regulating metabolism and growth (Forbes, McCarthy, & Norton, 2012). Since PAPP-A is an IGFBP5 protease, I investigated if PAPP-A promoted adipose tissue growth *in vitro*. The presence of recombinant human PAPP-A stimulated the angiogenic growth of adipose tissue explants from pregnant women, suggesting its role in one of the early stages of adipose tissue expansion.

PAPP-A activity has been reported as the protease of IGFBP2, IGFBP4 and IGFBP5 (Gyrup & Oxvig, 2007). Besides the placenta, other tissues express PAPP-A including subcutaneous and visceral adipose tissue although these measurements were done in human preadipocytes from non-pregnant individuals (Hou, Clemmons, & Smeekens, 2005) and in mice (Harstad & Conover, 2014). IGFBP4 proteolysis by PAPP-A was detected in the conditioned media of epicardial preadipocytes (Conover et al., 2019) and in visceral adipose tissue explants of human subjects (Davidge-Pitts et al., 2014), indicating adipose-derived synthesis of the protease and the capacity for PAPP-A to cleave IGFBPs in the adipose tissue microenvironment. I cannot rule out the possibility that in the adipose tissue of pregnant women PAPP-A is also cleaving IGFBP2 and

IGFBP4 to a lesser extent and considering that these are experiments with human samples, I cannot control the native presence of other IGFBPs that are also substrates of PAPP-A.

Our lab has done the adipose tissue angiogenesis assay utilizing subcutaneous human explants in the presence of IGFBP4. The results showed that addition of IGFBP4 decreased the formation of capillary sprouting, possibly since IGF was being sequestered by the binding protein (Gealekman et al., 2014). Thus, in the case of pregnancy, the upregulation of *IGFBP5* could indicate an increase of IGFBP5 protein in the adipose tissue microenvironment and further sequestering of IGFs and increasing its local bioavailability. According to the results obtained from the *in vitro* assay, I can conclude that the cleavage by PAPPA is coordinating the initial stages of adipose tissue expandability in late gestation possibly through IGFBP5 proteolysis.

In the literature it has been reported that PAPP-A can cleave IGFBP5 in the absence of IGF1 (Laursen et al., 2001) and that IGFBP5 can function as a growth factor independent of IGF1 in intestinal smooth muscle cells (Kuemmerle & Zhou, 2002) and in osteoblasts derived from *IGF1* null mice (Miyakoshi et al., 2001). Therefore, there are diverse roles for IGFBP5 in the IGF signaling

176

pathway that unfortunately I am not able to isolate in the approach I am using to measure *in vitro* human adipose tissue expandability.

Besides PAPP-A, ADAM12 (Shi, Xu, Loechel, Wewer, & Murphy, 2000) and PAPP-A2 (Kramer, Lamale-Smith, & Winn, 2016) are metalloproteases that cleave IGFBBP5 and are also secreted by the placenta. From these two proteases, ADAM 12 has been described to be expressed by mouse white and brown fat and in human lipomas (Kawaguchi et al., 2003). ADAM 12 was identified as an inducer of alterations in the extracellular matrix favoring the morphological change of preadipocytes in the process of differentiation to mature adipocytes, indicating a direct role of metalloproteases in adipose tissue remodeling during adipogenesis (Kawaguchi et al., 2003). Since the role of ADAM12 in adipose tissue growth has been described, I can test if PAPP-A is the pregnancy-specific protease stimulating a direct effect in adipose tissue expansion via IGFBP5. Additional insight for my conclusion can be obtained with an experiment where adipose tissue explants from pregnant women are cultured in the presence of recombinant PAPP-A or ADAM12 and measure the capacity of adipose tissue expandability *in vitro* while testing if the conditioned media has the cleaved fragments of IGFBP5. Concurrently, I can measure if PAPP-A presence enhances receptor activation by probing for the phosphorylated version of the insulin and IGF receptor.

177

Pregnant Papp-a knockout mice exhibit insulin resistance and impaired adipose tissue growth in gestation.

In the last part of chapter 3, I studied the possibility of utilizing *Papp-a* knockout mice as an animal model for GDM due to the association of PAPP-A with maternal glycemic state and adipose tissue expandability. The metabolic phenotyping and analysis of adipose tissue histology resulted in three main findings that are comparable with gestational diabetes in humans. Pregnant knockout mice are unable to undergo the morphological changes in adipose tissue that occur in pregnant wild-type dams, they exhibit insulin resistance, and have an excessive hepatic lipid accumulation.

In a normal pregnancy, as was reported with the wild-type controls, there were distinct changes in adipocyte size and number that were mainly noted by an increase in the number of small adipocytes in both subcutaneous and visceral fat pads indicating the proliferation and differentiation of adipocyte progenitors. This is supported by the enhanced expansion capacity of inguinal adipose tissue explants in wild-type pregnant dams. The role of Papp-a in murine adipose tissue remodeling in gestation was evident as in the knockouts there were no changes in adipocyte distribution between non-pregnant and pregnant mice.

The severe insulin resistance and hepatic lipid content in the pregnant *Papp-a* knockout was also demonstrated in pregnant *Pparg2* (Peroxisome proliferator-activated receptor gamma isoform-2) knockout mice (Vivas et al., 2016). PPARγ2 is a transcription factor predominantly present in the adipose tissue that regulates adipogenesis and insulin sensitivity (Werman et al., 1997) (Medina-Gomez et al., 2005). The *Pparg2* KO had decreased expression of lipid metabolism genes in subcutaneous adipose tissue and contained increased inflammation in the parametrial fat pad (Vivas et al., 2016). It is possible that the phenotypic similarities between *Papp-a* KO and *Pparg2* KO are mediated by the impaired adaptation of adipose tissue to the metabolic demands of gestation.

I also observed that pregnant *Papp-a* KO mice had excess triglyceride accumulation in their livers, characteristic of an insulin resistant state (Perry, Samuel, Petersen, & Shulman, 2014). This liver fat accumulation has a strong resemblance to that observed in GDM (Lee et al., 2019) (Mehmood et al., 2018) (Foghsgaard et al., 2017). Outside of pregnancy, fatty livers have also been observed in rats with growth hormone (GH) deficiency (Kuramoto et al., 2010). These rats have increased triglyceride content in their livers and non-alcoholic steatohepatitis, which was rescued with Igf-1 supplementation (H Nishizawa et al., 2012). Is possible that the local sequestering of Igf-1 by Igfbps and absence of proteolysis by Papp-a diminishes Igf-1 availability and is contributing to the

179

fatty liver in the pregnant *Papp-a* knockout. To test the mentioned hypothesis, I would have to quantify the amount of free Igf-1 and Igfbp-Igf-1 complex in liver samples of wild-type and *Papp-a* knockout pregnant dams. These experiments will provide relevant information regarding the pregnancy-specific effects of the IGF system on hepatic lipid metabolism.

One interesting result observed in the *Papp-a* knockouts was that they exhibited a fast glucose clearance, an effect not affected by pregnancy. I was not able to perform the hyperinsulinemic-euglycemic clamp on the pregnant *Papp-a* knockouts due to their small size and difficulty for the arterial catheterization. However, the increased insulin-stimulated muscle glucose uptake in the non-pregnant *Papp-a* knockouts could explain the feature of enhanced glucose tolerance.

The results presented from the pregnant *Papp-a* knockout dams demonstrate that Papp-a is fundamental in the adaptations of adipose tissue physiology and insulin sensitivity to gestation. A suitable experiment to support this conclusion is the analysis of the insulin/IGF signaling pathway molecules in the basal and insulin stimulated state of liver, muscle and adipose tissue to confirm the insulin resistance phenotype observed in the pregnant *Papp-a* knockout mice.

Future directions

Investigate the alterations of insulin/IGF signaling and other features of adipose
tissue expandability in normoglycemic and GDM pregnant women

A priority in the field of maternal metabolism is to unravel the molecular
mechanisms that are causing GDM. The phenotype of impaired adipose tissue in
GDM offers an ideal setting to study how alterations in adipose tissue
metabolism contribute to the development of glucose intolerance in gestation.
Insight into this physiology can be obtained by conducting a longitudinal study.
The time of assessment will include pre-pregnancy, early, mid, and late gestation
where a hyperinsulinemic-euglycemic clamp will be done in addition to needle
biopsies of subcutaneous adipose in the basal and insulin-stimulated state. Since
the percentage of women that will develop GDM is lower than those that will
remain normoglycemic during gestation (~4.8% GDM prevalence in
Massachusetts (Deputy, Kim, Conrey, & Bullard, 2018)) the prospective subjects
recruited for the GDM cohort will be screened for high risk factors of this disease.
The experimental approach will include measurements of whole and cleaved
IGFBP5 as well as activation of the molecules involved in the insulin/IGF
signaling pathway in the fat samples. In addition, the process of mild
inflammation can be assessed by determining the presence of pro- and anti-
inflammatory cytokines and activation state (M1/M2) of adipose tissue residing

181

macrophages. Last, the remodeling of the extracellular matrix in the expanding adipose tissue and its relationship with insulin sensitivity can be determined from the collected fat biopsies by analyzing the changes along gestation of extracellular matrix components and receptors.

Characterize the crosstalk between placental PAPP-A and adipose tissue IGFBP5 in human pregnancy

A subset of the subjects from the longitudinal study can then be included in an investigation to test the model of placental PAPP-A and adipose tissue IGFBP5 crosstalk presented in this thesis. At the time of cesarean section, samples of subcutaneous and omental adipose tissue and placenta are collected. Fat explants are embedded in Matrigel, following the protocol of the *in vitro* adipose tissue expandability assay. Placental explants are kept in culture. Then, the conditioned media from the placenta will be used to treat the adipose tissue explants and measure if it enhances capillary growth. To confirm the PAPP-A proteolytic cleavage of IGFBP5, intact and the peptide fragments of IGFBP5 will be determined from the adipose tissue explants treated with the placental conditioned media.

Determine if PAPP-A is associated with adverse neonatal outcomes

GDM increases the risk of neonatal adiposity, highlighting the effect of maternal glucose intolerance in offspring metabolism. The positive association between low levels of PAPP-A and metabolic risk can be further explored in relationship to adverse neonatal outcomes. Hence, I propose a prospective investigation to study the association between the circulating levels of maternal PAPP-A in the first trimester of gestation and neonatal adiposity. The cohort of the study consists of a multiethnic population of singleton gestations. Serum plasma for PAPP-A quantification will be collected between weeks 11-14 of gestation and values will be adjusted for gestational age (PAPP-A MoM). Neonatal adiposity will be measured between 1-3 days after birth using the PEAPOD system, an infant-sized air-displacement plethysmograph. PEAPOD has been shown to provide accurate and reliable assessments of infant body composition (Ellis et al., 2007) (Deierlein, Thornton, Hull, Paley, & Gallagher, 2012). An association between low PAPP-A MoM and increased neonatal adiposity could indicate how early exposure of maternal phenotypes alter offspring metabolism to an extent that the effect is maintained postnatally.

183

Explore if the maternal maladaptations to gestation observed in the Papp-a knockouts are tissue-specific

Besides impaired adipose tissue expansion, the whole-body knockout of *Papp-a* results in the presence of insulin resistance and fatty liver. The regulation of IGFBPs proteolysis and subsequent IGF signaling is more locally regulated, indicating the possibility of tissue specific adaptations to gestation. Generating an adipose tissue specific *Papp-a* knockout strain will explore if the systemic insulin resistance and increased liver triglyceride accumulation observed in the pregnant *Papp-a* knockouts occur specifically due to the effects of impaired adipose tissue growth and ectopic lipid accumulation. It is possible that the insulin resistance and fatty liver phenotype is still present with the tissue specific deletion. This effect could indicate that the specific disruption of the IGF/insulin signaling pathway in the adipose tissue is responsible for the maternal maladaptation to gestation characteristic of the *Papp-a* knockout mice.

Concluding remarks

The maternal metabolic adaptations to gestation are based on increasing blood glucose, reducing insulin sensitivity in peripheral organs, and weight gain. The increase in weight is partly attributed to expanding adipose tissue stores which encompasses a series of depot-specific cellular and molecular events that regulate maternal glucose metabolism. The placenta, as an endocrine organ, secretes proteins that also regulate glucose metabolism via interaction with metabolic tissues. My thesis employed different translational approaches that characterized the cellular and molecular mechanisms modulating glycemic state in gestation.

The results presented in this thesis include cross-sectional studies demonstrating the adaptations of adipose tissue expansion in gestation and how alterations in this physiology could lead to the development of gestational diabetes. In a retrospective study included in this work, I showed the association between a placental protease, PAPP-A, and the development of gestational diabetes. By developing a novel *in vitro* technique to recapitulate adipose tissue expandability, I showed the stimulatory effect of PAPP-A on adipose tissue growth in pregnancy. The adaptations of adipose tissue expandability are possibly mediated by interaction of placental PAPP-A and adipose tissue IGFBP5, which is highly induced in the fat of pregnant women (Figure 4.1). The effect of PAPP-A

185

on adipose tissue expansion in gestation was further explored in *Papp-a* knockout pregnant mice and the results of the animal experiments highlight the role of Papp-a in mediating insulin sensitivity and the adaptations of adipose tissue to pregnancy.

I hope my work on the metabolic adaptations of adipose tissue and glucose metabolism in pregnancy provide insight and motivate future studies investigating the molecular basis of gestational diabetes. Specifically, research exploring the potential role of PAPP-A as an early biomarker and therapeutic for gestational diabetes.
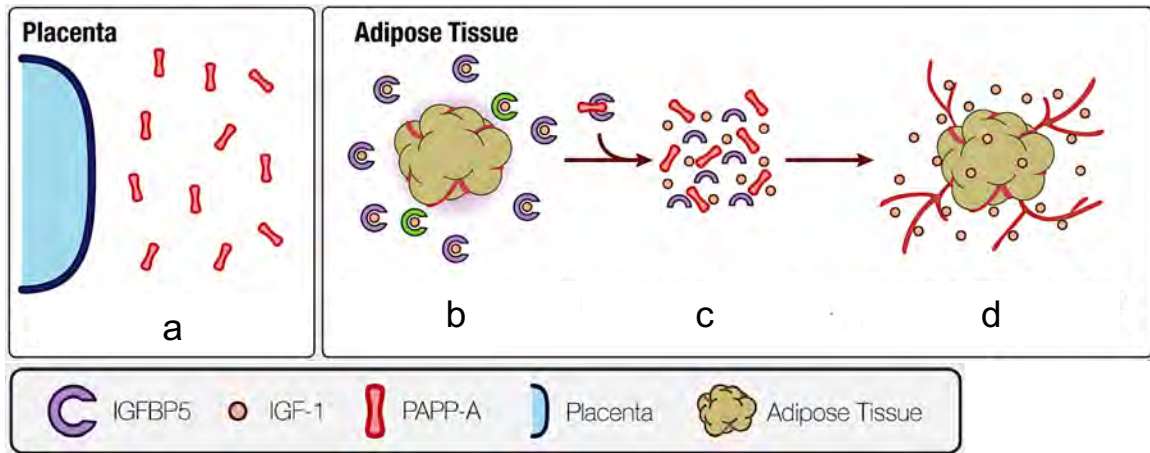
Figure 4. 1 Model for crosstalk between placental PAPP-A and adipose tissue IGFBP-5 in gestation.

(a) During pregnancy, the placenta produces PAPP-A which is secreted into the maternal circulation. **(b)** In response to pregnancy, maternal adipose tissue increases the production of IGFBP5 in its local microenvironment. **(c)** PAPP-A reaches the adipose tissue and cleaves IGFBP5, causing the release of IGF-1. **(d)** IGF-1 is free to bind the IGF receptor and promote the intracellular signaling pathways driving adipose tissue expansion via angiogenesis.

187

Appendix: Adipose Tissue Angiogenesis Assay

Abstract

Changes in adipose tissue mass must be accompanied by parallel changes in microcirculation. Investigating the mechanisms that regulate adipose tissue angiogenesis could lead to better understanding of adipose tissue function and reveal new potential therapeutic strategies. Angiogenesis is defined as the formation of new capillaries from existing microvessels. This process can be recapitulated *in vitro*, by incubation of tissue in extracellular matrix components in the presence of pro-angiogenic factors. Here, we describe a method to study angiogenesis from adipose tissue fragments obtained from mouse and human tissue. This assay can be used to define effects of diverse factors added *in vitro*, as well as the role of endogenously produced factors on angiogenesis. We also describe approaches to quantify angiogenic potential for the purpose of enabling comparisons between subjects, thus providing information on the role of physiological conditions of the donor on adipose tissue angiogenic potential.

Introduction

The adipose tissue of mammals has evolved as a preferred storage site for excess calories in the form of triacylglycerol, and also as a critically important endocrine organ, which controls whole body metabolic homeostasis. One of the unique features of adipose tissue is its ability to massively expand in response to chronic positive energy balance, and to decrease in size under conditions in which stored calories are mobilized for use in other organs. Adipose tissue expansion results from an increase in adipocyte size, as well as from the differentiation of precursors into new adipocytes. As is the case for any tissue, changes in adipose tissue mass must be accompanied by parallel changes in microcirculation (Cho et al., 2007) (Christiaens & Lijnen, 2010) (Crandall, Hausman, & Kral, 1997). Adequate vascularization is required to deliver nutrients and oxygen to all cells in the tissue, to remove waste products, and to allow the tissue to functionally interact with the rest of the organism through the sensing and production of hormones and growth factors. In the case of adipose tissue, inadequate microcirculation could impair appropriate triglyceride storage by preventing access to circulating lipoproteins under fed conditions; it could also prevent adequate fuel delivery to other organs during fasting. Recent data suggest that adipose tissue microcirculatory alterations occur in type 2 diabetes, raising the possibility that impaired vascular development may be pathogenic in this disease (Hodson, Humphreys, Karpe, & Frayn, 2013) (Hosogai et al., 2007)

189

(Michailidou et al., 2012) (Pasarica et al., 2009) (Rausch, Weisberg, Vardhana, & Tortoriello, 2008). In support of an important role for adipose tissue angiogenesis, increased production of pro-angiogenic factors, in particular VEGF, by adipose tissue improves whole body metabolism in high fat diet-fed mice (Michailidou et al., 2012) (Sung et al., 2013) (Wree et al., 2012). Thus, investigating the mechanisms that regulate adipose tissue angiogenesis could lead to better understanding of adipose tissue function and potentially reveal new therapeutic strategies.

Research on complex processes, such as tissue vascularization, can benefit from *in vitro* models that mimic important features of the process. In the area of angiogenesis, significant information has been derived from the aorta ring assay, in which aortic rings dissected from rat or mouse thoracic aortas generate outgrowths of branching microvessels (Aplin, Fogel, Zorzi, & Nicosia, 2008) (Baker et al., 2012). The formation of sprouts can be visualized by light microscopy of live cultures, and branching microvessels are composed of the same cell types that operate in vivo. The formation of aortic ring sprouts is regulated by endogenous and exogenously added pro- and anti-angiogenic factors. Thus, this assay has been extremely valuable in dissecting the basic mechanisms of angiogenesis.

Here we present an adaptation of the aorta ring assay, which we have used to assess the angiogenic capacity of adipose tissue from mice and humans (Gealekman et al., 2008) (Gealekman et al., 2012) (Gealekman et al., 2011). We have found that angiogenic capacity of adipose tissue *in vitro* reflects the physiological conditions of the donor. For example, adipose tissue angiogenesis, but not that of aorta, is enhanced in *ob/ob* hyperphagic mice, and in response to stimuli that increase adipose tissue growth, such as thiazolidinediones (Gealekman et al., 2008). Angiogenic capacity also differs among human adipose tissue depots and correlates with insulin sensitivity (Gealekman et al., 2011). Thus, this assay can be used to dissect endogenous factors that regulate adipose tissue angiogenesis under different physiological conditions.

Materials

Medium, instruments, and culture dishes

- Matrigel™ Basement Membrane Matrix, Growth Factor Reduced, Phenol Red-free, *LDEV-Free (BD Biosciences, San Jose, CA, catalog # 356231). Matrigel comes in bottles of 10 ml. To avoid freeze–thaw cycles and contamination, it is dispensed into 1 ml aliquots and stored at 20°C.

- EBM-2 medium supplemented with EGM-2 MV (Lonza, Basel, Switzerland, BulletKit, CC-3202)

- Dulbecco's phosphate-buffered saline (DPBS) (Life Technologies Corp-Gibco®, Carlsbad, CA, catalog # 14190)

- Dispase (BD Biosciences, San Jose, CA, catalog # 354235) enzyme is used for proteolysis of Matrigel. Aliquot dispase in 1.5 ml tubes and store at 20°C. Try to avoid multiple freeze–thaw cycle.

- 50 mM EDTA

- Trypsin-Versene (Lonza, Basel, Switzerland, catalog # 17-161E)

- Formaldehyde (Ted Pella, Inc., Redding, CA, catalog #18505)

- Hoechst 33258, pentahydrate (Life Technologies Corp, Carlsbad, CA, catalog # 947743)

- Triton X-100 (Sigma-Aldrich, St. Louis, MO, catalog # T-9284)

- BSA (Sigma-Aldrich, St. Louis, MO, catalog # A3059)

192

- 96-well flat bottom multiwell plates (BD FalconTM, Franklin Lakes, NJ, catalog # 353072)

- 35 mm glass-bottom culture dishes (MatTek Corporation, Ashland, MA, catalog # P35G-1.5-14-C)

- Very fine point forceps (VWR International, Radnor, PA, catalog # 25607-856)

- Micro Surgery Scissors (IntegraTM-Miltex®, York, PA, catalog # 17-2150)

- Sterile pipettes, tips, and conical tubes

- Three 100 mm x 20 mm petri dishes

- Round bladed disposable scalpels (FEATHER® Safety Razor Co. Ltd, Osaka, Japan, catalog # 2975#10)

Adipose tissue samples

Sample collection of adipose tissue from mice or human subjects requires IACUC and IRB approval from the institution at which the procedure will be performed. In preliminary studies, only the epididymal adipose depot of mice was competent to form angiogenic sprouts *in vitro*, for reasons that are currently under investigation. Thus, all of our studies have been carried out with male mice on a C56BL/6 background, or on genetic variants such as the *ob/ob* mouse. For this assay, epididymal adipose tissue is dissected and processed for embedding as described in detail below.

193

This assay has also been used to measure angiogenesis from human adipose tissue. Explants from both subcutaneous and visceral adipose tissue depots develop capillary sprouts (Gealekman et al., 2011). However, differences in the extent of angiogenic growth have been seen between visceral and subcutaneous adipose tissue. Thus, the exact source of each adipose tissue sample (including morphometric and metabolic characteristics of human subjects and the exact location from which the adipose tissue sample is extracted) should be carefully tracked and kept as consistent as possible between subjects within a study. An additional factor that may affect the outcome of this assay is the time between the excision of adipose tissue from the patient and the embedding of the tissue pieces into Matrigel. Both the conditions in which adipose tissue samples are stored and the time between excision and embedding should be optimized and, at very least, kept consistent between the subjects being compared. For optimal results we recommend collecting adipose tissue pieces that do not exceed 1 g and storing them at room temperature in EGM-2 MV-supplemented EBM-2 medium. The time between excision of the adipose tissue from human subject and its embedding into Matrigel should be minimized, and in our laboratory is routinely under 3 h.

194

Methods

Sample preparation

Before starting

- Protocol should be performed in a Class II Biocabinet.

- Wear personal protective garment including the use of lab coat, double gloves, facial barrier protection, hair net, etc. Follow Human Tissue Handling Guidelines from your institution.

- Instruments for handling tissue should be previously sterilized.

- Remove aliquots of Matrigel from 20°C and place on ice to bring it to 4°C. Use 2.5 ml of Matrigel for 60 wells of a 96-well-multiwell plate.

Collection of mouse adipose tissue

- Male C57Bl/6 mice from 9 to 23 weeks of age, fed either normal chow or high-fat diet.

- Mice are sacrificed according to institutional protocols.

- Epididymal fat pads are harvested by dissection using iris scissors according to the proximity to the epididymis and vesicular gland, taking care not to include the internal spermatic artery/vein and caput epididymis.

195

- After harvesting, adipose tissue is placed into 50 ml conical tubes containing 25 ml of EGM-2 MV-supplemented EBM-2 medium in which it is stored until embedding.

Collection of human adipose tissue

- Tissue is obtained following IRB protocols. In our studies, human adipose tissue has been obtained from needle biopsies, bariatric surgery, or panniculectomy procedures.
- Tissue is cut into ~1 g fragments, from which large vessels and obvious connective tissue are removed using iris scissors.
- After harvesting, adipose tissue is placed into 50 ml conical tubes containing 25 ml of EGM-2 MV-supplemented EBM-2 medium in which it is stored until embedding.

Embedding procedure

1. Label 3 100 cm petri dishes as #1, 2, and 3.
2. Pipette 25 ml of EGM-2MV-supplemented EBM-2 medium in plate #1 and #3. Put 15 ml of medium in plate #2.
3. Using forceps, transfer tissue from 50 ml conical tube into plate #1 and wash it by gently moving it around the plate.
4. Using forceps and scalpel, cut the tissue into strips (Figure Ap.1). Use the

196

forceps to hold the piece and the scalpel to make the cuts, always moving in one direction (no upward or downward movement). Rinse the strip with a gentle mix in the medium on the plate. Move the tissue strips to plate #2.

5. In plate #2, cut the strips into small slices. Maintain the size of pieces constant. As a guide for size, you can place millimeter paper underneath plate #2. Each piece should not be greater than 1 mm^3. Once cut, move the piece to plate #3. Cut approximately 75–80 slices per tissue sample.

6. Obtain a small tray and fill with ice. Put 96-well plate over ice. Maintain the plate in ice during the following steps.

7. Dispense 40 μl of Matrigel into wells to be used. Do not use the wells around the perimeter of the plate. Keep Matrigel on ice at all times.

8. Using the forceps, place one piece of adipose tissue per well.

9. After embedding, take plate out of ice. Make sure each explant is in the middle of the well. Use forceps if accommodation is needed.

10. Incubate at 37°C in 5% CO_2 for 30 min.

11. Add 200 μl of EGM-2 MV-supplemented EBM-2 medium per well. Make sure to fill all wells in the plate, including the wells around the perimeter of the plate, which do not contain adipose tissue explants. Wells at the perimeter of the plate tend to evaporate faster and placing explants only in the wells located in the middle of the plate allows for maintenance of a constant level of medium in all wells containing the explants.

12. Incubate at 37°C in 5% CO_2. 100 μl of the medium should be replaced

    every other day.
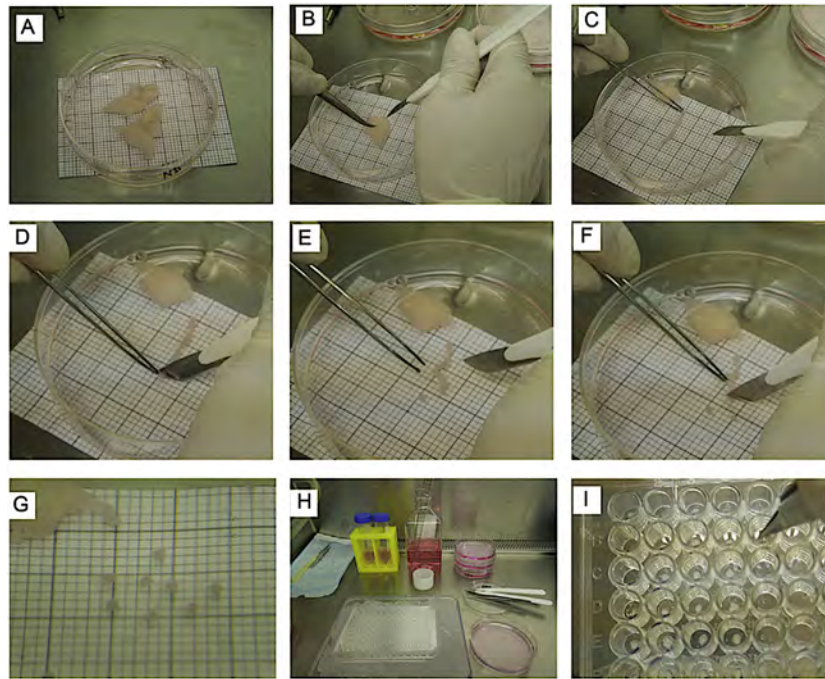
Figure Ap. 1 Embedding procedure.

(A) Adipose tissue samples placed in a 100 cm petri dish containing 25 ml of EGM-2 MV medium. The millimeter (mm) paper placed under the petri dish is used as a size reference. **(B)** Sample of adipose tissue in plate #2 containing 15 ml of EGM-2 MV medium. The scalpel and forceps are used to hold the fat and cut it into strips. **(C)** Piece of fat strip cut from the adipose tissue sample. Using the millimeter paper reference, the fat strip is aligned in order to cut the appropriate size of each slice (explant). **(D)** For the first cut, it is easier to start at one of the ends of the adipose tissue strip. The forceps are used to hold the fat while the scalpel is used to cut the slice. **(E)** The explant is aligned with one of the quadrants in the millimeter paper to verify adequate size. **(F)** The rest of the strip is cut into slices. The adipose tissue is held by forceps and the cut is done by the scalpel. While handling the forceps, avoid pulling or stretching the fat, since it may damage the tissue. **(G)** Individual slices cut to appropriate size and verified with the millimeter paper. **(H)** Display of workstation in the biocabinet before starting the embedding procedure. Explants were transferred to plate #3, containing 25 ml of EGM-2 MV medium. 96-multiwell plate is kept in a tray filled with ice for the embedding steps. **(I)** Embedding step. After the Matrigel is dispensed, forceps are used to place the explants, one per well. The explant is positioned at the center of the well.

199

Quantification of angiogenic potential

The mount of capillary growth can be evaluated using several approaches. Here we describe three independent strategies to quantify angiogenic potential, which we have successfully applied to both mouse and human samples. We recommend using at least two independent methods so correlation analysis can be performed to validate reproducibility of the data obtained.

Counting of capillary sprouts

A capillary sprout is defined as a branching structure of at least three cells connected to each other in a linear manner (Figure Ap.2 A, B). This structure is qualitatively different from other cell types that can also emerge from the explant, but which grow in a disorganized manner and typically adhere to the surface of the plate (Figure Ap.2 C, D). To detect capillary sprouts, imaging under sufficient magnification under phase contrast is required. In our laboratory we use a Zeiss Axiovert equipped with a 10 objective. Phase contrast images of embedded explants and emerging capillary sprouts from mouse adipose tissue at day 14 are shown in Figure Ap.2 E, and in Figure Ap.2 F, the structures that would be considered to be sprouts are delineated in red. As new sprouts emerge, they become interconnected and grow into the three-dimensional volume of the Matrigel; thus, counting should be performed early during the growth period. Sprouts begin to emerge after 4–5 days post-embedding of mouse epididymal fat

200

explants, and we quantify the number of sprouts per explant at day 7 and day 14 post-embedding. Because the definition of a sprout is somewhat subjective, it is necessary to have more than one individual perform the counting, and that the individuals performing the counting be blinded as to the experimental condition of the sample.
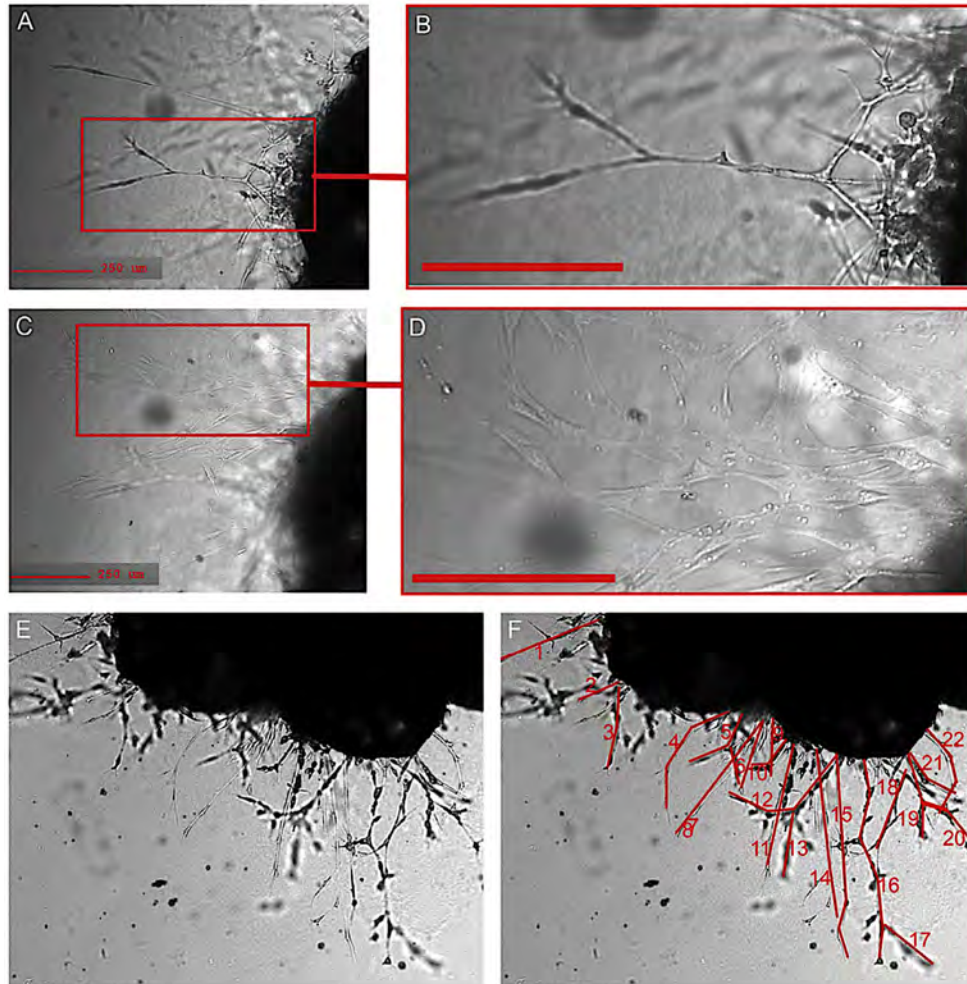
Figure Ap. 2 Cells emerging from mouse adipose tissue explant.

(A, B) Capillary sprout emerging from embedded mouse explant, displaying characteristic linear branching structure. **(C, D)** Focus set to the surface of the well, where fibroblastic adherent cells can be seen emerging from the explant, observed at a different optical plane of the image. **(E)** Phase contrast image of the explant and the capillary sprouts 14 days post-embedding. **(F)** Structures shown in red highlight formations that can be considered to be sprouts.

Because of the variability in the number of sprouts emerging from each explant, at least 25 explants must be analyzed for each experimental condition. The results are expressed as the average number of sprouts per explant. When studying mouse epididymal fat, there is a linear correlation between the number of explants that develop sprouts and the average number of sprouts per explant (Figure Ap.3). Thus, the percent of explants that display sprouting is an alternative way to quantify angiogenic potential.
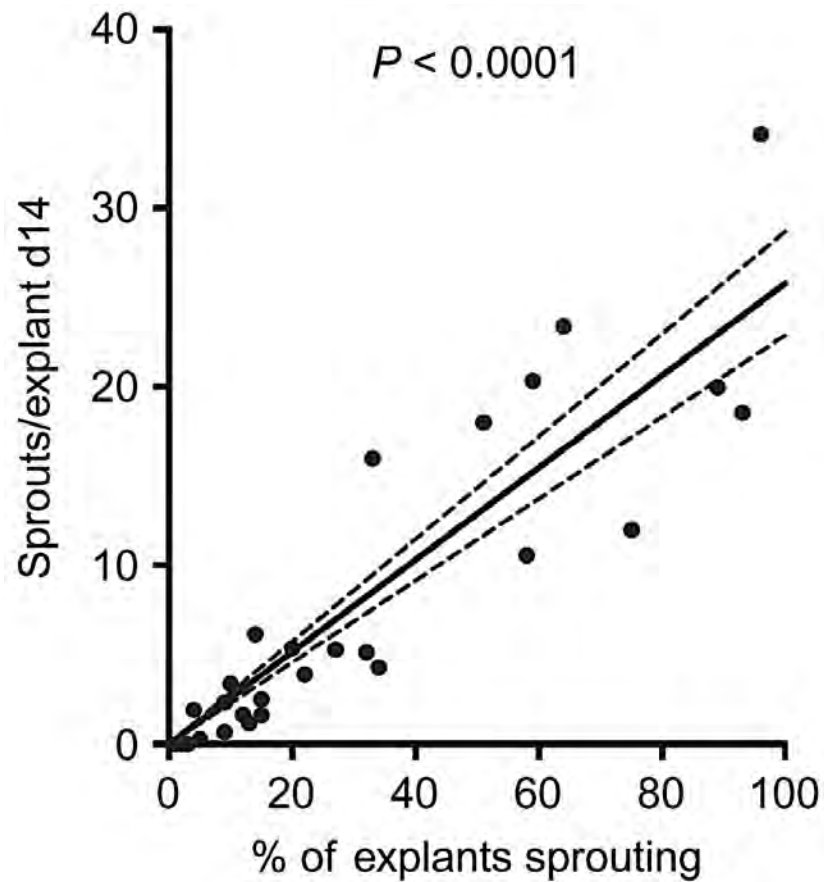
Figure Ap. 3 Linear correlation between the number of explants sprouting and the quantity of sprouts per explant from mouse adipose tissue.

Capillary sprouting was quantified in a study of 36 mice fed normal or high-fat diet for 3–30 weeks. 25–30 explants from each mouse were embedded. The percent of the embedded explants for each mouse displaying sprouts after 14 days of culture is plotted on the *x*-axis. The mean number of sprouts per explant (i.e., sum of sprouts in all explants/total number of explants embedded) is plotted on the *y*-axis. Linear regression was calculated using PRISM software.

Counting can also be performed on human explants, which form well defined capillaries with tight junctions defining primitive lumens (Figure Ap.4). Human explants develop many more sprouts compared to mouse (Figure Ap.5). After 11 days, the sprouts become highly branched and expand into the three-dimensional volume of the Matrigel, making counting more complex. Thus, counting of human sprouts is best done at days 5–7 post-embedding.
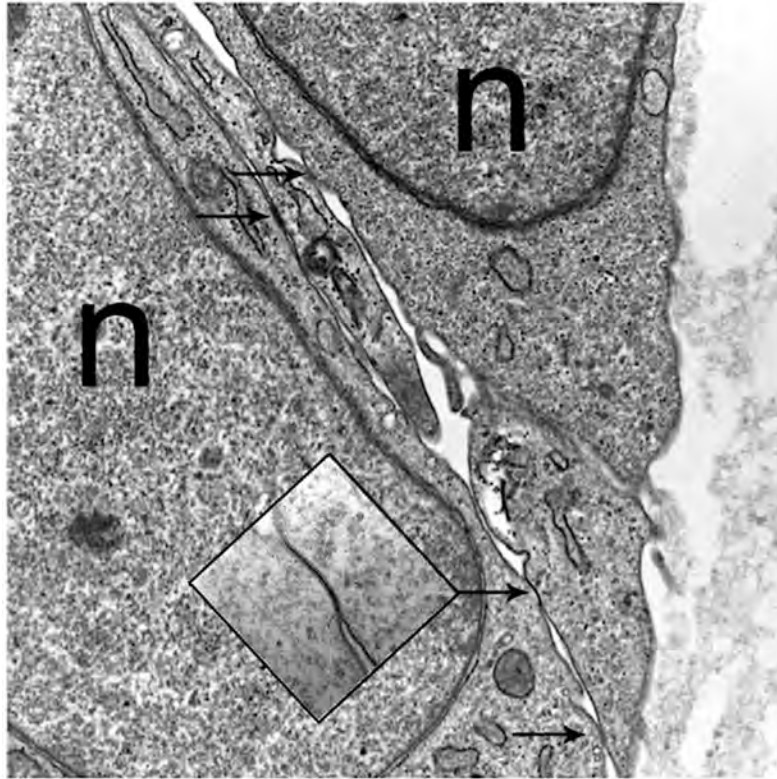
Figure Ap. 4 Electron micrograph of capillary sprouts from a human adipose tissue explant.

Arrows identify tight junctions. n, nucleus.
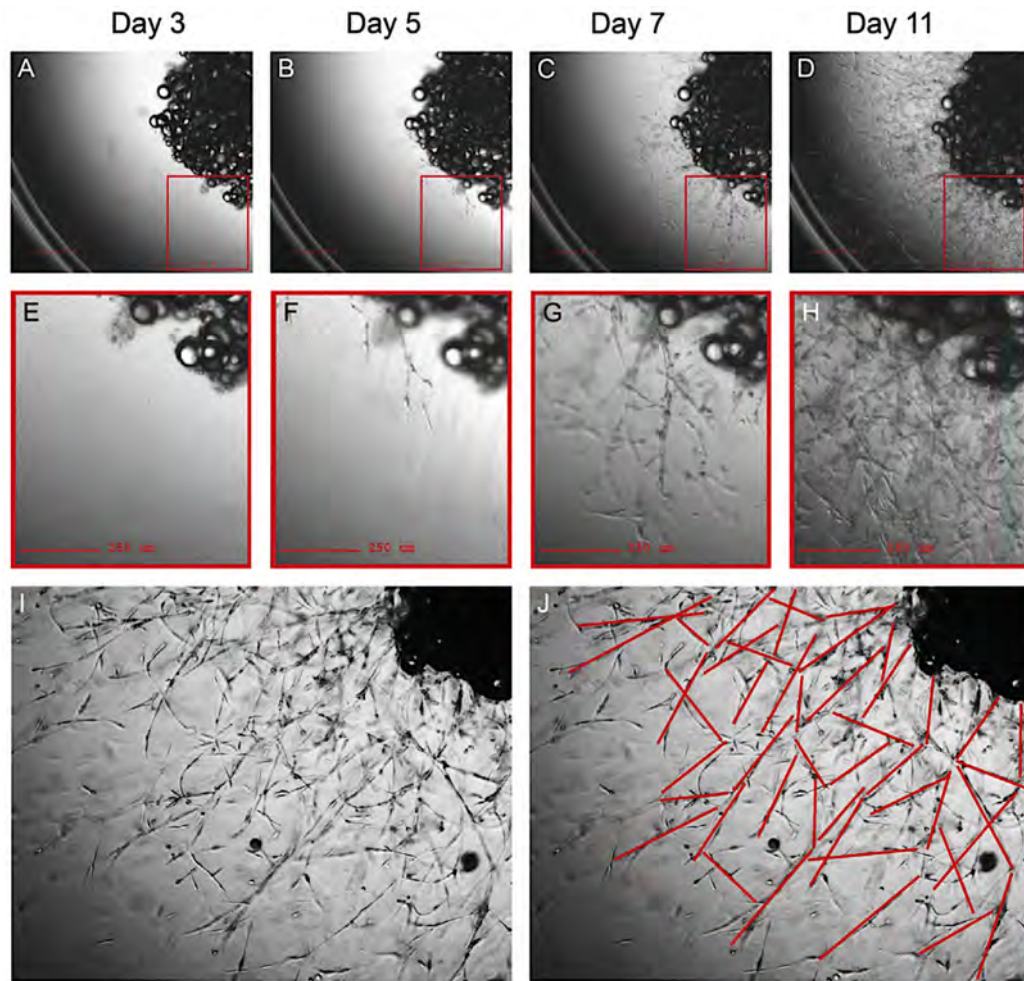
Figure Ap. 5 Capillary sprouting from human adipose tissue.

A human explant from subcutaneous adipose tissue at days 3 **(A, E)**, 5 **(B, F)** 7 **(C, G)**, and 11 **(D, H)** post-embedding. Capillary sprouting begins to be observed at day 5. After day 11, the growth is highly increased **(I, J)**, making difficult to identify all sprout formation.

207

Digital analysis of growth area

The capillary growth can be further analyzed by measuring the area of sprouting in each well. In our laboratory, we have used a Zeiss Axio Observer Z1 microscope equipped with an automated stage. Brightfield images of each well of a 96-well plate are acquired using a 2.5 objective and captured using an Andor Clara E interline CCD camera. The stage position, illumination and acquisition setting are controlled by Micro-manager open source microscopy software (Edelstein, Amodaj, Hoover, Vale, & Stuurman, 2010) using a multiwell plate plugin developed by Karl Bellve and Ben Czech (http://valelab.ucsf.edu/$MM/MMwiki/index.php/ Well_Plate_Plugin). The plugin is designed to handle standard SBS well plates from 24, 96, 384, and 1536 wells. The plugin will calculate the correct X, Y, and Z coordinate for each well position, and for any number of positions within each well. Imaging can then iterate through each well, starting at the first well. The plugin will move the stage down or up each column, until the last row, before moving to the next column and reversing direction. The zigzag path chosen for moving the stage is the fastest path on a Zeiss AxioObserver Z1. The starting well, or the ending well, can be selected to only work on a sub region. For our experiments, each well of a 96-well plate containing an explant is divided into four quadrants, with a 50 CCD pixel overlap. Five optical sections spaced at 150 mm are collected for each quadrant, and a montage of the quadrants is then generated for further analysis.

208

For further analysis, the composite image is imported into Fiji, an image processing package, which is a distribution of ImageJ, Java, Java 3D, and several plugins organized into a coherent menu structure (Schindelin et al., 2012). For calculation of the growth area, areas of explant and capillary sprout growth are delineated. Various parameters can then be extracted, including the area occupied by explant and sprouts (Figure Ap.6) as follows:

To measure areas in the image files:

1. Open Fiji

2. Open image to be analyzed

3. Visually examine in which plane the explant is more in focus. Use it for selecting the area of the explant.

4. In the tools menu, select "Freehand selections"

5. Select the area of the explant:

   1. Highlight the borders of the explant with the cursor, keeping pressed the left button on the mouse. If the button is released, the area selected will be automatically closed.

6. Edit>Selection>Add to Manager. Automatically, the selected area is added to ROI Manager. Keep the ROI Manager window open. ROI will allow you to select the area of growth in the same image and measure a series of parameters, including the area measurements.

209

7. Go back to the image and select the area of growth. Make sure to examine every plane. You can move around each plane while making the selection, so all the growth is included.

8. After selecting the area of growth, press "Add (t)" in the ROI Manager window.

9. In the ROI Manager window, select both areas
    1. "Shift"+"↓" if needed

10. Press "Measure" in the ROI Manager window. A "Results" window will appear. It contains different kinds of measurements, including area of the explant and growth.
    1. Item #1 is the area of the explant
    2. Item #2 is the area of the growth
    3. It is very important to maintain the order of measurements. First the explant, then the area of growth.

11. In the Results window, go to File>Save as
    1. Suggestion: Save results file with the well name (A2, B2, etc.) and a short identification of the sample. Keep consistency in naming, in case a program is developed to help in analysis.
    (Examples: A2_Control_Day7.txt, B7_Sample1_Day7.txt)

12. In the ROI Manager window, select "More>>," Save

    1. Save ROI file as a .zip. This will allow you to save both explant and growth area as .roi files. Suggestion: Name the .zip file with the well name (A2, B2, etc.) and a short identification of the sample. Keep consistency in naming, in case a program is developed to help in analysis. (Examples: A2_Control_Day7.zip, B7_Sample1_Day7.zip)

13. To open image files that were already measured

    1. Open Fiji

    2. Open desired image

    3. File>Open>Select file>Open ".zip" file

    4. In the ROI Manager window, select both areas

    5. "Shift"+"↓" if needed

    6. Mark "Show All"

    7. Both selected areas should appear in the active image
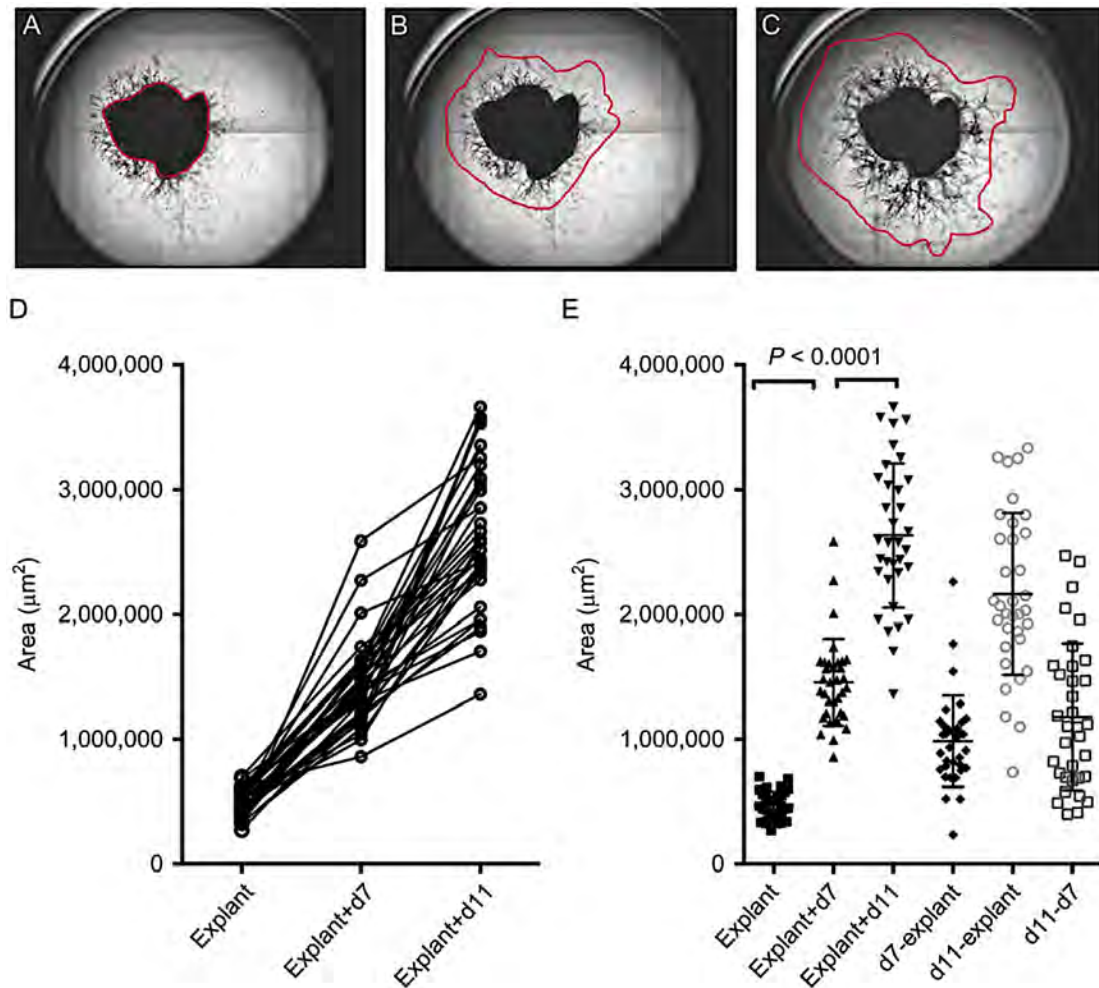
Figure Ap. 6 Digital Analysis of capillary growth area.

An example of montages generated from bright field images of quadrants of a single well from a 96-well-multiwell plate containing an explant from human omental adipose tissue. The region of the explant **(A)**, and of capillary growth at day 7 **(B)**, and day 11 **(C)** post-embedding is delineated. The areas are calculated for the selected regions highlighted in red. **(D)** Calculated areas of 34 explants from the same tissue sample growing in the same 96-well-multiwell plotted in a before–after format, revealing linear growth in all embedded explants over the culture period. **(E)** Scatter plot displaying the means and standard deviation of the values obtained for each explant at each time point, and values obtained after subtracting the area of the initial explant. Paired Student's *t*-test between time points

reveals highly significant differences, which can be used to compare angiogenic potential among different donors.

Immunofluorescence analysis of explants

Adipose tissue explants can also be analyzed by immunofluorescence, with the exception that embedding must be done on coverslips or glass-bottom culture dishes. In our laboratory we have used 35 mm glass-bottom culture dishes (MatTek Corporation). The use of glass-bottom culture dishes allows for examination of stained samples at higher magnifications. The protocol used for visualizing human Von Willebrand factor is as follows:

1. Dispense 100 μl of Matrigel to cover the bottom of each dish and embed explants and maintain in culture as described above.

2. On the desired day, wash samples three times in DPBS by gently aspirating medium from the side of the dish and using 3 ml of DPBS for each wash.

3. Prepare fresh 4% formaldehyde solution by diluting the supplied 16% solution in DPBS at 1:3 ratio. Make sure to use chemical hood with proper ventilation at all times while handling formaldehyde.

4. Inside of chemical hood, gently aspirate DPBS from the dishes with samples and add 1 ml of freshly prepared 4% formaldehyde solution into each dish. Incubate for 15 min at room temperature with very gentle shaking.

5. Gently remove 4% formaldehyde from the dish and wash again three times in DPBS, gently shaking for 5 min in each wash step.

6. Prepare permeabilizing solution by supplementing DPBS with 0.5% Triton X-100 and 1% BSA.

7. Permeabilize and block non-specific antibody attachment by incubating in 0.5% Triton X-100 1% BSA in DPBS for 60 min with gentle shaking. Use 2 ml of the solution per each well.

8. Remove solution and replace with primary antibody, in this case anti-human polyclonal rabbit Von Willebrand factor (Dako, catalog # A0082), diluted 1:100 in permeabilizing solution. Use at least 1 ml of antibody solution for each dish. Incubate overnight at 5°C with gentle shaking.

9. Remove primary antibody, and wash three times with DPBS, gently shaking for 5 min between each wash step.

10. Incubate for 1 h with secondary antibodies diluted in permeabilizing solution. The secondary antibody we have used is Alexa Fluor 488 (Invitrogen; Molecular probes, catalog # 11008, dilution 1:500).

11. Wash three times with DPBS, gently shaking for 5 min between each wash step.

12. Perform nuclear counter staining by incubating for 5 min with Hoechst 33258, pentahydrate diluted 1:5000 in DPBS.

13. Wash in DPBS three times.

Isolated cell analysis

After completing manual counting and digital assessments of capillary growth, cells comprising capillary sprouts can be harvested from the Matrigel for further analysis by western blotting, FACS, etc. To quantitatively recover the cells from each well, the following procedure is used:

Before starting

- Dispase is used for proteolysis of Matrigel. Dispase should be aliquoted in 1.5 ml volume vials and stored at 20 °C. Avoid multiple freeze–thaw cycles. Before use, dispase is thawed at 37°C.
- Most of the capillary cells grow in Matrigel, but some cells (e.g., fibro-blasts) attach to the bottom of the plate. Trypsin-Versene is used for detaching cells that remain adherent to the well after the dispase treatment.
- Materials and tools used, including jeweler's forceps and scissors, should be sterile.

1. Carefully, remove the medium by aspirating it from the wells. Be careful not to aspirate Matrigel or explants.

2. Rinse twice with 200 μl of sterile DPBS. Discard DPBS.

    Caution: In case of human tissue, discard medium and DPBS according to your institution's safety regulations.

215

3. Add 50 μl of dispase to each well. Incubate at 37°C for 1.5–2 h. *Make sure that all cells are detached and floating in the digested Matrigel by looking under the microscope after incubation.*

4. Prepare a 1:1 mixture of Trypsin-Versene and 50 mM EDTA.

5. Add 50 μl of the Trypsin-Versene/EDTA mixture to each well to stop dispase digestion and dislodge adherent cells. Gently mix by pipetting up and down. Incubate at 37°C for 10 min.

6. Use forceps to remove remaining explant from wells. Discard the explants in biomedical waste.

7. Add 50 μl of DPBS to each well. Mix by pipetting up and down.

8. Transfer the cell suspension from all wells to a 15 ml conical tube. Fill with EGM-2 MV-supplemented EBM-2 medium to achieve a final volume of 10 ml.

9. Centrifuge the tube containing the cells at 200xg for 10 min at room temperature.

10. Make sure the cells are pelleted down. Aspirate the supernatant and resuspend the pellet in 1 ml of fresh EGM-2 MV-supplemented EBM-2 medium.

11. Obtain cell concentration and viability. For this purpose, the Cellometer Auto T4 Cell Counter and Software was used (Nexcelom Bioscience).

12. Resuspend cells for further use.

216

Method limitations

1. There is significant variation between each individual explant, so quantitative analysis requires at least 25 explants per condition.

2. The capillary sprouts are defined by morphological criteria, so changes in the cellular composition, cell shape or cell motility could affect the result.

3. The Matrigel is relatively impermeable and thus penetration by large molecules such as nucleic acids, or viruses that could be used to interrogate the properties of the growing cells is difficult.

4. Immunostaining is complicated by non-specific attachment of antibodies to Matrigel, and therefore successful results depend on the availability of high affinity antibodies and molecules expressed at relatively high levels.

217

References

Abrams, B., & Selvin, S. (1995). Maternal weight gain pattern and birth weight. *Obstetrics & Gynecology*, *86*(2), 163–169. https://doi.org/10.1016/0029-7844(95)00118-B

Ahima, R. S., Prabakaran, D., Mantzoros, C., Qu, D., Lowell, B., Maratos-Flier, E., & Flier, J. S. (1996). Role of leptin in the neuroendocrine response to fasting. *Nature*, *382*(6588), 250–252. https://doi.org/10.1038/382250a0

Aitken, D., Barkai, G., Arbuzova, S., Spencer, K., Muller, F., Hallahan, T., … Cuckle, H. (2003). Frequency and clinical consequences of extremely high maternal serum PAPP-A levels. *Prenatal Diagnosis*, *23*(5), 385–388. https://doi.org/10.1002/pd.600

Akbay, E., Tıras, M. B., Yetkin, I., Törüner, F., Ersoy, R., Uysal, S., & Ayvaz, G. (2003). Insulin secretion and insulin sensitivity in normal pregnancy and gestational diabetes mellitus. *Gynecological Endocrinology*, *17*(2), 137–142. https://doi.org/10.1080/gye.17.2.137.142

Albrecht, S. S., Kuklina, E. V, Bansil, P., Jamieson, D. J., Whiteman, M. K., Kourtis, A. P., … Callaghan, W. M. (2010). Diabetes trends among delivery hospitalizations in the U.S., 1994-2004. *Diabetes Care*, *33*(4), 768–773. https://doi.org/10.2337/dc09-1801

Allard, J. B., & Duan, C. (2018). IGF-binding proteins: Why do they exist and why are there so many? *Frontiers in Endocrinology*, *9*(117), 1–12. https://doi.org/10.3389/fendo.2018.00117

Alligier, M., Gabert, L., Meugnier, E., Lambert-Porcheron, S., Chanseaume, E., Pilleul, F., … Laville, M. (2013). Visceral Fat Accumulation During Lipid Overfeeding Is Related to Subcutaneous Adipose Tissue Characteristics in Healthy Men. *The Journal of Clinical Endocrinology & Metabolism*, *98*(2), 802–810. https://doi.org/10.1210/jc.2012-3289

Alligier, M., Meugnier, E., Debard, C., Lambert-Porcheron, S., Chanseaume, E., Sothier, M., … Laville, M. (2012). Subcutaneous adipose tissue remodeling during the initial phase of weight gain induced by overfeeding in humans. *Journal of Clinical Endocrinology and Metabolism*, *97*(2), 183–192. https://doi.org/10.1210/jc.2011-2314

Altinova, A. E., Toruner, F., Bozkurt, N., Bukan, N., Karakoc, A., Yetkin, I., … Arslan, M. (2007). Circulating concentrations of adiponectin and tumor necrosis factor-α in gestational diabetes mellitus. *Gynecological Endocrinology*, *23*(3), 161–165. https://doi.org/10.1080/09513590701227960

Anderlová, K., Simjak, P., Cinkajzlova, A., Klouckova, J., Kratochvilova, H., Lacinová, Z., … Krsek, M. (2018). IGFs and IGF-Binding Proteins in

219

Pregnancy and Gestational Diabetes Mellitus. *Diabetes*, *67*(Supplement 1), 1412-P. https://doi.org/10.2337/db18-1412-P

Andersen, M., Nørgaard-Pedersen, D., Brandt, J., Pettersson, I., & Slaaby, R. (2017). IGF1 and IGF2 specificities to the two insulin receptor isoforms are determined by insulin receptor amino acid 718. *PLoS ONE, 12*(6), e0178885–e0178885. https://doi.org/10.1371/journal.pone.0178885

Andersson, D. P., Hogling, D. E., Thorell, A., Toft, E., Qvisth, V., Näslund, E., … Arner, P. (2014). Changes in subcutaneous fat cell volume and insulin sensitivity after weight loss. *Diabetes Care*, *37*(7), 1831–1836. https://doi.org/10.2337/dc13-2395

Angueira, A., Ludvik, A., Reddy, T., Wicksteed, B., Lowe, W., & Layden, B. (2015). New insights into gestational glucose metabolism: Lessons learned from 21st century approaches. *Diabetes*, *64*(2), 327–334. https://doi.org/10.2337/db14-0877

Anjana, M., Sandeep, S., Deepa, R., Vimaleswaran, K. S., Farooq, S., & Mohan, V. (2004). Visceral and central abdominal fat and anthropometry in relation to diabetes in Asian Indians. *Diabetes Care*, *27*(12), 2948–2953. https://doi.org/10.2337/diacare.27.12.2948

Anusree, S., Sindhu, G., Preetha Rani, M., & Raghu, K. (2018). Insulin resistance

in 3T3-L1 adipocytes by TNF-α is improved by punicic acid through upregulation of insulin signalling pathway and endocrine function, and downregulation of proinflammatory cytokines. *Biochimie*, *146*, 79–86. https://doi.org/10.1016/j.biochi.2017.11.014

Aplin, A. C., Fogel, E., Zorzi, P., & Nicosia, R. F. (2008). Chapter 7 The Aortic Ring Model of Angiogenesis. In *Angiogenesis* (Vol. 443, pp. 119–136). Academic Press. https://doi.org/10.1016/S0076-6879(08)02007-7

Arner, P. (2018). *Fat tissue growth and development in humans*. *Nestle Nutrition Institute Workshop Series* (Vol. 89). https://doi.org/10.1159/000486491

Atègbo, J., Grissa, O., Yessoufou, A., Hichami, A., Dramane, K., Moutairou, K., … Khan, N. (2006). Modulation of Adipokines and Cytokines in Gestational Diabetes and Macrosomia. *The Journal of Clinical Endocrinology & Metabolism*, *91*(10), 4137–4143. https://doi.org/10.1210/jc.2006-0980

Atilano, L., Lee-Parritz, A., Lieberman, E., Cohen, A., & Barbieri, R. (1999). Alternative methods of diagnosing gestational diabetes mellitus. *American Journal of Obstetrics & Gynecology*, *181*(5), 1158–1161. https://doi.org/10.1016/S0002-9378(99)70100-6

Attie, A., & Scherer, P. (2009). Adipocyte metabolism and obesity. *Journal of Lipid Research*, *50*(Suppl), S395–S399. https://doi.org/10.1194/jlr.R800057-

JLR200

Baer, R. J., Lyell, D. J., Norton, M. E., Currier, R. J., & Jelliffe-Pawlowski, L. L. (2016). First trimester pregnancy-associated plasma protein-A and birth weight. *European Journal of Obstetrics and Gynecology and Reproductive Biology*, *198*, 1–6. https://doi.org/10.1016/j.ejogrb.2015.12.019

Baker, M., Robinson, S. D., Lechertier, T., Barber, P. R., Tavora, B., D'Amico, G., … Hodivala-Dilke, K. (2012). Use of the mouse aortic ring assay to study angiogenesis. *Nature Protocols*, *7*, 89–104. Retrieved from https://doi.org/10.1038/nprot.2011.435

Bale, L., & Conover, C. (2005). Disruption of insulin-like growth factor-II imprinting during embryonic development rescues the dwarf phenotype of mice null for pregnancy-associated plasma protein-A. *Journal of Endocrinology, 186*(2), 325–331. https://doi.org/10.1677/joe.1.06259

Bale, L., West, S., & Conover, C. (2017). Inducible knockdown of pregnancy-associated plasma protein-A gene expression in adult female mice extends life span. *Aging Cell*, *16*(4), 895–897. https://doi.org/10.1111/acel.12624

Bao, W., Baecker, A., Song, Y., Kiely, M., Liu, S., & Zhang, C. (2015). Adipokine levels during the first or early second trimester of pregnancy and subsequent risk of gestational diabetes mellitus: A systematic review. *Metabolism:*

222

Clinical and Experimental, *64*(6), 756–764.
https://doi.org/10.1016/j.metabol.2015.01.013

Barbour, L., McCurdy, C., Hernandez, T., & Friedman, J. (2011). Chronically
increased S6K1 is associated with impaired IRS1 signaling in skeletal
muscle of GDM women with impaired glucose tolerance postpartum. *Journal
of Clinical Endocrinology and Metabolism*, *96*(5), 1431–1441.
https://doi.org/10.1210/jc.2010-2116

Barbour, L., McCurdy, C., Hernandez, T., Kirwan, J., Catalano, P., & Friedman,
J. (2007). Cellular mechanisms for insulin resistance in normal pregnancy
and gestational diabetes. *Diabetes Care*, *30*(Supplement 2), S112-119.
https://doi.org/10.2337/dc07-s202

Barnea, E. (1986). Placental and circulating pregnancy-associated plasma
protein A concentrates in normal and pathological term pregnancies.
Obstetrics and Gynecology, *68*(3), 382–386.
https://doi.org/10.1097/00006250-198609000-00019

Beattie, J., Allan, G. J., Lochrie, J. D., & Flint, D. J. (2006). Insulin-like growth
factor-binding protein-5 (IGFBP-5): a critical member of the IGF axis. *The
Biochemical Journal*, *395*(1), 1–19. https://doi.org/10.1042/BJ20060086

Bellamy, L., Casas, J. P., Hingorani, A. D., & Williams, D. (2009). Type 2

223

diabetes mellitus after gestational diabetes: a systematic review and meta-analysis. *The Lancet*, *373*, 1773–1779. https://doi.org/10.1016/S0140-6736(09)60731-5

Beneventi, F., Simonetta, M., Lovati, E., Albonico, G., Tinelli, C., Locatelli, E., & Spinillo, A. (2011). First trimester pregnancy-associated plasma protein-A in pregnancies complicated by subsequent gestational diabetes. *Prenatal Diagnosis*, *31*(6), 523–528. https://doi.org/10.1002/pd.2733

Berggren, E., O'Tierney-Ginn, P., Lewis, S., Presley, L., De-Mouzon, S., & Catalano, P. (2017). Variations in resting energy expenditure: impact on gestational weight gain. *American Journal of Obstetrics and Gynecology*, *217*(4), 445.e1-445.e6. https://doi.org/10.1016/j.ajog.2017.05.054

Bersinger, N., & Klopper, A. (1984). Observations on the source of pregnancy-associated plasma protein A (PAPP-A). *BJOG: An International Journal of Obstetrics & Gynaecology*, *91*(11), 1074–1076. https://doi.org/10.1111/j.1471-0528.1984.tb15078.x

Bischof, P. (1979). Purification and characterization of Pregnancy Associated Plasma Protein A (PAPP-A). *Archives of Gynecology*, *227*(4), 315–326. https://doi.org/10.1007/BF02109920

Bischof, P. (1984). The disappearance rate of pregnancy-associated plasma

224

protein-A (PAPP-A) after the end of normal and abnormal pregnancies. *Archives of Gynecology, 236*(2), 93–98.

Bischof, P. (1989). Three pregnancy proteins (PP12, PP14, and PAPP-A): their biological and clinical relevance. *American Journal of Perinatology*, *6*(2), 110–116. https://doi.org/10.1055/s-2007-999559

Bischof, P., DuBerg, S., Herrmann, W., & Sizonenko, P. C. (1981). Pregnancy-associated plasma protein-a (PAPP-A) and hCG in early pregnancy. *British Journal of Obstetrics and Gyneacology*, *88*(10), 973–975. https://doi.org/10.1111/j.1471-0528.1981.tb01683.x

Boucher, J., Kleinridders, A., & Kahn, C. R. (2014). Insulin Receptor Signaling in Normal and Insulin-Resistant States. *Cold Spring Harb Perspect Biol*, *6*, a009191. https://doi.org/10.1101/cshperspect.a009191

Bouloumié, A. (2002). Angiogenesis in adipose tissue. *Annales d'endocrinologie*, *63*(2), 91–95.

Brambati, B., Macintosh, M. C. M., Teisner, B., Maguiness, S., Shrimanker, K., Lanzani, A., … Grudzinskas, J. G. (1993). Low maternal serum levels of pregnancy associated plasma protein A (PAPP-A) in the first trimester in association with abnormal fetal karyotype. *BJOG: An International Journal of Obstetrics & Gynaecology*, *100*(4), 324–326. https://doi.org/10.1111/j.1471-

0528.1993.tb12973.x

Butte, N. (2000). Carbohydrate and lipid metabolism in pregnancy: Normal compared with gestational diabetes mellitus. *American Journal of Clinical Nutrition*, *71*(5), 1256S-1261S. https://doi.org/10.1093/ajcn/71.5.1256s

Butte, NF, Hopkinson, J., & Nicolson, M. (1997). Leptin in Human Reproduction : Serum Leptin Levels in Pregnant and Lactating Women. *Journal of Clinical Endocrinology & Metabolism*, *82*(2), 585–589. https://doi.org/10.1210/jc.82.2.585

Byun, D., Mohan, S., Yoo, M., Sexton, C., Baylink, D. J., & Qin, X. (2001). Pregnancy-associated plasma protein-A accounts for the insulin-like growth factor (IGF)-binding protein-4 (IGFBP-4) proteolytic activity in human pregnancy serum and enhances the mitogenic activity of IGF by degrading IGFBP-4 in vitro. *Journal of Clinical Endocrinology and Metabolism*, *86*(2), 847–854. https://doi.org/10.1210/jc.86.2.847

Cao, Y. (2007). Science in medicine Angiogenesis modulates adipogenesis and obesity. *Journal of Clinical Investigation*, *117*(9), 2362–2368. https://doi.org/10.1172/JCI32239.2362

Carobbio, S., Pellegrinelli, V., & Vidal-Puig, A. (2017). Adipose Tissue Function and Expandability as Determinants of Lipotoxicity and the Metabolic

226

Syndrome. In A. B. Engin & A. Engin (Eds.), *Obesity and Lipotoxicity* (pp. 161–196). Cham: Springer International Publishing. https://doi.org/10.1007/978-3-319-48382-5_7

Carpenter, M., & Coustan, D. (1982). Criteria for screening tests for gestational diabetes. *American Journal of Obstetrics and Gynecology*, *144*(7), 768–773. https://doi.org/10.1016/0002-9378(82)90349-0

Casagrande, S., Linder, B., & Cowie, C. (2018). Prevalence of gestational diabetes and subsequent Type 2 diabetes among U.S. women. *Diabetes Research and Clinical Practice*, *141*, 200–208. https://doi.org/10.1016/j.diabres.2018.05.010

Catalano, P. (2014). Trying to understand gestational diabetes. *Diabetic Medicine : A Journal of the British Diabetic Association*, *31*(3), 273–281. https://doi.org/10.1111/dme.12381

Catalano, P., Huston, L., Amini, S., & Kalhan, S. (1999). Longitudinal changes in glucose metabolism during pregnancy in obese women with normal glucose tolerance and gestational diabetes mellitus. *American Journal of Obstetrics and Gynecology*, *180*(4), 903–916. https://doi.org/10.1016/S0002-9378(99)70662-9

Catalano, P., Nizielski, S., Shao, J., Preston, L., Qiao, L., & Friedman, J. (2002).

Downregulated IRS-1 and PPARγ in obese women with gestational diabetes: relationship to FFA during pregnancy. *American Journal of Physiology-Endocrinology and Metabolism*, *282*(3), E522–E533. https://doi.org/10.1152/ajpendo.00124.2001

Catalano, P., Tyzbir, E., Roman, N., Amini, S., & Sims, E. (1991). Longitudinal changes in insulin release and insulin resistance in nonobese pregnant women. *American Journal of Obstetrics and Gynecology*, *165*(6), 1667–1672. https://doi.org/10.1016/0002-9378(91)90012-G

Catalano, P., Tyzbir, E., Wolfe, R., Calles, J., Roman, N., Amini, S., & Sims, E. (1993). Carbohydrate metabolism during pregnancy in control subjects and women with gestational diabetes. *American Journal of Physiology-Endocrinology and Metabolism*, *264*(1), E60–E67. https://doi.org/10.1152/ajpendo.1993.264.1.e60

Catalano, P., Tyzbir, E., Wolfe, R., Roman, N., Amini, S., & Sims, E. (1992). Longitudinal changes in basal hepatic glucose production and suppression during insulin infusion in normal pregnant women. *American Journal of Obstetrics & Gynecology*, *167*(4), 913–919. https://doi.org/10.1016/S0002-9378(12)80011-1

Chandna, A., Kuhlmann, N., Bryce, C., Greba, Q., Campanucci, V., & Howland,

J. (2015). Chronic maternal hyperglycemia induced during mid-pregnancy in

rats increases RAGE expression, augments hippocampal excitability, and

alters behavior of the offspring. *Neuroscience*, *303*, 241–260.

https://doi.org/10.1016/j.neuroscience.2015.06.063

Chao, W., & D'Amore, P. A. (2008). IGF2: Epigenetic regulation and role in

development and disease. *Cytokine and Growth Factor Reviews*, *19*(2),

111–120. https://doi.org/10.1016/j.cytogfr.2008.01.005

Chen, J., Bardes, E., Aronow, B., & Jegga, A. (2009). ToppGene Suite for gene

list enrichment analysis and candidate gene prioritization. *Nucleic Acids

Research*, *37*, W305–W311. https://doi.org/10.1093/nar/gkp427

Chen, J., Tan, B., Karteris, E., Zervou, S., Digby, J., Hillhouse, E., … Randeva,

H. (2006). Secretion of adiponectin by human placenta: Differential

modulation of adiponectin and its receptors by cytokines. *Diabetologia*,

49(6), 1292–1302. https://doi.org/10.1007/s00125-006-0194-7

Chen, Y., Lv, P., Du, M., Liang, Z., Zhou, M., & Chen, D. (2017). Increased

retinol-free RBP4 contributes to insulin resistance in gestational diabetes

mellitus. *Archives of Gynecology and Obstetrics*, *296*(1), 53–61.

https://doi.org/10.1007/s00404-017-4378-9

Cheung, N. W., & Byth, K. (2003). Population Health Significance of Gestational

Diabetes. *Diabetes Care*, *26*(7), 2005–2009.
https://doi.org/10.2337/diacare.26.7.2005

Cho, C.-H., Koh, Y. J., Han, J., Sung, H.-K., Lee, H. J., Morisada, T., … Koh, G.
Y. (2007). Angiogenic Role of LYVE-1–Positive Macrophages in
Adipose Tissue. *Circulation Research*, *100*(4), e47–e57.
https://doi.org/10.1161/01.RES.0000259564.92792.93

Choe, S. S., Huh, J. Y., Hwang, I. J., Kim, J. I., & Kim, J. B. (2016). Adipose
tissue remodeling: Its role in energy metabolism and metabolic disorders.
Frontiers in Endocrinology, *7*(30), 1–16.
https://doi.org/10.3389/fendo.2016.00030

Christiaens, V., & Lijnen, H. R. (2010). Angiogenesis and development of
adipose tissue. *Molecular and Cellular Endocrinology*, *318*(1), 2–9.
https://doi.org/10.1016/j.mce.2009.08.006

Cinti, S. (2015). The Adipose Organ : Implications For Prevention And Treatment
Of Obesity. Retrieved from https://ebook.ecog-obesity.eu/wp-
content/uploads/2015/02/ECOG-Obesity-eBook-The-Adipose-Organ-
Implications-For-Prevention-And-Treatment-Of-Obesity.pdf

Clemmons, D. R. (2012). Metabolic actions of insulin-like growth factor-I in
normal physiology and diabetes. *Endocrinology and Metabolism Clinics of*

230

North America, *41*(2), 425–443. https://doi.org/10.1016/j.ecl.2012.04.017

Coate, K. C., Smith, M. S., Shiota, M., Irimia, J. M., Roach, P. J., Farmer, B., … Moore, M. C. (2013). Hepatic glucose metabolism in late pregnancy normal versus high-fat and -fructose diet. *Diabetes*, *62*(3), 753–761. https://doi.org/10.2337/db12-0875

Combs, T. P., Berg, A. H., Obici, S., Scherer, P. E., & Rossetti, L. (2001). Endogenous glucose production is inhibited by the adipose-derived protein Acrp30. *Journal of Clinical Investigation*, *108*(12), 1875–1881. https://doi.org/10.1172/JCI14120

Conover, C., & Bale, L. (2007). Loss of pregnancy-associated plasma protein A extends lifespan in mice. *Aging Cell*, *6*(5), 727–729. https://doi.org/10.1111/j.1474-9726.2007.00328.x

Conover, C., Bale, L., Frye, R., & Schaff, H. (2019). Cellular characterization of human epicardial adipose tissue: highly expressed PAPP-A regulates insulin-like growth factor I signaling in human cardiomyocytes. *Physiological Reports*, *7*(4), e14006. https://doi.org/10.14814/phy2.14006

Conover, C., Bale, L., & Nair, K. (2016). Comparative gene expression and phenotype analyses of skeletal muscle from aged wild-type and PAPP-A-deficient mice. *Experimental Gerontology*, *80*, 36–42.

231

https://doi.org/10.1016/j.exger.2016.04.005

Conover, C., Bale, L., Overgaard, M., Johnstone, E., Laursen, U., Füchtbauer, E., … van Deursen, J. (2004). Metalloproteinase pregnancy-associated plasma protein A is a critical growth regulatory factor during fetal development. *Development*, *131*(5), 1187–1194. https://doi.org/10.1242/dev.00997

Conover, C., Bale, L., & Powell, D. (2013). Inducible knock out of pregnancy-associated plasma protein-a gene expression in the adult mouse: Effect on vascular injury response. *Endocrinology*, *154*(8), 2734–2738. https://doi.org/10.1210/en.2013-1320

Conover, C., Durham, S., Zapf, J., Masiarz, F., & Kiefer, M. (1995). Cleavage Analysis of Insulin-like Growth Factor (IGF)-dependent IGF-binding Protein-4 Proteolysis and Expression of Protease-resistant IGF-binding Protein-4 Mutants. *Journal of Biological Chemistry*, *270*(9), 4395–4400.

Conover, C., Oxvig, C., Overgaard, M., Christiansen, M., & Giudice, L. (1999). Evidence That the Insulin-Like Growth Factor Binding Protein-4 Protease in Human Ovarian Follicular Fluid Is Pregnancy Associated Plasma Protein-A. *The Journal of Clinical Endocrinology & Metabolism*, *84*(12), 4742–4745. https://doi.org/10.1210/jcem.84.12.6342

Corcoran, S. M., Achamallah, N., Loughlin, J. O., Stafford, P., Dicker, P., Malone, F. D., & Breathnach, F. (2018). First trimester serum biomarkers to predict gestational diabetes in a high-risk cohort: Striving for clinically useful thresholds. *European Journal of Obstetrics and Gynecology and Reproductive Biology*, *222*, 7–12. https://doi.org/10.1016/j.ejogrb.2017.12.051

Corvera, S., & Gealekman, O. (2014). Adipose tissue angiogenesis: impact on obesity and type-2 diabetes. *Biochimica et Biophysica Acta*, *1842*(3), 463–472. https://doi.org/10.1016/j.bbadis.2013.06.003

Coughlan, M. T., Oliva, K., Georgiou, H. M., Permezel, J. M. H., & Rice, G. E. (2001). Glucose-induced release of tumour necrosis factor-alpha from human placental and adipose tissues in gestational diabetes mellitus. *Diabetic Medicine*, *18*(11), 921–927. https://doi.org/10.1046/j.1464-5491.2001.00614.x

Crandall, D. L., Hausman, G. J., & Kral, J. G. (1997). A Review of the Microcirculation of Adipose Tissue: Anatomic, Metabolic, and Angiogenic Perspectives. *Microcirculation*, *4*(2), 211–232. https://doi.org/10.3109/10739689709146786

Crewe, C., An, Y. A., & Scherer, P. E. (2017). The ominous triad of adipose

233

tissue dysfunction: Inflammation, fibrosis, and impaired angiogenesis. *Journal of Clinical Investigation*, *127*(1), 74–82. https://doi.org/10.1172/JCI88883

D'Ippolito, S., Tersigni, C., Scambia, G., & Di Simone, N. (2012). Adipokines, an adipose tissue and placental product with biological functions during pregnancy. *BioFactors*, *38*(1), 14–23. https://doi.org/10.1002/biof.201

Davidge-Pitts, C., Escande, C. J., & Conover, C. A. (2014). Preferential expression of PAPPA in human preadipocytes from omental fat. *Journal of Endocrinology*, *222*(1), 87–97. https://doi.org/10.1530/joe-13-0610

De Souza, L. R., Berger, H., Retnakaran, R., Maguire, J. L., Nathens, A. B., Connelly, P. W., & Ray, J. G. (2016). First-Trimester Maternal Abdominal Adiposity Predicts Dysglycemia and Gestational Diabetes Mellitus in Midpregnancy. *Diabetes Care*, *39*(1), 61–64. https://doi.org/10.2337/dc15-2027

De Souza, L. R., Berger, H., Retnakaran, R., Vlachou, P. A., Maguire, J. L., Nathens, A. B., … Ray, J. G. (2016). Non-alcoholic fatty liver disease in early pregnancy predicts dysglycemia in mid-pregnancy: prospective study. *American Journal of Gastroenterology*, *111*(5), 665–670. https://doi.org/10.1038/ajg.2016.43

234

Deierlein, A. L., Thornton, J., Hull, H., Paley, C., & Gallagher, D. (2012). An anthropometric model to estimate neonatal fat mass using air displacement plethysmography. *Nutrition and Metabolism*, *9*, 1–5. https://doi.org/10.1186/1743-7075-9-21

del Aguila, L. F., Claffey, K. P., & Kirwan, J. P. (1999). TNF-α impairs insulin signaling and insulin stimulation of glucose uptake in C2C12 muscle cells. *American Journal of Physiology-Endocrinology and Metabolism*, *276*(5), E849–E855. https://doi.org/10.1152/ajpendo.1999.276.5.e849

Deputy, N., Kim, S., Conrey, E., & Bullard, K. (2018). Prevalence and Changes in Preexisting Diabetes and Gestational Diabetes Among Women Who Had a Live Birth — United States, 2012–2016. *MMWR and Morbidity and Mortality Weekly Report*, *67*, 1201–1207.

Diderholm, B., Stridsberg, M., Ewald, U., Lindeberg-Nordén, S., & Gustafsson, J. (2005). Increased lipolysis in non-obese pregnant women studied in the third trimester. *BJOG: An International Journal of Obstetrics & Gynaecology*, *112*(6), 713–718. https://doi.org/10.1111/j.1471-0528.2004.00534.x

Divoux, A., Tordjman, J., Veyrie, N., Hugol, D., Poitou, C., Aissat, A., … Cle, K. (2010). Fibrosis in Human Adipose Tissue : Composition , Distribution , and Link With Lipid Metabolism and Fat Mass Loss. *Diabetes*, *59*(11), 2817–

2825. https://doi.org/10.2337/db10-0585.A.D.

Domingos, A. I., Vaynshteyn, J., Voss, H. U., Ren, X., Gradinaru, V., Zang, F., …
Friedman, J. (2011). Leptin regulates the reward value of nutrient. *Nature Neuroscience*, *14*(12), 1562–1568. https://doi.org/10.1038/nn.2977

Doruk, M., Uğur, M., Oruç, A. S., Demirel, N., & Yildiz, Y. (2014). Serum
adiponectin in gestational diabetes and its relation to pregnancy outcome.
Journal of Obstetrics and Gynaecology, *34*(6), 471–475.
https://doi.org/10.3109/01443615.2014.902430

Driscoll, D. A., & Gross, S. J. (2008). First trimester diagnosis and screening for
fetal aneuploidy. *Genetics in Medicine*, *10*(1), 73–75.
https://doi.org/10.1097/GIM.0b013e31815efde8

Edelstein, A., Amodaj, N., Hoover, K., Vale, R., & Stuurman, N. (2010).
Computer control of microscopes using µManager. *Current Protocols in Molecular Biology*, *92*, 14.20.1-14.20.17.
https://doi.org/10.1002/0471142727.mb1420s92

Elias, I., Franckhauser, S., Ferré, T., Vilà, L., Tafuro, S., Muñoz, S., … Bosch, F.
(2012). Adipose tissue overexpression of vascular endothelial growth factor
protects against diet-induced obesity and insulin resistance. *Diabetes*, *61*(7),
1801–1813. https://doi.org/10.2337/db11-0832

Ellis, K., Yao, M., Shypailo, R., Urlando, A., Wong, W., & Heird, W. (2007). Body-composition assessment in infancy: Air-displacement plethysmography compared with a reference 4-compartment model. *American Journal of Clinical Nutrition*, *85*(1), 90–95.

Eriksson, B., Löf, M., Olausson, H., & Forsum, E. (2010). Body fat, insulin resistance, energy expenditure and serum concentrations of leptin, adiponectin and resistin before, during and after pregnancy in healthy Swedish women. *British Journal of Nutrition*, *103*(1), 50–57. https://doi.org/10.1017/S0007114509991371

Farahvar, S., Walfisch, A., & Sheiner, E. (2019). Gestational diabetes risk factors and long-term consequences for both mother and offspring: a literature review. *Expert Review of Endocrinology & Metabolism*, *14*(1), 63–74. https://doi.org/10.1080/17446651.2018.1476135

Fasshauer, M., Blüher, M., & Stumvoll, M. (2014). Adipokines in gestational diabetes. *The Lancet Diabetes and Endocrinology*, *2*(6), 488–499. https://doi.org/10.1016/S2213-8587(13)70176-1

Foghsgaard, S., Andreasen, C., Vedtofte, L., Andersen, E. S., Bahne, E., Strandberg, C., … Vilsbøll, T. (2017). Nonalcoholic fatty liver disease is prevalent in women with prior gestational diabetes mellitus and

237

independently associated with insulin resistance and waist circumference. *Diabetes Care*, *40*(1), 109–116. https://doi.org/10.2337/dc16-1017

Forbes, B. E., McCarthy, P., & Norton, R. S. (2012). Insulin-like growth factor binding proteins: A structural perspective. *Frontiers in Endocrinology*, *3*(38), 1–13. https://doi.org/10.3389/fendo.2012.00038

Forsum, E., Sadurskis, A., & Wager, J. (1989). Estimation of body fat in healthy Swedish women during pregnancy and lactation. *The American Journal of Clinical Nutrition*, *50*(3), 465–473. https://doi.org/10.1093/ajcn/50.3.465

Francis, E. C., Li, M., Hinkle, S., Chen, J., Chen, L., & Zhang, C. (2019). 1517-P: A Longitudinal Study of a Panel of Adipokines and Gestational Diabetes Risk. *Diabetes*, *68*(Supplement 1), 1517-P. https://doi.org/10.2337/db19-1517-P

Frank, A. P., de Souza Santos, R., Palmer, B. F., & Clegg, D. J. (2018). Determinants of body fat distribution in humans may provide insight about obesity-related health risks. *Journal of Lipid Research*, jlr.R086975. https://doi.org/10.1194/jlr.r086975

Friedman, J., Ishizuka, T., Shao, J., Huston, L., Highman, T., & Catalano, P. (1999). Impaired glucose transport and insulin receptor tyrosine phosphorylation in skeletal muscle from obese women with gestational

diabetes. *Diabetes*, *48*(9), 1807–1814.

Gaillard, R., Steegers, E. A. P., Franco, O. H., Hofman, A., & Jaddoe, V. W. V.
(2015). Maternal weight gain in different periods of pregnancy and childhood
cardio-metabolic outcomes. the Generation R Study. *International Journal of
Obesity*, *39*(4), 677–685. https://doi.org/10.1038/ijo.2014.175

Gariani, K., Egloff, M., Prati, S., Philippe, J., Boulvain, M., & Jornayvaz, F. R.
(2019). Consequences of the Adoption of the IADPSG versus Carpenter and
Coustan Criteria to Diagnose Gestational Diabetes: A Before-After
Comparison. *Exp Clin Endocrinol Diabetes*, *127*(7), 473–476.
https://doi.org/10.1055/a-0735-9469

Garten, A., Schuster, S., & Kiess, W. (2012). The Insulin-Like Growth Factors in
Adipogenesis and Obesity. *Endocrinology and Metabolism Clinics of North
America*, *41*(2), 283–295. https://doi.org/10.1016/j.ecl.2012.04.011

Garvey, W., Maianu, L., Hancock, J., Golichowski, A., & Baron, A. (1992). Gene
expression of GLUT4 in skeletal muscle from insulin-resistant patients with
obesity, IGT, GDM, and NIDDM. *Diabetes*, *41*(4), 465–475.

Gastaldelli, A., Miyazaki, Y., Pettiti, M., Matsuda, M., Mahankali, S., Santini, E.,
… Ferrannini, E. (2002). Metabolic effects of visceral fat accumulation in
type 2 diabetes. *Journal of Clinical Endocrinology and Metabolism*, *87*(11),

239

5098–5103. https://doi.org/10.1210/jc.2002-020696

Gealekman, O., Burkart, A., Chouinard, M., Nicoloro, S., Straubhaar, J., & Corvera, S. (2008). Enhanced angiogenesis in obesity and in response to PPARγ activators through adipocyte VEGF and ANGPTL4 production. *American Journal of Physiology-Endocrinology and Metabolism*, *295*(5), E1056–E1064. https://doi.org/10.1152/ajpendo.90345.2008

Gealekman, O., Gurav, K., Chouinard, M., Straubhaar, J., Thompson, M., Malkani, S., … Corvera, S. (2014). Control of Adipose Tissue Expandability in Response to High Fat Diet by the Insulin-like Growth Factor Binding Protein-4. *The Journal of Biological Chemistry*, *289*(26), 18327–18338. https://doi.org/10.1074/jbc.M113.545798

Gealekman, O., Guseva, N., Gurav, K., Gusev, A., Hartigan, C., Thompson, M., … Corvera, S. (2012). Effect of rosiglitazone on capillary density and angiogenesis in adipose tissue of normoglycaemic humans in a randomised controlled trial. *Diabetologia*, *55*(10), 2794–2799. https://doi.org/10.1007/s00125-012-2658-2

Gealekman, O., Guseva, N., Hartigan, C., Apotheker, S., Gorgoglione, M., Gurav, K., … Corvera, S. (2011). Depot-specific differences and insufficient subcutaneous adipose tissue angiogenesis in human obesity. *Circulation*,

240

123(2), 186–194. https://doi.org/10.1161/CIRCULATIONAHA.110.970145

Gérard, N., Delpuech, T., Oxvig, C., Overgaard, M., & Monget, P. (2004).
Proteolytic degradation of IGF-binding protein (IGFBP)-2 in equine ovarian
follicles: involvement of pregnancy-associated plasma protein-A (PAPP-A)
and association with dominant but not subordinated follicles. *Journal of
Endocrinology*, *182*(3), 457–466.

Getahun, D., Nath, C., Ananth, C. V, Chavez, M. R., & Smulian, J. C. (2008).
Gestational diabetes in the United States: temporal trends 1989 through
2004. *American Journal of Obstetrics & Gynecology*, *198*(5), 525.e1-525.e5.
https://doi.org/10.1016/j.ajog.2007.11.017

Giudice, I., Gianfranco, B., Di Nicolò, A., Daniela, M., Carrara, G., Randazzo, C.,
… Gulisano, A. (2015). Correlation of neonatal weight with maternal serum
levels of pregnancy-associated plasma protein-A during the first trimester of
pregnancy: a retrospective study. *Journal of Perinatal Medicine*.
https://doi.org/10.1515/jpm-2013-0249

Gray, S. L., & Vidal-Puig, A. J. (2007). Adipose Tissue Expandability in the
Maintenance of Metabolic Homeostasis. *Nutrition Reviews*, *65*(s1), S7–S12.
https://doi.org/10.1111/j.1753-4887.2007.tb00331.x

Griffin, J. F. T. (1983). Pregnancy-Associated Plasma Protein Levels at Term in

Normal Pregnancy, Preeclampsia and Essential Hypertension. *Australian and New Zealand Journal of Obstetrics and Gynaecology*, *23*(1), 11–14. https://doi.org/10.1111/j.1479-828X.1983.tb00150.x

Gude, M., Hjortebjerg, R., Oxvig, C., Thyoø, A., Magnusson, N., Bjerre, M., … Frystyk, J. (2016). PAPP-A, IGFBP-4 and IGF-II are secreted by human adipose tissue cultures in a depot-specific manner. *European Journal of Endocrinology*, *175*(6), 509–517. https://doi.org/10.1530/EJE-16-0569

Gupta, D., Krueger, C. B., & Lastra, G. (2012). Over-nutrition, Obesity and Insulin Resistance in the Development of β-Cell Dysfunction. *Current Diabetes Reviews*. https://doi.org/10.2174/157339912799424564

Gupta, R., Mepani, R., Kleiner, S., Lo, J., Khandekar, M., Cohen, P., … Spiegelman, B. (2012). Zfp423 expression identifies committed preadipocytes and localizes to adipose endothelial and perivascular cells. *Cell Metabolism*, *15*(2), 230–239. https://doi.org/10.1016/j.cmet.2012.01.010

Gur, E. B., Ince, O., Turan, G. A., Karadeniz, M., Tatar, S., Celik, E., … Guclu, S. (2014). Ultrasonographic visceral fat thickness in the first trimester can predict metabolic syndrome and gestational diabetes mellitus. *Endocrine*, *47*(2), 478–484. https://doi.org/10.1007/s12020-013-0154-1

Gyrup, C., Christiansen, M., & Oxvig, C. (2007). Quantification of proteolytically

active pregnancy-associated plasma protein-A with an assay based on
quenched fluorescence. *Clinical Chemistry*, *53*(5), 947–954.
https://doi.org/10.1373/clinchem.2006.080614

Gyrup, C., & Oxvig, C. (2007). Quantitative analysis of insulin-like growth factor-
modulated proteolysis of insulin-like growth factor binding protein-4 and -5
by pregnancy-associated plasma protein-A. *Biochemistry*, *46*(7), 1972–1980.
https://doi.org/10.1021/bi062229i

Han, J., Lee, J.-E., Jin, J., Lim, J. S., Oh, N., Kim, K., … Koh, G. Y. (2011). The
spatiotemporal development of adipose tissue. *Development*, *138*(22),
5027–5037. https://doi.org/10.1242/dev.067686

Hardie, L., Trayhurn, P., Abramovich, D., & Fowler, P. (1997). Circulating leptin in
women: A longitudinal study in the menstrual cycle and during pregnancy.
Clinical Endocrinology, *47*(1), 101–106. https://doi.org/10.1046/j.1365-
2265.1997.2441017.x

Harper, L. M., Mele, L., Landon, M. B., Carpenter, M. W., Ramin, S. M., Reddy,
U. M., … Tolosa, J. E. (2016). Carpenter-coustan compared with national
diabetes data group criteria for diagnosing gestational diabetes. *Obstetrics
and Gynecology*, *127*(5), 893–898.
https://doi.org/10.1097/AOG.0000000000001383

243

Harris, L. K., Crocker, I. P., Baker, P. N., Aplin, J. D., & Westwood, M. (2011). IGF2 Actions on Trophoblast in Human Placenta Are Regulated by the Insulin-Like Growth Factor 2 Receptor , Which Can Function as Both a Signaling and Clearance Receptor 1. *Biology of Reproduction*, *446*, 440–446. https://doi.org/10.1095/biolreprod.110.088195

Harstad, S. L., & Conover, C. A. (2014). Tissue-specific changes in pregnancy associated plasma protein-A expression with age in mice. *Experimental Gerontology*, *57*, 13–17. https://doi.org/10.1016/j.exger.2014.04.011

Hausman, G. J., & Richardson, R. L. (2004). Adipose tissue angiogenesis. *Journal of Animal Science*, *82*(3), 925–934.

Henegar, C., Tordjman, J., Achard, V., Lacasa, D., Cremer, I., Guerre-Millo, M., … Clement, K. (2008). Adipose tissue transcriptomic signature highlights the pathological relevance of extracellular matrix in human obesity. *Genome Biology*, *9*(1), R14. https://doi.org/10.1186/gb-2008-9-1-r14

Henson, M. C., Castracane, V. D., O'Neil, J. S., Gimpel, T., Swan, K. F., Green, A. E., & Wenliang, S. (1999). Serum leptin concentrations and expression of leptin transcripts in placental trophoblast with advancing baboon pregnancy. *Journal of Clinical Endocrinology and Metabolism*, *84*(7), 2543–2549. https://doi.org/10.1210/jc.84.7.2543

Henson, M., & Casatracane, D. (1998). Leptin in Pregnancy. *Biology of Reproduction*, *724*, 713–724.

Herrera, E. (2000). Metabolic adaptations in pregnancy and their implications for the availability of substrates to the fetus. *European Journal of Clinical Nutrition*, *54*(S1), S47–S51. https://doi.org/10.1038/sj.ejcn.1600984

Herrera, E., & Ortega-Senovilla, H. (2010). Maternal lipid metabolism during normal pregnancy and its implications to fetal development. *Clinical Lipidology*, *5*(6), 899–911.

Hesse, D., Trost, J., Schäfer, N., Schwerbel, K., Hoeflich, A., Schürmann, A., & Brockmann, G. A. (2018). Effect of adipocyte-derived IGF-I on adipose tissue mass and glucose metabolism in the Berlin Fat Mouse. *Growth Factors*, *36*(1–2), 78–88. https://doi.org/10.1080/08977194.2018.1497621

Hillier, T. A., Pedula, K. L., Schmidt, M. M., Mullen, J. A., Charles, M., & Pettitt, D. J. (2007). Childhood Obesity and Metabolic Imprinting. *Diabetes Care*, *30*(9), 2287 LP – 2292. https://doi.org/10.2337/dc06-2361

Hjortebjerg, R., Berryman, D. E., Comisford, R., List, E. O., Oxvig, C., Bjerre, M., … Kopchick, J. J. (2018). Depot-specific and GH-dependent regulation of IGF binding protein-4, pregnancy-associated plasma protein-A, and stanniocalcin-2 in murine adipose tissue. *Growth Hormone and IGF*

245

Research, *39*, 54–61. https://doi.org/10.1016/j.ghir.2018.01.001

Hodson, L., Humphreys, S. M., Karpe, F., & Frayn, K. N. (2013). Metabolic
Signatures of Human Adipose Tissue Hypoxia in Obesity. *Diabetes*, *62*(5),
1417–1425. https://doi.org/10.2337/db12-1032

Hoeflich, A., Minyao, W., Subburaman, M., Jurgen, F., Rudiger, W., Froehlich, T.,
… Wolf, E. (1999). Overexpression of Insulin-Like Growth Factor-Binding
Protein-2 in Transgenic Mice Reduces Postnatal Body Weight Gain.
Endocrinology, *140*(12), 5488–5496.

Hoffstedt, J., Arner, E., Wahrenberg, H., Andersson, D. P., Qvisth, V., Löfgren,
P., … Arner, P. (2010). Regional impact of adipose tissue morphology on the
metabolic profile in morbid obesity. *Diabetologia*, *53*(12), 2496–2503.
https://doi.org/10.1007/s00125-010-1889-3

Holly, J. (2004). Physiology of the IGF system. *Novartis Foundation Symposium*,
262, 19–26; disussion 26-35, 265–268.
https://doi.org/10.1002/0470869976.ch3

Hosni, A. A., Abdel-Moneim, A. A., Abdel-Reheim, E. S., Mohamed, S. M., &
Helmy, H. (2017). Cinnamaldehyde potentially attenuates gestational
hyperglycemia in rats through modulation of PPARγ, proinflammatory
cytokines and oxidative stress. *Biomedicine and Pharmacotherapy*, *88*, 52–

246

60. https://doi.org/10.1016/j.biopha.2017.01.054

Hosogai, N., Fukuhara, A., Oshima, K., Miyata, Y., Tanaka, S., Segawa, K., …
Shimomura, I. (2007). Adipose Tissue Hypoxia in Obesity and Its Impact on
Adipocytokine Dysregulation. *Diabetes*, *56*(4), 901–911.
https://doi.org/10.2337/db06-0911

Hou, J., Clemmons, D. R., & Smeekens, S. (2005). Expression and
characterization of a serine protease that preferentially cleaves insulin-like
growth factor binding protein-5. *Journal of Cellular Biochemistry*, *94*(3), 470–
484. https://doi.org/10.1002/jcb.20328

Huang, L., Liu, J., Feng, L., Chen, Y., Zhang, J., & Wang, W. (2014). Maternal
prepregnancy obesity is associated with higher risk of placental pathological
lesions. *Placenta*, *35*(8), 563–569.
https://doi.org/10.1016/j.placenta.2014.05.006

Huda, S. S., Forrest, R., Paterson, N., Jordan, F., Sattar, N., & Freeman, D. J.
(2014). In preeclampsia, maternal third trimester subcutaneous adipocyte
lipolysis is more resistant to suppression by insulin than in healthy
pregnancy. *Hypertension*, *63*(5), 1094–1101.
https://doi.org/10.1161/HYPERTENSIONAHA.113.01824

Huopio, H., Hakkarainen, H., Pääkkönen, M., Kuulasmaa, T., Voutilainen, R.,

Heinonen, S., & Cederberg, H. (2014). Long-term changes in glucose metabolism after gestational diabetes: a double cohort study. *BMC Pregnancy and Childbirth*, *14*(296), 1–9. https://doi.org/10.1186/1471-2393-14-296

Husslein, H., & Lausegger, F. (2012). Association between pregnancy-associated plasma protein-A and gestational diabetes requiring insulin treatment at 11-14 weeks of gestation. *Journal of Maternal-Fetal and Neonatal Medicine*, *25*(11), 2230–2233. https://doi.org/10.3109/14767058.2012.684170

Infante, A., & Rodríguez, C. I. (2018). Secretome analysis of in vitro aged human mesenchymal stem cells reveals IGFBP7 as a putative factor for promoting osteogenesis. *Scientific Reports*, *8*, 1–12. https://doi.org/10.1038/s41598-018-22855-z

International Association of Diabetes and Pregnancy Study Groups (IADPSG) Consensus Panel. (2010). International Association of Diabetes and Pregnancy Study Groups Recommendations on the Diagnosis and Classification of Hyperglycemia in Pregnancy. *Diabetes Care*, *33*(3), 676–682. https://doi.org/10.2337/dc09-1848

International Association of Diabetes in Pregnancy Study Group (IADPSG)

248

Working Group on Outcome Definitions, Feig, D., Corcoy, R., Jensen, D., Kautzky-Wille, A., Nolan, C., … McIntyre, H. (2015). Diabetes in pregnancy outcomes: A systematic review and proposed codification of definitions. *Diabetes/Metabolism Research and Reviews*, *31*, 680–690. https://doi.org/10.1002/dmrr

International Diabetes Federation. (2017). *Eighth edition 2017*. *IDF Diabetes Atlas, 8th edn. Brussels, Belgium: International Diabetes Federation, 2017*. https://doi.org/10.1016/S0140-6736(16)31679-8.

Isakson, P., Hammarstedt, A., Gustafson, B., & Smith, U. (2009). Impaired preadipocyte differentiation in human abdominal obesity: Role of Wnt, tumor necrosis factor-α, and inflammation. *Diabetes*, *58*(7), 1550–1557. https://doi.org/10.2337/db08-1770

Ishizuka, T., Klepcyk, P., Liu, S., Panko, L., Liu, S., Gibbs, E., & Friedman, J. (1999). Effects of overexpression of human GLUT4 gene on maternal diabetes and fetal growth in spontaneous gestational diabetic C57BLKS/J Lepr(db/+) mice. *Diabetes*, *48*(5), 1061–1069.

Jawerbaum, A., & White, V. (2010). Animal models in diabetes and pregnancy. *Endocrine Reviews*, *31*(5), 680–701. https://doi.org/10.1210/er.2009-0038

Jones, C., & Fox, H. (1976). Placental changes in gestational diabetes. An

ultrastructural study. *Obstetrics and Gynecology*, *48*, 247–280.

Joslin, E. P. (1915). Pregnancy and Diabetes Mellitus. *Boston Medical and Surgical Journal*, *173*(23), 841–849.

Kabir, M., Catalano, K. J., Ananthnarayan, S., Kim, S. P., Van Citters, G. W., Dea, M. K., & Bergman, R. N. (2005). Molecular evidence supporting the portal theory: a causative link between visceral adiposity and hepatic insulin resistance. *American Journal of Physiology-Endocrinology and Metabolism*, *288*(2), E454–E461. https://doi.org/10.1152/ajpendo.00203.2004

Kampmann, F. B., Thuesen, A. C. B., Hjort, L., Olsen, S. F., Pires, S. M., Tetens, I., & Grunnet, L. G. (2018). Exposure to Gestational Diabetes Is a Stronger Predictor of Dysmetabolic Traits in Children Than Size at Birth. *The Journal of Clinical Endocrinology & Metabolism*, *104*(5), 1766–1776. https://doi.org/10.1210/jc.2018-02044

Kautzky-Willer, A., Pacini, G., Tura, A., Bieglmayer, C., Schneider, B., Ludvik, B., … Waldhäusl, W. (2001a). Increased plasma leptin in gestational diabetes. *Diabetologia*, *44*(2), 164–172.

Kautzky-Willer, A., Pacini, G., Tura, A., Bieglmayer, C., Schneider, B., Ludvik, B., … Waldhäusl, W. (2001b). Increased plasma leptin in gestational diabetes. *Diabetologia*, *44*(2), 164–172. https://doi.org/10.1007/s001250051595

Kavak, Z. N., Basgul, A., Elter, K., Uygur, M., & Gokaslan, H. (2006). The efficacy of first-trimester PAPP-A and free BhCG levels for predicting adverse pregnancy outcome. *Journal of Perinatal Medicine*, *34*, 145–148. https://doi.org/10.1515/JPM.2006.026

Kawaguchi, N., Sunberg, C., Kveiborg, M., Moghadaszadeh, B., Asmar, M., Dietrich, N., … Wewer, U. (2003). ADAM12 induces actin cytoskeleton and extracellular matrix reorganization during early adipocyte differentiation by regulating 1 integrin function. *Journal of Cell Science*, *116*(19), 3893–3904. https://doi.org/10.1242/jcs.00699

Keller, P., Gburcik, V., Petrovic, N., Gallagher, I. J., Nedergaard, J., Cannon, B., & Timmons, J. A. (2011). Gene-chip studies of adipogenesis-regulated microRNAs in mouse primary adipocytes and human obesity. *BMC Endocrine Disorders*, *11*(1), 7. https://doi.org/10.1186/1472-6823-11-7

Kieffer, T. J., Heller, R. S., Leech, C. A., Holz, G. G., & Habener, J. F. (1997). Leptin Suppression of Insulin Secretion by the Activation of ATP-Sensitive K+ Channels in Pancreatic B-Cells. *Diabetes*, *46*(6), 1087–1093. https://doi.org/10.2337/diab.46.6.1087

Kim, C., Newton, K., & Knopp, R. (2002). Gestational Diabetes and the Incidence of Type 2 Diabetes. *Diabetes Care*, *25*(10), 1862–1868.

https://doi.org/10.2337/dc09-1679

Kim, H., Rosenfeld, R., & Oh, Y. (1997). Biological roles of insulin-like growth factor binding proteins (IGFBPs). *Experimental & Molecular Medicine*, *29*(2), 85–96. https://doi.org/10.1038/emm.1997.13

Kim, J. (2009). Hyperinsulinemic--Euglycemic Clamp to Assess Insulin Sensitivity In Vivo. In C. Stocker (Ed.), *Type 2 Diabetes: Methods and Protocols* (pp. 221–238). Totowa, NJ: Humana Press. https://doi.org/10.1007/978-1-59745-448-3_15

Kim, JI, Huh, J., Sohn, J., Choe, S., Lee, Y., Lim, C., … Kim, J. (2015). Lipid-Overloaded Enlarged Adipocytes Provoke Insulin Resistance Independent of Inflammation. *Molecular and Cellular Biology*, *35*(10), 1686–1699. https://doi.org/10.1128/mcb.01321-14

Kim, JY, van de Wall, E., Laplante, M., Azzara, A., Trujillo, M., Hofmann, S., … Scherer, P. (2007). Obesity-associated improvements in metabolic profile through expansion of adipose tissue. *The Journal of Clinical Investigation*, *117*(9), 2621–2637. https://doi.org/10.1172/JCI31021

King, J. (2000). Physiology of pregnancy and nutrient metabolism. *American Journal of Clinical Nutrition*, *71*, 1218S-1225S.

Kinoshita, T., & Itoh, M. (2006). Longitudinal variance of fat mass deposition during pregnancy evaluated by ultrasonography: The ratio of visceral fat to subcutaneous fat in the abdomen. *Gynecologic and Obstetric Investigation*, *61*(2), 115–118. https://doi.org/10.1159/000089456

Kirwan, J. P., Hauguel-De Mouzon, S., Lepercq, J., Challier, J.-C., Huston-Presley, L., Friedman, J. E., … Catalano, P. (2002). TNF-α Is a Predictor of Insulin Resistance in Human Pregnancy. *Diabetes*, *51*(7), 2207–2213. https://doi.org/10.2337/diabetes.51.7.2207

Kiss, A. C., Lima, P. H., Sinzato, Y. K., Takaku, M., Takeno, M. A., Rudge, M. V., & Damasceno, D. C. (2009). Animal models for clinical and gestational diabetes: maternal and fetal outcomes. *Diabetology & Metabolic Syndrome*, *1*(1), 21. https://doi.org/10.1186/1758-5996-1-21

Kitzmiller, J. L., Dang-Kilduff, L., & Taslimi, M. M. (2007). Gestational diabetes after delivery: Short-term management and long-term risks. *Diabetes Care*, *30*(SUPPL. 2), S225–S235. https://doi.org/10.2337/dc07-s221

Kjos, S. L., Peters, R. K., Xiang, A., Henry, O. A., Montoro, M., & Buchanan, T. A. (1995). Predicting Future Diabetes in Latino Women With Gestational Diabetes: Utility of Early Postpartum Glucose Tolerance Testing. *Diabetes*, *44*(5), 586–591. https://doi.org/10.2337/diab.44.5.586

253

Klement, R., & Fink, M. (2016). Dietary and pharmacological modification of the

insulin/IGF-1 system: Exploiting the full repertoire against cancer.

Oncogenesis, *5*, e193. https://doi.org/10.1038/oncsis.2016.2

Knopp, R. H., Saudek, C. D., Arky, R. A., & O'sullivan, J. B. (1973). Two phases

of adipose tissue metabolism in pregnancy: Maternal adaptations for fetal

growth. *Endocrinology*, *92*(4), 984–988. https://doi.org/10.1210/endo-92-4-

984

Kopp-Hoolihan, L. E., van Loan, M. D., Wong, W. W., & King, J. C. (2017). Fat

mass deposition during pregnancy using a four-component model. *Journal

of Applied Physiology*, *87*(1), 196–202.

https://doi.org/10.1152/jappl.1999.87.1.196

Koukkou, E., Watts, G., & Lowy, C. (1996). Serum lipid, lipoprotein and

apolipoprotein changes in gestational diabetes mellitus: A cross-sectional

and prospective study. *Journal of Clinical Pathology*, *49*(8), 634–637.

Kramer, A. W., Lamale-Smith, L. M., & Winn, V. D. (2016). Differential expression

of human placental PAPP-A2 over gestation and in preeclampsia. *Placenta*,

37, 19–25. https://doi.org/10.1016/j.placenta.2015.11.004

Kristensen, T., Oxvig, C., Sand, O., Hundahl Moeller, N. P., & Sottrup-Jensen, L.

(1994). Amino acid sequence of human pregnancy-associated plasma

protein A derived from cloned cDNA. *Biochemistry*, *33*(6), 1592–1598.

https://doi.org/10.1021/bi00172a040

Kucukural, A., Yukselen, O., Ozata, D. M., Moore, M. J., & Garber, M. (2019). DEBrowser: interactive differential expression analysis and visualization tool for count data. *BMC Genomics*, *20*(1), 6. https://doi.org/10.1186/s12864-018-5362-x

Kuemmerle, J., & Zhou, H. (2002). Insulin-like growth factor-binding protein-5 (IGFBP-5) stimulates growth and IGF-I secretion in human intestinal smooth muscle by Ras-dependent activation of p38 MAP kinase and Erk1/2 pathways. *Journal of Biological Chemistry*, *277*(23), 20563–20571. https://doi.org/10.1074/jbc.M200885200

Kuhl, C. (1991). Insulin Secretion and Insulin Resistance in Pregnancy and GDM. Implications for Diagnosis and Management. *Diabetes*, *40*(SUPPL 2), 18–24.

Kulaksizoglu, S., Kulaksizoglu, M., Kebapcilar, A. G., Torun, A. N., Ozcimen, E., & Turkoglu, S. (2013). Can first-trimester screening program detect women at high risk for gestational diabetes mellitus? *Gynecological Endocrinology*, *29*(2), 137–140. https://doi.org/10.3109/09513590.2012.708800

Kuramoto, K., Tahara, S., Sasaki, T., Matsumoto, S., Kaneko, T., Kondo, H., …

Shinkai, T. (2010). Spontaneous dwarf rat: A novel model for aging research. *Geriatrics and Gerontology International*, *10*(1), 94–101. https://doi.org/10.1111/j.1447-0594.2009.00559.x

Kusminski, C., & Scherer, P. (2012). Mitochondrial dysfunction in white adipose tissue. *Trends in Endocrinology and Metabolism*, *23*(9), 435–443. https://doi.org/10.1016/j.tem.2012.06.004

Kwak, S. H., Choi, S. H., Kim, K., Jung, H. S., Cho, Y. M., Lim, S., … Jang, H. C. (2013). Prediction of type 2 diabetes in women with a history of gestational diabetes using a genetic risk score. *Diabetologia*, *56*(12), 2556–2563. https://doi.org/10.1007/s00125-013-3059-x

Lain, K., & Catalano, P. (2007). Metabolic changes in pregnancy. *Clinical Obstetrics and Gynecology*, *50*(4), 938–948. https://doi.org/10.1097/GRF.0b013e31815a5494

Landy, H. J., Gómez-Marín, O., & O'Sullivan, M. J. (1996). Diagnosing gestational diabetes mellitus: use of a glucose screen without administering the glucose tolerance test. *Obstetrics & Gynecology*, *87*(3), 395–400. https://doi.org/10.1016/0029-7844(95)00460-2

Lappas, M., Permezel, M., & Rice, G. E. (2004). Release of proinflammatory cytokines and 8-isoprostane from placenta, adipose tissue, and skeletal

muscle from normal pregnant women and women with gestational diabetes mellitus. *Journal of Clinical Endocrinology and Metabolism*, *89*(11), 5627–5633. https://doi.org/10.1210/jc.2003-032097

Lappas, M., Yee, K., Permezel, M., & Rice, G. E. (2005). Release and regulation of leptin, resistin and adiponectin from human placenta, fetal membranes, and maternal adipose tissue and skeletal muscle from normal and gestational diabetes mellitus-complicated pregnancies. *Journal of Endocrinology*, *186*(3), 457–465. https://doi.org/10.1677/joe.1.06227

Larciprete, G., Valensise, H., Vasapollo, B., Altomare, F., Sorge, R., Casalino, B., … Arduini, D. (2003). Body composition during normalpregnancy: reference ranges. *Acta Diabetologica*, *40*(1), s225–s232. https://doi.org/10.1007/s00592-003-0072-4

Laursen, L. S., Overgaard, M. T., Soe, R., Boldt, H. B., Sottrup-Jensen, L., Giudice, L. C., … Oxvig, C. (2001). Pregnancy-associated plasma protein-A (PAPP-A) cleaves insulin-like growth factor binding protein (IGFBP)-5 independent of IGF: Implications for the mechanism of IGFBP-4 proteolysis by PAPP-A. *FEBS Letters*, *504*, 36–40. https://doi.org/10.1016/S0014-5793(01)02760-0

Lee, S. M., Kwak, S. H., Koo, J. N., Oh, I. H., Kwon, J. E., Kim, B. J., … Park, J.

S. (2019). Non-alcoholic fatty liver disease in the first trimester and subsequent development of gestational diabetes mellitus. *Diabetologia*, *62*(2), 238–248. https://doi.org/10.1007/s00125-018-4779-8

Leguy, C. C., Brun, S., Pidoux, G., Salhi, H., Choiset, A., Menet, C. C., … Guibourdenche, J. (2014). Pattern of secretion of pregnancy-associated plasma protein-A (PAPP-A) during pregnancies complicated by fetal aneuploidy, in vivo and in vitro. *Reproductive Biology and Endocrinology*, *12*, 129. https://doi.org/10.1186/1477-7827-12-129

Leturque, A., Ferre, P., Burnol, A.-F., Kande, J., Maulard, P., & Girard, J. (1986). Glucose Utilization Rates and Insulin Sensitivity In Vivo in Tissues of Virgin and Pregnant Rats. *Diabetes*, *35*, 172–177.

Lewitt, M., Dent, M., & Hall, K. (2014). The Insulin-Like Growth Factor System in Obesity, Insulin Resistance and Type 2 Diabetes Mellitus. *Journal of Clinical Medicine*, *3*(4), 1561–1574. https://doi.org/10.3390/jcm3041561

Lin, D., Chun, T. H., & Kang, L. (2016). Adipose extracellular matrix remodelling in obesity and insulin resistance. *Biochemical Pharmacology*, *119*, 8–16. https://doi.org/10.1016/j.bcp.2016.05.005

Lönn, M., Mehlig, K., Bengtsson, C., & Lissner, L. (2010). Adipocyte size predicts incidence of type 2 diabetes in women. *The FASEB Journal*, *24*(1), 326–331.

https://doi.org/10.1096/fj.09-133058

Lovati, E., Beneventi, F., Simonetta, M., Laneri, M., Quarleri, L., Scudeller, L., …
   Corazza, G. R. (2013). Gestational diabetes mellitus: Including serum
   pregnancy-associated plasma protein-A testing in the clinical management
   of primiparous women? A case–control study. *Diabetes Research and
   Clinical Practice*, *100*(3), 340–347.
   https://doi.org/10.1016/j.diabres.2013.04.002

Lowe, W. L., Scholtens, D. M., Kuang, A., Linder, B., Lawrence, J. M., Lebenthal,
   Y., … Metzger, B. E. (2019). Hyperglycemia and adverse Pregnancy
   Outcome follow-up study (HAPO FUS): Maternal gestational diabetes
   mellitus and childhood glucose metabolism. *Diabetes Care*, *42*(3), 372–380.
   https://doi.org/10.2337/dc18-1646

Lu, Q., Li, M., Zou, Y., & Cao, T. (2014). Induction of adipocyte hyperplasia in
   subcutaneous fat depot alleviated type 2 diabetes symptoms in obese mice.
   Obesity, *22*(7), 1623–1631. https://doi.org/10.1002/oby.20705

Malcolm, J. (2012). Through the looking glass: gestational diabetes as a
   predictor of maternal and offspring long-term health. *Diabetes/Metabolism
   Research and Reviews*, *28*(4), 307–311. https://doi.org/10.1002/dmrr.2275

Maridas, D. E., DeMambro, V. E., Le, P. T., Mohan, S., & Rosen, C. J. (2017).

IGFBP4 Is required for adipogenesis and influences the distribution of

adipose depots. *Endocrinology*, *158*(10), 3488–3500.

https://doi.org/10.1210/en.2017-00248

Mazaki-Tovi, S., Vaisbuch, E., Tarca, A. L., Kusanovic, J. P., Than, N. G.,

Chaiworapongsa, T., … Romero, R. (2015). Characterization of Visceral and

Subcutaneous Adipose Tissue Transcriptome and Biological Pathways in

Pregnant and Non-Pregnant Women: Evidence for Pregnancy-Related

Regional-Specific Differences in Adipose Tissue. *PloS ONE*, *10*(12),

e0143779. https://doi.org/10.1371/journal.pone.0143779

McLaughlin, T., Lamendola, C., Liu, A., & Abbasi, F. (2011). Preferential fat

deposition in subcutaneous versus visceral depots is associated with insulin

sensitivity. *Journal of Clinical Endocrinology and Metabolism*, *96*(11),

E1756–E1760. https://doi.org/10.1210/jc.2011-0615

Medina-Gomez, G., Virtue, S., Lelliott, C., Boiani, R., Campbell, M.,

Christodoulides, C., … Vidal-puig, A. (2005). The Link Between Nutritional

Status and Insulin Sensitivity Is Dependent on the Adipocyte-Specific

Peroxisome Proliferator-Activated Receptor-γ2. *Diabetes*, *54*, 1706–1716.

Mehmood, S., Margolis, M., Ye, C., Maple-Brown, L., Hanley, A. J., Connelly, P.

W., … Retnakaran, R. (2018). Hepatic fat and glucose tolerance in women

with recent gestational diabetes. *BMJ Open Diabetes Research and Care*, *6*, e000549. https://doi.org/10.1136/bmjdrc-2018-000549

Mele, J., Muralimanoharan, S., Maloyan, A., & Myatt, L. (2014). Impaired mitochondrial function in human placenta with increased maternal adiposity. *American Journal of Physiology-Endocrinology and Metabolism*, *307*(5), E419–E425. https://doi.org/10.1152/ajpendo.00025.2014

Metzger, B. E. (2007). Long-term outcomes in mothers diagnosed with gestational diabetes mellitus and their offspring. *Clinical Obstetrics and Gynecology*, *50*(4), 972–979. https://doi.org/10.1097/GRF.0b013e31815a61d6

Michailidou, Z., Turban, S., Miller, E., Zou, X., Schrader, J., Ratcliffe, P. J., … Seckl, J. R. (2012). Increased Angiogenesis Protects against Adipose Hypoxia and Fibrosis in Metabolic Disease-resistant 11β-Hydroxysteroid Dehydrogenase Type 1 (HSD1)-deficient Mice. *Journal of Biological Chemistry*, *287*(6), 4188–4197. https://doi.org/10.1074/jbc.M111.259325

Min, S. Y., Kady, J., Nam, M., Rojas-Rodriguez, R., Berkenwald, A., Kim, J. H., … Corvera, S. (2016). Human "brite/beige" adipocytes develop from capillary networks, and their implantation improves metabolic homeostasis in mice. *Nature Medicine*, *22*(3), 312–318. https://doi.org/10.1038/nm.4031

261

Miyakoshi, N., Richman, C., Kasukawa, Y., Linkhart, T. A., Baylink, D. J., & Mohan, S. (2001). Evidence that IGF-binding protein-5 functions as a growth factor. *The Journal of Clinical Investigation*, *107*, 73–81. https://doi.org/10.1172/JCI10459

Mohan, S., & Baylink, D. (2002). IGF-binding proteins are multifunctional and act via IGF-dependent and -independent mechanisms. *Journal of Endocrinology*, *175*(1), 19–31. https://doi.org/10.1677/joe.0.1750019

Monaghan, J. M., Godber, I. M., Lawson, N., Kaur, M., Wark, G., Teale, D., & Hosking, D. J. (2004). Longitudinal changes of insulin-like growth factors and their binding proteins throughout normal pregnancy. *Annals of Clinical Biochemistry*, *41*(3), 220–226. https://doi.org/10.1258/000456304323019596

Monget, P., Mazerbourg, S., Delpuech, T., Maurel, M., Manière, S., Zapf, J., … Overgaard, M. (2003). Pregnancy-Associated Plasma Protein-A Is Involved in Insulin-Like Growth Factor Binding Protein-2 (IGFBP-2) Proteolytic Degradation in Bovine and Porcine Preovulatory Follicles: Identification of Cleavage Site and Characterization of IGFBP-2 Degradation. *Biology of Reproduction*, *68*(1), 77–86. https://doi.org/10.1095/biolreprod.102.007609

Moore-Simas, T., & Corvera, S. (2014). The Roles of Adipose Tissue and Inflammation in Gestational Diabetes Mellitus. *Internal Medicine*, *S6*(010), 1–

7. https://doi.org/10.4172/2165-8048.s6-010

Moore, M. C., Menon, R., Coate, K. C., Gannon, M., Smith, M. S., Farmer, B., & Williams, P. E. (2010). Diet-induced impaired glucose tolerance and gestational diabetes in the dog. *Journal of Applied Physiology*, *110*(2), 458–467. https://doi.org/10.1152/japplphysiol.00768.2010

Moore Simas, T. A., Doyle Curiale, D. K., Hardy, J., Jackson, S., Zhang, Y., & Liao, X. (2010). Efforts needed to provide Institute of Medicine-recommended guidelines for gestational weight gain. *Obstetrics and Gynecology*, *115*(4), 777–783. https://doi.org/10.1097/aog.0b013e3181d56e12

Mørkrid, K., Jenum, A. K., Sletner, L., Vårdal, M. H., Waage, C. W., Nakstad, B., … Birkeland, K. I. (2012). Failure to increase insulin secretory capacity during pregnancy-induced insulin resistance is associated with ethnicity and gestational diabetes. *European Journal of Endocrinology*, *167*(4), 579–588. https://doi.org/10.1530/EJE-12-0452

Murphy, L. J. (1998). Insulin-like growth factor-binding proteins: Functional diversity or redundancy? *Journal of Molecular Endocrinology*, *21*(2), 97–107. https://doi.org/10.1677/jme.0210097

Musial, B., Fernandez-Twinn, D. S., Vaughan, O. R., Ozanne, S. E., Voshol, P.,

Sferruzzi-Perri, A. N., & Fowden, A. L. (2016). Proximity to delivery alters insulin sensitivity and glucose metabolism in pregnant mice. *Diabetes*, *65*(4), 851–860. https://doi.org/10.2337/db15-1531

Myers, M. G., Cowley, M. A., & Münzberg, H. (2008). Mechanisms of Leptin Action and Leptin Resistance. *Annual Review of Physiology*, *70*(1), 537–556. https://doi.org/10.1146/annurev.physiol.70.113006.100707

National Diabetes Data Group. (1979). Classification and diagnosis of diabetes mellitus and other categories of glucose intolerance. *Diabetes*, *28*(12), 1039–1057.

Neeland, I., Turer, A., Ayers, C., Powell-Wiley, T., Vega, G., Farzaneh-Far, R., … De Lemos, J. (2012). Dysfunctional adiposity and the risk of prediabetes and type 2 diabetes in obese adults. *JAMA - Journal of the American Medical Association*, *308*(11), 1150–1159. https://doi.org/10.1001/2012.jama.11132

Nishimura, S., Manabe, I., Nagasaki, M., Hosoya, Y., Yamashita, H., Fujita, H., … Sugiura, S. (2007). Adipogenesis in Obesity Requires Close Interplay Between Differentiating Adipocytes, Stromal Cells, and Blood Vessels. *Diabetes*, *56*(6), 1517–1526.

Nishizawa, H, Takahashi, M., Fukuoka, H., Iguchi, G., Kitazawa, R., & Takahashi, Y. (2012). GH-independent IGF-I action is essential to prevent

the development of nonalcoholic steatohepatitis in a GH-deficient rat model. *Biochemical and Biophysical Research Communications*, *423*, 295–300. https://doi.org/10.1016/j.bbrc.2012.05.115

Nishizawa, Haruki, Pryor-Koishi, K., Suzuki, M., Kato, T., Kogo, H., Sekiya, T., … Udagawa, Y. (2008). Increased levels of pregnancy-associated plasma protein-A2 in the serum of pre-eclamptic patients. *Molecular Human Reproduction*, *14*(10), 595–602. https://doi.org/10.1093/molehr/gan054

Noctor, E., & Dunne, F. (2015). Type 2 diabetes after gestational diabetes: The influence of changing diagnostic criteria. *World Journal of Diabetes*, *6*(2), 234. https://doi.org/10.4239/wjd.v6.i2.234

Nordström, A., Hadrévi, J., Olsson, T., Franks, P. W., & Nordström, P. (2016). Higher prevalence of type 2 diabetes in men than in women is associated with differences in visceral fat mass. *Journal of Clinical Endocrinology and Metabolism*, *101*(10), 3740–3746. https://doi.org/10.1210/jc.2016-1915

Nyegaard, M., Overgaard, M. T., Su, Y.-Q., Hamilton, A. E., Kwintkiewicz, J., Hsieh, M., … Giudice, L. C. (2010). Lack of Functional Pregnancy-Associated Plasma Protein-A (PAPPA) Compromises Mouse Ovarian Steroidogenesis and Female Fertility. *Biology of Reproduction*, *82*(6), 1129–1138. https://doi.org/10.1095/biolreprod.109.079517

265

O'Tierney-Ginn, P., Presley, L., Myers, S., & Catalano, P. (2015). Placental growth response to maternal insulin in early pregnancy. *The Journal of Clinical Endocrinology and Metabolism*, *100*(1), 159–165. https://doi.org/10.1210/jc.2014-3281

Okuno, S., Akazawa, S., Yasuhi, I., Kawasaki, E., Matsumoto, K., Yamasaki, H., … Nagataki, S. (1995). Decreased expression of the GLUT4 glucose transporter protein in adipose tissue during pregnancy. *Hormone and Metabolic Research*, *27*(5), 231–234. https://doi.org/10.1055/s-2007-979946

Ott, R., Stupin, J. H., Melchior, K., Schellong, K., Ziska, T., Dudenhausen, J. W., … Plagemann, A. (2018). Alterations of adiponectin gene expression and DNA methylation in adipose tissues and blood cells are associated with gestational diabetes and neonatal outcome. *Clinical Epigenetics*, *10*, 131. https://doi.org/10.1186/s13148-018-0567-z

Ouchi, N., Parker, J. L., Lugus, J. J., & Walsh, K. (2011). Adipokines in inflammation and metabolic disease. *Nature Reviews Immunology*, *11*(2), 85–97. https://doi.org/10.1038/nri2921

Overgaard, M. T., Haaning, J., Boldt, H. B., Olsen, I. M., Laursen, L. S., Christiansen, M., … Oxvig, C. (2000). Expression of recombinant human pregnancy-associated plasma protein-A and identification of the proform of

eosinophil major basic protein as its physiological inhibitor. *Journal of Biological Chemistry*, *275*(40), 31128–31133. https://doi.org/10.1074/jbc.M001384200

Oxvig, C. (2015). The role of PAPP-A in the IGF system: location, location, location. *Journal of Cell Communication and Signaling*, *9*(2), 177–187. https://doi.org/10.1007/s12079-015-0259-9

Pasarica, M., Sereda, O. R., Redman, L. M., Albarado, D. C., Hymel, D. T., Roan, L. E., … Smith, S. R. (2009). Reduced adipose tissue oxygenation in human obesity evidence for rarefaction, macrophage chemotaxis, and inflammation without an angiogenic response. *Diabetes*, *58*(3), 718–725. https://doi.org/10.2337/db08-1098

Patel, S., Fraser, A., Smith, G. D., Lindsay, R. S., Sattar, N., Nelson, S. M., & Lawlor, D. A. (2012). Associations of gestational diabetes, existing diabetes, and glycosuria with offspring obesity and cardiometabolic outcomes. *Diabetes Care*, *35*(1), 63–71. https://doi.org/10.2337/dc11-1633

Patif, N., Cox, D. R., Bhat, D., Faham, M., Myers, R. M., Peterson, A. S., … Friedman, J. M. (1995). Leptin levels in human and rodent: Measurement of plasma leptin and ob RNA in obese and weight-reduced subjects. *Nature Medicine*, *1*(11), 1155–1161. https://doi.org/10.1038/nm1195-1155

Pedersen, J. F., Sørensen, S., & Ruge, S. (1995). Human placental lactogen and pregnancy-associated plasma protein A in first trimester and subsequent fetal growth. *Acta Obstetricia et Gynecologica Scandinavica*, *74*(7), 505–508. https://doi.org/10.3109/00016349509024379

Pellegrinelli, V., Peirce, V. J., Howard, L., Virtue, S., Türei, D., Senzacqua, M., … Vidal-Puig, A. (2018). Adipocyte-secreted BMP8b mediates adrenergic-induced remodeling of the neuro-vascular network in adipose tissue. *Nature Communications*, *9*(1), 1–18. https://doi.org/10.1038/s41467-018-07453-x

Pereira, T. J., Fonseca, M. A., Campbell, K. E., Moyce, B. L., Cole, L. K., Hatch, G. M., … Dolinsky, V. W. (2015). Maternal obesity characterized by gestational diabetes increases the susceptibility of rat offspring to hepatic steatosis via a disrupted liver metabolome. *Journal of Physiology*, *593*(14), 3181–3197. https://doi.org/10.1113/JP270429

Pérez-Pérez, A., Toro, A., Vilariño-García, T., Maymó, J., Guadix, P., Dueñas, J. L., … Sánchez-Margalet, V. (2018). Leptin action in normal and pathological pregnancies. *Journal of Cellular and Molecular Medicine*, *22*(2), 716–727. https://doi.org/10.1111/jcmm.13369

Perry, R. J., Samuel, V. T., Petersen, K. F., & Shulman, G. I. (2014). The role of hepatic lipids in hepatic insulin resistance and type 2 diabetes. *Nature, 510*,

84–91. https://doi.org/10.1038/nature13478

Petry, C. J., Ong, K. K., Hughes, I. A., Acerini, C. L., Frystyk, J., & Dunger, D. B.
(2017). Early pregnancy-associated plasma protein a concentrations are
associated with third trimester insulin sensitivity. *Journal of Clinical
Endocrinology and Metabolism*, *102*(6), 2000–2008.
https://doi.org/10.1210/jc.2017-00272

Pirani, B. B. K., Campbell, D. M., & MacGillivray, I. (1973). Plasma volume in
normal first pregnancy. *BJOG: An International Journal of Obstetrics &
Gynaecology*, *80*, 884–887. https://doi.org/10.1111/j.1471-
0528.1973.tb02146.x

Plante, I., Stewart, M., & Laird, D. (2011). Evaluation of Mammary Gland
Development and Function in Mouse Models. *Journal of Visualized
Experiments*, (53), 2–6. https://doi.org/10.3791/2828

Plows, J. F., Yu, X., Broadhurst, R., Vickers, M. H., Tong, C., Zhang, H., …
Baker, P. N. (2017). Absence of a gestational diabetes phenotype in the
LepRdb/+ mouse is independent of control strain, diet, misty allele, or parity.
Scientific Reports, *7*, 45130. https://doi.org/10.1038/srep45130

Porter, S. A., Massaro, J. M., Hoffmann, U., Vasan, R. S., O'Donnel, C. J., & Fox,
C. S. (2009). Abdominal subcutaneous adipose tissue: A protective fat

depot? *Diabetes Care*, *32*(6), 1068–1075. https://doi.org/10.2337/dc08-2280

Poveda, N. E., Garcés, M. F., Darghan, A. E., Jaimes, S. A. B., Sánchez, E. P., Díaz-Cruz, L. A., … Caminos, J. E. (2018). Triglycerides/Glucose and Triglyceride/High-Density Lipoprotein Cholesterol Indices in Normal and Preeclamptic Pregnancies: A Longitudinal Study. *International Journal of Endocrinology*, *2018*(Article ID 8956408), 1–10. https://doi.org/10.1155/2018/8956404

Pusukuru, R., Shenoi, A. S., Kyada, P. K., Ghodke, B., Mehta, V., Bhuta, K., & Bhatia, A. (2016). Evaluation of Lipid Profile in Second and Third Trimester of Pregnancy. *Journal of Clinical and Diagnostic Research*, *10*(3), QC12–QC16. https://doi.org/10.7860/JCDR/2016/17598.7436

Qiao, L., Chu, K., Wattez, J.-S., Lee, S., Gao, H., Feng, G.-S., … Shao, J. (2019). High-fat feeding reprograms maternal energy metabolism and induces long-term postpartum obesity in mice. *International Journal of Obesity*, (Epub ahead of print). https://doi.org/10.1038/s41366-018-0304-x

Qiao, L., Wattez, J. S., Lee, S., Nguyen, A., Schaack, J., Hay, W. W., & Shao, J. (2017). Adiponectin deficiency impairs maternal metabolic adaptation to pregnancy in mice. *Diabetes*, *66*(5), 1126–1135. https://doi.org/10.2337/db16-1096

Qin, X., Sexton, C., Byun, D., Strong, D. D., Baylink, D. J., & Mohan, S. (2002). Differential regulation of pregnancy associated plasma protein (PAPP)-A during pregnancy in human and mouse. *Growth Hormone and IGF Research*, *12*(5), 359–366. https://doi.org/10.1016/S1096-6374(02)00046-1

Rajkumar, K., Krsek, M., Dheen, S. T., & Murphy, L. J. (1996). Impaired glucose homeostasis in insulin-like growth factor binding protein-1 transgenic mice. *The Journal of Clinical Investigation*, *98*(8), 1818–1825. https://doi.org/10.1172/JCI118982

Ranheim, T., Haugen, F., Staff, A. C., Braekke, K., Harsem, N. K., & Drevon, C. A. (2004). Adiponectin is reduced in gestational diabetes mellitus in normal weight women. *Acta Obstetricia et Gynecologica Scandinavica*, *83*(4), 341–347. https://doi.org/10.1111/j.0001-6349.2004.00413.x

Rausch, M. E., Weisberg, S., Vardhana, P., & Tortoriello, D. V. (2008). Obesity in C57BL/6J mice is characterized by adipose tissue hypoxia and cytotoxic T-cell infiltration. *International Journal Of Obesity*, *32*, 451–463. https://doi.org/10.1038/sj.ijo.0803744

Rebuffe-Scrive, M., Enk, L., Crona, N., Lönnroth, P., Abrahamsson, L., Smith, U., & Björntorp, P. (1985). Fat cell metabolism in different regions in women. Effect of menstrual cycle, pregnancy, and lactation. *Journal of Clinical*

271

Investigation, *75*(6), 1973–1976. https://doi.org/10.1172/JCI111914

Reilly, S. M., Ahmadian, M., Zamarron, B. F., Chang, L., Uhm, M., Poirier, B., … Saltiel, A. R. (2015). A subcutaneous adipose tissue-liver signalling axis controls hepatic gluconeogenesis. *Nature Communications*, *6*, 1–12. https://doi.org/10.1038/ncomms7047

Resi, V., Basu, S., Haghiac, M., Presley, L., Minium, J., Kaufman, B., … Hauguel-de Mouzon, S. (2012). Molecular inflammation and adipose tissue matrix remodeling precede physiological adaptations to pregnancy. *American Journal of Physiology-Endocrinology and Metabolism*, *303*(7), E832–E840. https://doi.org/10.1152/ajpendo.00002.2012

Retnakaran, R., Hanley, A. J. G., Raif, N., Connelly, P. W., Sermer, M., & Zinman, B. (2004). Reduced Adiponectin Concentration in Women With Gestational Diabetes. *Diabetes Care*, *27*(3), 799–800. https://doi.org/10.2337/diacare.27.3.799

Riddle, S., & Nommsen-Rivers, L. (2016). A Case Control Study of Diabetes During Pregnancy and Low Milk Supply. *Breastfeeding Medicine*, *11*(2), 80–85. https://doi.org/10.1089/bfm.2015.0120

Roberts, C., & Leroith, D. (1988). 11 Molecular aspects of insulin-like growth factors, their binding proteins and receptors. *Baillière's Clinical*

272

Endocrinology and Metabolism, *2*(4), 1069–1085.

https://doi.org/10.1016/S0950-351X(88)80030-2

Rojas-Rodriguez, R., Gealekman, O., Kruse, M. E., Rosenthal, B., Rao, K., Min, S., … Corvera, S. (2014). Adipose tissue angiogenesis assay. *Methods in Enzymology*, *537*, 75–91.

Rojas-Rodriguez, R., Lifshitz, L. M., Bellve, K. D., Min, S. Y., Pires, J., Leung, K., … Moore Simas, T. A. (2015). Human adipose tissue expansion in pregnancy is impaired in gestational diabetes mellitus. *Diabetologia*, *58*, 2106–2114. https://doi.org/10.1007/s00125-015-3662-0

Ruan, H., Hacohen, N., Golub, T. R., Parijs, L. Van, & Lodish, H. F. (2002). Tumor Necrosis Factor-α Suppresses Adipocyte-Specific Genes and Activates Expression of Preadipocyte Genes in 3T3-L1 Adipocytes. *Diabetes*, *51*, 1319–1336. https://doi.org/10.2337/diabetes.51.5.1319

Rupnick, M., Panigrahy, D., Zhang, C., Dallabrida, S., Lowell, B., Langer, R., & Folkman, M. (2002). Adipose tissue mass can be regulated through the vasculature. *Proceedings of the National Academy of Sciences of the United States of America*, *99*(16), 10730–10735. https://doi.org/10.1073/pnas.162349799

Rutkowski, J., Stern, J., & Scherer, P. (2015). Beyond the cell: The cell biology of

fat expansion. *The Journal of Cell Biology*, *208*(5), 501–512. https://doi.org/10.1083/jcb.201105099

Ryan, E., Sullivan, M., & Skyler, J. (1985). Insulin Action During Pregnancy: Studies with the Euglycemic Clamp Technique. *Diabetes*, *34*(4), 380–389. https://doi.org/10.2337/diab.34.4.380

Rydén, M., Andersson, D. P., Bergström, I. B., & Arner, P. (2014). Adipose tissue and metabolic alterations: Regional differences in fat cell size and number matter, but differently: A cross-sectional study. *Journal of Clinical Endocrinology and Metabolism*, *99*(10), E1870–E1876. https://doi.org/10.1210/jc.2014-1526

Sacks, D. A., Hadden, D. R., Maresh, M., Deerochanawong, C., Dyer, A. R., Metzger, B. E., … The HAPO Study Cooperative Research Group. (2012). Frequency of gestational diabetes mellitus at collaborating centers based on IADPSG consensus panel-recommended criteria: the Hyperglycemia and Adverse Pregnancy Outcome (HAPO) Study. *Diabetes Care*, *35*(3), 526–528. https://doi.org/10.2337/dc11-1641

Savvidou, M. D., Syngelaki, A., Muhaisen, M., Emelyanenko, E., & Nicolaides, K. H. (2012). First trimester maternal serum free β-human chorionic gonadotropin and pregnancy-associated plasma protein A in pregnancies

complicated by diabetes mellitus. *BJOG*, *119*, 410–416.

https://doi.org/10.1111/j.1471-0528.2011.03253.x

Schindelin, J., Arganda-Carreras, I., Frise, E., Kaynig, V., Longair, M., Pietzsch,

T., … Cardona, A. (2012). Fiji: an open-source platform for biological-image

analysis. *Nature Methods*, *9*(7), 676–682.

https://doi.org/10.1038/nmeth.2019

Scholtens, D. M., Kuang, A., Lowe, L. P., Hamilton, J., Lawrence, J. M.,

Lebenthal, Y., … HAPO Follow-Up Study Cooperative Research Group.

(2019). Hyperglycemia and Adverse Pregnancy Outcome Follow-Up Study

(HAPO FUS): Maternal Glycemia and Childhood Glucose Metabolism.

Diabetes Care, *42*(3), 381–392. https://doi.org/10.2337/dc18-2021

Sethi, J., & Vidal-Puig, A. (2007). Thematic review series: adipocyte biology.

Adipose tissue function and plasticity orchestrate nutritional adaptation.

Journal of Lipid Research, *48*(6), 1253–1262.

https://doi.org/10.1194/jlr.R700005-JLR200

Shi, Z., Xu, W., Loechel, F., Wewer, U. M., & Murphy, L. J. (2000). ADAM 12, a

disintegrin metalloprotease, interacts with insulin-like growth factor-binding

protein-3. *Journal of Biological Chemistry*, *275*(24), 18574–18580.

https://doi.org/10.1074/jbc.M002172200

275

Shinar, S., Berger, H., De Souza, L. R., & Ray, J. G. (2019). Difference in Visceral Adipose Tissue in Pregnancy and Postpartum and Related Changes in Maternal Insulin Resistance. *Journal of Ultrasound in Medicine*, *38*(3), 667–673. https://doi.org/10.1002/jum.14737

Siddle, K. (2011). Signalling by insulin and IGF receptors: Supporting acts and new players. *Journal of Molecular Endocrinology*, *47*(1), R1-10. https://doi.org/10.1530/JME-11-0022

Silha, J. V, Gui, Y., & Murphy, L. J. (2002). Impaired glucose homeostasis in insulin-like growth factor-binding protein-3-transgenic mice. *American Journal of Physiology-Endocrinology and Metabolism*, *283*(5), E937–E945. https://doi.org/10.1152/ajpendo.00014.2002

Singh, C. K., Kumar, A., Hitchcock, D. B., Fan, D, Goodwin, R., Lavoie, H. A., … Singh, U. S. (2011). Resveratrol prevents embryonic oxidative stress and apoptosis associated with diabetic embryopathy and improves glucose and lipid profile of diabetic dam. *Molecular Nutrition and Food Research*, *55*(8), 1186–1196. https://doi.org/10.1002/mnfr.201000457

Sivan, E., Chen, X., Homko, C., Reece, E., & Boden, G. (1997). Longitudinal Study of Carbohydrate Metabolism in Healthy Obese Pregnant Women. *Diabetes Care*, *20*(9), 1470–1475.

Smith, A., Choufani, A., Ferreira, J., & Weksberg, R. (2007). Growth Regulation, Imprinted Genes, and Chromosome 11p15.5. *Pediatric Research*, *61*(5), 43R-47R. https://doi.org/10.1203/pdr.0b013e3180457660

Smith, R., Bischof, P., Hughes, G., & Klopper, A. (1979). Studies on pregnancy-associated plasma protein A in the third trimester of pregnancy. *BJOG: An International Journal of Obstetrics & Gynaecology*, *86*(11), 882–887. https://doi.org/10.1111/j.1471-0528.1979.tb10716.x

Snel, M., Jonker, J. T., Schoones, J., Lamb, H., De Roos, A., Pijl, H., … Jazet, I. M. (2012). Ectopic fat and insulin resistance: Pathophysiology and effect of diet and lifestyle interventions. *International Journal of Endocrinology*, *2012*, Article ID 983814. https://doi.org/10.1155/2012/983814

Snijders, R., Spencer, K., Souter, V., Nicolaides, K. H., & Tul, N. (2003). A screening program for trisomy 21 at 10-14 weeks using fetal nuchal translucency, maternal serum free β-human chorionic gonadotropin and pregnancy-associated plasma protein-A. *Ultrasound in Obstetrics and Gynecology*, *13*(4), 231–237. https://doi.org/10.1046/j.1469-0705.1999.13040231.x

Soheilykhah, S., Mojibian, M., Rahimi-Saghand, S., Rashidi, M., & Hadinedoushan, H. (2011). Maternal serum leptin concentration in

gestational diabetes. *Taiwanese Journal of Obstetrics and Gynecology*, *50*(2), 149–153. https://doi.org/10.1016/j.tjog.2011.01.034

Sonagra, A. D., Biradar, S. M., Dattatreya, K., & Murthy, J. (2014). Normal Pregnancy- A State of Insulin Resistance. *Journal of Clinical and Diagnostic Research*, *8*(11), CC01–CC03. https://doi.org/10.7860/JCDR/2014/10068.5081

Spencer, M., Unal, R., Zhu, B., Rasouli, N., McGehee Jr, R. E., Peterson, C. A., & Kern, P. A. (2011). Adipose tissue extracellular matrix and vascular abnormalities in obesity and insulin resistance. *The Journal of Clinical Endocrinology and Metabolism*, *96*(12), E1990–E1998. https://doi.org/10.1210/jc.2011-1567

Spicer, L., & Aad, P. (2007). Insulin-Like Growth Factor (IGF) 2 Stimulates Steroidogenesis and Mitosis of Bovine Granulosa Cells Through the IGF1 Receptor: Role of Follicle-Stimulating Hormone and IGF2 Receptor. *Biology of Reproduction*, *77*(1), 18–27. https://doi.org/10.1095/biolreprod.106.058230

Sreelakshmi, P. R., Nair, S., Soman, B., Alex, R., Vijayakumar, K., & Kutty, V. R. (2015). Maternal and neonatal outcomes of gestational diabetes: A retrospective cohort study from Southern India. *Journal of Family Medicine*

278

and Primary Care, *4*(3), 395–398.

Stephens, J., Lee, J., & Pilch, P. (1997). Tumor Necrosis Factor- α -induced Insulin Resistance in 3T3-L1 Adipocytes Is Accompanied by a Loss of Insulin Receptor Substrate-1 and GLUT4 Expression without a Loss of Insulin Receptor-mediated Signal Transduction. *Journal of Biological Chemistry*, *272*(2), 971–976. https://doi.org/10.1074/jbc.272.2.971

Straughen, J. K., Trudeau, S., & Misra, V. K. (2013). Changes in adipose tissue distribution during pregnancy in overweight and obese compared with normal weight women. *Nutrition and Diabetes*, *3*(e84), 1–5. https://doi.org/10.1038/nutd.2013.25

Summers, S. A. (2006). Ceramides in insulin resistance and lipotoxicity. *Progress in Lipid Research*, *45*(1), 42–72. https://doi.org/10.1016/j.plipres.2005.11.002

Sun, K., Kusminski, C., & Scherer, P. (2011). Adipose tissue remodeling and obesity. *The Journal of Clinical Investigation*, *121*(6), 2094–2101. https://doi.org/10.1172/JCI45887.2094

Sung, H. K., Doh, K. O., Son, J. E., Park, J. G., Bae, Y., Choi, S., … Nagy, A. (2013). Adipose vascular endothelial growth factor regulates metabolic homeostasis through angiogenesis. *Cell Metabolism*, *17*(1), 61–72.

279

https://doi.org/10.1016/j.cmet.2012.12.010

Sutcliffe, R. G., Sutherland, H. W., Bowman, A. W., Maclean, A. B., Horne, C. H. W., Jandial, V., … Kukulska-Langlands, B. M. (1982). Studies on the concentration of pregnancy-associated plasma protein-a during normal and complicated pregnancy. *Placenta*, *3*(1), 71–79. https://doi.org/10.1016/s0143-4004(82)80020-9

Svensson, H., Wetterling, L., Bosaeus, M., Odén, B., Odén, A., Jennische, E., … Lönn, M. (2016). Body fat mass and the proportion of very large adipocytes in pregnant women are associated with gestational insulin resistance. *International Journal of Obesity*, *40*(4), 646–653. https://doi.org/10.1038/ijo.2015.232

Syngelaki, A., Kotecha, R., Pastides, A., Wright, A., & Nicolaides, K. H. (2015). First-trimester biochemical markers of placentation in screening for gestational diabetes mellitus. *Metabolism*, *64*(11), 1485–1489. https://doi.org/10.1016/j.metabol.2015.07.015

Tang, W., Zeve, D., Suh, J. M., Bosnakovski, D., Kyba, M., Hammer, R. E., … Graff, J. M. (2008). White fat progenitor cells reside in the adipose vasculature. *Science*, *322*(5901), 583–586. https://doi.org/10.1126/science.1156232

Taniguchi, C. M., Emanuelli, B., & Kahn, C. R. (2006). Critical nodes in signalling pathways:insights into insulin action. *Nature Reviews Molecular Cell Biology*, *7*, 85–96. https://doi.org/10.1038/nrm1837

Tchernof, A., & Després, J.-P. (2013). Pathophysiology of Human Visceral Obesity: An Update. *Physiological Reviews*, *93*(1), 359–404. https://doi.org/10.1152/physrev.00033.2011

Tchoukalova, Y. D., Votruba, S. B., Tchkonia, T., Giorgadze, N., Kirkland, J. L., Jensen, M. D., … Kirklandc, J. L. (2014). Regional differences in cellular mechanisms of adipose tissue gain with overfeeding. *Proceedings of the National Academy of Sciences of the United States of America*, *107*(42), 18226–18231. https://doi.org/10.1073/pnas.1005259107

The HAPO Study Cooperative Research Group. (2008). Hyperglycemia and Averse Pregnancy Outcomes. *The New England Journal of Medicine*, *358*(19), 1991–2002.

Tokarz, V. L., MacDonald, P. E., & Klip, A. (2018). The cell biology of systemic insulin function. *Journal of Cell Biology*, *217*(7), 1–17. https://doi.org/10.1083/jcb.201802095

Tornehave, D., Chemnitz, J., Teisner, B., Folkersen, J., & Westergaard, J. G. (1984). Immunohistochemical demonstration of pregnancy-associated

281

plasma protein A (PAPP-A) in the syncytiotrophoblast of the normal placenta at different gestational ages. *Placenta*, *5*, 427–431. https://doi.org/10.1016/S0143-4004(84)80023-5

Tran, K., Gealekman, O., Frontini, A., Zingaretti, M., Morroni, M., Giordano, A., … Cinti, S. (2012). The vascular endothelium of the adipose tissue gives rise to both white and brown fat cells. *Cell Metabolism*, *15*(2), 222–229. https://doi.org/10.1016/j.cmet.2012.01.008

Trayhurn, P., & Beattie, J. H. (2008). Physiological role of adipose tissue: white adipose tissue as an endocrine and secretory organ. *Proceedings of the Nutrition Society*, *60*(3), 329–339. https://doi.org/10.1079/pns200194

Trejo-González, N. L., Chirino-Galindo, G., & Palomar-Morales, M. (2015). Antiteratogenic capacity of resveratrol in streptozotocin-induced diabetes in rats. *Revista Peruana de Medicina Experimental y Salud Publica*, *32*(3), 457–463.

Tsiotra, P. C., Halvatsiotis, P., Patsouras, K., Maratou, E., Salamalekis, G., Raptis, S. A., … Boutati, E. (2018). Circulating adipokines and mRNA expression in adipose tissue and the placenta in women with gestational diabetes mellitus. *Peptides*, *101*, 157–166. https://doi.org/10.1016/j.peptides.2018.01.005

Uebel, K., Pusch, K., Gedrich, K., Schneider, K. T. M., Hauner, H., & Bader, B. L. (2014). Effect of maternal obesity with and without gestational diabetes on offspring subcutaneous and preperitoneal adipose tissue development from birth up to year-1. *BMC Pregnancy and Childbirth*, *14*(138), 1–13. https://doi.org/10.1186/1471-2393-14-138

Usui, C., Asaka, M., Kawano, H., Aoyama, T., Ishijima, T., Sakamoto, S., & Higuchi, M. (2010). Visceral Fat Is a Strong Predictor of Insulin Resistance Regardless of Cardiorespiratory Fitness in Non-Diabetic People. *Journal of Nutritional Science and Vitaminology*, *56*(2), 109–116. https://doi.org/10.3177/jnsv.56.109

Veilleux, A., Caron-Jobin, M., Noël, S., Laberge, P. Y., & Tchernof, A. (2011). Visceral adipocyte hypertrophy is associated with dyslipidemia independent of body composition and fat distribution in women. *Diabetes*, *60*(5), 1504–1511. https://doi.org/10.2337/db10-1039

Verboven, K., Wouters, K., Gaens, K., Hansen, D., Bijnen, M., Wetzels, S., … Jocken, J. W. (2018). Abdominal subcutaneous and visceral adipocyte size, lipolysis and inflammation relate to insulin resistance in male obese humans. *Scientific Reports*, *8*(1), 4677. https://doi.org/10.1038/s41598-018-22962-x

Virtue, S., & Vidal-Puig, A. (2010). Adipose tissue expandability, lipotoxicity and

283

the Metabolic Syndrome — An allostatic perspective. *Biochimica et Biophysica Acta (BBA) - Molecular and Cell Biology of Lipids*, *1801*(3), 338–349.

Vivas, Y., Díez-Hochleitner, M., Izquierdo-Lahuerta, A., Corrales, P., Horrillo, D., Velasco, I., … Medina-Gomez, G. (2016). Peroxisome Proliferator-Activated Receptor γ 2 Modulates Late-Pregnancy Homeostatic Metabolic Adaptations. *Molecular Medicine*, *22*, 724–736. https://doi.org/10.2119/molmed.2015.00262

Wajchenberg, B. L. (2000). Subcutaneous and Visceral Adipose Tissue : *Endocrine Reviews*, *21*(6), 697–738.

Wald, N., Stone, R., Cuckle, H. S., Grudzinskas, J. G., Barkai, G., Brambati, B., … Fuhrmann, W. (1992). First trimester concentrations of pregnancy associated plasma protein A and placental protein 14 in Down syndrome. *BMJ*, *305*(6844), 28. https://doi.org/10.1136/bmj.305.6844.28

Wapner, R., Thom, E., Simpson, J. L., Pergament, E., Silver, R., Filkins, K., … Jackson, L. (2003). First-Trimester Screening for Trisomies 21 and 18. *The New England Journal of Medicine*, *349*(15), 1405–1413.

Wells, G., Bleicher, K., Han, X., McShane, M., Chan, Y. F., Bartlett, A., … Lau, S. M. (2015). Maternal diabetes, large-for-gestational-age births, and first

trimester pregnancy-associated plasma protein-A. *Journal of Clinical Endocrinology and Metabolism*, *100*(6), 2372–2379. https://doi.org/10.1210/jc.2014-4103

Werman, A., Hollenberg, A., Solanes, G., Bjørbæk, C., Vidal-Puig, A. J., & Flier, J. S. (1997). Ligand-independent Activation Domain in the N Terminus of Peroxisome Proliferator-activated Receptor γ (PPARγ). *Journal of Biological Chemistry*, *272*(32), 20230–20235. https://doi.org/10.1074/jbc.272.32.20230

Werner, H., Weinstein, D., & Bentov, I. (2008). Similarities and differences between insulin and IGF-I: structures, receptors, and signalling pathways. *Archives of Physiology and Biochemistry*, *114*(1), 17–22. https://doi.org/10.1080/13813450801900694

Wernstedt Asterholm, I., Tao, C., Morley, T. S., Wang, Q. a., Delgado-Lopez, F., Wang, Z. V., & Scherer, P. E. (2014). Adipocyte inflammation is essential for healthy adipose tissue expansion and remodeling. *Cell Metabolism*, *20*(1), 103–118. https://doi.org/10.1016/j.cmet.2014.05.005

White, V., Jawerbaum, A., Mazzucco, M. B., Gauster, M., Desoye, G., & Hiden, U. (2017). IGF2 stimulates fetal growth in a sex- and organ-dependent manner. *Pediatric Research*, *83*(1), 183–189. https://doi.org/10.1038/pr.2017.221

285

Wicklow, B. A., Sellers, E. A. C., Sharma, A. K., Kroeker, K., Nickel, N. C., Philips-Beck, W., & Shen, G. X. (2018). Association of Gestational Diabetes and Type 2 Diabetes Exposure In Utero With the Development of Type 2 Diabetes in First Nations and Non–First Nations Offspring. *JAMA Pediatrics*, *172*(8), 724–731. https://doi.org/10.1001/jamapediatrics.2018.1201

Wiznitzer, A., Mayer, A., Novack, V., Sheiner, E., Gilutz, H., Malhotra, A., & Novack, L. (2009). Association of lipid levels during gestation with preeclampsia and gestational diabetes mellitus: a population-based study. *American Journal of Obstetrics and Gynecology*, *201*(5), 482.e1-482.e8. https://doi.org/10.1016/j.ajog.2009.05.032

Wolf, M., Sauk, J., Shah, A., Vossen Smirnakis, K., Jimenez-Kimble, R., Ecker, J. L., & Thadhani, R. (2004). Inflammation and Glucose Intolerance. A prospective study of gestational diabetes mellitus. *Diabetes Care*, *27*, 21–27.

Wree, A., Mayer, A., Westphal, S., Beilfuss, A., Canbay, A., Schick, R. R., … Vaupel, P. (2012). Adipokine expression in brown and white adipocytes in response to hypoxia. *Journal of Endocrinological Investigation*, *35*(5), 522–527. https://doi.org/10.3275/7964

Wright, D., Silva, M., Papadopoulos, S., Wright, A., & Nicolaides, K. H. (2015). Serum pregnancy-associated plasma protein-A in the three trimesters of

pregnancy: Effects of maternal characteristics and medical history. *Ultrasound in Obstetrics and Gynecology*, *46*(1), 42–50. https://doi.org/10.1002/uog.14870

Xin, X., Rodrigues, M., Umapathi, M., Kashiwabuchi, F., Ma, T., Babapoor-Farrokhran, S., … Sodhi, A. (2013). Hypoxic retinal Müller cells promote vascular permeability by HIF-1–dependent up-regulation of angiopoietin-like 4. *Proceedings of the National Academy of Sciences*, *110*(36), E3425–E3434. https://doi.org/10.1073/pnas.1217091110

Yamada, P. M., Mehta, H. H., Hwang, D., Roos, K. P., Hevener, A. L., & Lee, K. W. (2010). Evidence of a role for insulin-like growth factor binding protein (IGFBP)-3 in metabolic regulation. *Endocrinology*, *151*(12), 5741–5750. https://doi.org/10.1210/en.2010-0672

Yamashita, H., Shao, J., Ishizuka, T., Klepcyk, P. J., Muhlenkamp, P., Qiao, L., … Friedman, J. E. (2001). Gestational Diabetes in Heterozygous Lepr db/+ Mice: Effects on Placental Leptin and Fetal Growth. *Endocrinology*, *142*(7), 2888–2897.

Yamauchi, T., Kamon, J., Waki, H., Terauchi, Y., Kubota, N., Hara, K., … Murakami, K. (2001). The fat-derived hormone adiponectin reverses insulin resistance associated with both lipoatrophy and obesity. *Nature Medicine*,

7(8), 941–946.

Yang, Q., Wang, P., Du, X., Wang, W., Zhang, T., & Chen, Y. (2018). Direct
repression of IGF2 is implicated in the anti-angiogenic function of microRNA-
210 in human retinal endothelial cells. *Angiogenesis*, *21*(2), 313–323.
https://doi.org/10.1007/s10456-018-9597-6

Yu, H., Mistry, J., Nicar, M. J., Khosravi, M. J., Diamandis, A., Van Doorn, J., &
Juul, A. (1999). Insulin-like growth factors (IGF-I, free IGF-I, and IGF-II) and
insulin- like growth factor binding proteins (IGFBP-2, IGFBP-3, IGFBP-6, and
ALS) in blood circulation. *Journal of Clinical Laboratory Analysis*, *13*(4), 166–
172. https://doi.org/10.1002/(SICI)1098-2825(1999)13:4<166::AID-
JCLA5>3.0.CO;2-X

Zhang, C., Olsen, S. F., Hinkle, S. N., Gore-Langton, R. E., Vaag, A., Grunnet, L.
G., … Hu, F. B. (2019). Diabetes and Women's Health (DWH) Study: an
observational study of long-term health consequences of gestational
diabetes, their determinants and underlying mechanisms in the USA and
Denmark. *BMJ Open*, *9*(4), e025517. https://doi.org/10.1136/bmjopen-2018-
025517

Zhang, M., Hu, T., Zhang, S., & Zhou, L. (2015). Associations of Different
Adipose Tissue Depots with Insulin Resistance: A Systematic Review and

Meta-analysis of Observational Studies. *Scientific Reports*, *5*, 18495.

Retrieved from https://doi.org/10.1038/srep18495

Zhao, Y. N., Li, Q., & Li, Y. C. (2014). Effects of body mass index and body fat

percentage on gestational complications and outcomes. *Journal of*

Obstetrics and Gynaecology Research, *40*(3), 705–710.

https://doi.org/10.1111/jog.12240

Zhou, T., Sun, D., Li, X., Heinza, Y., Nisa, H., Hu, G., … Qi, L. (2018).

Prevalence and Trends in Gestational Diabetes Mellitus among Women in

the United States, 2006–2016. *Diabetes*, *67*(Supplement 1), 121-OR.

https://doi.org/10.2337/db18-121-OR

Zhu, Y., Mendola, P., Albert, P. S., Bao, W., Hinkle, S. N., Tsai, M. Y., & Zhang,

C. (2016). Insulin-like growth factor axis and gestational diabetes mellitus: A

longitudinal study in a multiracial cohort. *Diabetes*, *65*(11), 3495–3504.

https://doi.org/10.2337/db16-0514